Vol. 56 DECEMBER, 1952 No. 9

THE JOURNAL OF PHYSICAL CHEMISTRY

(Registered in U. S. Patent Office)

Founded by Wilder D. Bancroft

SYMPOSIUM ON THE THERMODYNAMICS OF IRREVERSIBLE SYSTEMS

R. A. Oriani: Irreversible Phenomena in Metallurgy 1025

R. T. Cox: The Statistical Method of Gibbs in Irreversible Thermodynamics 1030

Eugene M. Holleran and Hugh M. Hulburt: A Relation among the Kinetic Theory Cross-Section Integrals and New Relations Involving the Transport Properties of Gases 1034

Harold Grad: Statistical Mechanics of Dynamical Systems with Integrals Other than Energy 1039

John G. Kirkwood and Bryce Crawford, Jr.: The Macroscopic Equations of Transport 1048

CONTRIBUTED PAPERS

Fausto W. Lima: On the Viscosity of Binary Liquid Mixtures 1052

W. West, B. H. Carroll and D. H. Whitcomb: The Adsorption of Sensitizing Dyes in Photographic Emulsions 1054

C. W. Hoerr and H. J. Harwood: The Solubilities of Oleic and Linoleic Acids in Common Organic Solvents 1068

W. O. Milligan and Harry B. Whitehurst: Magnetic Properties of Adsorbed Vapors 1073

W. J. Priest: Particle Growth in the Aqueous Polymerization of Vinyl Acetate 1077

J. Rooley, C. S. Rohrer and O. W. Brown: The Catalytic Activity of Reduced Nickel Molybdate and Reduced Nickel Chromate 1082

Lyman Chalkley: The Extent of the Photochemical Reduction of Phosphotungstic Acid 1084

R. K. Iler: Linear Polymetaphosphates—Quaternary Ammonium Salts 1086

F. H. MacDougall and Leo E. Topol: Ionic Equilibria in Aqueous and Mixed Solvent Solutions of Silver Acetate and Silver Monochloroacetate 1090

Frank E. Young, Francis T. Jones and Harold J. Lewis: D-Fructose–Water Phase Diagram 1093

Darleane Christian Hoffman and Don S. Martin, Jr.: Hot Atom Chemistry. Photonuclear Preparation of Cobalt-58, Cobalt 58m 1097

H. Kacser: The Probability Factor in Bimolecular Reactions. I. Uncomplicated Ion-Dipole Systems 1101

Albert W. Jache and George H. Cady: Solubility of Fluorides of Metals in Liquid Hydrogen Fluoride 1106

Additions and Corrections 1110

Author Index 1111

Subject Index 1116

Founded by Wilder D. Bancroft

THE JOURNAL OF PHYSICAL CHEMISTRY

(Registered in U. S. Patent Office)

Published monthly (except July, August and September) by the American Chemical Society at 20th and Northampton Sts., Easton, Pa.

Entered as second-class matter at the Post Office at Easton, Pennsylvania.

The *Journal of Physical Chemistry* is devoted to the publication of selected symposia in the broad field of physical chemistry and to other contributed papers.

Manuscripts originating in the British Isles, Europe and Africa should be sent to F. C. Tompkins, The Faraday Society, 6 Gray's Inn Square, London W. C. 1, England.

Manuscripts originating elsewhere should be sent to W. Albert Noyes, Jr., Department of Chemistry, University of Rochester, Rochester 3, N. Y.

Correspondence regarding accepted copy, proofs and reprints should be directed to Assistant Editor, Allen D. Bliss, Department of Chemistry, Simmons College, 300 The Fenway, Boston 15, Mass.

Business Office: American Chemical Society, 1155 Sixteenth St., N. W., Washington 6, D. C.

Advertising Office: American Chemical Society, 332 West 42nd St., New York 18, N. Y.

Articles must be submitted in duplicate, typed and double spaced. They should have at the beginning a brief Abstract, in no case exceeding 300 words. Original drawings should accompany the manuscript. Lettering at the sides of graphs (black on white or blue) may be pencilled in, and will be typeset. Figures and tables should be held to a minimum consistent with adequate presentation of information. Photographs will not be printed on glossy paper except by special arrangement. All footnotes and references to the literature should be numbered consecutively and placed on the manuscript at the proper places. Initials of authors referred to in citations should be given. Nomenclature should conform to that used in *Chemical Abstracts*, mathematical characters marked for italic, Greek letters carefully made or annotated, and subscripts and superscripts clearly shown. Articles should be written as briefly as possible consistent with clarity and should avoid historical background unnecessary for specialists.

Symposium papers should be sent in all cases to Secretaries of Divisions sponsoring the symposium, who will be responsible for their transmittal to the Editor. The Secretary of the Division by agreement with the Editor will specify a time after which symposium papers cannot be accepted. The Editor reserves the right to refuse to publish symposium articles, for valid scientific reasons. Each symposium paper may not exceed four printed pages (about sixteen double spaced typewritten pages) in length except by prior arrangement with the Editor.

Remittances and orders for subscriptions and for single copies, notices of changes of address and new professional connections, and claims for missing numbers should be sent to the American Chemical Society, 1155 Sixteenth St., N. W., Washington 6, D. C. Changes of address for the *Journal of Physical Chemistry* must be received on or before the 30th of the preceding month.

Claims for missing numbers will not be allowed (1) if received more than sixty days from date of issue (because of delivery hazards, no claims can be honored from subscribers in Central Europe, Asia, or Pacific Islands other than Hawaii) (2) if loss was due to failure of notice of change of address to be received before the date specified in the preceding paragraph, or (3) if the reason for the claim is "missing from files."

Annual Subscription: $8.00 to members of the American Chemical Society, $10.00 to non-members. Postage free to countries in the Pan American Union; Canada, $0.40; all other countries, $1.20. Single copies, $1.25; foreign postage, $0.15; Canadian postage $0.05.

The American Chemical Society and the Editors of the *Journal of Physical Chemistry* assume no responsibility for the statements and opinions advanced by contributors to THIS JOURNAL.

The American Chemical Society also publishes *Journal of the American Chemical Society*, *Chemical Abstracts*, *Industrial and Engineering Chemistry*, *Chemical and Engineering News* and *Analytical Chemistry*. Rates on request.

THE JOURNAL OF PHYSICAL CHEMISTRY

(Registered in U. S. Patent Office) (Copyright, 1952, by the American Chemical Society)

Founded by Wilder D. Bancroft

VOLUME 56 DECEMBER 26, 1952 NUMBER 9

IRREVERSIBLE PHENOMENA IN METALLURGY

BY R. A. ORIANI

General Electric Research Laboratory, Schenectady, New York

Received July 2, 1952

The assumptional background and the structure of the thermodynamics of irreversible processes are very briefly reviewed, and it is demonstrated that application of this thermodynamics to metallurgical phenomena may be advantageous in helping to identify the proper forces and fluxes and in elucidating the cross-effects when more than one force is operating. However, because of the singleness of the type of driving force usually encountered in metallurgy, cross-effects are relatively rare, so that applications of this thermodynamics to metallurgical processes are limited. The relevant features of multicomponent diffusion with and without phase transformations, formation of oxide and sulfide films, and grain boundary migration are described in order to assess the bearing of the theory of irreversible thermodynamics on typical irreversible metallurgical phenomena. The theory of plastic deformation cannot profit from this thermodynamics.

Foreword

This paper was presented at a symposium on the thermodynamics of irreversible systems sponsored by the American Chemical Society at Buffalo, New York. Of the various developments of thermodynamics designed to apply to irreversible phenomena, that one based on Onsager's reciprocity relations, and further developed by the Belgian school, has attained a compact and comprehensive formulation and has enjoyed extensive application in various fields of physical chemistry. It is therefore of interest to examine what bearing this thermodynamics may have on the irreversible phenomena of metallurgy.

Introduction

As a scientific discipline, metallurgy, the study of the atomic and microstructural properties of metals, is one of the youngest branches of physics and chemistry, though it has a long history of practical "know-how." Its scientific development has had to await the rise of such refined techniques as X-ray diffraction on the one hand and, on the other, the application of quantum mechanics to metallic cohesion. Theoretical understanding is impeded by the well-appreciated difficulties inherent in the condensed phases. Though the periodic structure of solid metals has allowed much greater progress in certain directions than has been the case with liquids, nevertheless, it has turned out that many of the interesting metallurgical properties depend on deviations from periodicity in ways which are just now beginning to be understood. Experimental progress has been hindered by the existence of phenomena which are history-dependent, making it difficult to characterize completely a test material. There are also reactions and transformations which, though driven by small free energy changes, have very great consequences for the physical characteristics of the metals. These reactions are often irreversible, and are therefore incompletely and inadequately described by classical thermodynamics.

It is in connection with this last class of phenomena that the metallurgist may wish to look for help to the thermodynamics based on Onsager's principle and recently formulated by de Groot.[1] Indeed, it seems that a worthwhile purpose would be served by a tentative exploration of such phenomena, to see whether or not the thermodynamics of irreversible processes can offer guidance and assistance to the metallurgist. Some work along this line has already been accomplished and will be described. For the most part, however, it will be necessary to restrict ourselves to an account of the relevant features of the phenomena, and simply to indicate the possibility of contributions from this thermodynamics. A secondary purpose for this paper will be to draw the attention of chemists to

---

(1) S. R. de Groot, "Thermodynamics of Irreversible Processes," Interscience Publishers, Inc., New York, N. Y., 1951.

the very interesting physical chemical problems to be found in metallurgy.

Thermodynamic Background.—The essential points of the thermodynamics based on Onsager's work may be stated briefly. Any generalized force, *e.g.*, temperature gradient, chemical affinity, can give rise to any generalized flux, or current, *e.g.*, mass transport, energy flow. If the phenomenon can be adequately represented by a linear relation between the forces X_k and the fluxes J_i, *i.e.*, if

$$J_i = \sum_{k=1}^{n} L_{ik}X_k, \ (i = 1,2,\cdots, n) \qquad (1)$$

then the matrix of the phenomenological coefficients L_{ik} is symmetric provided that the forces and the fluxes are properly chosen. This proper specification depends upon being able to write down the entropy production as a sum of products of conjugated forces and fluxes. The validity of the scheme depends not only on the Boltzmann H-theorem, the property of microscopic reversibility, and Onsager's hypothesis of the regression of fluctuations, but also on the ability to define thermodynamical quantities outside of thermostatic equilibrium, and upon the acceptance of Gibbs' relation

$$T\mathrm{d}S = \mathrm{d}U + P\mathrm{d}V - \sum_i \mu_i \mathrm{d}M_i \qquad (2)$$

for non-equilibrium states. The complex question of the legitimacy of this interrelated set of assumptions and hypotheses has been examined by several authors in the light of kinetic theory; for our present purpose it will suffice to state that if deviations from equilibrium are not too large, the set of assumptions is valid.[2,3]

This type of thermodynamics, together with the attendant statistical mechanics, gives us in principle at least, a means of ascertaining whether or not we are justified in using thermodynamical variables in certain situations. We are also given a means of determining which are the proper forces and fluxes to use in formulating a problem, by calculating the entropy production as a quadratic form. Then also, and most importantly, through the symmetry of the matrix of the coefficients L_{ik} in equation (1) we acquire a powerful tool for establishing necessary relations among cross-effects. In metallurgical studies, one or more of these benefits from the thermodynamics of irreversible processes may apply. It may be remarked in passing, however, that since the matter of justifying the use of thermodynamical coördinates and relations in specific instances is a very complex one indeed, we are really no better off than formerly. Human scientific nature being what it is, we will continue to use thermodynamic variables in every situation in the pious hope that there is at least approximate justification, until stubborn facts force another approach. Therefore, we are left with but two aspects of this thermodynamics to apply in the field of metallurgy, the specification of forces and fluxes, and the elucidation of the cross-effects from the simultaneous operation of more than one force.

Diffusion.—The chief factor limiting the velocities of reaction and transformation in metallurgy is the transport of matter in the solid state. This is a very slow process, especially when compared with the transport of heat and of electricity. This disproportionateness is in sharp contrast with the similarity of the rates of mass and heat transport in gases, and of mass and electrical transport by ions in liquids. The very different orders of magnitude of these transport processes in solids makes it highly improbable that any interference effects between them will ever be of importance in metallurgy. If we exclude the thermoelectric effect, heat and electrical conduction *per se*, the Hall effect and other properties of semi-conductors from the domain of metallurgy, electronic motions need be considered only rarely. Temperature inhomogeneities certainly do arise in metallurgy, but usually only as accidental, short-lived fluctuations, the chief consequence of which is to make a temperature specification unprecise as to its time and space coördinates. However, there is never enough time in metallurgical phenomena for the slow transport of matter to respond to a temperature gradient, as there is in gaseous thermal diffusion, particularly since the high thermal conductivity of metals so markedly diminishes spatial variation of temperature. Therefore, temperature gradient as a driving force, with which other generalized forces could conceivably give rise to interesting cross-effects, is practically non-attainable in metallurgy.

However, the possibility exists that a study of the Soret effect in solid binary alloys may yield important information about the atomic interactions in metals. To my knowledge, no data exist in the literature on the magnitude of the disparity in concentration produced by a temperature gradient in solid metals, although there are data for some solid sulfides and halides.[4] At present in our laboratory we are carrying out some experiments to furnish only the order of magnitude of the effect; if it proves large enough to be interesting, more elaborate experiments will be set up. The state of the theory for correlating the Soret coefficient in solids with the atomic or molecular interactions is very discouraging, since there is no theory; the reasons for the want are self-evident when one recalls the difficulties encountered in the case of gases. Nevertheless, some semi-empirical, useful approach ought to be possible, perhaps along the lines of order–disorder theory by the nearest-neighbor approximation. A paper by Prigogine and others,[5] and one by Denbigh,[6] have made a beginning in the correlation of Soret coefficients in binary liquids with molecular interactions of the components.

Except for this situation, where a temperature gradient is artificially maintained in order to study the Soret effect as such, examples of cross-effects

---

(2) The quantitative aspect of this question has been examined by Prigogine[2a] for the Enskog–Chapman model of a gas, who found that if the distribution function of particle velocities can be well represented by the Maxwell–Boltzmann distribution plus one correction term, then the thermodynamics of irreversible processes gives the same results as kinetic theory.

(3) Ref. 1, Chap. XI.

(4) H. Reinhold, *Z. physik. Chem.*, **A141**, 137 (1929); *Z. Elektrochem.*, **35**, 627 (1929).

(5) I. Prigogine, L. de Brouckere and R. Amand, *Physica*, **16**, 577 (1950).

(6) K. G. Denbigh, *Trans. Faraday Soc.*, **48**, 1 (1952).

between driving forces can be found only in isothermal diffusion in multicomponent systems. Long accustomed to writing Fick's law of proportionality between flux and concentration gradient for a binary alloy, some metallurgists have in the past opposed the introduction of the chemical potential gradient as the driving force in diffusion. These objections are well countered by the thermodynamics of irreversible processes, and the experiments of Darken,[7] designed to prove that a component can flow spontaneously "up-hill" against a concentration gradient at uniform temperature, helped to establish the greater significance of the chemical potential gradient. In the case of three or more components, the flux of any one species must depend not only on the chemical potential gradient of that component but also on those of the other constituents. Darken has presented the Onsager phenomenology to the metallurgist[8] and has suggested critical experiments to show just how important are the terms arising from the influence of the chemical potential gradient of the i'th species on the flow of the j'th component. If such terms are negligible, a certain amount of simplification is possible for diffusion in multicomponent systems; if not, each flux must be represented as a function of all the partial molal free energy gradients, and only Onsager's reciprocal relations offer an element of simplification.

In passing it may be mentioned that it has been possible to measure the diffusion through grain boundaries in metals and that along free surfaces, as distinct from the diffusion through the volume, or the lattice, of the metal[9] (see Fig. 1). These different diffusion paths are of great interest from the point of view of casting light on the nature of surfaces and of interfaces between grains, as well as on the mechanism of the diffusion process. For radiosilver diffusing in silver, the activation energies for lattice, grain boundary and surface diffusion are in the proportions 4.6:2:1.

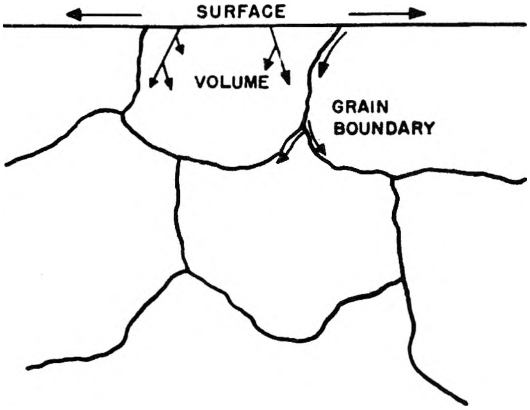

Fig. 1.—The various diffusion paths in a polycrystalline metal.

In 1947, Smigelskas and Kirkendall[10] found that inert markers, such as molybdenum wires set into a diffusion couple move during the diffusion. This phenomenon came as a surprise to metallurgists who were unfamiliar with the work of Hartley[11] who used similar techniques for the somewhat different case of diffusion of solvents into high polymers. These observations have been checked and extended, notably by da Silva and Mehl,[12] for many binary alloy systems. The crux of the matter has been shown by Darken[13] to lie in what type of motion we choose to call diffusion, whether the motion of a component relative to the center of mass of the system or the motion relative to an observer. That the center of mass should in general have a motion relative to the observer is a consequence of the difference in size and mass between atoms A and B. This results in the transfer of A by random motions across a volume-fixed section to be greater or less than that of B. Consequently, a hydrostatic pressure tends to be built up in the region of the solution which contributes least to the volume-rate of transfer. This pressure is relieved by a mass-flow of A and B together, that is, of the whole solution, and the inert Kirkendall markers share the motion of the solution as a whole.[14]

However, in the Kirkendall effect the motion of the markers is much greater than can explained simply by the change of density with composition. Atomistically, it is impossible to account for a mass flow relative to markers, when larger than that due simply to a density–composition variation, if diffusion takes place solely by simple interchange of neighboring atoms, or by the ring mechanism proposed by Zener[15] (see Fig. 2). Exchange of atoms on lattice sites with those in interstitial positions may give rise to a Kirkendall effect, but a net current of interstitial atoms is very unlikely in the common f.c.c. metals. Seitz[16] points out that it seems most probable that the large motion of the markers is due to the existence of a vacancy current, the mechanism in diffusion being largely the exchange of atoms with lattice vacancies.

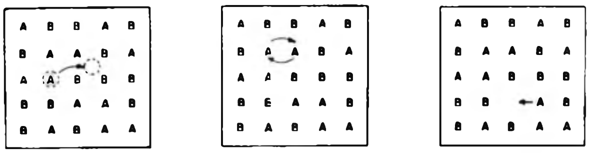

INTERSTITIAL. DIRECT INTERCHANGE. VACANCY.

Fig. 2.—Three possible mechanisms for diffusion in the solid state.

Faced with the necessity of explicitly considering the motion of vacancies, Bardeen and Herring[17] have developed phenomenological equations with the vacancies treated as one of the constituents of the alloy. With the reasonable hypotheses that

---

(7) L. S. Darken, *Trans. Am. Inst. Mining Met. Engrs.*, **180**, 430 (1949).

(8) L. S. Darken in "Atom Movements," seminar published by the American Society for Metals, 1951.

(9) D. Turnbull, *ibid.*

(10) A. D. Smigelskas and E. O. Kirkendall, *Trans. Am. Inst. Mining Met. Engrs.*, **171**, 130 (1947).

(11) G. S. Hartley, *Trans. Faraday Soc.*, **42B**, 6 (1946).

(12) L. C. C. da Silva and R. F. Mehl, *J. Metals*, 155 (1951).

(13) L. S. Darken, *Trans. Am. Inst. Mining Met. Engrs.*, **175**, 184 (1948).

(14) G. S. Hartley and J. Crank, *Trans. Faraday Soc.*, **45**, 801 (1949).

(15) C. Zener, *Acta Cryst.*, **3** 346 (1950).

(16) F. Seitz, from "Phase Transformations in Solids," John Wiley and Sons, Inc., New York, N. Y., 1951.

(17) J. Bardeen and C. Herring, in "Atom Movements" published by the American Society for Metals, 1951.

lattice sites are conserved, and that the vacancies remain in local equilibrium concentration because of the action of dislocations, which can serve as sources and sinks for vacancies, these authors show that the Kirkendall effect follows from the fact that when vacancies are considered as a third component, there are no restrictions on the flow of matter. That is, the sum of the flows of the two atomic species need not equal zero, since, in general, there is a non-vanishing current of vacancies. For the case of a radioisotope diffusing through the corresponding normal atomic species, the vacancy current must vanish; for this situation, Bardeen and Herring show that the diffusion coefficient for the radioisotope differs from the self-diffusion coefficient by a cross-term. By some considerations of the kinetics of diffusion *via* vacant sites, they estimate this disparity to be of the order of 10%. The writer[18] has pointed out that the conditions for the vanishing of the vacancy current are likely to be fulfilled in ideal solid solutions, so that the Kirkendall effect should be small in such alloys.

Diffusion with Chemical Reaction or Phase Transformation.—In metallurgy there are numerous examples where diffusion is produced by, or is accompanied by, a chemical reaction or a phase transformation. From the purely phenomenological point of view, the presence of the reaction adds nothing novel; the force driving the reaction has a tensorial character different from the force driving the diffusion, and hence by Curie's theorem[1] there can be no interference effects. The only influence of the reaction is to affect the boundary conditions for the diffusion equations. However, there are certain difficulties in setting up the phenomenology in useful form.

In the formation of oxide or sulfide films on metals there can in general be migration of cations, anions, electrons, atoms and vacancies. The fact that some of these particles are charged and that they move in an electrical field does not introduce new forces; rather, the chemical potential of the ions acquires[19,20] a term ($z_k e\phi$) in addition to the ordinary chemical potential of the uncharged atom, and the term for the electrons is simply ($e\phi$). (In these expressions, e is the electronic charge, z_k the valence of the k'th ion, and ϕ the electrical potential.) Wagner[21,22] has developed equations for the rate of film formation based on independent migration of the various species. The great utility of these relations is due to the fact that they can be expressed in terms of transport numbers or diffusivities which can be obtained from other measurements, and this convenience is made possible by the assumption of independence of migration. Many oxides and sulfides, *e.g.*, Cu_2O, FeO and Ag_2S form with only the cations and the electrons as the mobile agents, so that the simple equations are sufficient. However, when more than one ionic species is mobile, as is the case with Fe_3O_4, or when a binary alloy is being oxidized, the assumption of independence of migration may not be warranted. The writer has developed an equation taking account of two mobile ions plus electrons with cross-effects among them, which, however, although of the right form, is too complex to be useful. There appears to be room for application of Onsager thermodynamics here, and the need will be felt more as data of the requisite precision accumulate.

When an alloy is cooled to a temperature at which the previously existing solid solution is no longer stable, a precipitate often appears and grows. At any holding temperature, the precipitate that forms from the parent phase is that one which of all possible precipitates has the structure, composition, orientation and state of strain such that the product of nucleation rate and growth rate is a maximum, and this usually means that the free energy of the critical size nucleus is a minimum. The usual limitation to the rate of growth of precipitates in solid solutions is the diffusion of matter. If ΔC is the composition difference between precipitate and the parent phase, and if ΔF_v is the free energy change per unit volume of particle, then at a given particle size and temperature the growth-rate is proportional[23] to $-\Delta F_v/\Delta C$. From the phenomenological point of view we are concerned only with the formulation of the free energy change as the driving force for diffusion through the parent phase. It can be shown that for small amounts of undercooling, the precipitate is apt to be incoherent, that is, there is no matching of lattices between precipitate particles and matrix phase (see Fig. 3); thus, the precipitate is relatively unstrained but has a large interfacial free energy which may be a function of the difference in orientation between the two lattices. On the other hand, if the amount of undercooling is large, the precipitate may be coherent with the matrix, with a consequent strain energy occasioned by the elastic deformation of particle or matrix in order to produce matching of lattices. The ΔF_v should ideally take into account the strain energy and the interfacial free energy and their dependence on shape and orientation.

The formation of pearlite from a solid solution of iron and carbon is an interesting example of the decomposition of a solid solution. The parent phase precipitates out the compound Fe_3C in layers alternating with another solid solution, with a characteristic spacing between the lamellae (see Fig. 4). E. S. Machlin[24] of Columbia University is at present treating this problem by the methods of irreversible thermodynamics.

Grain Growth.—When a metal that has been cold-worked is heated, a temperature is reached at which recrystallization occurs; new grains are nucleated and grow at the expense of the old grains. At a subsequent stage, not sharply demarcated from the first, some of the new grains grow at the expense of the others; this is sometimes termed normal grain growth. Furthermore, under certain

---

[18] R. A. Oriani, General Electric Research Laboratory report.

[19] M. H. Hebb, *J. Chem. Phys.*, **20**, 185 (1952).

[20] C. Herring and M. H. Nichols, *Rev. Modern Phys.*, **21**, 185 (1949).

[21] C. Wagner, *Z. physik. Chem.*, **B21**, 25 (1933).

[22] C. Wagner, in "Atom Movements," published by the American Society for Metals, 1951.

[23] J. C. Fisher, J. H. Hollomon and J. G. Leschen, to be published in *Ind. Eng. Chem.*

[24] E. S. Machlin, private communication.

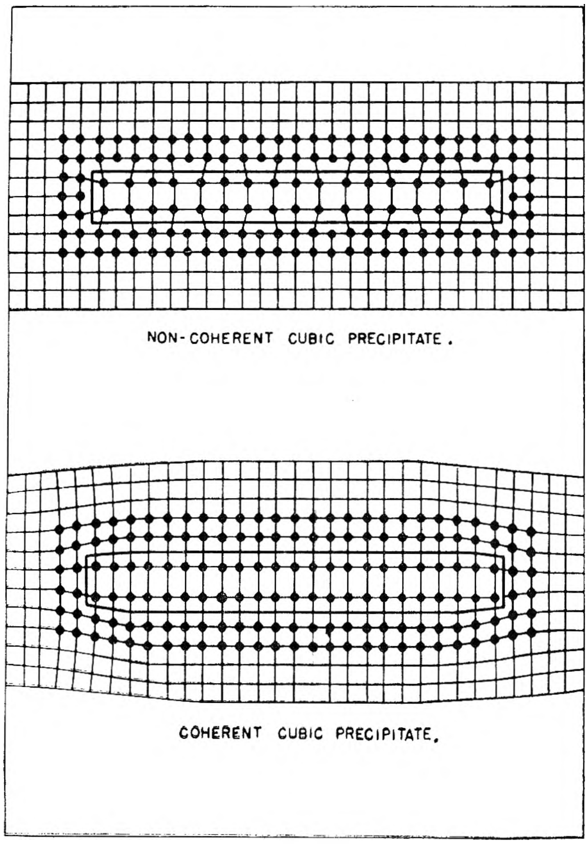

Fig. 3.—Coherency and non-coherency of a solid precipitate in a matrix. (Courtesy of J. C. Fisher, J. H. Hollomon, and J. G. Leschen.)

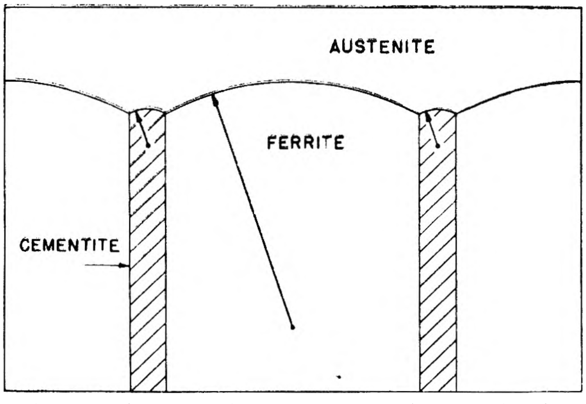

Fig. 4.—The formation of ferrite and cementite from austenite, showing the characteristic lamellae. (Courtesy of J. C. Fisher.)

conditions, on prolonged annealing of the specimen, a small number of grains begin to grow rapidly, devouring the surrounding fine-grained matrix. This coarsening process has been called secondary recrystallization, or exaggerated grain growth.[25]

There is general agreement that primary recrystallization is a mechanism for replacing strained regions of metal with strain-free grains, thereby lowering the free energy of the system. There is also general agreement that the interfacial free energy of the grain boundaries has a role in the normal and in the exaggerated types of grain growth, but there has been confusion as to the proper formulation. Ewing and Rosenhain[26] first suggested that the primary driving force in grain growth is the decrease of interfacial free energy of grain boundaries. Beck[27] proposed that grain growth might be described by taking the rate of motion of the grain boundary as proportional to the interfacial free energy per unit volume, and this leads to a mean grain diameter varying with the square root of the time. Burke[28] showed that the same equation, which is sometimes supported by experience, may be obtained by considering the rate of migration of individual boundaries to be proportional to their curvatures. The phenomenology of irreversible thermodynamics supplies a uniform point of view for all types of grain growth: that the flux of the atoms, which become detached from one grain and attached to the adjacent one, is proportional to the difference between the chemical potentials of the atoms immediately on either side of the grain boundary. This point of view has been clearly stated by Turnbull.[29] In the case of primary recrystallization, the difference in chemical potential occurs by virtue of the different states of strain of the two grains. In normal and exaggerated grain growth, the difference in chemical potential is relatable through the Kelvin equation to the quotient of grain boundary interfacial free energy by the radius of curvature of the boundary. It is easy to show that the same parabolic relation between grain diameter and time for normal growth is obtained from this formulation. The fact that during normal grain growth the extent of grain boundary area decreases should be regarded primarily as a consequence, not a cause, of the grain growth. The constant of proportionality between the flux of atoms and the difference in chemical potential is the mobility of the atoms during their passage from one grain to another. Therefore, it should be relatable to the diffusivity of atoms in grain boundaries for all types of grain growth, and this appears to be true.[28,30]

As a grain boundary sweeps through a region of specimen, it accumulates impurity atoms in the grain boundary phase. This accumulation conceivably can affect the motion of the grain boundary by virtue of the functional dependence of interfacial energy on composition, which affects the driving force, and by virtue of the effect of composition on the atomic mobility through the grain boundary.

Conclusion

Thus we see that the theory of irreversible thermodynamics has some bearing on the problems of metallurgy, but its contributions can only be fairly modest when compared with those in other fields. This relative poverty of application is due essentially to the singleness of the type of driving force usually encountered in metallurgy. The biggest experimental contribution that at present

---

[25] J. E. Burke, in "Atom Movements," published by the American Society for Metals, 1951.

[26] J. A. Ewing and W. Rosenhain, *Proc. Roy. Soc. (London)*, **67**, 112 (1900).

[27] P. A. Beck, J. C. Kremer, L. J. Demer and M. L. Holzworth, *Trans. Am. Inst. Mining Met. Engs.*, **175**, 372 (1948).

[28] J. E. Burke, *ibid.*, **180**, 73 (1949).

[29] D. Turnbull, *ibid.*, **191**, 661 (1951).

[30] F. D. Rosi, B. H. Alexander and C. A. Dube, *J. Metals*, 189 (1952).

can be made in this field is to determine the relative importance of the cross-effect diffusivities in multicomponent diffusion. If these are found to be negligible, important simplifications can be effected.

Nothing has been said in connection with plastic deformation of metals. The reason for this omission is that the objections raised by Bridgman[31] to the application of classical thermostatics to objects in states which are completely surrounded by irreversibility are just as valid when directed against the present thermodynamic theory, because this theory also demands equilibrium states as reference states. I do not believe that anything useful can be said at present about the thermodynamics of plastically strained bodies, except to point out that there are grounds for expecting progress on this score, independently of Onsager thermodynamics, from the development of the concepts and techniques of the dislocation theory,[32] and from such experiments as those by Taylor and Quinney,[33] Suzuki[34] and Kanzaki[35] on the energy stored in a metal by deformation.

(31) P. W. Bridgman, *Revs. Modern Phys.*, **22**, 56 (1950).

(32) A. H. Cottrell, "Progress in Metal Physics," Vol. I, Butterworth's Scientific Publications, London, 1949.

(33) G. D. Taylor and H. Quinney, *Proc. Roy. Soc.* (*London*), **A143**, 307 (1934).

(34) T. Suzuki, *Sci. Rpts. Research Inst. Tohoku Univ.*, **1**, 193 (1949).

(35) H. Kanzaki, *J. Phys. Soc. Japan*, **6**, 90 (1951); **6**, 456 (1951).

THE STATISTICAL METHOD OF GIBBS IN IRREVERSIBLE THERMODYNAMICS

By R. T. Cox

Department of Physics, The Johns Hopkins University, Baltimore, Maryland

Received July 2, 1952

The method of Gibbs, in which the ensemble is one of systems rather than molecules, gives results which, like those of thermodynamics, are independent of molecular structure. If $f_1, f_2, \ldots$ are probabilities of quantized states of the system, the approach to equilibrium is described by equations $\mathrm{d}f_i/\mathrm{d}t = \Sigma_j(f_j\lambda_{ji} - f_i\lambda_{ij})$, in which $\lambda_{ji} = \lambda_{ij}$, if the system is isolated with a given energy. When the approach is through stages of quasi-equilibrium, in which the entropy is maximum except that several variables $n', n'', \ldots$ have average values different from those at equilibrium, it is found approximately that

$$\mathrm{d} <n^\alpha>/\mathrm{d}t = \Sigma_\beta g^{\alpha\beta}\partial S/\partial<n^\beta>$$

where

$$g^{\alpha\beta} = g^{\beta\alpha} = [2k \exp (S_0/k)]^{-1} \Sigma_i\Sigma_j(n^\alpha{}_i - n^\alpha{}_j)(n^\beta{}_i - n^\beta{}_j)\lambda_{ij}$$

S is the entropy and S_0 its value at equilibrium. $g^{\alpha\beta} = g^{\beta\alpha}$ is Onsager's principle of reciprocity. The transitions of the system give rise to random forces on neighboring bodies, results of which are viscosity and Brownian motion. A generalized Rayleigh dissipation function R is obtained by which $S = -\partial A/\partial T - \partial R/\partial \dot{T}$ and $<Q> = -\partial A/\partial q - \partial R/\partial \dot{q}$, where A is the work function, q a coördinate of one of the bodies, Q the corresponding force, $\dot{q}$ the rate of change of q, and $\dot{T}$ the rate of change of the temperature T. The motion of the bodies in phase-space is described by a modification of Gibbs' equation for the density-in-phase, from which equations of Brownian motion may be obtained.

Irreversible phenomena may be studied for the insight they can give into molecular structure and molecular processes. Those for whom this is the main interest will be drawn toward the statistical method of Maxwell and Boltzmann, in which a thermodynamic system is treated as a statistical ensemble of molecules, and the macroscopically observable quantities of thermodynamics are described as aggregates or averages of the molecular variables. The same phenomena may also be studied with a different purpose. This purpose, which is the traditional one of thermodynamics, is to derive from the least possible hypothesis relations between observable quantities, especially those relations which hold for all systems, whatever their molecular structure. An extreme adherent to this purpose might regard the molecular variables of the Boltzmann method as so many superfluous parameters, introduced in the equations only to be discarded later, and their presence would seem to him to mar the logical economy of the theory. Such a person—and others less extreme in their view—will incline toward the statistical method of Gibbs, in which the entire thermodynamic system is taken as the statistical unit and the statistical ensemble comprises a great number of like systems. This method yields general principles independent of structure, like the laws of thermodynamics.

The two methods may be contrasted in another way, with one another and with the quasi-thermodynamic method, by distinguishing the two kinds of microscopic detail in which we may be interested. A thermodynamic system has microscopic detail in structure and its processes have microscopic detail in time. The method of molecular kinetic theory takes account of both kinds of detail, the quasi-thermodynamic method ignores both, while the method of Gibbs ignores the molecular details of structure but takes account of the microscopic details of change. It is possible to base a general theory of irreversible processes on the intermittency of change, that is, the microscopic detail of processes in time. This is because macroscopic change in thermodynamic systems results from an unbalance, usually small, among a great many contrary microscopic changes. Random inequalities in the opposing processes give rise to fluctuations and persistent ones to irreversible phenomena.

The assumptions sufficient for such a theory and a few of their consequences are the subject of this paper. It should be said at the beginning that many of the consequences are familiar, being known by other methods. The simplicity of the assumptions from which they are derived here may, I hope, be of some interest, and the close connection of the theory with classical thermodynamics may appeal to any who, like myself, regard thermodynamics as the queen of the natural sciences.

Let us consider a thermodynamic system, the structure of which determines a series of quantized states. Let f_i denote the probability that the system is in the quantized state i and let $\lambda_{ij}\mathrm{d}t$ denote the probability of the transition in the time $\mathrm{d}t$ to another quantized state j, when it is given that the system is initially in the state i. Then the rate of change of f_i is given by

$$\dot{f}_i = \Sigma_j(f_j\lambda_{ji} - f_i\lambda_{ij}) \tag{1}$$

If the system is isolated, λ_{ij} is zero for any states of unequal energy. If also the system is free from forces, like those of magnetism, which are odd functions of momentum, then the principle of microscopic reversibility is applicable in the form

$$\lambda_{ji} = \lambda_{ij} \tag{2}$$

and thus

$$\dot{f}_i = \Sigma_j(f_j - f_i)\lambda_{ij} \tag{3}$$

Let n denote some variable of the system having the value n_i when the system is in the state i. Then the average value of n is given by

$$<n> = \Sigma_i n_i f_i$$

and

$$\mathrm{d}<n>/\mathrm{d}t = \Sigma_i n_i \dot{f}_i = \Sigma_i\Sigma_j n_i(f_j - f_i)\lambda_{ij}$$

Alternatively, by an exchange of the labels i and j,

$$\mathrm{d}<n>/\mathrm{d}t = \Sigma_i\Sigma_j n_j(f_i - f_j)\lambda_{ji}$$

Adding these two expressions for $\mathrm{d}<n>/\mathrm{d}t$ and making use of the fact that $\lambda_{ji} = \lambda_{ij}$, we have

$$\mathrm{d}<n>/\mathrm{d}t = -{}^1/_2\Sigma_i\Sigma_j(n_i - n_j)(f_i - f_j)\lambda_{ij} \tag{4}$$

There are many systems which are subject to such constraints that transitions are frequent among states for which some variable n has the same value, whereas transitions in which n changes are much less frequent. Such a system quickly attains a partial equilibrium, characterized by a slowly changing average value of n, and this equilibrium remains practically undisturbed as $<n>$ changes gradually during the much slower approach to the ultimate equilibrium. Thus, for example, a gas may be in practically complete equilibrium in each of two chambers, while its passage through a fine opening between them slowly diminishes a difference in pressure. Or a solid may dissolve in a liquid so slowly that the solution remains practically homogeneous in concentration and temperature. Or a slow chemical reaction may go on in a gas without producing appreciable gradients of temperature or pressure.

By eq. (3), the probabilities of the states will not be constant until they are all equal and each of them has the value $1/W$, where W is the number of states with energies equal to the given energy of the system. During this change the entropy, given by

$$S = -k\Sigma_i f_i \ln f_i \tag{5}$$

continually increases, approaching its ultimate equilibrium value $k \ln W$. We suppose now that the entropy more quickly attains the greatest value consistent with the slowly changing value of $<n>$. This is not a consequence of any of the preceding general equations but an assumption intended to describe a system of the special kind we are considering. The assumption requires that $\ln f_i$ be a linear function of n_i, so that

$$f_i = e^{M + Nn_i} \tag{6}$$

Thus all states having equal values of n are equally probable, in agreement with the supposition that transitions among such states are much more frequent than transitions in which n changes.

By eqs. (5) and (6)

$$\partial S/\partial<n> = -k\Sigma_i(\partial f_i/\partial<n>)(M + Nn_i) = -kM\Sigma_i\partial f_i/\partial<n> - kN\Sigma_i n_i\partial f_i/\partial<n>$$

Now $\Sigma_i f_i = 1$ and $\Sigma_i n_i f_i = <n>$. Hence $\Sigma_i\partial f_i/\partial<n> = 0$, and $\Sigma_i n_i\partial f_i/\partial<n> = 1$. Thus

$$N = -\frac{1}{k}\frac{\partial S}{\partial<n>} \tag{7}$$

Also by eq. (6)

$$\partial f_i/\partial N = (\partial M/\partial N + n_i)f_i$$

whence, summing with respect to i, we find

$$\partial M/\partial<n> = -\Sigma_i n_i f_i = -<n>$$

and therefore

$$\partial f_i/\partial N = (n_i - <n>)f_i \tag{8}$$

At equilibrium, $f_i = 1/W$ and therefore

$$(\partial f_i/\partial N)_0 = (n_i - <n>_0)/W \tag{9}$$

If the system is near enough to equilibrium that the first-order term is sufficient when $\mathrm{d}<n>/\mathrm{d}t$ is expressed as a power series in N, then approximately, by eq. (4) and (9)

$$\mathrm{d}<n>/\mathrm{d}t = -{}^1/_2N\Sigma_i\Sigma_j(n_i - n_j)^2(\lambda_{ij}/W)$$

or, by eq. (7)

$$\mathrm{d}<n>/\mathrm{d}t = g\partial S/\partial<n> \tag{10}$$

where g is a positive quantity given by

$$2kg = \Sigma_i\Sigma_j(n_i - n_j)^2(\lambda_{ij}/W) \tag{11}$$

Since λ_{ij}/W is the number of transitions per unit time from state i to state j at equilibrium, $2kg$ is the mean square rate of change of n at equilibrium. A frequently interesting case is that in which n is the number of molecules of a certain kind in the system or in one of its phases and does not change in a transition between states unless by ±1. In this case $(n_i - n_j)^2$ has only the two values 0 and 1, and $2kg$ is simply the average number of times n changes in one unit of time.

A generalization of the preceding result leads to Onsager's principle. If the approach to equilibrium is controlled by the disequilibrium not of one but of several variables, n', n'', . . ., then a calculation similar to that just made leads to the result

$$\mathrm{d}<n^\alpha>/\mathrm{d}t = \Sigma_\beta g^{\alpha\beta}\partial S/\partial<n^\beta> \tag{12}$$

where

$$g^{\alpha\beta} = g^{\beta\alpha} = \Sigma_i\Sigma_j(n^\alpha{}_i - n^\alpha{}_j)(n^\beta{}_i - n^\beta{}_j)\lambda_{ij}/(2kW) \tag{13}$$

The equality of $g^{\alpha\beta}$ and $g^{\beta\alpha}$ expresses Onsager's principle for a system free from magnetic and Coriolis forces.[1]

---

(1) John S. Thomsen (doctoral dissertation, Johns Hopkins, not yet published) has given a derivation, by the method employed here, of Onsager's principle for a system in a magnetic or Coriolis field.

Thus far it has been supposed that the system is isolated. This is an unnecessary restriction and often an inconvenient one. Usually we shall wish to consider a system in thermal contact with an environment at some uniform temperature T. A system in equilibrium with such an environment has the greatest entropy consistent with the average value of its energy, and the probabilities of its states are in the canonical distribution given by

$$f_i = e^{(A-E_i)/kT} \qquad (14)$$

where E_i is the energy of the system in the state i and A is the Helmholtz free energy or work function.

When the system is not in equilibrium the probabilities change according to eq. (1). In this case, λ_{ji} is not in general equal to λ_{ij}, because transitions can occur with an exchange of energy between the system and its environment. However, we may regard the environment as a large heat-bath at temperature T and apply the principles of conservation of energy and microscopic reversibility to the system and environment together, regarded as a single compound system. In this way it may be shown[2] that

$$\lambda_{ji}e^{-E_j/kT} = \lambda_{ij}e^{-E_i/kT} \qquad (15)$$

By this relation and eq. (1) we may express the rate of change of f_i in the form

$$\dot{f}_i = \Sigma_j(f_j e^{E_j/kT} - f_i e^{E_i/kT})\mu_{ij} \qquad (16)$$

where

$$\mu_{ij} = \mu_{ji} = \lambda_{ji}e^{-E_j/kT} \qquad (17)$$

The equality of μ_{ij} and μ_{ji} plays in this case a part similar to that which the equality of λ_{ij} and λ_{ji} plays in the case of the isolated system and leads to similar results. For example, in place of eq. (12) we now find[3]

$$\mathrm{d}\langle n^\alpha\rangle/\mathrm{d}t = -\Sigma_\beta G^{\alpha\beta}\partial A/\partial\langle n^\beta\rangle \qquad (18)$$

where

$$G^{\alpha\beta} = G^{\beta\alpha} = \Sigma_i\Sigma_j(n^\alpha{}_i - n^\alpha{}_j)(n^\beta{}_i - n^\beta{}_j)\mu_{ij}e^{A_0/kT}/(2kT) \qquad (19)$$

Here $2kTG^{\alpha\alpha}$ is the mean square rate of change of n^α.

Another use of eq. (16) is in the description of viscous forces. When the system is in the state i, the force it exerts on a macroscopic body in a position described by the coördinate q is $-\partial E_i/\partial q$, and the average force is given by

$$\langle Q\rangle = -\Sigma_i f_i\partial E_i/\partial q$$

When the probabilities of the states are in the canonical distribution, it is well known that

$$\langle Q\rangle = -\partial A/\partial q$$

in agreement with the familiar thermodynamic relation. A small regular motion of the body will produce a small disturbance of the equilibrium. For a first approximation to the rate of change of f_i, eq. (14) may be differentiated to give

$$\dot{f}_i = \frac{\dot{q}}{kT}\frac{\partial(A - E_i)}{\partial q}e^{(A - E_i)/kT}$$

whence, by eq. (16)

$$\frac{\dot{q}}{kT}\frac{\partial(A - E_i)}{\partial q}e^{(A - E_i)/kT} = \Sigma_j(f_j e^{E_j/kT} - f_i e^{E_i/kT})\mu_{ij}$$

This equation is satisfied for arbitrary values of $\dot{q}$ if we let

$$f_i = e^{(A - E_i)/kT}(1 + \kappa_i\dot{q}) \qquad (20)$$

where the quantities κ_i are determined by the equations

$$\partial(A - E_i)/\partial q = kTe^{E_i/kT}\Sigma_j(\kappa_j - \kappa_i)\mu_{ij} \qquad (21)$$

and

$$\Sigma_i e^{(A - E_i)/kT}\kappa_i = 0 \qquad (22)$$

Multiplying together the corresponding members of eq. (20) and (21), summing with respect to i, and making changes of labels allowed by the fact that $\mu_{ji} = \mu_{ij}$, we find

$$\partial A/\partial q - \Sigma_i f_i\partial E_i/\partial q = -\sigma\dot{q}$$

where

$$\sigma = {}^1/_2 kTe^{A/kT}\Sigma_i\Sigma_j(\kappa_i - \kappa_j)^2\mu_{ij} \qquad (23)$$

Thus

$$\langle Q\rangle = -\partial A/\partial q - \sigma\dot{q} \qquad (24)$$

The first term on the right is the elastic force and the second is the viscous force.

Extending this result to several coördinates, we find

$$\langle Q^\alpha\rangle = -\partial A/\partial q^\alpha - \Sigma_\beta\sigma^{\alpha\beta}\dot{q}^\beta \qquad (25)$$

where

$$\sigma^{\alpha\beta} = \sigma^{\beta\alpha} = {}^1/_2 kTe^{A/kT}\Sigma_i\Sigma_j(\kappa^\alpha{}_i - \kappa^\alpha{}_j)(\kappa^\beta{}_i - \kappa^\beta{}_j)\mu_{ij} \qquad (26)$$

The equality of $\sigma^{\alpha\beta}$ and $\sigma^{\beta\alpha}$ gives the reciprocal relations of Rayleigh[4]

$$\partial\langle Q^\alpha\rangle/\partial\dot{q}^\beta = \partial\langle Q^\beta\rangle/\partial\dot{q}^\alpha \qquad (27)$$

and makes it possible to derive the viscous forces from the Rayleigh dissipation function, defined by

$$R = {}^1/_2\Sigma_\alpha\Sigma_\beta\sigma^{\alpha\beta}\dot{q}^\alpha\dot{q}^\beta \qquad (28)$$

This calculation can be extended to the case in which not only the macroscopic coördinates, q', q'', . . . but also the temperature of the environment is changing. We then find a generalized Rayleigh dissipation function such that

$$\langle Q^\alpha\rangle = -\partial A/\partial q^\alpha - \partial R/\partial\dot{q}^\alpha \qquad (29)$$

$$S = -\partial A/\partial T - \partial R/\partial\dot{T} \qquad (30)$$

This adds the reciprocal relation

$$\partial S/\partial\dot{q}^\alpha = \partial\langle Q^\alpha\rangle/\partial\dot{T} \qquad (31)$$

to the reciprocities of Rayleigh, in analogy with the Maxwell relation for equilibrium, $\partial S/\partial q^\alpha = \partial\langle Q^\alpha\rangle/\partial T$. This generalized Rayleigh function may be used to state the Carnot theorem in the form of an equation

$$\oint(J/T)\mathrm{d}t = -2\oint(R/T)\mathrm{d}t \qquad (32)$$

where J is the rate of flow of heat into the system.

An extension of these calculations due to Walter[5] includes the case in which the chemical potentials of the environment are changing and thus causing an exchange of matter between the system and the environment.

In the preceding discussion of viscous forces, the macroscopic coördinates have been taken as inde-

---

(2) The derivation is given in *Rev. Modern Phys.*, **22**, 238 (1950).

(3) This result also was given by Thomsen.

(4) Rayleigh, "The Theory of Sound," Vol. I, 2nd. Ed., The Macmillan Co., Ltd., London, 1894, p. 102.

(5) Lloyd S. Walter, doctoral dissertation, Johns Hopkins, not yet published.

pendent variables. They generally are so in the physical sense that they can be varied arbitrarily at will. In the case of very small bodies, however, the Brownian motion becomes important and these coördinates must be regarded as statistical variables.

Let q, p and H denote the coördinate, momentum and Hamiltonian function of a body with one degree of freedom. Let $F\,\mathrm{d}q\,\mathrm{d}p$ denote the probability that the coördinate is in the element $\mathrm{d}q$ and the momentum in the element $\mathrm{d}p$. In classical statistical mechanics F would be subject to the equation of Gibbs

$$\frac{\partial F}{\partial t} + \frac{\partial F}{\partial q}\frac{\partial H}{\partial p} - \frac{\partial F}{\partial p}\frac{\partial H}{\partial q} = 0$$

However, in addition to the force derived from the Hamiltonian, there also acts on the body a force exerted by the thermodynamic system, and this force changes intermittently with the transitions of the system from one state to another. To take account of this force, let $F_\mathrm{i}\,\mathrm{d}q\,\mathrm{d}p$ denote the probability that the coördinate is in the element $\mathrm{d}q$, the momentum is in the element $\mathrm{d}p$, and the system is in the state i. Then

$$F = \Sigma_\mathrm{i} F_\mathrm{i} \tag{33}$$

and the equation of Gibbs is replaced by

$$\frac{\partial F_\mathrm{i}}{\partial t} + \frac{\partial F_\mathrm{i}}{\partial q}\frac{\partial H}{\partial p} - \frac{\partial F_\mathrm{i}}{\partial p}\frac{\partial (H + E_\mathrm{i})}{\partial q} = \Sigma_\mathrm{j}(F_\mathrm{j}e^{E_\mathrm{j}/kT} - F_\mathrm{i}e^{E_\mathrm{i}/kT})\mu_\mathrm{ij} \tag{34}$$

The right-hand member of this equation is the contribution which the transitions of the system make to the rate of change of F_i.

The solution at equilibrium is

$$F_\mathrm{i} = Ce^{-(H + E_\mathrm{i})/kT} \tag{35}$$

whence we can derive the familiar expressions for the average kinetic energy and the virial.

Except at equilibrium, there is no exact general solution, because E_i and μ_ij are functions of q which are different for systems of different structure. Near equilibrium, however, it can be shown[6] that approximately

$$F_\mathrm{i} = Fe^{(A - E_\mathrm{i})/kT}(1 + \kappa_\mathrm{i}\langle p\rangle_\mathrm{q}/m) \tag{36}$$

where κ_i has the same meaning as before, the Hamiltonian has been assumed to have the form $V(q) + {}^1/_2p^2/m$, and $\langle p\rangle_\mathrm{q}$ denotes the average momentum at a given value of q. In this solution, F satisfies the equations

$$\frac{\partial F}{\partial t} + \frac{\partial F}{\partial q}\frac{p}{m} - \frac{\partial F}{\partial p}\left[\frac{\partial (A + V)}{\partial q} + \frac{\sigma\langle p\rangle_\mathrm{q}}{m}\right] = 0 \tag{37}$$

and

$$\frac{\partial F}{\partial p} + \frac{(p - \langle p\rangle_\mathrm{q})F}{mkT} = 0 \tag{38}$$

where σ is given by eq. (23).

From these equations it is possible to derive certain results concerning averages in Brownian motion. For example, for a particle in a field-free space or in a uniform force field, we find

$$\langle (p - \langle p\rangle)^2\rangle/m = kT + Ae^{-2\beta t} \tag{39}$$

$$\beta\langle (p - \langle p\rangle)(q - \langle q\rangle)\rangle = kT - Ae^{-2\beta t} + Be^{-\beta t} \tag{40}$$

$$\beta^2 m\langle (q - \langle q\rangle)^2\rangle = 2kT\beta t + Ae^{-2\beta t} - 2Be^{-\beta t} + C \tag{41}$$

where $\beta = \sigma/m$ and A, B and C are constants determined by the initial conditions.

By eq. (41), when the transient terms have become negligible

$$\mathrm{d}\langle (q - \langle q\rangle)^2\rangle/\mathrm{d}t = 2kT/\sigma$$

the result predicted by Einstein and verified by the experiments of J. Perrin. Equations similar to those given above have been obtained by Ornstein,[7] Fürth[8] and, from a general equation of Kramers,[9] by Wang and Uhlenbeck.[10]

[6] The calculations are given in a paper now awaiting publication in *Rev. Modern Phys.*

[7] L. S. Ornstein, *Proc. Acad. Sci. Amsterdam*, **21**, 96 (1919).

[8] R. Fürth *Z. Physik*, **2**, 244 (1920).

[9] H. A. Kramers, *Physica*, **7**, 284 (1940).

[10] M. C. Wang and G. E. Uhlenbeck, *Rev. Modern Phys.*, **17**, 323 (1945).

A RELATION AMONG THE KINETIC THEORY CROSS-SECTION INTEGRALS AND NEW RELATIONS INVOLVING THE TRANSPORT PROPERTIES OF GASES[1]

By EUGENE M. HOLLERAN AND HUGH M. HULBURT

Department of Chemistry, St. John's University, Brooklyn, N. Y.

Received July 2, 1952

A recurrence relation among the kinetic theory cross-section integrals is derived for spherically symmetrical intermolecular potentials. Its use as a check on previous calculations of the integrals is illustrated. It is also used to derive new relations between the integrals and the transport properties of gases. These equations are shown to be very exacting tests for the correspondence between a postulated molecular model and experimental measurements. Predictions of the Lennard-Jones 13,7 potential are compared with experimental data for argon by means of one of these equations. Finally, the recurrence formula is used to derive new relations among the transport properties themselves. The sign of the thermal diffusion ratio, R_T, is shown to depend simply on the magnitude of the slope of ln D *vs.* ln T. The thermal diffusion ratio for isotopic mixtures is found as a function of the coefficients of viscosity and diffusion of either pure isotope. Values of R_T for argon calculated from this equation agree well with experimental data. A simple relation between diffusion and thermal diffusion for Lorentzian mixtures is shown to be a good approximation for other mixtures near the inversion temperatures.

The exact kinetic theory of Enskog and Chapman relates the transport properties of dilute gases to certain collision cross-section integrals, $H^{(l,m)}$, which are functions of the temperature, T, and the parameters, p_i, in terms of which the intermolecular potential is expressed. For the present purpose these integrals are most conveniently defined as

$$H^{(l,m)}(T, p_i) = {}^1/_2(kT)^{-\frac{m+1}{2}} \int_0^\infty e^{-x/kT} x^{\frac{m-1}{2}} \textcircled{H}^{(l)} \mathrm{d}x \quad (1)$$

where k is Boltzmann's constant and

$$x = \mu g^2/2 \quad (2)$$

in which μ is the reduced mass of the two molecules involved in the collision, and g is the magnitude of their relative velocity before interaction. For spherically symmetrical intermolecular potentials the quantities $\textcircled{H}^{(l)}$ are functions of x and p_i only. This can be seen from equations (3), (4) and (5).

$$\textcircled{H}^{(l)}(x, p_i) = \int_0^\infty [1 - P_l(\cos\theta)]\, b\, \mathrm{d}b \quad (3)$$

where b is the distance of closest approach the molecules would experience if they did not interact, and θ is the angle through which one molecule is deflected considering the other stationary. For spherically symmetrical potentials

$$\theta(x, p_i, b) = \pi - 2\int_0^t \frac{x^{1/2}\,\mathrm{d}y}{[(1 - y^2)x - \Phi(b/y, p_i)]^{1/2}} \quad (4)$$

where $y \equiv b/r$; r is the separation of centers; $\Phi(r, p_i)$ is the intermolecular potential; $t(x, b, p_i)$ is the maximum value of y and may be found as the least positive root of the equation

$$(t^2 - 1)x + \Phi(b/t, p_i) = 0 \quad (5)$$

For certain very simple potential models, such as elastic spheres, the dependence of θ and $\textcircled{H}$ on x disappears, and the $H^{(l,m)}$ are then not functions of T.

Since T and x are independent variables, and assuming that the parameters, p_i, are independent of T, we can easily verify from eq. (1) that for any T

$$H^{(l,m+2)} = \frac{m+1}{2}H^{(l,m)} + \frac{\mathrm{d}H^{(l,m)}}{\mathrm{d}\ln T} \quad (6)$$

Equation (6) is a general recurrence relation which must be obeyed at all temperatures by the cross-section integrals determined by any temperature-independent, spherically symmetrical intermolecular potential.

These relations may be used in two ways: (a) to check calculations of the integrals, and (b) to derive new relations involving the transport properties. Some examples of the former will be considered first.

Check of Previous Calculations.—The $\Omega^{(l)}(r)$ of Chapman and Cowling[2] are related to the $H^{(l,m)}$ defined above as follows for $l = 1$ and 2.

$$H^{(l,m)} = \frac{3}{4-l}\left[\frac{\mu}{2\pi kT}\right]^{1/2} \Omega^{(l)}\left(\frac{m-3}{2}\right) \quad (7)$$

Their integrals should therefore obey the relations

$$\Omega^{(l)}(r + 1) = [r + 3/2]\,\Omega^{(l)}(r) + \frac{\mathrm{d}\,\Omega^{(l)}(r)}{\mathrm{d}\ln T} \quad (8)$$

That they do is illustrated by the results given by them for the inverse power model which can be expressed as

$$\Omega^{(l)}(r) = AT^b(r + {}^1/_2 + b)! \quad (9)$$

where A and b are independent of r and T. The correct value from this of $AT^b(r + {}^3/_2 + b)!$ for $\Omega^{(l)}(r + 1)$ follows simply from eq. (8) also.

The $W^{(l)}(n)$ of Hirschfelder, Bird and Spotz[3] are related to the $H^{(l,m)}$ as follows, for $l = 1$ or 2.

$$H^{(l,m)} = \frac{3\,r_0^2}{4-l}\,W^{(l)}\left(\frac{m-3}{2}\right) \quad (10)$$

where r_0 is a constant length. These authors give $W^{(l)}(n)$ for the Lennard-Jones 13,7 model as functions of $x \equiv \epsilon/kT$, where ϵ is the potential minimum, in the form $W^{(l)}(n) = x^{n+2}Q^{(l)}(n)$ where $Q^{(l)}(n)$ is the sum of various powers and exponentials of x. Combining this with eq. (6) and (10) we find that

$$Q^{(l)}(n + 1) = -\frac{\mathrm{d}Q^{(l)}(n)}{\mathrm{d}x} \quad (11)$$

The discrepancies between eq. (11) and the exponential terms in the expressions given are no more

---

[1] This paper was not presented at the Symposium but is considered by the presiding officer and the authors to be of such a nature that it should appear with the symposium papers.

[2] S. Chapman and T. G. Cowling, "The Mathematical Theory of Non-Uniform Gases," The Cambridge University Press, New York, N. Y., 1939.

[3] J. O. Hirschfelder, R. B. Bird and E. L. Spotz, *J. Chem. Phys.*, **16**, 968 (1948).

serious than the use which was made of $C_p^{-q}e^{-\frac{qx}{p}}$ to approximate $C/(x + p)^q$, since if the reverse substitution is made the resulting expressions obey eq. (11) exactly, except for a typographical error where the coefficient of $e^{-0.5867x}$ in the expression for $W^{(1)}(1)$ should be -0.02159 instead of -0.2159. The tabulated values were calculated with the correct coefficient.

It is perhaps unnecessary to emphasize that agreement of any results with eq. (6) does not imply that they are the correct values of $H^{(l,m)}$ for a given molecular model, but is a check only on the final integration involved in the calculations, namely, that in eq. (1).

In the foregoing examples eq. (1) was integrated analytically and the probability of error was small. Equation (6) is more valuable as an independent check when the integration is performed by quadrature. Any significant errors may then be discovered by finding $\frac{\mathrm{d}H^{(l,m)}}{\mathrm{d}\ln T}$ from a plot of the results. In this way the $H^{(l,m)}$ of Holleran and Hulburt for the square-well model[4] can be shown to follow eq. (6) very closely.

The $\Omega^{(l,k)}$ given by Jones[5] for the Lennard-Jones 9,5 model are related to the $H^{(l,m)}$ as

$$H^{(l,m)} = r_0^2(2q)^{1/2}\,\Omega^{(l,k)} \tag{12}$$

where $q = 2(\epsilon/kT)^{1/2}$, and should therefore obey the relation

$$2\Omega^{(l,k+2)} = (k + {}^1/_2)\Omega^{(l,k)} - \frac{\mathrm{d}\ \Omega^{(l,k)}}{\mathrm{d}\ln q} \tag{13}$$

The values of $\Omega^{(l,k)}$ tabulated by Jones were obtained as the sum of two terms, one integrated analytically using an approximate empirical equation for Ⓗ$^{(l)}$ and the other a correction term integrated numerically. It is easy to show that the expressions given for the first terms obey an equation of the form of eq. (13), but it is difficult to decide whether or not the same is true, as it should be, for the correction terms. The accuracy with which these terms can be found as the difference between the given $\Omega^{(l,k)}$'s and the analytic terms is small, and the number of values given is too few to determine the slopes with certainty.

An additional relationship which is the same for all the various definitions of the cross-section integrals may be derived from eq. (6). This relates the useful quantities B and C, defined below, which are usually tabulated with the results for a given potential model.

$$B = \frac{5H^{(1,7)} - H^{(1,9)}}{5H^{(1,5)}} \qquad C = \frac{2H^{(1,7)}}{5H^{(1,5)}} \tag{14}$$

Subscripts of 12 or 11 on these quantities signify that they refer to the interaction of two molecules whose force fields are different or identical, respectively. Such subscripts will be omitted whenever either may be used.

Application of eq. (6) to the definitions of B and C leads to the equations

$$B = \frac{1}{5}\left[3 - 2\frac{\mathrm{d}\ln H^{(1,5)}}{\mathrm{d}\ln T} - \frac{\mathrm{d}^2\ln H^{(1,5)}}{\mathrm{d}\ln T^2} - \left(\frac{\mathrm{d}\ln H^{(1,5)}}{\mathrm{d}\ln T}\right)^2\right] \tag{15}$$

and

$$C = 2/5\left[3 + \frac{\mathrm{d}\ln H^{(1,5)}}{\mathrm{d}\ln T}\right] \tag{16}$$

which when combined give

$$B = \frac{C}{2}\left[4 - 5/2\,C - \frac{\mathrm{d}\ln C}{\mathrm{d}\ln T}\right] \tag{17}$$

Since Eq. (6) has already been used to check the results for several molecular models the discussion of Eq. (17) will be limited to a few illustrations of its use as a spot check at temperatures for which $\frac{\mathrm{d}\ln C}{\mathrm{d}\ln T} = 0$. For elastic spheres C is constant at 1.2, and eq. (17) gives the correct value of 0.6 for B. For the Lennard-Jones 9,5 model C approaches unity at low temperatures, and B approaches 0.75 as eq. (17) requires. For the Lennard-Jones 13,7 model C becomes constant at 1.138 for $\frac{kT}{\epsilon} > 30$, and B is constant at the required 0.657, the given values wavering between the extremes of 0.6567 and 0.6575. Checks at maxima and minima in ln C *vs.* ln T for these models show similar agreements.

Relations Involving the Transport Coefficients.—The first approximation from the general theory to the coefficient of diffusion, D, may be written in the form

$$D = \frac{KT^{3/2}}{H^{(1,5)}} \tag{18}$$

where K is known and constant at constant pressure. Appropriate subscripts may be supplied here, although for the transport coefficients they have a somewhat different interpretation, 12 signifying a binary mixture and 11 a pure gas, so that D_{11} is the coefficient of self diffusion.

If the derivative in eq. (16) is found from eq. (18) assuming constant pressure we obtain

$$\frac{9 - 5C}{2} = \frac{\mathrm{d}\ln D}{\mathrm{d}\ln T} \tag{19}$$

Similarly we find from eq. (15) and (18)

$$5B = 5\frac{\mathrm{d}\ln D}{\mathrm{d}\ln T} - \left(\frac{\mathrm{d}\ln D}{\mathrm{d}\ln T}\right)^2 + \frac{\mathrm{d}^2\ln D}{\mathrm{d}\ln T^2} - \frac{9}{4} \tag{20}$$

The second approximation to the coefficient of diffusion, D_2 is related to the first approximation, D_1, as

$$D_2 = \frac{D_1}{1 - \Delta} \tag{21}$$

The quantity Δ depends in general on the composition of the mixture and is given by a rather complicated expression. For heavy isotopes Chapman and Cowling give the simplified expression

$$\Delta = \frac{5\,(C - 1)^2}{8A - 4B + 11} \tag{22}$$

where

$$A = \frac{2H^{(2,7)}}{15H^{(1,5)}} \tag{23}$$

Table I includes Δ as a function of kT/ϵ according to eq. (22) and the Lennard-Jones 13,7 model.

---

(4) E. M. Holleran and H. M. Hulburt, *J. Chem. Phys.*, **19**, 232 (1951).

(5) R. C. Jones, *Phys. Rev.*, **59**, 1019 (1941).

TABLE I

Δ AND $p = \dfrac{\mathrm{d}\ln(1-\Delta)}{\mathrm{d}\ln T}$ FOR HEAVY ISOTOPES ACCORDING TO THE LENNARD-JONES 13,7 MODEL

kT/ϵ	$\Delta \times 10^5$	$p \times 10^4$
0.3	13	6
.5	4	− 1
.7	5	2
~ .98	0	0
1.1	1	− 6
1.3	3	−14
1.5	55	−23
2.0	157	−41
2.5	264	−50
3.0	364	−55
3.5	438	−50
4.0	500	−45
5.0	585	−36
6.0	656	−27
7.0	687	−19
8.0	720	−15
9.0	730	−11
10	753	− 9
20	785	− 3
~35	795	0
80	793	<1
400	789	<1

Considering eq. (21) we obtain, correct to the second approximation to D

$$\frac{9-5C}{2} = \frac{\mathrm{d}\ln D}{\mathrm{d}\ln T} + \frac{\mathrm{d}\ln(1-\Delta)}{\mathrm{d}\ln T} \tag{24}$$

Equation (20) may be modified in a similar manner. Values of $\mathrm{d}\ln(1-\Delta)/\mathrm{d}\ln T$ estimated graphically are also given in Table I. Since $\mathrm{d}\ln D/\mathrm{d}\ln T$ is usually near two, it is seen that for heavy isotopes the right sides of eq. (19) and (24) agree very closely, the greatest difference being about 0.3% when kT/ϵ is approximately 3. This close agreement probably holds over a considerable temperature range for non-isotopic mixtures as well, since the exact expression for Δ includes the factor $(C-1)^2$ which causes the last term in eq. (24) to vanish at the temperatures for which C is unity and $\mathrm{d}\ln D/\mathrm{d}\ln T$ is two. It seems likely therefore that eq. (19) can be used instead of eq. (24) without appreciable error in many cases.

Some relations involving thermal diffusion can now be derived. The thermal diffusion ratio, R_T, defined only for a mixture, is given by the general theory as

$$R_T = \frac{\alpha}{\alpha_h} = \frac{1}{\alpha_h}\left[\frac{5(C_{12}-1)(x_1S_1 - x_2S_2)}{x_1^2Q_1 + x_2^2Q_2 + x_1x_2Q_{12}}\right] \tag{25}$$

where α is the thermal diffusion constant and is given by the expression in brackets; α_h is α as calculated from the same expression for the hard sphere potential model and is a constant independent of T; x_1 and x_2 are the mole fractions of the heavier and lighter components, respectively, and S_1, S_2, Q_1, Q_2 and Q_{12} are expressions involving the masses of the molecules, m_1 and m_2, and the $H^{(l,m)}$ with the various subscripts 11, 12 and 22.

An approximation of eq. (25) for isotopes has been given by Jones and may be written as

$$R_T = \frac{16.9\,(C-1)(A+1)}{A(8A-4B+11)} \tag{26}$$

Subscripts are unnecessary in eq. (26) because for isotopes $H_{11}^{(l,m)}$ equals $H_{12}^{(l,m)}$.

Since experimental values of R_T are always less than one, the denominator of eq. (26) cannot change sign. For the potential models that have been investigated it is always positive. Therefore according to eq. (26) the sign of R_T is always the same as the sign of $(C-1)$. According to the more general eq. (25) the sign of R_T also depends on the composition of the mixture, but the temperature dependence of the sign is still determined by the factor $(C-1)$. Rearranging eq. (19) we find that at constant pressure

$$C_{12} - 1 = \frac{2}{5}\left(2 - \frac{\mathrm{d}\ln D_{12}}{\mathrm{d}\ln T}\right) \tag{27}$$

so that

$$\operatorname{sign} R_T = \operatorname{sign}\left(2 - \frac{\mathrm{d}\ln D_{12}}{\mathrm{d}\ln T}\right) \tag{28}$$

and in particular R_T will be zero at those temperatures at which $\dfrac{\mathrm{d}\ln D_{12}}{\mathrm{d}\ln T} = 2$. Since eq. (24) reduces to eq. (19) when $C = 1$, eq. (28) holds for the second approximation to D as well as the first. When this equation is applied to mixtures of isotopes D_{12} may be replaced by D_{11} if desired.

For some mixtures the sign of R_T may be reversed once as the composition is varied,[6,7] so that for part of the composition range the "equals" sign of eq. (28) must be replaced by a "does not equal" sign.

It is interesting to compare eq. (28) with a result derived by Waldmann[8] for the special case of a Lorentzian mixture which is one for which $x_1 >> x_2$ and $m_1 >> m_2$

$$\alpha = \left(\frac{\partial\ln D_{12}}{\partial\ln T}\right)_p - 2 \tag{29}$$

Since the $H^{(l,m)}$ are independent of temperature for hard spheres, eq. (29) and (18) give $\alpha_h = -1/2$, so that we have for constant pressure

$$R_T = 2\left(2 - \frac{\mathrm{d}\ln D_{12}}{\mathrm{d}\ln T}\right) \tag{30}$$

Comparison with eq. (27) shows that for the Lorentzian mixture

$$R_T = 5\,(C_{12} - 1) \tag{31}$$

For mixtures of isotopes we find, by substituting from eqs. (19) and (20) into eq. (26)

$$R_T = \frac{8.43\left(2 - \dfrac{\mathrm{d}\ln D}{\mathrm{d}\ln T}\right)(A+1)}{A\left[10A + 16 - 5\dfrac{\mathrm{d}\ln D}{\mathrm{d}\ln T} + \left(\dfrac{\mathrm{d}\ln D}{\mathrm{d}\ln T}\right)^2 - \dfrac{\mathrm{d}^2\ln D}{\mathrm{d}\ln T^2}\right]} \tag{32}$$

We can consider A an experimentally determined quantity since for heavy isotopes it is related to the coefficients of self diffusion and viscosity, η, as follows, according to the first approximation to these coefficients

$$A = \frac{\rho D_{11}}{3\eta_{11}} \tag{33}$$

---

(6) K. E. Grew, *Nature*, **160**, 320 (1942).

(7) S. Chapman, *Proc. Roy. Soc. (London)*, **A177**, 38 (1940).

(8) L. Waldmann, *Z. Naturforsch.*, **5a**, 322 (1950).

where ρ is the density of the gas in the diffusion experiments. Equation (32) therefore interrelates η, D and R_T for isotopes.

Discussion of Results.—The equations that have been derived are of three types.

A.—Equations (6), (15), (16) and (17) are relations among the cross-section integrals and should be obeyed by the results calculated for all spherically symmetrical, temperature independent potentials. The use of these equations to check computations of the integrals has been illustrated.

B.—Equations (19), (20), (24) and (31) are relations between the integrals and the transport properties. They should presumably be obeyed only by the correct intermolecular potential. They may therefore be used to check the correspondence between experimental observations and the predictions of a postulated potential. Considerations given below show that for this purpose they should be as exacting as the most rigorous test previously available.

C.—Equations (28) and (32) are relations among the transport properties themselves and are independent of the intermolecular potential as long as it is spherically symmetrical and temperature independent. They can be used to gain information about one property from measurements of others. Waldmann's equation, eq. (29), and its other form, eq. (30), are also relations of this type.

Until the present time by far the strictest test of a postulated potential model has been the predicted relation between the thermal diffusion ratio and the cross section integrals, as expressed in eq. (25) and its approximation for isotopes, eq. (26). For the reasons which follow a postulated model should experience this same order of difficulty in satisfying any of the equations of Type B above. This is to be expected of eq. (31) since it is itself the expression for thermal diffusion for a special mixture, and since the values of R_T it gives for the Lennard-Jones 13,7 model do not differ very greatly from those calculated for isotopes from eq. (25) and (26) by Grew[9] and Winters.[10] Equations (19) and (20) should be just as difficult to fit because $\dfrac{\mathrm{d}\ln D}{\mathrm{d}\ln T}$ is very sensitively related to R_T through the factor $\left(2 - \dfrac{\mathrm{d}\ln D}{\mathrm{d}\ln T}\right)$ as in eq. (30) and (32). It may also be observed that eq. (19) and (20) should be much harder to satisfy than eq. (18) or (21) since the correct value of $\dfrac{\mathrm{d}\ln D}{\mathrm{d}\ln T} \equiv \dfrac{T\,\mathrm{d}D}{D\,\mathrm{d}T}$ involves not only the correct D for a given temperature but the correct slope of D *vs.* T as well. Equation (24) may be even more exacting although, as in the case of argon discussed below, the second derivative may contribute only a few per cent. to the value of B.

Comparison with Experiment.—The quantity C as a function of kT/ϵ for the Lennard-Jones and square-well potentials passes through a minimum. Assuming that the C's resulting from actual intermolecular potentials behave similarly we expect that R_T, because of the factor $(C - 1)$, will also have a minimum and in general two inversion temperatures if the minimum is negative. We also expect from eq. (19) that the slope of ln D *vs.* ln T will exhibit a maximum, and that the curve will be sigmoid in general appearance. According to eq. (28) one can estimate from such a plot the temperature regions of positive and negative R_T and the inversion temperatures.

The maximum slope of the ln D *vs.* ln T curves predicted by the Lennard-Jones model is 2.33 at $kT/\epsilon = 0.49$ for the indices 9,5 and 2.033 at $kT/\epsilon = 0.64$ for the indices 13,7. For the square-well model the inflection point occurs at various values of kT/ϵ with various slopes depending on a parameter, d. Some values of d permit a maximum slope of less than two and thus a minimum R_T greater than zero. The Lennard-Jones model with higher indices may behave similarly.

Winn[11] has recently reported measurements of the temperature variation of the self diffusion coefficient for a number of gases. Except for oxygen, for which the values seem somewhat erratic and which is not spherically symmetrical anyhow, plots from these data of ln D *vs.* ln T all appear to show the high temperature portion of the expected sigmoid curves. It seems likely therefore that for many gases the lower portion of the curves, including the maximum slope and the R_T inversion temperatures, occurs at temperatures too low for observation at convenient pressures.

However, in the case of argon $\dfrac{\mathrm{d}\ln D}{\mathrm{d}\ln T}$ appears to be near the critical value of two at the lowest experimental temperatures. Because of this and for the following additional reasons argon was chosen for quantitative comparisons: argon is spherically symmetrical; more experimental D values are given for argon than for any other gas, permitting a better estimation of $\dfrac{\mathrm{d}\ln D}{\mathrm{d}\ln T}$; R_T data are available for argon isotopes.

The experimental values of ln D were fitted by the method of least squares to a polynomial in ln T, the cubic being chosen as the simplest that would permit a maximum in the slope and a minimum in R_T. The equation obtained is

$$\ln D = -12.660 + 1.5864 \ln T + 0.13371 (\ln T)^2 - 0.013089 (\ln T)^3 \quad (34)$$

The values of $n = \dfrac{\mathrm{d}\ln D}{\mathrm{d}\ln T}$ found by differentiating eq. (34) and those found from eq. (19) and (24) according to the Lennard-Jones 13,7 model are compared in Table II. The viscosity value of $\epsilon/k = 124.0°$ which was used has been shown by Winn to give a good reproduction of the D_{11} data. It is difficult to decide whether the discrepancies between the n's are due mainly to the inadequacy of the model or to the uncertainty of the slope as calculated from the data by way of eq. (34). Doubt is cast on the Lennard-Jones values by the fact that Winters has shown that this model fails to fit the argon R_T data of Stier.[12] A definite decision could of course be made with the help of more abundant diffusion data. Since the disagreement between the

---

(9) K. E. Grew, *Proc. Phys. Soc. (London)*, **62A**, 655 (1949.)

(10) E. R. S. Winters, *Trans. Faraday Soc.*, **46**, 81 (1950).

(11) E. B. Winn, *Phys. Rev.*, **80**, 1024 (1950).

(12) L. G. Stier, *ibid.*, **62**, 548 (1942).

TABLE II

COMPARISON OF OBSERVED AND CALCULATED VALUES OF $n = \frac{\mathrm{d}\ln D}{\mathrm{d}\ln T}$ AND R_T FOR ARGON ISOTOPES

T, °K.	n obsd. (34)	n 13,7 (19)	n 13,7 (24)	$\frac{\mathrm{d}^2 \ln D}{\mathrm{d}\ln T^2}$ (34)	D obsd. (34)	$\eta \times 10^4$ obsd.	R_T obsd.	R_T Calcd. (32)	$2(2 - n)$
75	2.009	2.033	2.033						−0.02
100	1.985	2.018	2.018						.03
130	1.958	1.982	1.982	0.1149	0.0378	1.070	0.07	0.08	.08
150	1.940	1.956	1.957	.1261	.0496	1.222	.13	.11	.12
200	1.901	1.893	1.896	.1488	.0867	1.594	.21	.19	.20
250	1.866	1.846	1.850	.1663	.132	1.947	.26	.25	.27
300	1.834	1.808	1.813	.1806	.185	2.270	.31	.31	.33
350	1.805	1.778	1.783	.1927	.245	2.56	.35	.36	.39

n's is greatest near the critical value of two, an experimental determination of the thermal diffusion inversion temperature would also be helpful. The Lennard-Jones 13,7 model predicts this will be about 115°K., and eq. (28) with n calculated from eq. (34), predicts it will be about 85°K.

Using eq. (20), discrepancies also also arise between the Lennard-Jones 13,7 predictions and the n and $\frac{\mathrm{d}^2 \ln D}{\mathrm{d}\ln T^2}$ found from eq. (34), but these values for $\mathrm{d}^2 \ln D/\mathrm{d}\ln T^2$ are probably too unreliable for the comparison to be significant.

Table II also compares the experimental values of R_T with those calculated from viscosity and diffusion data according to eq. (32) for the temperature range overlapped by the available D_{11} and R_T data. The experimental values of R_T were estimated from a plot of Stier's values; D, n and $\frac{\mathrm{d}^2 \ln D}{\mathrm{d}\ln T^2}$ were calculated from eq. (34) and its derivatives. The values of η are due to Johnston and Grilly[13] except for the value at 350°K. which was interpolated from the data of Trautz.[14]

The agreement between the observed and calculated R_T values is considered good. If this agreement is not simply fortuitous the values of n calculated from eq. (34) cannot be far wrong since R_T is very sensitive to slight changes in this quantity. The Lennard-Jones 13,7 values of n would then be in error, and we note that the use of these values in eq. (32) considerably worsens the agreement with the experimental R_T values.

Table II also shows that $2(2-n)$ is a good approximation in this temperature range for the thermal diffusion ratio of this non-Lorentzian mixture. Such a result should be expected for any mixture at temperatures not far from the inversion temperatures, since at these points eq. (30) holds for non-Lorentzian mixtures as well as Lorentzian. The quantity $5(C - 1)$ is then similarly useful in this range as an approximation to the predicted values of R_T for a given potential model.

Equation (32) may be written as $R_T = z(2 - n)$ where z, instead of being 2, varies in the case of argon from 1.90 to 1.86 as the temperature rises from 129 to 720°K. In this case then 4.7 is a better multiplier than 5 for $(C - 1)$.

We note finally that if the second approximation to D is used in the derivation of eq. (32) the only important change is in the factor $\left(2 - \frac{\mathrm{d}\ln D}{\mathrm{d}\ln T}\right)$ which becomes $\left(2 - \frac{\mathrm{d}\ln D}{\mathrm{d}\ln T} - \frac{\mathrm{d}\ln(1 - \Delta)}{\mathrm{d}\ln T}\right)$. Since R_T is about twice this factor we see from Table I that the correction to the calculated R_T amounts at most to an increase of one in the second decimal place.

---

[13] H. L. Johnston and E. R. Grilly, *J. Phys. Chem.*, **46**, 948 (1942).

[14] Landolt-Börnstein, "Physical Chemical Tables," fifth edition, Vol. 1, Julius Springer, Berlin, 1935.

STATISTICAL MECHANICS OF DYNAMICAL SYSTEMS WITH INTEGRALS OTHER THAN ENERGY

By HAROLD GRAD

Institute for Mathematics and Mechanics, New York University, New York 3, N. Y.

Received August 15, 1952

Statistical mechanics is generalized to include a complete set of integrals. This leads to a generalization of classical thermodynamics and generalized macroscopic conservation equations. Application is made to the integral of angular momentum and to the theory of irreversible thermodynamics.

Introduction

Conventionally, statistical mechanics and thermodynamics are based on the energy, fluid dynamics on momentum as well, while the other integrals of classical particle dynamics, notably the angular momentum, are ignored or relegated to a footnote. If the theory is generalized to include a complete set of integrals, it is found possible to give a more rational presentation to the whole of classical statistical mechanics.

The aim of statistical mechanics is the derivation of the macroscopic properties of matter entirely from the microscopic properties of molecules. It is found necessary to supplement molecular information by two fundamental postulates: (1) the number of time-independent integrals is small compared to the total number of degrees of freedom—it is usually assumed, implicitly, that there is only one integral, the energy; (2) the probability distribution in phase space is absolutely continuous—this supplants the more restrictive hypothesis of equal *a priori* probabilities to equal volumes.

The first result is the derivation of a generalization of the microcanonical distribution for an isolated system. Then follow derivations of a generalized canonical distribution for a system in "thermal" equilibrium with its surroundings, grand canonical distribution for a system free to exchange molecules with its surroundings, and a further distribution valid for a system in mechanical equilibrium with the surroundings. Corresponding to each of these physical situations is its own thermodynamical structure with a few significant differences. In particular, the entropy function is different in the canonical and grand canonical cases, thereby resolving the Gibbs Paradox purely classically, without recourse to quantum mechanics. Corresponding to the set of integrals is a set of generalized temperatures which, in "thermal" equilibrium, are equal to those of the surroundings. For the grand canonical distribution this is true of the chemical potentials and in mechanical equilibrium of certain general "forces." A generalized expression of the second law is discovered in which appears an entropy with the usual "increasing" properties. In non-equilibrium, conservation equations are derived for each integral, and generalizations of the usual results of irreversible thermodynamics are obtained by consideration of the entropy production.

In particular, interesting results are obtained for the integral of angular momentum. In a rigid body rotation, additional "hidden" internal energy and angular momentum are found; equipartition of energy is lost; chemical equilibria are dependent on angular velocity. In non-equilibrium, the stress tensor is found to be asymmetric in general (this effect is very small, however), and the force system in a fluid is generalized to include a couple per unit area as well as a force per unit area.

This talk is based on a paper[1] to which references are made for proofs and further discussion of some results; the material on the grand canonical distribution and the derivation of the conservation equations supplements that paper.

Statistical Mechanics and Thermodynamics

We assume the existence of a time-independent Hamiltonian $H(q_i, p_i)$, $i = 1 \ldots s$, and the validity of the canonical equations

$$\frac{\mathrm{d}q_i}{\mathrm{d}t} = \frac{\partial H}{\partial p_i}, \quad \frac{\mathrm{d}p_i}{\mathrm{d}t} = -\frac{\partial H}{\partial q_i} \tag{1}$$

Solution of these equations gives the motion of the system, $q_i(t)$, $p_i(t)$; geometrically this is a curve with parameter t (*path*) in the $2s$-dimensional *phase space* $P:(q_i, p_i)$. In this way the differential equations (1) define a steady flow of the phase space into itself with parameter t. This flow is incompressible, and the volume element $\mathrm{d}P$ is preserved since the divergence of the flow velocity vanishes

$$\sum_{i=1}^{s}\left[\frac{\partial}{\partial q_i}\left(\frac{\mathrm{d}q_i}{\mathrm{d}t}\right) + \frac{\partial}{\partial p_i}\left(\frac{\mathrm{d}p_i}{\mathrm{d}t}\right)\right] = \sum_{i=1}^{s}\left(\frac{\partial^2 H}{\partial q_i \partial p_i} - \frac{\partial^2 H}{\partial p_i \partial q_i}\right) = 0$$

A time-independent integral is a function $\epsilon(P)$ which has a constant value on each path. Alternatively, every path must lie entirely within a $(2s - 1)$-dimensional manifold $\epsilon(P) = $ constant. If we have r distinct integrals, $\epsilon_1(P) \ldots \epsilon_r(P)$, each path will lie in a $(2s - r)$-dimensional intersection of the manifolds $\epsilon_i(P) = $ constant, and, if $r = 2s - 1$, the intersection is the path itself. In general there do not exist as many as $2s - 1$ independent integrals, and in this case we may call the system *ergodic*. For example, on a billiard table the phase space is four-dimensional, coördinates (x,y) and velocities (u,v). Two integrals are u^2 and v^2 since either u or v changes sign on reflection at a cushion; however, no third integral exists which is not a function of u^2 and v^2. The reason for this is that all paths (except the periodic ones—of measure zero) meander about the whole table coming arbitrarily close to every point (x,y) and even spending, on the average, equal times in equal areas. This is the case

---

(1) H. Grad, *Comm. Pure and Appl. Math.*, **5**, No. 4 (1952).

more generally for any ergodic system; almost every path "fills" the $(2s - r)$-manifold to which it belongs and, in particular, the infinite time average of any phase function $\phi(P)$ over a path is equal to the corresponding $(2s - r)$-dimensional phase average. Our fundamental postulate is that the number of integrals, r, is small compared to $2s$. This is, in a sense, a gap in the theory since this postulate is, in principle, provable for any given dynamical system. However there exist mathematical theorems which (interpreted broadly) assert that almost any system chosen at random will have no integrals other than the known ones.[1,2] Such a statement is, for our purposes, even more significant than would be the proof of ergodicity of any particular dynamical system.

Following the usual procedure when it is impossible practically to obtain complete information about the state of a system (*i.e.*, all the coördinates q_i and p_i), we introduce an *a priori* probability density $f(P)$ with the property that $\int_D f(P)\mathrm{d}P$ is the probability of finding the state P within the domain D. Implied is the possibility of generating the probability $f(P)$ by repeated experiments with the macroscopic variables fixed. This is the second postulate, namely, that no finite probability is concentrated on a manifold of dimension lower than the full phase space; the cumulative probability distribution is absolutely continuous. The state of a system is now specified by a function $f(P)$ instead of by a point P. In general, the probability will vary with time, $f(P,t)$. The variation in time is determined by the flow in the phase space, explicitly by Liouville's equation

$$\frac{\partial f}{\partial t} + \sum_{i=1}^{s}\left(\frac{\partial H}{\partial p_i}\frac{\partial f}{\partial q_i} - \frac{\partial H}{\partial q_i}\frac{\partial f}{\partial p_i}\right) = 0 \qquad (2)$$

We define a state of equilibrium by the condition that the probability density $f(P)$ be independent of time. It follows that $f(P)$ is a function of the integrals $\epsilon_1(P) \ldots \epsilon_r(P)$ since this is the general time-independent solution of (2). We now have a probability density defined in the r-dimensional ϵ-space. This general solution represents many physical situations; given the situation we must decide which solution is appropriate to describe it. The first problem we consider is an isolated system. The values of the ϵ_i are constant and therefore presumably known. Consequently the behavior of any system with different values of the ϵ_i is irrelevant, and we are led to a probability distribution concentrated on the $(2s - r)$-manifold ϵ = constant, or, in r-space, concentrated at a point[3]; this distribution we call *microcanonical*. Although a system must be allowed to interact with its surroundings in order to treat thermodynamics, all the thermodynamical functions can be computed for an isolated system. To start, we follow the formalism of Khinchin,[4] generalizing it to more than one integral.

It is convenient to use the uniform notation x_i, $i = 1 \ldots 2s$ for (q_i, p_i), $i = 1 \ldots s$; also we write x and ϵ for x_i and ϵ_i and $\mathrm{d}x$ and $\mathrm{d}\epsilon$ for the elements of volume in $2s$ and in r-space. The bounded domain V_c defined by $\epsilon_i < c_i$ has volume $V(c)$

$$V(c) = \int_{V_c} \mathrm{d}x, \qquad (3)$$

and we define

$$\Omega(c) = \frac{\partial^r}{\partial c_1 \ldots \partial c_r} V(c) \qquad (4)$$

$\Omega(c)$ is the limit of the volume of a thin shell $c_i < \epsilon_i < c_i + \mathrm{d}c_i$ divided by $\mathrm{d}c$. It is easily proved that

$$\int_{a_i<\epsilon_i<b_i} f(\epsilon)\mathrm{d}x = \int_a^b f(\epsilon)\Omega(\epsilon)\mathrm{d}\epsilon \qquad (5)$$

This converts a $2s$-fold integral into an r-fold integral. We remark that if the ϵ_i depend on any parameters λ_i, $\epsilon_i(x,\lambda)$, these parameters will also appear in $V(c,\lambda)$ and $\Omega(c,\lambda)$; also, if we consider a variety of systems with different numbers of molecules, n, the parameter n (or $n_1 \ldots n_m$ if there are m different kinds of molecules) will appear in V and Ω. We now define the entropy by[5]

$$S(\epsilon,\lambda,n) = \log \Omega \qquad (6)$$

generalized temperatures by

$$\theta_i = \frac{\partial S}{\partial \epsilon_i} \qquad (7)$$

forces by

$$Y_i = \frac{\partial S}{\partial \lambda_i} \qquad (8)$$

and potentials by[5]

$$\mu_i = \frac{\partial S}{\partial n_i} \qquad (9)$$

Summarizing

$$\mathrm{d}S = \theta\cdot\mathrm{d}\epsilon + Y\cdot\mathrm{d}\lambda + \mu\cdot\mathrm{d}n \qquad (10)$$

All this is, of course, purely formal, and it will become thermodynamics only with a discussion of the interaction between two or more systems.

Denoting by C the complete system $(x_1 \ldots x_{2s}) = x$, we consider the two *components* $C' : (x_1 \ldots x_k) = x'$ and $C'' : (x_{k+1} \ldots x_{2s}) = x''$. We state that the two components are in thermal equilibrium if

$$\epsilon(x) = \epsilon'(x') + \epsilon''(x'') \qquad (11)$$

in mechanical equilibrium if

$$\lambda = \lambda' + \lambda'' \qquad (12)$$

and in diffusional equilibrium if

$$n = n' + n'' \qquad (13)$$

The condition (11), *weak interaction*, would seem to be even more rigorously valid for two isolated systems. This contingency is eliminated by the postulate that $\epsilon_1 \ldots \epsilon_r$ are all the integrals of the system; if the components were isolated, ϵ_i' and ϵ_i'' would be integrals separately. The simplest example of condition (12) is when λ is volume and the two components are separated by a movable wall. In principle, any combination of isolation and the three types of equilibrium is possible. For example, the components could be isolated with regard to

---

(2) P. R. Halmos, *Bull. Am. Math. Soc.*, **55**, No. 11 (1949).

(3) This requires a modification of the absolute continuity postulate, see ref. 1.

(4) A. I. Khinchin, "Mathematical Foundations of Statistical Mechanics," Dover Publications, Inc., New York, N. Y., 1949.

(5) The conventional entropy is kS and chemical potential $-kT\mu$.

one integral ϵ_i and in interaction with regard to another; some parameters λ could be fixed and others variable; a semipermeable membrane could allow one type of molecule to mix and not another. Of course, most of these combinations are of no interest; for example, diffusional without thermal equilibrium.

In the case of thermal equilibrium we have

$$V(c) = \int_{V_c} \mathrm{d}x = \int \mathrm{d}x' \int_{\epsilon'' < c - \epsilon'} \mathrm{d}x'' = \int V''(c - \epsilon')\mathrm{d}x' \tag{14}$$

Similarly, for thermal and mechanical equilibrium

$$V(c,\lambda) = \int V''(c - \epsilon', \lambda - \lambda')\,\mathrm{d}x'\,\mathrm{d}\lambda' \tag{15}$$

while for thermal and diffusional equilibrium

$$V(c,n) = \sum_{n'} \int \frac{n!}{n'!\,(n - n')!} V''(c - \epsilon', n - n')\mathrm{d}x' \tag{16}$$

The factorials[6] enter because $V''(c - \epsilon', n - n')$ is the volume for a fixed choice of the n' molecules, and V_c contains a distinct region for every different choice of these molecules. Application of (4) and (5) yields

$$\Omega(\epsilon,\lambda,n) = \int \Omega''(\epsilon - \epsilon',\lambda,n)\Omega'(\epsilon',\lambda,n)\mathrm{d}\epsilon' \tag{17}$$

$$\Omega(\epsilon,\lambda,n) = \int \Omega''(\epsilon - \epsilon', \lambda - \lambda', n)\Omega'(\epsilon',\lambda',n)\mathrm{d}\epsilon'\,\mathrm{d}\lambda' \tag{18}$$

$$\frac{\Omega(\epsilon,\lambda,n)}{n!} = \sum_{n'} \int \frac{\Omega''(\epsilon - \epsilon', \lambda, n - n')}{(n - n')!} \frac{\Omega'(\epsilon',\lambda,n')}{n'!}\mathrm{d}\epsilon' \tag{19}$$

The convolution form of these integrals suggests the use of Laplace transforms

$$Z(\theta,\lambda,n) = \int e^{-\theta\cdot\epsilon}\Omega(\epsilon,\lambda,n)\,\mathrm{d}\epsilon \tag{20}$$

$$\begin{aligned} \Lambda(\theta,\alpha,n) &= \int e^{-\alpha\cdot\lambda}Z(\theta,\lambda,n)\mathrm{d}\lambda \qquad (21) \\ &= \int e^{-\alpha\cdot\lambda - \theta\cdot\epsilon}\Omega(\epsilon,\lambda,n)\mathrm{d}\epsilon\,\mathrm{d}\lambda \end{aligned}$$

$$\begin{aligned} \Xi(\theta,\lambda,\mu) &= \sum_n \frac{1}{n!} e^{-\mu\cdot n}Z(\theta,\lambda,n) \qquad (22) \\ &= \sum_n \int \frac{1}{n!} e^{-\mu\cdot n - \theta\cdot\epsilon}\Omega(\epsilon,\lambda,n)\mathrm{d}\epsilon \end{aligned}$$

and similarly for Z', Z'', etc. Of course

$$Z = Z'Z'' \tag{23}$$

$$\Lambda = \Lambda'\Lambda'' \tag{24}$$

$$\Xi = \Xi'\Xi'' \tag{25}$$

Anticipating our results, we shall find that the integrals ϵ_i are fixed in an isolated system whereas the temperatures θ_i are fixed in thermal equilibrium: the parameters λ_i are fixed in isolation and the forces α_i in mechanical equilibrium; the composition n_i is fixed in isolation and the potentials μ_i if there is diffusion. The technique is to take Laplace transforms with respect to integrals and parameters which are not fixed; the new variables which are introduced will be found to have fixed values.

A further group of formulas (ref. 1 for derivation) is the following for the probability density $f'(x')$ induced in the component C' by a microcanonical distribution of the whole system on the manifold $\epsilon = c$

$$f'(x') = \frac{\Omega''(c - \epsilon',\lambda,n)}{\Omega(c,\lambda,n)} \tag{26}$$

$$f'(x',\lambda') = \frac{\Omega''(c - \epsilon', \lambda - \lambda', n)}{\Omega(c,\lambda,n)} \tag{27}$$

$$f'_{n'}(x') = \frac{n!}{n'!\,(n - n')!} \frac{\Omega''(c - \epsilon',\lambda,n - n')}{\Omega(c,\lambda,n)} \tag{28}$$

The normalization is $\int f'(x')\mathrm{d}x' = 1$, $\int f'(x',\lambda')\mathrm{d}x'\mathrm{d}\lambda' = 1$, and $\sum_{n'} \int f'_{n'}(x')\mathrm{d}x' = 1$; $f'(x')$ is the probability that molecule 1 has coördinate x_1, etc.; $f'_{n'}(x')$ is the probability that *a* molecule has coördinate x_1, etc.

Now we state a theorem concerning Laplace transforms which is of fundamental importance; for a proof see ref. 1. Suppose $\psi(x)$ is a non-negative function and is positive for x in X. Assume that

$$\Psi(y) = \int e^{-y\cdot x}\psi(x)\mathrm{d}x \tag{29}$$

exists for y in some set Y. Construct the function

$$\Phi_\xi(y) = y\cdot\xi + \log \Psi(y) = \log \int e^{y\cdot(\xi - x)}\psi(x)\mathrm{d}x \tag{30}$$

Theorem.—To every ξ in X there exists a unique minimum of $\Phi_\xi(y)$ with respect to y; this is attained at the unique value of y determined implicitly by

$$\xi_i + \frac{\mathrm{d}}{\mathrm{d}y_i} \log \Psi = 0 \tag{31}$$

With these preliminaries, we can derive the canonical distribution and thermodynamics of a system C' in thermal equilibrium with a large component C''. Formula (26) can be rewritten in the form

$$f'(x') = e^{-\theta\cdot\epsilon'} \frac{e^{-\theta\cdot(c - \epsilon')}\,\Omega''(c - \epsilon')}{e^{-\theta\cdot c}\,\Omega(c)} \tag{32}$$

and we choose for $\theta_i(c,\lambda'',n'')$ the value

$$\theta_i = \frac{\partial}{\partial c_i} \log \Omega''(c,\lambda'',n'') \tag{33}$$

This value of θ makes $e^{-\theta\cdot(c - \epsilon')}\ \Omega''(c - \epsilon')$ stationary as a function of ϵ' at $\epsilon' = 0$, and, if C'' is a *large component*, $e^{-\theta\cdot(c - \epsilon')}\ \Omega''(c - \epsilon')$ will scarcely vary while ϵ' ranges sufficiently for $e^{-\theta\cdot\epsilon'}$ to become sensibly zero; consequently

$$f'(x') \sim (\text{constant})e^{-\theta\cdot\epsilon'}$$

or

$$f'(x') \sim \frac{e^{-\theta\cdot\epsilon'}}{Z'(\theta,\lambda',n')} \tag{34}$$

evaluating the constant by the condition $\int f'(x')\cdot \mathrm{d}x' = 1$. The large component condition can be satisfied, for example, by taking n'' large compared to n' if $\log \Omega''(c)$ is convex in c and C''_{ij} (see equation (37)) approaches infinity with n''.

All physical properties of the system C' are determinable from its distribution function, $f'(x')$. The surroundings enter only in the values of the parameters θ_i which have the same values for every (small) component C' which is put into contact with this reservoir; hence we call the θ_i (generalized) temperatures. Since we are interested only in the system C', we drop the accent and consider

$$f(x) = \frac{e^{-\theta\cdot\epsilon}}{Z(\theta,\lambda,n)} \tag{35}$$

The mean value of ϵ_i is given by

$$E_i = \frac{1}{Z}\int \epsilon_i e^{-\theta\cdot\epsilon}\mathrm{d}x = -\frac{\partial}{\partial\theta_i} \log Z \tag{36}$$

and its dispersion by

$$C_{ij} = \frac{1}{Z}\int (\epsilon_i - E_i)(\epsilon_j - E_j)e^{-\theta\cdot\epsilon}\mathrm{d}x = \frac{\partial^2}{\partial\theta_i\partial\theta_j} \log Z \tag{37}$$

---

(6) If there are several species of molecules, $n!$ is replaced by the product $n_1!\,n_2!\ldots$

It can be verified that the relative dispersion is small if n is large; we conclude that E_i is *the* observed value of ϵ_i. Now, identifying $\psi(x)$ in (29) with $\Omega(\epsilon)$, we find that for every value a_i that is a possible value of ϵ_i, a unique θ_i, determined by $E_i(\theta) = a_i$, minimizes $\theta\cdot a + \log Z(\theta)$. In particular, the observed value E_i can be given any value by choice of θ_i—*i.e.*, by choice of a reservoir. The minimum value we call entropy

$$S(E,\lambda,n) = \theta\cdot E + \log Z \tag{38}$$

(θ is replaced by its value in terms of E), and we introduce the following auxiliary quantities

$$X_{ij} = -\int \frac{\partial\epsilon_i}{\partial\lambda_j} f(x)\mathrm{d}x \tag{39}$$

$$Y_j = \frac{\partial}{\partial\lambda_i}\log Z = \sum_i \theta_i X_{ij} \tag{40}$$

$$\mu_i = \frac{\partial}{\partial n_i}\log Z \tag{41}$$

We have

$$\mathrm{d}\log Z = -E\cdot\mathrm{d}\theta + Y\cdot\mathrm{d}\lambda + \mu\cdot\mathrm{d}n \tag{42}$$

and

$$\begin{aligned}\mathrm{d}S &= \theta\cdot\mathrm{d}E + Y\cdot\mathrm{d}\lambda + \mu\cdot\mathrm{d}n \\ &= \sum_i \theta_i(\mathrm{d}E_i + \sum_j X_{ij}\mathrm{d}\lambda_j) + \sum_i \mu_i\mathrm{d}n_i\end{aligned} \tag{43}$$

For the system of many integrals we may define quantities as we please and discover their properties; for the system of one integral, energy, a macroscopic theory already exists, and we should show the equivalence. We will not go into this here; the results are $\theta = \frac{1}{kT}$, $X = p$ if $\lambda = V$, and $kT\mathrm{d}S = \mathrm{d}E + p\mathrm{d}V$.

For the general case, we justify the name "entropy" by stating a few properties that follow immediately from the minimum property. If the system is transferred from a reservoir, θ', to another, θ, with parameters fixed, then

$$S - S' > \theta\cdot(E - E') \tag{44}$$

and

$$(E - E')\cdot(\theta - \theta') < 0 \tag{45}$$

The second inequality states that "in general" E "flows" from lower θ to higher θ. If two systems with energy and entropy functions $E(\theta)$, $S(E)$ and $\bar{E}(\theta)$, $\bar{S}(E)$, originally at temperatures θ' and θ'', are both transferred to a reservoir at a temperature θ such that

$$E(\theta') + \bar{E}(\theta)'' = E(\theta) + \bar{E}(\theta)$$

then

$$S + \bar{S} > S' + \bar{S}''$$

In other words, bringing two systems at different temperatures into contact with no total change in "energy" increases the entropy (this can also be proved without the intervention of reservoirs).

In view of all this, we interpret (43) as a generalization of the second law (the integrating factor property of the temperature does not seem to be highly significant when there is more than one integral). Also we note that C_{ij} (which is positive definite in the indices i,j) is a generalization of the specific heat at constant volume.

Next we turn to the case of thermal and mechanical equilibrium. Just as before we arrive at the distribution of a small component

$$f(x,\lambda) = \frac{e^{-\theta\cdot\epsilon-\alpha\cdot\lambda}}{\Lambda(\theta,\alpha,n)} \tag{46}$$

The entropy is again defined as the minimum of the function (30) where, as before, ψ is Ω, but now x ranges through ϵ and λ and y through θ and α; we have

$$\left.\begin{aligned} E_i &= \int \epsilon_i f(x)\mathrm{d}x = -\frac{\partial}{\partial\theta_i}\log\Lambda \\ L_i &= \int \lambda_i f(x)\mathrm{d}x = -\frac{\partial}{\partial\alpha_i}\log\Lambda \\ \mu_i &= \frac{\partial}{\partial n_i}\log\Lambda \\ S(E,L,n) &= \theta\cdot E + \alpha\cdot L + \log\Lambda \\ \mathrm{d}S &= \theta\cdot\mathrm{d}E + \alpha\cdot\mathrm{d}L + \mu\cdot\mathrm{d}n \end{aligned}\right\} \tag{47}$$

In thermal equilibrium, the temperatures θ_i are fixed, in mechanical equilibrium, the forces α_i. L_i is the observed value of λ_i. In particular, with $\lambda = V$, if there were a macroscopic theory of mechanical equilibrium similar to that of thermal equilibrium, we could now conclude that α is an "empirical pressure" and by using a perfect gas as a "thermometer" conclude that $\alpha = p/kT$ universally. The first two entropy inequalities become

$$\begin{gathered} S - S' > \theta\cdot(E - E') + \alpha\cdot(L - L) \\ (E - E')\cdot(\theta - \theta') + (L - L')\cdot(\alpha - \alpha') < 0 \end{gathered} \tag{48}$$

and the third one is unaltered (the total volume is held fixed as well as the total energy); we have an entropy increase due to a "flow" of volume from lower to higher pressure.

For the case of thermal and diffusional equilibrium, the distribution of a small component is *grand canonical* (see footnote (6))

$$f_n(x) = \frac{e^{-\theta\cdot\epsilon-\mu\cdot n}}{n!\Xi(\theta,\lambda,\mu)} \tag{49}$$

The entropy is again taken to be the minimum of the function (30), this time with ϵ and n as variables and $\Omega/n!$ as ψ. We have

$$\left.\begin{aligned} E_i &= \sum_n \int \epsilon_i f(x)\mathrm{d}x = -\frac{\partial}{\partial\theta_i}\log\Xi \\ N_i &= \sum_n \int n_i f(x)\mathrm{d}x = -\frac{\partial}{\partial\mu_i}\log\Xi \\ Y_i &= \frac{\partial}{\partial\lambda_i}\log\Xi \\ S(E,\lambda,N) &= \theta\cdot E + \mu\cdot N + \log\Xi \\ \mathrm{d}S &= \theta\cdot\mathrm{d}E + Y\cdot\mathrm{d}\lambda + \mu\cdot\mathrm{d}N \end{aligned}\right\} \tag{50}$$

We conclude that in diffusional equilibrium the potentials μ_i are fixed. N_i is the observed value of n_i. The entropy inequalities are now

$$\begin{gathered} S - S' > \theta\cdot(E - E') + \mu.(N - N') \\ (E - E')\cdot(\theta - \theta') + (N - N')\cdot(\mu - \mu') < 0 \end{gathered} \tag{51}$$

There is an entropy increase due to a flow of molecules from low to high μ.

We have introduced four different thermodynamical structures; a natural question is whether the various functions are the same. Although they are not identical, a simple application of steepest descent shows them to be asymptotically equivalent (with one important exception) as the size of the system increases. For example, solution of the implicit relation

$$\theta = \frac{\mathrm{d}}{\mathrm{d}\epsilon} \log \Omega(\epsilon)$$

for $\epsilon(\theta)$ gives the asymptotic value

$$\epsilon(\theta) = -\frac{\mathrm{d}}{\mathrm{d}\theta} \log Z(\theta)$$

Also, $S(E)$ is asymptotically the same function as $\log \Omega(\epsilon)$ except for a term $\log n!$ in the case of diffusional equilibrium. This is closely connected with the problem of additivity. It is immediately evident from the definitions that the four entropies are additive in the situations to which they apply; for example

$$\log \Omega = \log \Omega' + \log \Omega''$$

for two isolated systems

$$\log Z + \theta \cdot E = \log Z' + \theta \cdot E' + \log Z'' + \theta \cdot E''$$

for systems in thermal contact, etc. Of course, all definitions are found to be additive for isolated systems, provided, however, that certain precautions are observed: namely, that both ϵ' and ϵ'' are integrals, λ' and λ'' are individual parameters, and the diffusional entropy is defined only when we take n' and n'' separately as parameters. Care must be taken in other cases to use the correct entropy. An important special case of additivity is homogeneity, *i.e.*, the quality of being proportional to the size of the system. We shall consider such quantities per unit volume rather than per unit mass or per molecule which are more common. The appropriate thermodynamics to use is the grand canonical since the insertion of a purely conceptual barrier clearly creates two components in diffusional equilibrium. We consider V to be so divided into V_1 and V_2 and note that

$$\log \Xi\ (\theta,\lambda,V,\mu) = \log \Xi\ (\theta,\lambda,V_1,\mu) + \log \Xi\ (\theta,\lambda,V_2,\mu)$$

The λ_i here signify all parameters other than V (*e.g.*, molecular constants) and, for simplicity, are assumed to be independent of the size of the system. It is an elementary fact that a function satisfying the equation $f(V_1 + V_2) = f(V_1) + f(V_2)$ is proportional to V; in other words, $\log \Xi/V$ is a function of θ, λ and μ. The same follows for E, N and S from (50), and, in addition

$$\log \Xi = \frac{pV}{kT} \tag{52}$$

using the fact that the "force" corresponding to V is p/kT. We define

$$\left.\begin{aligned} N_i &= V\nu_i \\ E_i &= Ve_i \\ Y_i &= Vy_i \\ S &= Vs(\epsilon,\lambda,\nu) \end{aligned}\right\} \tag{53}$$

and conclude that

$$s = \theta \cdot e + \mu \cdot \nu + \frac{p}{kT}$$

$$\mathrm{d}s = \theta \cdot \mathrm{d}e + y \cdot \mathrm{d}\lambda + \mu \cdot \mathrm{d}\nu \tag{54}$$

Since we have found the grand canonical entropy to be homogeneous, the same cannot be true of the other entropies because of the $n!$ We conclude that insertion or removal of a barrier in a homogeneous substance changes its entropy if molecular flow is not allowed through the barrier; this is even the case using the grand canonical entropy. When a barrier is removed between two gases of differing μ and identical p and T, diffusion takes place so we expect an increase of entropy; however, the same diffusion takes place even if, to our knowledge, the gases are identical. Whereas previously a molecule once observed on one side would always remain there, this knowledge is lost when the barrier is removed.

Quantum mechanically, all entropies are found to be homogeneous since interchange of two identical molecules is not an event (*cf.* ref. 7); however, in order to know whether there is a change of entropy when a barrier is removed, one must first decide whether the two gases are identical.

It is possible to treat chemical equilibria classically but, of course, only rather artificially. Given two types of atom, A and B, and their joint Hamiltonian, we adopt some rule for stating when they should be considered a molecule, AB, for example when the intermolecular distance is smaller than some fixed value. At every point in the phase space we can then assign parameters n_A, n_B, n_{AB} for the number of molecules of each type. More generally, we assume a chemical reaction (in a perfect gas) involving the molecules A_i

$$\sum_i a_i A_i = 0 \tag{55}$$

where the composition in terms of atoms B_j is

$$A_i = \sum_j a_{ij} B_j \tag{56}$$

the condition for balancing equation (55) is

$$\sum_i a_i a_{ij} = 0, \quad j = 1, 2, \ldots \tag{57}$$

Let n_r be the number of molecules A_r and n_s' the (fixed) number of atoms B_s; clearly

$$\Sigma n_i a_{ij} = n'_j \tag{58}$$

If n_i° is a possible composition of the system, then all others consistent with the reaction (55) are given by

$$n_i = n_i^\circ + \beta a_i, \quad \beta = 0, \pm 1, \pm 2, \ldots \tag{59}$$

An elementary computation yields

$$Z(\theta,\lambda,n^\circ) = \sum_\beta \prod_r \frac{Z_r(\theta,\lambda,n_r)}{n_r!} \prod_s \frac{N_s!}{(a_{rs})^{n_r}}$$

The β-summation can be approximated by steepest descents, and to first order the condition on β (*i.e.*, on n_r) is easily seen to be

$$\frac{\partial}{\partial \beta} \sum_r \log \frac{Z_r(n_r^\circ + \beta a_r)}{(n_r^\circ + \beta a_r)!} = 0$$

or

$$\sum_r a_r \frac{\partial}{\partial n_r} \log \left(\frac{Z_r}{n_r!}\right) = 0$$

which is, asymptotically

$$\sum_r a_r \mu_r = 0 \tag{60}$$

for the grand canonical potentials, μ_r.

---

(7) E. Schrödinger, "Statistical Thermodynamics" Cambridge University Press, London, 1948.

The significance of these results, compared to the thermodynamics of energy alone, will become clearer with an example. We take a perfect gas with molecules of arbitrary internal structure and consider the integrals of momentum and angular momentum as well as energy. It is found (see ref. 1) that the system is translating and rotating as a rigid body with local velocity[8]

$$\mathbf{u} = -\frac{\theta_2 + \theta_3 \times \mathbf{x}}{\theta_1} \tag{61}$$

and angular velocity

$$\omega = -\frac{\theta_3}{\theta_1} \tag{62}$$

$\theta_1 = 1/kT$, θ_2, and θ_3 are the temperatures corresponding to energy, momentum and angular momentum. For thermal equilibrium

$$Z = \prod_r z_r^{n_r} \tag{63}$$

where

$$z_r = \left(\frac{2\pi m_r}{\theta_1}\right)^{s_r/2} \sigma_r \tau_r \tag{64}$$

$$\sigma_r = \int \exp\left[\frac{1}{2} m_r u^2/kT\right] dx \tag{65}$$

(a threefold integration over the volume, V), and τ_r is a function of $\theta_3^2/\theta_1 = \omega^2/kT = w$ which can be written as a complicated integral over the internal coördinates of molecule r. The results are conveniently expressed in terms of the parameter

$$I_r = \frac{2}{w}\frac{d}{dw} \log \tau_r \tag{66}$$

namely

$$\left.\begin{aligned} E_1 &= \sum_r \int \left(\frac{s_r}{2} kT + \frac{1}{2} m_r u^2 + \frac{1}{2} I_r \omega^2\right) \nu_r dx \\ \mathbf{E}_2 &= \sum_r \int m_r \mathbf{u} \nu_r dx \\ \mathbf{E}_3 &= \sum_r \int (m_r \mathbf{x} \times \mathbf{u} + I_r \omega) \nu_r dx \\ S &= \sum_r \int \left[\frac{s_r}{2}(1 + \log 2\pi m_r + \log kT) + \right. \\ &\qquad \left. \log n_r/\nu_r + g_r \right] \nu_r dx \end{aligned}\right\} \tag{67}$$

where

$$g_r = \left(1 - w\frac{d}{dw}\right) \log \tau_r \tag{68}$$

I_r is a sort of average moment of inertia of the molecule; for a rigid sphere it is exactly the moment of inertia; for a dumb-bell molecule of radius a, it is a function of $m_r\omega^2 a^2/2kT$ which, for small values of this parameter, reduces to the moment of inertia of a shell of radius a.

For diffusional equilibrium, we find

$$\log \Xi = \sum_r z_r e^{-\mu_r} \tag{69}$$

$$N_r = z_r e^{-\mu_r} \tag{70}$$

The expressions for E_i are the same, but

$$S = \sum_r \int \left[\frac{s_r}{2}(1 + \log 2\pi m_r + \log kT) + 1 - \log \nu_r + g_r\right] \nu_r dx \tag{71}$$

and

$$\left.\begin{aligned} \mu_r &= \log \frac{z_r}{N_r} \\ &= \frac{1}{2} s_r \log (2\pi m_r + \log kT) + \log \sigma_r + \\ &\qquad \log \tau_r \\ &= \frac{1}{2} s_r (\log 2\pi m_r + \log kT) - \log \nu_r + \\ &\qquad m_r u^2/2kT + \log \tau_r \end{aligned}\right\} \tag{72}$$

We see that the "temperature" corresponding to momentum is essentially the translational velocity, and to angular momentum, the angular velocity. The expressions for the energy, entropy, etc., become familiar only when expressed in terms of an integral over the local parameters $\mathbf{u}(x)$ and $\nu(x)$. The extra terms $I\omega$, $\frac{1}{2}I\omega^2$, and g are unconventional but, in general, extremely small. In a coördinate system moving with velocity $\mathbf{u}$, the energy per internal degree of freedom is not quite $\frac{1}{2}kT$. In chemical equilibria, the concentrations are determined by the condition $\Sigma a_r \mu_r = 0$. Essentially, the parameter σ_r takes the place of volume and N_r/σ_r the concentration. The variation of each ν_r with radius is known beforehand.

Continuum Mechanics

To use thermodynamics for non-equilibrium states of continua, it is necessary to postulate the existence of point functions which satisfy the same equations of state as in equilibrium. Extensive quantities are given by densities (say with respect to volume); for example

$$\left.\begin{aligned} E_i &= \int_D e_i(x,t)\, dx \\ S &= \int_D s(x,t)\, dx \\ N_i &= \int_D \nu_i(x,t)\, dx \end{aligned}\right\} \tag{73}$$

are the "amount" of ϵ_i and of entropy and the number of molecules within D—evidently we must use the diffusional thermodynamics. The dynamical statement that ϵ_i is constant for an isolated system is generalized to the statement that E, for any domain D, varies only by flow through the boundary, B; *i.e.*, we postulate the existence of a flow quantity, $\mathbf{Q}(x,t)$, which is the rate of flow of ϵ per unit area through an element of surface. Specifically

$$\frac{d}{dt}\int_D e\, dx + \oint_B \mathbf{Q} \cdot d\mathbf{A} = 0 \tag{74}$$

where D is a domain moving at the macroscopic flow velocity $\mathbf{u}$. From the condition that (74) holds for an arbitrary domain, D, follows the differential equation

$$\frac{\partial e}{\partial t} + \operatorname{div}(e\mathbf{u} + \mathbf{Q}) = 0 \tag{75}$$

Similarly, from the condition that

$$\frac{d}{dt}\int_D \nu_i\, dx = 0 \tag{76}$$

for a domain D moving at the flow velocity of the substance i, follows the equation

---

(8) The scalar or vector character of greek symbols is not indicated explicitly but should be clear from the context.

$$\frac{\partial \nu_i}{\partial t} + \mathrm{div}(\nu_i \mathbf{u}_i) = 0 \qquad (77)$$

The flow velocity, **u**, is identified with the thermodynamic velocity, *i.e.*, the temperature corresponding to the integral of momentum. The $\mathbf{u}_i$ are not thermodynamic coördinates, but, from the equation of state, momentum $= \rho\mathbf{u}$, where

$$\begin{aligned} \rho &= \Sigma \rho_i \\ \rho_i &= m_i \nu_i \end{aligned} \qquad (78)$$

follows the relation

$$\rho\mathbf{u} = \Sigma\, \rho_i \mathbf{u}_i \qquad (79)$$

For the entropy, using (54) and dropping the parameters λ, we have

$$\frac{\partial s}{\partial t} = \Sigma\, \theta_i \frac{\partial e_i}{\partial t} + \Sigma\, \mu_i \frac{\partial \nu_i}{\partial t} \qquad (80)$$

and a little manipulation leads to

$$\frac{\partial s}{\partial t} + \mathrm{div}\,(s\mathbf{u}) = \frac{p}{kT}\,\mathrm{div}\,\mathbf{u} - \Sigma\,\theta_i\,\mathrm{div}\,\mathbf{Q}_i - \Sigma\,\mu_i\,\mathrm{div}\,(\nu_i \mathbf{v}_i) \qquad (81)$$

where

$$\mathbf{v}_i = \mathbf{u}_i - \mathbf{u} \qquad (82)$$

Integrating (81) over a fixed domain D yields

$$\begin{aligned} \frac{\mathrm{d}S}{\mathrm{d}t} + \oint s\mathbf{u}\cdot d\mathbf{A} = &- \sum_i \oint \mu_i \nu_i \mathbf{v}_i \cdot \mathrm{d}\mathbf{A} \\ &+ \int \left(\frac{p}{kT}\mathrm{div}\,\mathbf{u} - \sum_i \theta_i\,\mathrm{div}\,\mathbf{Q}_i \right) \mathrm{d}x \\ &+ \sum_i \int \nu_i \mathbf{v}_i \cdot \mathrm{grad}\,\mu_i\,\mathrm{d}x \end{aligned} \qquad (83)$$

Before interpreting this in general, consider the energy and momenta

$$\left.\begin{aligned} e_1 &= \frac{1}{2}\rho u^2 + \bar{e} \\ e_2^i &= \rho u^i \\ e_3^{ij} &= \rho(x^i u^j - x^j u^i) + \sum_r \nu_r I_r \omega^{ij} \\ &= M^{ij} + m^{ij} \end{aligned}\right\} \qquad (84)$$

and the corresponding flow parameters

$$\left.\begin{aligned} Q_1^r &= \sum_i u^i P^{ir} + \sum_{i,j} \frac{1}{2}\omega^{ij} q^{ijr} + q^r \\ Q_2^{ir} &= P^{ir} \\ Q_3^{ijr} &= x^i P^{jr} - x^j P^{ir} + q^{ijr} \end{aligned}\right\} \qquad (85)$$

The momentum flow is given by a stress tensor, P^{ij}, the angular momentum flow by the moment of the stress tensor plus an additional flow, the energy flow by the work corresponding to these two terms plus an additional heat flow, q^r. Equations for M^{ij} and m^{ij} separately can be obtained by multiplying the momentum equation by **x**

$$\begin{aligned} \frac{\partial M^{ij}}{\partial t} + \sum_r \frac{\partial}{\partial x^r}(\rho u^r M^{ij} + x^i P^{jr} - x^j P^{ir}) &= P^{ji} - P^{ij} \\ \frac{\partial m^{ij}}{\partial t} + \sum_r \frac{\partial}{\partial x^r}(\rho u^r m^{ij} + q^{ijr}) &= P^{ij} - P^{ji} \end{aligned} \qquad (86)$$

The coupling between internal and external angular momentum is the asymmetric part of the stress tensor which does not vanish in general. Similarly, equations for $^1/_2\rho u^2$ and $\bar{e}$ separately can be obtained.

Using these results, we evaluate for use in (83)

$$\begin{aligned} \int \left(\frac{p}{kT}\,\mathrm{div}\,\mathbf{u} - \Sigma\,\theta_i\,\mathrm{div}\,\mathbf{Q}_i \right) \mathrm{d}x &= - \oint \frac{1}{kT}\,\mathbf{q}\cdot\mathrm{d}\mathbf{A} - \int \frac{1}{kT^2}\,\mathbf{q}\cdot\mathrm{grad}\,T\,\mathrm{d}x \\ &- \sum_{i,r} \int \frac{1}{kT}\,p^{ir}\left(\frac{\partial u^i}{\partial x^r} + \omega^{ir}\right)\mathrm{d}x \\ &- \sum_{i,j,r} \int \frac{1}{2kT}\,q^{ijr}\,\frac{\partial w^{ij}}{\partial x^r}\,\mathrm{d}x \end{aligned} \qquad (87)$$

where

$$p^{ir} = P^{ir} - p\delta^{ir} \qquad (88)$$

Following the procedures of irreversible thermodynamics, we call q^i, q^{ijr}, p^{ij} and $\nu^i\mathbf{v}^i$ fluxes and $\partial T/\partial x^r$, $\partial\omega^{ij}/\partial x^r$, $\partial u^i/\partial x^r + \omega^{ir}$ and $\partial\mu_i/\partial x^r$ forces and assume that the fluxes are a homogeneous linear function of the forces. Limiting ourselves to orthogonally invariant isotropic coefficients, we obtain the groups (q^i, q^{ijr}, $\nu^i\mathbf{v}^i$) and p^{ij}. For the stress we obtain three scalar viscosity coefficients for the trace, symmetric and asymmetric parts of $\partial u^i/\partial x^j + \omega^{ir}$. In particular, the asymmetric part of the stress tensor is proportional to the difference between ω and $^1/_2$ curl **u**. For q^i we obtain a scalar heat conductivity, a scalar coefficient for each species of molecule coupling q^i with potential gradients, and a single coefficient for ω gradients. For $\nu^i\mathbf{v}^i$ there is a scalar diffusion coefficient for each pair of molecular species and a thermal diffusion and ω coefficient for each species. For q^{ijr} there are three scalars coupling it with ω gradients, one with temperature gradients, and one for each species of potential gradients. Estimates of the size of some of these coefficients are given in ref. 1. The total number of coefficients is reduced by consideration of the Onsager relations and $\Sigma\rho_i\mathbf{v}_i = 0$. From (72) we see that grad μ has gradients of temperature, pressure, concentration and ω; (the $m_r u^2/2kT$ can be dropped since $\Sigma\nu_r\mathbf{v}_r m_r = 0$). This fact would be quite unintelligible without the "cross" terms in the assumed linear relation between forces and fluxes.

For the general case, ignoring the term p div $(\mathbf{u}/kT)$ in (83)

$$\int \theta_i\,\mathrm{div}\,\mathbf{Q}_i\,\mathrm{d}x = \oint \theta_i \mathbf{Q}_i\cdot\mathrm{d}\mathbf{A} - \int \mathbf{Q}_i\cdot\mathrm{grad}\,\theta_i\,\mathrm{d}x$$

which has a boundary flow $\mathbf{Q}_i\theta_i$ (*cf.* $\mathbf{q}/kT$) and suggests a transport relation

$$\mathbf{Q}_i \sim \mathrm{grad}\,\theta_i \qquad (89)$$

It is possible to justify some of the preceding considerations on a molecular basis. Following the method of Irving and Kirkwood[9] for the derivation of the classical conservation equations, we will indicate the derivation of a conservation equation for the general integral, ϵ. For this purpose it is not necessary to restrict ourselves to Hamiltonian systems, so we take the generalization of Liouville's equation

$$\frac{\partial f}{\partial t} + \sum_{i=1}^{n} \left[\frac{\partial}{\partial \mathbf{x}_i}\cdot(\xi_i f) + \frac{\partial}{\partial \xi_i}\cdot(\mathbf{F}_i f) + \frac{\partial}{\partial \mathbf{q}_i}\cdot(\mathbf{p}_i f) + \frac{\partial}{\partial \mathbf{p}_i}\cdot(\mathbf{G}_i f) \right] = 0 \qquad (90)$$

The coördinates are not canonical; $\mathbf{x}_i$ is the position vector of the center of molecule i, $\xi_i = \mathrm{d}\mathbf{x}_i/\mathrm{d}t$

---

(9) J. H. Irving and J. G. Kirkwood, *J. Chem. Phys.*, **18**, No. 6 (1950).

is its velocity, $\mathbf{q}_i$ represents the internal coördinates, $\mathbf{p}_i = d\mathbf{q}_i/dt$ the velocities; the symbol $(\cdot)$ refers to a summation of the 3 external or $s - 3$ internal degrees of freedom, as the case may be. $\mathbf{F}_i$ is the acceleration of the center of molecule i, $\mathbf{G}_i$ of the internal coördinates; we write

$$\mathbf{F}_i = \sum_{j=1}^{n} \mathbf{F}_{ij} \qquad \mathbf{G}_i = \sum_{j=1}^{n} \mathbf{G}_{ij} \tag{91}$$

and assume that

$$\begin{aligned} \mathbf{F}_{ii} &= \mathbf{F}_{11}(P_i) \qquad \mathbf{G}_{ii} = \mathbf{G}_{11}(P_i) \\ \mathbf{F}_{ij} &= \mathbf{F}_{12}(P_i,P_j) \qquad \mathbf{G}_{ij} = \mathbf{G}_{12}(P_i,P_j) \end{aligned} \tag{92}$$

P_i represents all the coördinates $(\mathbf{x}_i, \xi_i, \mathbf{q}_i, \mathbf{p}_i)$.

We consider two cases; the integral ϵ can be written

$$\text{(a)} \quad \epsilon = \sum_{i=1}^{n} \epsilon_i \quad , \quad \epsilon_i = \epsilon_1(P_i)$$

or

$$\text{(b)} \quad \begin{aligned} \epsilon &= \sum_{i=1}^{n} \epsilon_i + \sum_{i<j} \epsilon_{ij} \\ \epsilon_i &= \epsilon_1(P_i) \quad , \quad \epsilon_{ij} = \epsilon_{12}(P_i,P_j); \end{aligned}$$

We assume that $f(P) = f(P_1 \ldots P_n)$ is symmetric in the n (identical) molecules. In order to compute the amount of ϵ in a domain, it must be localized with respect to the molecules; ϵ_i is, of course, assumed to be localized at P_i; we adopt the further convention that ϵ_{ij} is localized one-half at P_i and one-half at P_j. From this it is easy to show that in case (a) the density of ϵ in P_1 is

$$n\epsilon_1 f_1 \tag{93}$$

and in case (b) it is

$$n\epsilon_1 f_1 + \frac{1}{2}n(n-1)\int \epsilon_{12} f_{12}\, dP_2 \tag{94}$$

The notation is

$$\begin{aligned} f_1 = f_1(P_1) &= \int f(P)\frac{dP}{dP_1} = \int f(P_1 \ldots P_n)\, dP_2 \ldots dP_n \\ f_{12} = f_{12}(P_1,P_2) &= \int f(P)\frac{dP}{dP_1 dP_2} \end{aligned} \tag{95}$$

etc. We integrate through (90) with respect to dP/dP_1, then multiply by $n\epsilon_1$, and finally integrate with respect to dP_1/dx_1 to get

$$\begin{aligned} \frac{\partial}{\partial t}(\nu\bar{\epsilon}_1) + \frac{\partial}{\partial \mathbf{x}_1}\cdot(\nu\overline{\epsilon_1\xi_1}) - (n-1)\nu\left(\overline{\frac{\partial\epsilon_1}{\partial\xi_1}\cdot\mathbf{F}_{12}} + \overline{\frac{\partial\epsilon_1}{\partial\mathbf{p}_1}\cdot\mathbf{G}_{12}}\right) \\ = \nu\left(\overline{\xi_1\cdot\frac{\partial\epsilon_1}{\partial\mathbf{x}_1}} + \overline{\mathbf{p}_1\cdot\frac{\partial\epsilon_1}{\partial\mathbf{q}_1}} + \overline{\mathbf{F}_{11}\cdot\frac{\partial\epsilon_1}{\partial\xi_1}} + \overline{\mathbf{G}_{11}\cdot\frac{\partial\epsilon_1}{\partial\mathbf{p}_1}}\right) \end{aligned} \tag{96}$$

It has been assumed that f vanishes at the extreme range of integration (or is periodic) for all variables. We define the mean value

$$\bar{\psi} = \frac{\int \psi f\, dP/dx_1}{\int f\, dP/dx_1} = \frac{n}{\nu}\int \psi f\, dP/dx_1 \tag{97}$$

where

$$\nu = n \int f\, dP/dx_1 \tag{98}$$

is the number density in physical space. Also, note that in case (a)

$$e = \nu\bar{\epsilon}_1 \tag{99}$$

is the volume density of ϵ. Similarly, integrating through (90) with respect to dP/dP_1dP_2, then multiplying by $n\epsilon_{12}$ and integrating with respect to dP_2dP_1/dx_1, we obtain

$$\begin{aligned} \frac{\partial}{\partial t}(\nu\bar{\epsilon}_{12}) + \frac{\partial}{\partial \mathbf{x}_1}\cdot(\nu\overline{\epsilon_{12}\xi_1} - (n-2)\nu[\overline{(1,2,3)} + \overline{(2,1,3)}] \\ = \nu\left(\overline{\frac{\partial\epsilon_{12}}{\partial\mathbf{x}_1}\cdot\xi_1} + \overline{\frac{\partial\epsilon_{12}}{\partial\mathbf{x}_2}\cdot\xi_2} + \overline{\frac{\partial\epsilon_{12}}{\partial\mathbf{q}_1}\cdot\mathbf{p}_1} + \overline{\frac{\partial\epsilon_{12}}{\partial\mathbf{q}_2}\cdot\mathbf{p}_2}\right) \\ + \nu[\overline{(1,2,1)} + \overline{(1,2,2)} + \overline{(2,1,1)} + \overline{(2,1,2)}] \end{aligned} \tag{100}$$

where

$$\left.\begin{aligned} (i,j) &= \frac{\partial\epsilon_i}{\partial\xi_i}\cdot\mathbf{F}_{ij} + \frac{\partial\epsilon_i}{\partial\mathbf{p}_i}\cdot\mathbf{G}_{ij} \\ (i,j)^* &= \frac{\partial\epsilon_{ij}^*}{\partial\xi_i}\cdot\mathbf{F}_{ij} + \frac{\partial\epsilon_{ij}^*}{\partial\mathbf{p}_i}\cdot\mathbf{G}_{ij} \\ (i,j,k) &= \frac{\partial\epsilon_{ij}}{\partial\xi_i}\cdot\mathbf{F}_{ik} + \frac{\partial\epsilon_{ij}}{\partial\mathbf{p}_i}\cdot\mathbf{G}_{ik} \end{aligned}\right\} \tag{101}$$

In case (b)

$$\left.\begin{aligned} e &= \nu\overline{\epsilon_{12}^*} \\ \epsilon_{12}^* &= \epsilon_1 + \frac{1}{2}(n-1)\epsilon_{12} \end{aligned}\right\} \tag{102}$$

Up to now we have not made use of the fact that ϵ is an integral. We assume that all external forces are included in $\mathbf{F}_{ii}$ and $\mathbf{G}_{ii}$—if these are dropped the system is isolated. If molecule 1 is isolated, $d\epsilon_1/dt = 0$, which leads to the identity

$$\frac{\partial\epsilon_1}{\partial\mathbf{x}_1}\cdot\xi_1 + \frac{\partial\epsilon_1}{\partial\mathbf{q}_1}\cdot\mathbf{p}_1 = 0 \tag{103}$$

If the system consisting of molecules 1 and 2 is isolated, then $\frac{d}{dt}(\epsilon_1 + \epsilon_2) = 0$ in case (a) and $d/dt\,(\epsilon_1 + \epsilon_2 + \epsilon_{12}) = 0$ in case (b), leading to the identities

$$(1,2) + (2,1) = 0 \tag{104}$$

and

$$\begin{aligned} \frac{\partial\epsilon_{12}}{\partial\mathbf{x}_1}\cdot\xi_1 + \frac{\partial\epsilon_{12}}{\partial\mathbf{x}_2}\cdot\xi_2 + \frac{\partial\epsilon_{12}}{\partial\mathbf{q}_1}\cdot\mathbf{p}_1 + \frac{\partial\epsilon_{12}}{\partial\mathbf{q}_2}\cdot\mathbf{p}_2 \\ + (1,2) + (2,1) + (1,2,2) + (2,1,1) = 0 \end{aligned} \tag{105}$$

Similarly, for a system of three molecules in case (b)

$$(1,2,3) + (2,1,3) + (1,3,2) + (2,3,1) + (3,1,2) + (3,2,1) = 0 \tag{106}$$

By the use of these identities, for case (a) we can obtain

$$\begin{aligned} \frac{\partial}{\partial t}(\nu\bar{\epsilon}_1) + \frac{\partial}{\partial \mathbf{x}_1}\cdot(\nu\overline{\epsilon_1\xi_1}) - \nu\overline{(1,1)} \\ + \frac{1}{2}(n-1)\nu[\overline{(2,1)} - \overline{(1,2)}] = 0 \end{aligned} \tag{107}$$

and for case (b)

$$\begin{aligned} \frac{\partial}{\partial t}(\nu\overline{\epsilon_{12}^*}) + \frac{\partial}{\partial \mathbf{x}_1}\cdot(\nu\overline{\epsilon_{12}^*\xi_1}) - \nu\overline{(1,1)}^* + \\ \frac{1}{2}(n-1)\nu[\overline{(2,1)} - \overline{(1,2)}] + \\ \frac{1}{6}(n-1)(n-2)\nu[\overline{(1,3,2)} + \\ \overline{(3,1,2)} - \overline{(3,2,1)} - \overline{(2,3,1)}] = 0 \end{aligned} \tag{108}$$

In order to put these equations into the desired form (75), the brackets [ ] must be shown to be equivalent to divergence expressions. This can always be done in infinitely many ways. The flow quantity, $\mathbf{Q}$, is not defined uniquely by the differential equation (75), so we must consider the original definition leading to the integral form (74).

But first we insert a simple formula of Irving and Kirkwood. By differentiating under the integral sign, we verify that the divergence of the vector function

$$\mathbf{K}(\mathbf{x}) = \frac{1}{2}\int \mathbf{y}\,\mathrm{d}y \int_0^1 \varphi(\mathbf{x} - \alpha\mathbf{y}, \mathbf{x} + (1 - \alpha)\mathbf{y})\,\mathrm{d}\alpha \qquad (109)$$

is

$$\int \frac{1}{2}\,[\varphi(\mathbf{y},\mathbf{x}) - \varphi(\mathbf{x},\mathbf{y})]\mathrm{d}y$$

or simply $\int \varphi(\mathbf{x},\mathbf{y})\mathrm{d}y$ if $\varphi(\mathbf{x},\mathbf{y}) = -\varphi(\mathbf{y},\mathbf{x})$. This formula can be applied directly to (107) and (108) since the expressions in brackets have the form $\int \varphi(\mathbf{x},\mathbf{y})\mathrm{d}y$ with $\varphi(\mathbf{x},\mathbf{y}) = -\varphi(\mathbf{y},\mathbf{x})$.

In order to compute the flow of ϵ into a domain D passing through a given element of its surface, it is first necessary to localize the flow of ϵ. For that part of the flow which is carried with the molecules, this has already been done by the localization of ϵ itself; this is responsible for the terms $\frac{\partial}{\partial \mathbf{x}_1}\cdot(\nu\overline{\epsilon_1\xi_1})$ in (107) and $\frac{\partial}{\partial \mathbf{x}_1}\cdot(\overline{\epsilon_{12}^{*}\xi_1})$ in (108). There remains the flow of ϵ due to intermolecular forces. In case (a) it seems natural to localize the flow between two molecules along their line of centers; in case (b) this is not so natural since a force of molecule 1 on molecule 2 can transfer ϵ to molecule 3; nevertheless some justification can be given, and this is assumed. Without carrying out the computations, we state that the result takes the form of $\mathbf{K}(\mathbf{x})$ in (109) except that the range of integration of α depends on the domain D as well as on the point $\mathbf{x}$. In other words, an expression has been obtained for the flow $\mathbf{Q}$, but it is not a point function of $\mathbf{x}$ and t. The same computation shows that (109) *is* exact if the domain D is a half-space. Consequently, by changing the definition of "the flow of ϵ across $\mathrm{d}A$," we obtain a point function $\mathbf{Q}(\mathbf{x},t)$ which, when integrated over the whole boundary, gives the correct total flow into any domain D; (the difference between the two $\mathbf{Q}$'s has zero divergence). The discrepancy between the two $\mathbf{Q}$'s is on the order of the molecular radius compared to the radius of curvature of the surface—in general this is extremely small.

Using (109), we obtain for $\mathbf{Q}$ the expressions

$$\mathbf{Q}_a = \nu\overline{\epsilon_1\mathbf{c}_1} + n(n - 1)\mathbf{K}_a \qquad (110)$$

$$\mathbf{Q}_b = \nu\overline{\epsilon^{*}\mathbf{c}_1} + n(n - 1)\mathbf{K}_a + \frac{1}{2}n(n - 1)(n - 2)\mathbf{K}_b$$

where

$$\varphi_a(\mathbf{x}_1,\mathbf{x}_2) = \int\left(\frac{\partial\epsilon_1}{\partial\xi_1}\cdot\mathbf{F}_{12} + \frac{\partial\epsilon_1}{\partial\mathbf{p}_1}\cdot\mathbf{G}_{12}\right)f_{12}\,\frac{\mathrm{d}P_1}{\mathrm{d}x_1}\,\frac{\mathrm{d}P_2}{\mathrm{d}x_2} \qquad (111)$$

$$\varphi_b(\mathbf{x}_1,\mathbf{x}_2) = \int\left(\frac{\partial\epsilon_{13}}{\partial\xi_1}\cdot\mathbf{F}_{12} + \frac{\partial\epsilon_{13}}{\partial\mathbf{p}_1}\cdot\mathbf{G}_{12} + \frac{\partial\epsilon_{13}}{\partial\xi_3}\cdot\mathbf{F}_{12} + \frac{\partial\epsilon_{13}}{\partial\mathbf{p}_3}\cdot\mathbf{G}_{12}\right)f_{123}\,\frac{\mathrm{d}P_1}{\mathrm{d}x_1}\,\frac{\mathrm{d}P_2}{\mathrm{d}x_2}\,\mathrm{d}P_3$$

and

$$\mathbf{c}_1 = \xi_1 - \mathbf{u} \qquad (112)$$

Equation (77) is obtained by setting $\epsilon_1 = 1$ in (107) and identifying $\bar{\xi}_1$ with $\mathbf{u}$.

For the conservation of momentum, $\epsilon_1 = m\xi_1$, and we have

$$\left.\begin{aligned} P^{ij} &= \nu\overline{c_1^i c_1^j} + n(n - 1)K^{ij} \\ \varphi^i &= \int mF_{12}^i f_{12}\,\frac{\mathrm{d}P_1}{\mathrm{d}x_1}\,\frac{\mathrm{d}P_2}{\mathrm{d}x_2} \end{aligned}\right\} \qquad (113)$$

For central forces, $F_{12}^i = (x_2^i - x_1^i)F^{*}(|\mathbf{x}_2 - \mathbf{x}_1|)$, and

$$\mathbf{K}^{ij} = \frac{1}{2}\,m\int y^i y^j F^{*}(y)\mathrm{d}y\int_0^1 f_{12}\,(\mathbf{x}_1 - \alpha\mathbf{y}, \mathbf{x}_2 + (1 - \alpha)\mathbf{y})\mathrm{d}\alpha$$

so the stress tensor is symmetric. If, in addition, f_{12} depends on $|\mathbf{x}_2 - \mathbf{x}_1|$ alone, K^{ij} is diagonal. If F_{12} is not central, it gives rise to non-diagonal and asymmetric components of K^{ij} which are, *a priori*, of the same order of magnitude.

For the conservation of angular momentum

$$\left.\begin{aligned} \epsilon_1^{ij} &= m(x_1^i\xi_1^j - x_1^j\xi_1^i) + \mu_1^{ij} \\ \nu\overline{\mu_1^{ij}} &= m^{ij} \end{aligned}\right\} \qquad (114)$$

where μ_1^{ij} is a function of $\mathbf{p}_1$ and $\mathbf{q}_1$ only. We find

$$\left.\begin{aligned} q^{ijk} &= \nu\overline{\mu^{ij}c^k} - n(n - 1)K^{ijk} \\ \varphi^{ij} &= \int\frac{\partial\mu_1^{ij}}{\partial\mathbf{p}_1}\cdot\mathbf{G}_{12}\,f_{12}\frac{\mathrm{d}P_1}{\mathrm{d}x_1}\,\frac{\mathrm{d}P_2}{\mathrm{d}x_2} \end{aligned}\right\} \qquad (115)$$

To obtain the energy flux in the form (85), it is necessary to introduce in each molecule a rigid coördinate system thereby defining w_1^{ij}, the angular velocity of the molecule. We make the identification

$$\omega^{ij} = \overline{w}_1^{ij} \qquad (116)$$

and write

$$\overline{w}_1^{ij} = \omega^{ij} + w_1^{ij\prime} \qquad (117)$$

The energy is put in the form

$$\epsilon_1 = \frac{1}{2}m\xi_1^2 + \sum_{i,j}\frac{1}{2}w_1^{ij}\mu_1^{ij} + \epsilon_1' \qquad (118)$$

where w_1^{ij} is a function of $\mathbf{p}_1$ and $\mathbf{q}_1$ alone, and ϵ_1' of all the coördinates P_1; ϵ_{12} is allowed to be a function of all the coördinates P_1 and P_2. For a rigid molecule, $\epsilon_1' = 0$. We obtain

$$q^r = \nu\left(\frac{1}{2}\,\overline{mc_1^2c_1^r} + \sum_{i,j}\frac{1}{2}\,\overline{w^{ij\prime}\mu^{ij}c_1^r} + \overline{\epsilon_1'c_1^r} + \frac{1}{2}(n - 1)\overline{\epsilon_{12}c_1^r}\right) + n(n - 1)K_a^r + \frac{1}{2}\,n(n - 1)(n - 2)K_b^r \qquad (119)$$

where

$$\varphi_a = \int\left(m\mathbf{c}_1\cdot\mathbf{F}_{12} + \sum_{i,j}\frac{1}{2}\,\frac{\partial}{\partial\mathbf{p}_1}\,(w^{ij\prime}\mu^{ij})\cdot\mathbf{G}_{12} + \frac{\partial\epsilon_1'}{\partial\xi_1}\cdot\mathbf{F}_{12} + \frac{\partial\epsilon_1'}{\partial\mathbf{p}_1}\cdot\mathbf{G}_{12}\right)f_{12}\,\frac{\mathrm{d}P_1}{\mathrm{d}x_1}\,\frac{\mathrm{d}P_2}{\mathrm{d}x_2} \qquad (120)$$

$$\varphi_b = \int\frac{\partial\epsilon_{13}}{\partial\xi_1}\cdot\mathbf{F}_{12} + \frac{\partial\epsilon_{13}}{\partial\mathbf{p}_1}\cdot\mathbf{G}_{12} + \frac{\partial\epsilon_{13}}{\partial\xi_3}\cdot\mathbf{F}_{12} + \frac{\partial\epsilon_{13}}{\partial\mathbf{p}_3}\cdot\mathbf{G}_{12}\,f_{123}\,\frac{\mathrm{d}P_1}{\mathrm{d}x_1}\,\frac{\mathrm{d}P_2}{\mathrm{d}x_2}\,\mathrm{d}P_3$$

This formula can be written in many alternative forms using the symmetry relations (106) and interchanging molecules 2 and 3.

These results can easily be generalized to the case of several species of molecules. Also, formulas are easily derived for the "partial integrals" ϵ_{12} alone, translational kinetic energy alone, the momentum of a single species of molecule alone, etc. In such cases, some, but not all of the identities (103)–(106) will hold.

THE MACROSCOPIC EQUATIONS OF TRANSPORT*

BY JOHN G. KIRKWOOD AND BRYCE CRAWFORD, JR.

Sterling Chemistry Laboratory, Yale University, New Haven, Connecticut and School of Chemistry, University of Minnesota, Minneapolis, Minnesota

Received August 18, 1952

The equations of continuity, motion and of energy and entropy transport in multi-component, chemically reacting fluid mixtures are formulated on the basis of the postulate of partial local thermodynamic equilibrium. In this approximation, it is assumed that a thermodynamic temperature can be defined at each point in the fluid and that the intensive thermodynamic functions, chemical potentials, partial specific enthalpies, partial specific entropies, etc., possess their equilibrium values as functions of the local temperature and densities of the several components. It is shown that the postulate of partial local equilibrium uniquely determines a dissipation function in terms of the diffusion and heat currents, the chemical potential and temperature gradients, the viscous stresses and the local free energy increments of the several chemical reactions. When phenomenological relations between the viscous stresses, heat current, diffusion currents and the rate of strain, temperature gradient and chemical potential gradients are introduced into the equations of transport, a system of partial differential equations is obtained which determines the velocity field and the local thermodynamic state of the fluid in terms of initial and boundary conditions. The analysis leads to a generalization of results previously obtained by Eckart, Curtiss and Hirschfelder, and others. Chemical reactions are treated in terms of a relaxation-time spectrum which characterizes the lag behind equilibrium.

The extension of thermodynamics to apply to irreversible processes has received considerable attention since the early work of Eckart,[1] Tolman and Fine,[2] and Onsager.[3] We may refer to the recent monographs of Prigogine,[4] de Groot[5] and Denbigh.[6]

In the present paper we formulate the equations of transport from the purely macroscopic standpoint, using the approximation of local thermodynamic equilibrium, with a somewhat different view. Our object is to obtain the general equations governing the behavior in time and space of any multicomponent, chemically reacting fluid, to the approximation indicated.

The Hydrodynamic Equations

We consider an element of fluid, and assume we may adequately describe its state at time t by giving its specific energy E, its density ρ, its composition in terms of weight fractions x_α, and its velocity $\mathbf{u}$. For a system in equilibrium, these quantities will be constant in space and in time; for our flow system, they will vary both in space and in time, with the substantial derivative, $\mathrm{d}/\mathrm{d}t$, being connected to the time-derivative at a fixed point, $\partial/\partial t$, by the usual relation

$$\mathrm{d}/\mathrm{d}t = \partial/\partial t + \mathbf{u}\cdot\nabla \qquad (1)$$

The flow pattern may be characterized in terms of the heat current, diffusion currents and chemical reactions occurring. The material currents might be described in terms of the local mean velocity $\mathbf{u}_\alpha$ for each component α; and indeed we shall have occasion to consider these *total fluxes* $\rho_\alpha\mathbf{u}_\alpha$. But we assume that these velocities $\mathbf{u}_\alpha$ do not greatly differ, and we shall describe the material currents in terms of the mean velocity $\mathbf{u}$ given by

$$\rho\mathbf{u} = \Sigma_\alpha\rho_\alpha\mathbf{u}_\alpha;\ \ \rho_\alpha = x_\alpha\rho \qquad (2)$$

and the diffusion currents

$$\mathbf{j}_\alpha = \rho_\alpha(\mathbf{u}_\alpha - \mathbf{u}) \ \ ; \ \ \Sigma_\alpha\mathbf{j}_\alpha = 0 \qquad (3)$$

Thus motion is divided into the convective motion described by $\mathbf{u}$ and the diffusive motions $\mathbf{j}_\alpha$. We shall ultimately linearize our equations with respect to the latter.

To describe the chemical processes, we may first write the chemical equation for the rth reaction as

$$0 = \Sigma_\alpha\nu_\alpha^r\mathrm{A}_\alpha \qquad (4)$$

where A_α is the chemical symbol for component α and ν_α is the number of *grams* of α produced per gram of reaction. (We note that $\Sigma_\alpha\nu_\alpha^r = 0$.) Next we introduce the progress variable λ_r, equal to the grams of reaction occurred per gram of original sample; then in a sample of mass m the change of mass of α, m_α, will be

$$\mathrm{d}m_\alpha = m\Sigma_r\nu_\alpha^r\mathrm{d}\lambda_r \qquad (5)$$

Our first task is to relate the changing state of the fluid to the flow pattern. We may begin this with the aid of the basic relations of hydrodynamics, the equation of motion and the equations of continuity of matter and of energy.

Equations of Continuity of Matter.—The overall equation of continuity of matter, for the fluid element as a whole, is of course

$$\frac{\mathrm{d}\rho}{\mathrm{d}t} + \rho\nabla\cdot\mathbf{u} = 0 \qquad (6)$$

However, we may also apply the continuity principle separately to each component α, relating the change of local density of that component, ρ_α, to the divergence of the total flux $\rho_\alpha\mathbf{u}_\alpha$ and the local source ϕ_α.

---

* This study was begun at the California Institute of Technology in 1950–51, when B. L. C. was a Guggenheim Fellow on Sabbatical leave from the University of Minnesota.

(1) C. Eckart, *Phys. Rev.*, **58**, 267, 269, 919 (1940).

(2) R. C. Tolman and P. C. Fine, *Rev. Modern Phys.*, **20**, 51 (1948).

(3) L. Onsager, *Phys. Rev.*, **37**, 405 (1931); **38**, 2265 (1931).

(4) I. Prigogine, "Étude Thermodynamique des processes irreversibles," Desoer, Liege, 1947.

(5) S. R. deGroot, "Thermodynamics of Irreversible Processes," Interscience Publishers, Inc., New York, N. Y., 1951.

(6) K. G. Denbigh, "Thermodynamics of the Steady State," John Wiley and Sons, Inc., New York, N. Y., 1951.

The local source ϕ_α is just the mass of α produced per unit volume per unit time by chemical reaction. In terms of our progress variables, we may apply eq. (5) to our element of fluid and we see that

$$\phi_\alpha = \rho\Sigma_r \nu_\alpha^r \dot{\lambda}_r \tag{7}$$

So the equation of continuity of α becomes

$$\frac{\partial \rho_\alpha}{\partial t} + \nabla\cdot(\rho_\alpha \mathbf{u}_\alpha) = \rho\Sigma_r \nu_\alpha^r \dot{\lambda}_r \tag{8}$$

or, after some rearrangement to express this in our chosen variables

$$\rho\frac{\mathrm{d}x_\alpha}{\mathrm{d}t} + \nabla\cdot\mathbf{j}_\alpha = \rho\Sigma_r \nu_\alpha^r \dot{\lambda}_r \tag{9}$$

So we have the rate of change of composition given in terms of the diffusion currents and the chemical reactions.

The Equation of Motion.—The equation of motion for the *convective* motion of the element as a whole is

$$\rho\frac{\mathrm{d}\mathbf{u}}{\mathrm{d}t} = \nabla\cdot\sigma + \rho\mathbf{X} \tag{10}$$

or

$$\frac{\partial \rho\mathbf{u}}{\partial t} = \nabla\cdot(\sigma - \rho\mathbf{u}\,\mathbf{u}) + \rho\mathbf{X} \tag{11}$$

where σ is the stress tensor and $\rho\mathbf{X}$ describes the force acting on the element due to external fields. Presumably these outside forces might act selectively on the different components; the total effect of selective forces $\rho_\alpha\mathbf{X}_\alpha$ would then be $\rho\mathbf{X} = \Sigma_\alpha\rho_\alpha\mathbf{X}_\alpha$.

The Energy Equation.—From hydrodynamics alone, we may write down the energy balance for an element of fluid and simplify it with the aid of the equations of continuity and of motion to give

$$\rho\frac{\mathrm{d}E}{\mathrm{d}t} = \sigma:\nabla\,\mathbf{u} + \Sigma_\alpha\mathbf{j}_\alpha\cdot\mathbf{X}_\alpha - \nabla\cdot\mathbf{j}_E \tag{12}$$

where $\mathbf{j}_E$ is an energy-transport vector including the effects of both heat flow and diffusion; E is of course the specific internal energy. (If the external forces $\mathbf{X}_\alpha$ are derivable from a potential, this is *not* included in E.) This is as far as one can go from hydrodynamics; after introducing the local-equilibrium assumption, we shall re-examine this equation.

The Assumption of Local Equilibrium

We now introduce the assumption that all of the thermodynamic functions of state exist for each element of fluid, with values determined by the local state variables (say ρ and E) according to the equilibrium relations. Thus the local temperature T may be defined by the same function $T(\rho,E)$ as is given by measurements on equilibrium systems.

The validity of this assumption has been discussed elsewhere[4]; ultimately, of course, it must be validated either by experiment or by microscopic theoretical analysis. The question thus lies beyond the scope of our discussion here.

By this assumption, then, we may write E as a function of T, p and x_α; indeed, we may write

$$E = \Sigma_\alpha x_\alpha \bar{E}_\alpha \tag{13}$$

where the partial specific energies $\bar{E}_\alpha$ are precisely those defined in equilibrium thermodynamics. We may also re-examine the energy equation by generalizing from relations valid for equilibrium states. For an equilibrium system of mass m and total energy E_t, we have

$$\mathrm{d}E_t = \left(\frac{\partial E_t}{\partial T}\right)_{p,m}\mathrm{d}T + \left(\frac{\partial E_t}{\partial p}\right)_{T,m}\mathrm{d}p + \Sigma_\alpha\bar{E}_\alpha\mathrm{d}m_\alpha \tag{14}$$

If the system is closed, $\mathrm{d}m_\alpha = 0$, and moreover we may write

$$\mathrm{d}E_t = \mathrm{d}q_r - p\mathrm{d}V \tag{15}$$

whence

$$\begin{aligned}\mathrm{d}q_r &= \left[\left(\frac{\partial E_t}{\partial T}\right)_{p,m}\mathrm{d}T + \left(\frac{\partial E_t}{\partial p}\right)_{T,m}\mathrm{d}p\right] \\ &\quad + p\left[\left(\frac{\partial V}{\partial T}\right)_{p,m}\mathrm{d}T + \left(\frac{\partial V}{\partial p}\right)_{T,m}\mathrm{d}p\right] \\ &= \left[\frac{\partial E_t}{\partial T}\mathrm{d}T + \frac{\partial E_t}{\partial p}\mathrm{d}p\right] + p\mathrm{d}V\end{aligned} \tag{16}$$

Inserting this in (14), we find

$$\mathrm{d}E_t = \mathrm{d}q_r - p\mathrm{d}V + \Sigma_\alpha\bar{E}_\alpha\mathrm{d}m_\alpha \tag{17}$$

If we include kinetic energy and external forces, the direct generalization is

$$\begin{aligned}\frac{\partial}{\partial t}\left[\Sigma_\alpha\rho_\alpha\left(\bar{E}_\alpha + \frac{\mathbf{u}_\alpha^2}{2}\right)\right] &= \Sigma_\alpha\rho_\alpha\mathbf{u}_\alpha\cdot\mathbf{X}_\alpha + \nabla\cdot(\mathbf{u}\cdot\sigma) - \nabla\cdot\mathbf{q} \\ &\quad - \nabla\cdot\left[\Sigma_\alpha\rho_\alpha\mathbf{u}_\alpha\left(\bar{E}_\alpha + \frac{\mathbf{u}^2}{2}\right)\right]\end{aligned} \tag{18}$$

If we now linearize with respect to $\mathbf{j}_\alpha$, and utilize the continuity and force equations, we obtain

$$\rho\frac{\mathrm{d}E}{\mathrm{d}t} = \sigma:\nabla\mathbf{u} - \nabla\cdot\mathbf{q} - \Sigma_\alpha\nabla\cdot\mathbf{j}_\alpha\bar{E}_\alpha + \Sigma_\alpha\mathbf{j}_\alpha\cdot\mathbf{X}_\alpha \tag{19}$$

in which a separation has been effected between the energy transport associated with diffusion currents, and that due to pure heat flow.

There exists a certain arbitrariness in the definition of heat flow for open systems, even in the field of equilibrium states. Our definition, based on the first law of thermodynamics, seems to us to follow from a clear-cut operational distinction between heat and work. Certain authors prefer to base the definition of heat flow on the second law, in the form

$$\mathrm{d}S = \mathrm{d}q'/T + \Sigma_\alpha\,\bar{S}_\alpha\,\mathrm{d}\,m_\alpha$$

The heat flow then becomes identified with $\mathbf{q}'$ rather than $\mathbf{q}$ (see equations (23) and (24) below). While it is true that $\mathbf{q}'$ enters as a fundamental quantity in the linear relations between currents and forces (equations (26) below), the difference term $p\Sigma_\alpha\mathbf{j}_\alpha\bar{V}_\alpha$ is clearly operationally distinguishable as the work associated with the volume increment produced by diffusion of the several components into the element at constant T and p. If the heat flow is defined as $\mathbf{q}'$, then the energy equation (18) must be treated rather artificially, with partial enthalpies $\bar{H}_\alpha$ replacing the $\bar{E}_\alpha$, and with a somewhat unrealistic deletion of the work associated with the diffusion-produced volume increment from the work term of which it is properly an operational part. However, if used consistently, either definition of the heat flow leads to correct results.

The Entropy Equation.—The local-equilibrium assumption also permits us to define the specific entropy of our element of fluid through the relation

$$dE = TdS - p\,\mathrm{d}(1/\rho) + \Sigma_\alpha \mu_\alpha\,\mathrm{d}x_\alpha \qquad (20)$$

We may note that the chemical potential μ_α used here does *not* include the potential of the external forces $\mathbf{X}$; also that in using the term $p\,\mathrm{d}(1/\rho)$ we are limiting ourselves to a fluid. Since we have expressions for $(\mathrm{d}E/\mathrm{d}t)$, $(\mathrm{d}\rho/\mathrm{d}t)$ and $(\mathrm{d}x_\alpha/\mathrm{d}t)$ we may easily get an equation for $(\mathrm{d}S/\mathrm{d}t)$. In order to have this in the most useful form, we shall manipulate the terms to get an equation of the form

$$\frac{\mathrm{d}S}{\mathrm{d}t} = \frac{\Phi}{T} - \nabla\cdot\mathbf{j}_S \qquad (21)$$

i.e., an "entropy source" term and a term involving the divergence of an "entropy flow". The entropy source term we have written for convenience as a dissipation function divided by T; we shall arrange for Φ to be in the form

$$\Phi = \Sigma_i \mathbf{j}_i\cdot\mathbf{F}_i \qquad (22)$$

where the $\mathbf{j}_i$ are "currents" and the $\mathbf{F}_i$ "conjugate forces," gradients being very satisfactory as forces. This will permit us to apply Onsager's relations to the $\mathbf{j}_i$ and $\mathbf{F}_i$ so chosen.

If we carry out this algebra, we find the form (21) easily achieved, with Φ a sum of four terms

$$\begin{aligned}
\phi_1 &= (\sigma + p\,\mathbf{1}) : \nabla\mathbf{u}\\
\phi_2 &= -\rho\Sigma_r \Delta F_r \dot{\lambda}_r\\
\phi_3 &= -\Sigma_\alpha \mathbf{j}_\alpha\cdot\nabla_T\mu\\
\phi_4 &= -\mathbf{q}'\cdot\nabla \ln T\\
\mathbf{j}_S &= (\mathbf{q}'/T) + \Sigma_\alpha \mathbf{j}_\alpha \bar{S}_\alpha \qquad (23)
\end{aligned}$$

where

$$\begin{aligned}
\Delta F_r &= \Sigma_\alpha \nu_\alpha^r \mu_\alpha\\
\nabla_T\mu_\alpha' &= \nabla\mu_\alpha' + \bar{S}_\alpha\nabla T\\
&= \nabla\mu_\alpha - \mathbf{X}_\alpha + \bar{S}_\alpha\nabla T\\
\mathbf{q}' &= \mathbf{q} - \Sigma_\alpha \mathbf{j}_\alpha p\bar{V}_\alpha \qquad (24)
\end{aligned}$$

The four contributions to Φ represent the dissipation due to convection, chemical reaction, diffusion and heat flow, respectively. In the first, both flow and force are (second-order) tensors; in the second, both are scalars; in the two last, both are vectors.

The inclusion of the external force $\mathbf{X}_\alpha$ in the gradient $\nabla\mu_\alpha'$ is made here for convenience. If $\mathbf{X}_\alpha$ is derivable from a potential, one could express this inclusion by saying that μ_α' is the chemical potential *including* the external potential. Inclusion or exclusion is merely a matter of convenience in writing the equations; we have written ours in the fashion which seemed to us most easily adapted to specific problems likely to arise. In particular cases, as when the external force is a rapidly varying function of time, explicit treatment of the $\mathbf{X}_\alpha$ may be strongly indicated.

We may note that electrical conductance is included in our equations in the diffusion terms. If component α carries a charge Z_α (per gram), then the current $\mathbf{i}$ is given by $\Sigma_\alpha Z_\alpha \mathbf{j}_\alpha$; in the presence of an external electric field of strength $\mathbf{E}$, the force $\mathbf{X}_\alpha = Z_\alpha\mathbf{E}$ will apply to this component; and the dissipation term $\Sigma_\alpha \mathbf{j}_\alpha\cdot\mathbf{X}_\alpha$ included in ϕ_3 gives the electrical dissipation $\mathbf{i}\cdot\mathbf{E}$.

The Phenomenological Relations

Experience shows that in many systems the flows and forces of equations (23) are linearly related. We must treat scalars, vectors and tensors separately, for the entities of different tensorial character cannot interact (Curie's theorem). We shall also defer discussion of chemical reaction. Thus we may now introduce the phenomenological relations

$$\sigma = -[p + \left(\tfrac{2}{3}\eta - \varphi\right)(\nabla\cdot\mathbf{u})]\mathbf{1} + 2\eta\dot{\epsilon} \qquad (25a)$$

$$\dot{\epsilon} = \mathrm{sym}\,(\nabla\mathbf{u}) \qquad (25b)$$

$$\begin{aligned}
-\mathbf{q}' &= \Omega_{00}\nabla \ln T + \Sigma_\alpha\Omega_{0\alpha}\nabla_T\mu_\alpha'\\
-\mathbf{j}_\alpha &= \Omega_{\alpha 0}\nabla \ln T + \Sigma_\beta\Omega_{\alpha\beta}\nabla_T\mu'_\beta \qquad (26)
\end{aligned}$$

Equations (25) express the conventional Newtonian stress tensor; η and φ are the coefficients of shear and volume viscosity, respectively. Equations (26) express the general linear dependence of heat flow and diffusion on the gradients of temperature and chemical potential.

The flows and gradients have been chosen to be those appearing together in the dissipation functions of (23). For this choice, Onsager has shown[3] that the matrix Ω of the coefficients in (26) is symmetric; *i.e.*, that $\Omega_{\alpha\beta} = \Omega_{\beta\alpha}$. These reciprocity relations are most useful; their application to specific problems, especially in steady-state flow, has been discussed elsewhere.[4-6]

The introduction of these relations has also been used to find the requirements for Φ to be positive.[7] That Φ should be positive—*i.e.*, that the occurrence of irreversible processes should cause an increase of entropy in each element of fluid—may be construed as a (slightly strengthened) form of the second law. Introducing (25) into (23) yields

$$\phi_1 = \varphi(\nabla.\mathbf{u})^2 + 2\eta\left[\dot{\epsilon} - \frac{1}{3}(tr\,\dot{\epsilon})\mathbf{1}\right]:\left[\dot{\epsilon} - \frac{1}{3}(tr\,\dot{\epsilon})\mathbf{1}\right] \qquad (27)$$

which is essentially positive if the viscosity coefficients η and φ are positive. Introducing (26) into (23) gives for $\phi_3 + \phi_4$ a quadratic form in the gradients $\nabla\ln T$ and $\nabla_T\mu_\alpha'$; this is positive if the matrix Ω is positive-definite.

We may note that a different set of (vector) currents and forces may be used. The desirable properties are that the dissipation function be of the form (22), and that the matrix of coefficients in the linear relations similar to (26) be symmetric and positive-definite. If we transform the currents $\mathbf{j}_i$ to a new set $\mathbf{j}_i'$ by any orthogonal homogeneous linear transformation, and the forces $\mathbf{F}_i$ to new forces $\mathbf{F}_i'$ by the same transformation, these properties will be retained.

The Transport Equations

We now wish to recast our equations to obtain a general set of transport equations describing the state of the fluid as a function of space and time. We choose for our independent variables $\mathbf{u}$, T, p and x_α; other variables such as ρ and μ_α may be written as functions of these.

Actually, we already have equations for the change of x_α and $\mathbf{u}$, equations (9) and (10). We need to eliminate ρ and S from equations (6) and

(7) C. F. Curtiss and J. O. Hirschfelder, *J. Chem. Phys.*, **18**, 171 (1950).

(21). To this end, we use the thermodynamic relations

$$\rho\kappa C_V\,\mathrm{d}T = \kappa(\rho\,T\,\mathrm{d}S) + \beta T(\mathrm{d}p/\rho) + \Sigma_\alpha(\rho\,\mathrm{d}x_\alpha)[\beta T\,\overline{V}_\alpha - \kappa T\,\overline{S}_\alpha] \quad (28)$$

$$\rho\kappa C_V\,\mathrm{d}p = \beta(\rho T\mathrm{d}S) + \rho C_p(\mathrm{d}p/\rho) + \Sigma_\alpha(\rho\,\mathrm{d}x_\alpha)[\rho C_p\overline{V}_\alpha - \beta T\overline{S}_\alpha] \quad (29)$$

Here β and κ are the usual volume-expansion and compressibility coefficients

$$\beta = \frac{1}{V}\left(\frac{\partial V}{\partial T}\right)_p, \ \kappa = -\frac{1}{V}\left(\frac{\partial V}{\partial p}\right)_T \quad (30)$$

The introduction of equations (6), (9) and (21) thus leads to

$$\rho\kappa C_V\frac{\mathrm{d}T}{\mathrm{d}t} = [\kappa\phi_1 - \beta T(\nabla.\mathbf{u})] - \kappa\nabla.\mathbf{q}' - \Sigma_r\rho\dot{\lambda}_r\,(\kappa\Delta H_r - \beta T\Delta V_r) - \Sigma_\alpha\,[\kappa\mathbf{j}_\alpha\cdot\nabla\overline{H}'_\alpha + (\nabla\cdot\mathbf{j}_\alpha)\beta T\overline{V}_\alpha] \quad (31)$$

$$\rho\kappa C_V\frac{\mathrm{d}p}{\mathrm{d}t} = [\beta\,\phi_1 - \rho C_p(\nabla.\mathbf{u})] - \beta\nabla.\mathbf{q}' - \Sigma_r\rho\dot{\lambda}_r\,(\beta\Delta H_r - \rho C_p\Delta V_r) - \Sigma_\alpha\,[\beta\mathbf{j}_\alpha\cdot\nabla\,\overline{H}'_\alpha + (\nabla\cdot\mathbf{j}_\alpha)\,\rho C_p\overline{V}_\alpha] \quad (32)$$

where $\nabla\overline{H}'_\alpha$ is defined analogously to $\nabla\mu'_\alpha$ and ΔH_r, ΔV_r analogously to ΔF_r, equations (24). We may also rewrite equation (10) in the Navier–Stokes form

$$\rho\frac{\mathrm{d}\mathbf{u}}{\mathrm{d}t} = \rho\mathbf{X} - \nabla p + \eta\nabla^2\mathbf{u} + \left(\frac{1}{3}\eta + \varphi\right)\nabla\left(\nabla\cdot\mathbf{u}\right) \quad (33)$$

and we may add a formal expression of chemical kinetics

$$\frac{\mathrm{d}\lambda_r}{\mathrm{d}t} = \mathrm{f}_r\,(T;\ \rho_\alpha) \quad (34)$$

Equations (31) to (34) and (9), together with (26), form a complete set of partial differential equations describing the behavior of the variables T, p, x_α and $\mathbf{u}$ in terms of functions of these variables and of the external forces X_α. Thus the velocity field and the thermodynamic state of the fluid at every point are determined as a function of initial and boundary conditions.

Chemical Reaction

The equations we have thus found are reasonably satisfactory save for that governing reaction rate; chemical kinetics does not fit into the scheme of linear relations between flows and forces. Without discussing the microscopic reasons for this, we accept the experimental fact that the approximation of setting $\dot{\lambda}_r$ proportional to ΔF_r is not a good one.

We therefore approach the problem by dividing λ_r into two variables

$$\lambda_r = \lambda_r^0 + \xi_r \quad (35)$$

where λ_r^0 is the *equilibrium* value of the progress of the rth reaction, for the temperature, pressure and over-all composition of the fluid element. The new variable ξ_r will then measure the deviation from equilibrium, or the "lag" of the rth reaction in its attempt to maintain equilibrium.

The equation determining λ_r^0 is easily found from the condition that

$\Delta F_r = 0$ at $\lambda_r = \lambda_r^0$:

$$0 = \Sigma_\alpha\nu_\alpha^r\frac{\mathrm{d}\mu_\alpha}{\mathrm{d}t} = -\Delta S_r\frac{\mathrm{d}T}{\mathrm{d}t} + \Delta V_r\frac{\mathrm{d}p}{\mathrm{d}t} + \Sigma_\beta\Delta g_\beta^r\frac{\mathrm{d}x_\beta}{\mathrm{d}t} \quad (36)$$

$$\Delta g_\beta^r = \Sigma_\alpha\nu_\alpha^r g_{\alpha\beta};\ g_{\alpha\beta} = (\partial\mu_\alpha/\partial x_\beta)_{T,p,x_\gamma}$$

The introduction of (9) leads to the set of equations for the $\dot{\lambda}_r^0$:

$$\Sigma_s G^{rs}\frac{\mathrm{d}\lambda_s^0}{\mathrm{d}t} = \Delta S_r\frac{\mathrm{d}T}{\mathrm{d}t} - \Delta V_r\frac{\mathrm{d}p}{\mathrm{d}t} + \frac{1}{\rho}\Sigma_\beta\Delta g_\beta^r\,(\nabla\cdot\mathbf{j}_\beta) \quad (37)$$

$$G^{rs} = \Sigma_\alpha\Sigma_\beta\,\nu_\beta^s\nu_\alpha^r g_{\alpha\beta}$$

which may be combined with (31) to (33) and (9) to obtain the complete description of the fluid assuming no lag in the chemical reactions.

Chemical lag may then be treated in terms of relaxation behavior. If we expand the rate function f_r of equation (34) about the equilibrium point $(\lambda_1^0, \lambda_2^0, \ldots)$, and linearize, we have

$$\dot{\lambda}_r = \dot{\xi}_r + \dot{\lambda}_r^0 = \Sigma_s\beta_{rs}\xi_s \quad (38)$$

$$\beta_{rs} = \rho\Sigma_\alpha\nu_\alpha^s\left(\frac{\partial\mathrm{f}_r}{\partial\rho_\alpha}\right)$$

where the derivative is evaluated at the equilibrium point. We may note that the linearization used here sets the rates proportional to *concentrations;* this will be exact for some types of reaction, and should in any case be a better approximation than linearization in ΔF_r.

Equation (38) gives us a set of linear equations in the ξ_r, with a forcing function $\dot{\lambda}_r^0$ which is known from the set (37). Such a set of equations can be solved in terms of "relaxation times." If we define the determinantal function

$$\Delta(z) = |z\,\delta_{rs} - \beta_{rs}| \quad (39)$$

with minors $\Delta_{rs}(z)$ and roots κ_n, then we may write the solutions of (38) by the method of Laplace[8] transforms

$$\xi_r = \Sigma_n\Sigma_s\frac{\Delta_{rs}(\kappa_n)}{\Delta'(\kappa_n)}\xi_s^0\,e^{-t/\tau_n} - \frac{1}{2\pi i}\Sigma_s\int_{c-i\infty}^{c+i\infty}\frac{\Delta_{rs}(z)}{\Delta(z)}\,\dot{\Lambda}_s\,(z)\,e^{zt}\,\mathrm{d}z \quad (40)$$

where the ξ_s^0 are the values of ξ_s at $t = 0$, $\dot{\Lambda}_s(z)$ is the transform of $\dot{\lambda}_s^0$, and the relaxation times

$$\tau_n = -1/\kappa_n \quad (41)$$

Thus the effect of the initial conditions will die away according to these relaxation times; and when the functions $\dot{\Lambda}_s$ are inserted, the lag of the chemical reactions behind the equilibrium values λ_r^0 will also be expressed in terms of the spectrum of relaxation times.

---

(8) G. Doetsch, "Theorie und Anwendung der Laplace-Transformation," Dover, New York, 1943, pp. 329 ff.

ON THE VISCOSITY OF BINARY LIQUID MIXTURES[1]

BY FAUSTO W. LIMA

Department of Chemistry, Escola Politecnica, University of São Paulo, Brasil

Received October 23, 1951

A formula for the viscosity of binary liquid mixtures as a function of the viscosity and the density of the pure components and the density of the mixtures is proposed. It is applied to binary mixtures of toluene, bromobenzene and nitrobenzene at different temperatures and to mixtures of primary alcohols and organic acids in benzene and carbon tetrachloride at 25°. The formula accounts for the presence of the minima found in the graph for viscosity *versus* concentration and it applies when there are large differences in the viscosities of the pure components.

Introduction

By the application of the notions of parachor and molar refraction to mixtures of pure compounds much success has been achieved in the study of surface tension and refractive index of mixtures. The following reasoning will illustrate the above. Let F equal an additive-constitutive property such as parachor or molar refraction. F is always the product of a molar volume M/d (M = molecular weight in grams and d = density in g./cc.) times a function of a physical property: $\gamma^{1/4}$ in the case of parachor and $(n^2 - 1)/(n^2 + 2)$ in the case of molar refraction (γ = surface tension and n = refractive index). By putting this function of a physical property $\gamma^{1/4}$ or $(n^2 - 1)/(n^2 + 2)$ as $f(p)$, then $F = f(p)\ M/d$ for a pure compound. Now, if, for the ith component of a mixture of i components, the additive-constitutive property is designated by F_i, the molecular weight by M_i, and the density of the mixture by d, the function of the physical property for the mixture by $f(p)$, the value of F for this mixture as has been shown by Smyth[2] and co-workers and others, is obtained by

$$F = \Sigma_i x_i F_i = x_1F_1 + x_2F_2 + x_3F_3 + \ldots \quad (1)$$

or by

$$F = f(p)\Sigma_i x_i M_i/d = f(p) \times (x_1M_1 + x_2M_2 + x_3M_3 + \ldots)/d \quad (2)$$

(x_i is the mole fraction of the ith component of the mixture)

By equating formulas (1) and (2) we get

$$f(p) = d\Sigma_i x_i F_i/\Sigma_i x_i M_i = \frac{x_1F_1 + x_2F_2 + x_3F_3 + \ldots}{x_1M_1 + x_2M_2 + x_3M_3 + \ldots}\,d \quad (3)$$

and thus the physical property p (surface tension or refractive index) is obtained in terms of the properties of the components. The values of F_i can be calculated from the additivity of group or atomic values for the molecule.

Katz and co-workers[3] applied this type of reasoning to the notion of parachor and were able to predict the value of surface tension for three binary mixtures at temperatures up to 90° and pressures up to 100 atmospheres. The application of formula (3) to the case of molar refraction was made by Smyth, Engel and Wilson,[2] Koening-Gresmann[4a] and Welhm.[4b]

The present work was undertaken to establish whether or not formula (3) could be applied to Souders' viscosity constant I[5]

$$I = M\ (\log \log \eta + k)/d$$

(η = viscosity in millipoise; k = constant = 2.9 in Souders' work; the logarithms are on decimal base). By using formula (3) the viscosity of a binary mixture can be calculated as

$$\log \log \eta = d(x_1I_1 + x_2I_2)/(x_1M_1 + x_2M_2) - k \quad (4)$$

The values of I_1 and I_2 can be calculated from Souders' work.[5]

To test formula (4) viscosity and density measurements were made on binary mixtures of toluene, bromobenzene and nitrobenzene using various concentrations at temperatures from 25 to 35°.

Experimental and Results

Viscosities were determined by an Ostwald type viscometer. Densities were measured in pycnometers provided with a thermometer and a glass cap to prevent evaporation. Temperatures were controlled within ±0.03°. Viscometers, pycnometers and the flasks in which mixtures were stored were cleaned with dichromate–sulfuric acid solution, rinsed with dust-free distilled water and dried. That the viscometer constant remained uniform was verified at intervals during the experiment. For every mixture the times of flow were recorded five times and the results averaged; the agreement among the flow times for every mixture was within less than 0.2%. The liquids used were purified by distillation and crystallization. After purification, the refractive index and density were determined and were found to be in very good agreement with values listed in the literature. Differential evaporation of the two components during an experiment cannot be completely eliminated. However the surface of the liquid which is in contact with air is small and the differential evaporation in most mixtures is not appreciable.

Eight mixtures were made for every pair of compounds and results at 25, 30 and 35° are presented in Tables I, II and III, together with the values calculated with formula (4). For the toluene–bromobenzene mixture measurements were made at 25 and 30°, only.

TABLE I

OBSERVED AND CALCULATED VISCOSITIES IN TOLUENE–NITROBENZENE MIXTURES

Mole fraction nitrobenzene	25° Obsd.	25° Calcd.	30° Obsd.	30° Calcd.	35° Obsd.	35° Calcd.
0.000	5.52	5.52	5.25	5.25	4.86	4.86
.115	6.22	6.20	5.86	5.80	5.54	5.49
.227	7.02	6.95	6.60	6.58	6.18	6.08
.344	8.03	7.96	7.43	7.42	6.94	6.99
.457	8.94	9.09	8.37	8.48	7.83	7.96
.577	10.30	10.55	9.56	9.79	9.22	9.21
.675	11.69	11.83	10.80	10.97	10.42	10.25
.787	13.74	13.80	12.52	12.71	11.57	11.96
.870	15.42	15.68	14.20	14.13	13.13	13.28
1.000	18.20	18.20	16.82	16.82	15.50	15.50

---

[1] Part of this material was submitted to the University of Wisconsin as Thesis in partial fulfillment of the requirements for the Master's Degree in Chemistry, June, 1950. Presented at the XIIth International Congress of Pure and Applied Chemistry, New York, September, 1951.

[2] C. P. Smyth, E. W. Engel and E. B. Wilson, Jr., *J. Am. Chem. Soc.*, **51**, 1736 (1929).

[3] D. L. Katz and C. J. Reno, *Ind. Eng. Chem., Ind. Ed.*, **35**, 1091 (1943); D. L. Katz and C. F. Weinang, *ibid.*, **35**, 239 (1943).

[4] (a) M. L. Koening-Gressmann, Thesis, University of Munich, 1938; (b) J. Welhm, Thesis, University of Konigsberg, 1934.

[5] M. Souders, Jr., *J. Am. Chem. Soc.*, **60**, 154 (1938).

TABLE II

OBSERVED AND CALCULATED VISCOSITIES IN BROMOBENZENE–NITROBENZENE MIXTURES

Mole fraction nitrobenzene	25° Obsd.	25° Calcd.	30° Obsd.	30° Calcd.	35° Obsd.	35° Calcd.
0.000	10.68	10.68	10.08	10.08	9.38	9.38
.117	11.06	11.40	10.36	10.52	9.73	9.83
.225	11.64	12.00	10.75	11.21	10.15	10.45
.345	12.27	12.75	11.30	11.86	10.60	11.05
.464	12.96	13.55	12.09	12.58	11.17	11.72
.554	13.52	14.17	12.46	13.17	11.73	12.28
.676	14.65	15.15	13.55	14.20	12.51	13.05
.790	15.56	16.20	14.59	15.17	13.45	13.99
.887	16.73	17.20	15.51	15.96	14.23	14.60
1.000	18.20	18.20	16.82	16.82	15.50	15.50

TABLE III

OBSERVED AND CALCULATED VISCOSITIES OF TOLUENE–BROMOBENZENE MIXTURES

Mole fraction bromobenzene	25° Obsd.	25° Calcd.	30° Obsd.	30° Calcd.
0.000	5.52	5.52	5.25	5.25
.129	6.13	5.92	5.74	5.57
.267	6.72	6.51	6.26	6.10
.379	7.20	7.00	6.74	6.56
.505	7.86	7.65	7.29	7.16
.629	8.51	8.29	7.92	7.77
.736	9.10	9.01	8.57	8.43
.853	9.81	9.72	9.20	9.10
.882	9.96	9.84	9.38	9.30
1.000	10.68	10.68	10.08	10.08

Since binary solutions of toluene, bromobenzene and nitrobenzene are almost ideal it was decided that the applicability of formula (4) should also be tested for non-ideal solutions. Formula (4) was applied to mixtures of primary alcohols and organic acids in benzene and carbon tetrachloride, at 25°, using the data of Jones and co-workers.[6] Table IV gives the maximum error in calculated viscosities. Although the maximum error, in some cases, is large, the average error is only 2.9% (the value of Souders' constant used was $k = 2.9000$).

TABLE IV

MAXIMUM ERROR IN CALCULATED VISCOSITIES FROM EQUATION (4)

Component B	Component A	Max. % error	% B at max. error
Methyl alcohol	Carbon tetrachloride	6.4	50
Ethyl alcohol	Carbon tetrachloride	5.3	70
Propyl alcohol	Carbon tetrachloride	7.8	20
Butyl alcohol	Carbon tetrachloride	10.8	20
Hexyl alcohol	Carbon tetrachloride	11.4	20
Heptyl alcohol	Carbon tetrachloride	7.3	80
Octyl alcohol	Carbon tetrachloride	3.7	20
Decyl alcohol	Carbon tetrachloride	5.4	20
Acetic acid	Carbon tetrachloride	4.8	15
Butyric acid	Carbon tetrachloride	5.0	15
Caproic acid	Carbon tetrachloride	9.0	80
Heptylic acid	Carbon tetrachloride	15.0	80
Caprylic acid	Carbon tetrachloride	3.6	15
Butyric acid	Benzene	5.5	50
Valeric acid	Benzene	4.8	50
Caproic acid	Benzene	3.4	40
Heptylic acid	Benzene	4.2	40
Caprylic acid	Benzene	3.3	60

Discussion

For the almost ideal solutions of bromobenzene, nitrobenzene and toluene, the constant k was taken as 2.9000. The decimals were taken empirically up to the fourth place, although Souders reports the mean value as being 2.9. The average error between observed values and the values calculated by formula (4) is ±2.4% for all the concentration ranges of these mixtures.

For the non-ideal solutions of primary alcohols and organic acids in benzene and carbon tetrachloride the same value for k (2.9000) was used, except for the mixtures of butyl alcohol, hexyl alcohol and amyl alcohol in benzene. For these the value of k was calculated knowing the viscosity of the mixtures at a known concentration when the resulting k was used. The maximum error was smaller than when the k of the universal value (2.9000) was used (Table V). Values for the acetic acid–carbon tetrachloride mixtures are also given in Table V.

TABLE V

MAXIMUM ERROR IN CALCULATED VISCOSITIES FROM EQUATION (4) USING THE UNIVERSAL VALUE FOR k AND A VALUE PREVIOUSLY DETERMINED

Component B	Component A	k	Max % error	% B at max. error
Butyl alcohol	Benzene	2.9000	15.0	80
		2.9184	6.0	40
Amyl alcohol	Benzene	2.9000	9.0	20
		2.9119	2.8	40
Hexyl alcohol	Benzene	2.9000	12.9	80
		2.9195	8.5	40
Acetic acid	Carbon tetrachloride	2.9000	4.8	15
		2.9060	1.8	80

Jones and co-workers[6] examined the many relationships suggested for the variation of the viscosity of a mixture of liquids with composition and came to the conclusion that they do not afford proper representations when applied to the binary systems carbon tetrachloride–acids and alcohols, and benzene–acids and alcohols. The equation of Arrhenius,[7] Kendall,[8] Lees,[9] Bingham,[10] Drucker and Kassel,[11] and Meyer and Mylius,[12] do not give curves with the minima in the graph for viscosity *versus* concentration in the mixtures containing the lower alcohols or the fatty acids. The formula of Kendall and Monroe,[13] Dolezalek and Schulze,[14] Sachanov and Rjachowsky,[15] Van der Wyk,[16] Lederer,[17] Powell, Roseveare and Eyring,[18] Tuomikoski,[19]

---

[6] W. J. Jones, S. T. Bowden, W. W. Yarnold and W. H. Jones, THIS JOURNAL, **52**, 753 (1948).

[7] S. Arrhenius, *Z. physik. Chem.*, **1**, 289 (1887).

[8] J. Kendall, *Medd. Vetenskapsadad. Nobelinst.*, **2**, n. 25, 1 (1913).

[9] C. H. Lees, *Phil. Mag.*, **1**, 139 (1901).

[10] E. C. Bingham, *Am. Chem. J.*, **35**, 195 (1906).

[11] K. Drucker and R. Kassel, *Z. physik. Chem.*, **76**, 376 (1911).

[12] J. Meyer and B. Mylius, *ibid.*, **95**, 374 (1920).

[13] J. Kendall and K. P. Monroe, *J. Am. Chem. Soc.*, **39**, 1798 (1917).

[14] F. Dolezalek and A. Schulze, *Z. physik. Chem.*, **83**, 74 (1913).

[15] A. Sachanov and N. Rjachowsky, *ibid.*, **86**, 532 (1914).

[16] A. J. A. Van der Wyk, *Nature*, **138**, 846 (1936).

[17] E. L. Lederer, *ibid.*, **139**, 27 (1937).

[18] R. E. Powell, W. E. Roseveare and H. Eyring, *Ind. Eng. Chem.*, **33**, 432 (1941).

[19] P. Tuomikoski, *Suomen. Kemistilehti*, **15B**, 19 (1942).

Lutschinski[20] and Kottler[21] cannot be applied when one of the components is partly associated.

In order to compare the results with formula (4) with other expressions, formula (4) was applied to n-octyl alcohol–carbon tetrachloride mixtures at 25°. The resulting data (Table VI) together with the values given by the application of the formulas of Kendall and Monroe,[13] Sachanov and Rjachowsky,[15] Ishikawa,[22] and Arrhenius,[7] indicates that only Sachanov–Rjachowsky formula gives better agreement than equation (4). However, as was observed by Jones and co-workers,[6] the Sachanov–Rjachowsky formula cannot be applied in a general fashion, for instance in the case of acetic acid–carbon tetrachloride mixture where a minimum occurs. Spells[23] and Macleod[24] equations give better results for this same mixture, in one region of concentration, than formula (4). Both equations are inapplicable when there is great disparity between the viscosities of the pure components.

The examination of all previous formulas shows a lack of generality; although for some types of mixtures they give good results, they are not applicable to all type of mixtures, for instance in the case where there is great disparity between the viscosities of the components, or when there is a minimum in the curve viscosity *versus* concentration. Although, in some cases, the application of formula (4) gives a large maximum error, formula (4) is quite general, and can be used for different types of mixtures and at different temperatures. The application of formula (4) to mixtures of normal paraffins, 2,4-dimethylpentane and benzene has been presented by Lima[25] in another paper.

Acknowledgments.—The author wishes to thank Professor Ethel L. French of the Chemistry Department, University of Rochester, for her kindness in improving the style in the manuscript.

TABLE VI

COMPARISON OF RESULTS OBTAINED BY VARIOUS FORMULAS FOR THE MIXTURES OF n-OCTYL ALCOHOL–CARBON TETRACHLORIDE, AT 25°

Weight % alcohol	Kendall Monroe	Sachanov Rjachowsky	Ishikawa	Arrhenius	Present work	Obsd.
0	9.02^a	9.02^a	9.02^a	9.02	9.02	9.02
5	10.72	9.98	10.63	10.94	10.33	10.00
10	12.58	11.27	12.33	13.05	11.61	11.39
15	14.61	12.86	14.13	15.33	13.23	12.97
20	16.80	14.74	16.03	17.83	15.07	14.70
40	27.23	24.83^a	24.83^a	29.28	24.49	24.83
50	33.41	31.23	30.14	35.84	30.48	3.124
60	40.23	38.41	36.23	42.72	35.31	38.47
80	55.7	54.8	51.6	57.6	51.05	55.8
100	73.3^a	73.3^a	73.3^a	73.3	73.3	73.3

^{a} Values used by the respective authors to calculate constants of their equations.

---

[20] G. P. Lutschinski, *Symposium on the Viscosity of Liquids and Colloids, Acad. Sc. U.S.S.R.*, **1**, 41 (1941).

[21] F. Kottler, THIS JOURNAL, **47**, 280 (1943); **48**, 76 (1944).

[22] T. Ishikawa, *Bull. Chem. Soc. Japan*, **4**, 7 (1929).

[23] K. E. Spells, *Trans. Faraday Soc.*, **32**, 537 (1936).

[24] D. B. Macleod, *ibid.*, **19**, 20 (1923).

[25] F. W. Lima, *J. Chem. Phys.*, **19**, 137 (1951).

THE ADSORPTION OF SENSITIZING DYES IN PHOTOGRAPHIC EMULSIONS[1]

BY W. WEST, B. H. CARROLL AND D. H. WHITCOMB

Communication No. 1468 from the Kodak Research Laboratories, Eastman Kodak Company, Rochester, N. Y.

Received December 15, 1951

Many cyanine dyes are adsorbed to the grains of photographic emulsions according to the Langmuir equation, the molecules in the saturated monolayer being oriented with their planes parallel and projecting away from the surface at an average intermolecular distance of about 4.6 Å. Less well adsorbed dyes often exhibit a discontinuity between adsorption as isolated molecules and a co-operative phase with different spectral characteristics. Polylayer adsorption also occurs, and merocyanines conform to Langmuir or approximate Freundlich curves according to the class. Non-planar dyes are feebly adsorbed compared with corresponding planar dyes. Heats of adsorption, determined from the Clapeyron–Clausius equation, are about 10 to 12 kcal. per mole for the first additions of well-adsorbed cyanine dyes in silver halide gelatin emulsions, and decrease with increasing coverage. Both electrostatic and van der Waals forces contribute to the adsorption of cyanines, while some kind of linkage between Ag^+ and doubly bonded S figures for certain merocyanines. While correlations appear between the adsorption and optical sensitization of individual dyes, relative adsorbability and relative efficiency of sensitization of different dyes are not, in general, parallel quantities. The inefficient optical sensitization of non-planar dyes cannot be explained by their low adsorbability, nor is supersensitization caused by any material increase of the strength of binding of the sensitizer to the silver halide in the presence of the supersensitizer.

Part I. Adsorption Isotherms and Heat of Adsorption

It has long been realized that a necessary condition for optical sensitization is the presence of the sensitizing dye in the adsorbed state at the surface of the silver halide grains in the photographic emulsion. Stimulated by the realization that the nature of dye adsorption on silver halide grains is of interest in the theory of optical sensitization Sheppard and Crouch[2] initiated, in 1928, the determination of adsorption isotherms in silver halide suspensions. This and subsequent studies by Sheppard and his co-workers[3,4] established some of the fundamentals of dye adsorption on silver halide for cyanine sensitizers. They recognized that typical cyanine dyes are flat molecules consisting of a coplanar arrangement of two heterocyclic nuclei linked by a methine or polymethine

---

[1] Read in part at the Symposium on the Colloid Chemistry of the Photographic Process, 119th National Meeting of the American Chemical Society, Boston, Mass., April 1–5, 1951

[2] S. E. Sheppard and H. Crouch, *J. Phys. Chem.*, **32**, 751 (1928).

[3] S. E. Sheppard, R. H. Lambert and R. L. Keenan, *ibid.*, **36**, 174 (1932).

[4] S. E. Sheppard, R. H. Lambert and R. D. Walker, *J. Chem. Phys.*, **7**, 265 (1938).

chain. For some representative cyanine sensitizers, the adsorption to silver halide grains dispersed in water or in gelatin solution was found to conform to the Langmuir isotherm. The saturation plateau indicated the formation of a monolayer of the flat dye cations oriented "edge-on" to the surface, in an arrangement somewhat resembling a pack of cards standing on edge. A second layer, differentiated in the isotherm as a step rising from the first-layer plateau, was found for some adsorbed dyes, while Davey[5] published isotherms for a few sensitizers which showed steps *below* the saturation level corresponding to the completion of the monolayer. He suggested that the first adsorbed molecules were held in a different manner from those adsorbed at higher concentration, possibly in a flat, in contrast to the edge-on orientation, and supported this supposition from differences in the spectral distribution of sensitivity in the emulsions with low and with high concentrations of dye. Rabinowitch and Natanson[6] also observed monolayer adsorption of some sensitizers of the pyronine and eosin classes, with, in some cases, superposed steps indicating polylayer adsorption.

These earlier studies were limited to a few sensitizing dyes of a restricted number of chemical classes. In the work described in the present communication, the object has been to make a systematic survey of the adsorption characteristics on silver halide grains of a large number of dyes embracing many classes of sensitizers; for example, cationic dyes of the 2,2′-cyanine, oxacarbocyanine and thiacarbocyanine classes, as well as un-ionized merocyanines of several classes, and some other miscellaneous sensitizers and desensitizers. The prime interest centered around any connection which might reveal itself between adsorption and optical sensitization, and the adsorptive systems examined were therefore normal photographic bromoiodide or chlorobromide suspensions in 7% aqueous gelatin solution; occasionally emulsions[7] of much lower gelatin content were used. The presence of gelatin does not seem to detract from the general interest afforded by these systems as examples of the adsorption of large molecules to ionogenic surfaces; the gelatin acts as a competitive adsorbate, and, in its presence, certain interesting details appear in the adsorption isotherms which are otherwise not so readily observed. Heats of adsorption, concerning which no satisfactory data seem previously to have been reported for these dyes, were determined for several dyes from the 40° and 60° isotherms by means of the Clapeyron–Clausius equation; and, in connection with the phenomenon of supersensitization,[8–10] the adsorption of several two component dye mixtures was studied.

The experimental technique consisted in adding a known weight of dye dissolved in a definite volume of methyl alcohol or other solvent to ten times the volume of liquid emulsion at the desired temperature. Equilibration was effected by mechanical tumbling in a water thermostat and checked by measurements of the isotherm after 3 and after 24 hours. Most dyes were practically in equilibrium with the surface after 3 hours, and some after 15 minutes, but sometimes 24 hours or longer were required for the last amounts of dye to be taken up. The emulsion was then centrifuged in a stoppered tube in a thermostated machine (International centrifuge size-1, type SB, with conical head, at 4000 r.p.m.) and the amount of unadsorbed dye in the aqueous phase was determined spectrophotometrically by means of a Beckman spectrophotometer, model DU, the adsorbed dye being computed by difference. For a number of dyes, satisfactory checks were made between the values of the adsorbed dye so computed and the amount of dye liberated from the centrifuged grains by dissolving them in concentrated aqueous thiourea. Extraction with butyl alcohol after dissolving the silver halide in sodium thiosulfate or sodium cyanide solutions yielded low results. The pH and pAg were adjusted as desired.

For the less soluble dyes, the limit to which the concentration can be extended in the isotherm is determined by the point at which precipitation of dye occurs, recognizable by microscopic search of the centrifuged aqueous phase for dye crystals or by presence of obvious precipitate on the surface of the centrifuged grains. Precipitation from supersaturated solution in gelatin is often slow, and it is sometimes possible to extend the isotherm to the region in which the adsorbed dye is in equilibrium with a supersaturated solution.

Two emulsions were used, each containing 7% gelatin after addition of the dye solution. Emulsion A was a bromoiodide with a projective area (estimated from microscopic analysis) of 4.03 × 10^3 sq. cm. per gram of silver halide. The grains of this emulsion were mostly flat truncated triangles or hexagons; the thickness of the triangular grains was about one-fifth the side of the grain, regarded as an equilateral triangle or, for the others, about one-half the regular hexagonal side. For equilateral triangular prisms whose height is one-fifth the side of the base, the ratio of the total surface to that of the base is 3.4, while for hexagonal prisms whose height is one-half the length of the side, the ratio is 3.2. The true form of the grains is not, of course, prismatic, but, as a likely approximation, the total area of the emulsion grains has been assumed to be 3.3 times the projective area, *i.e.*, 13.3 × 10^3 sq. cm. per gram of silver halide (*cf.* reference 11). The pH and pAg of the emulsion were 6.5 and 8.5, respectively, except when specially adjusted to other values.

Emulsion B was a chlorobromide with a projective area of 5.60 × 10^3 sq. cm. per gram of halide, and, on the assumption of the same shape factor as for A, a total surface of 18.5 × 10^3 sq. cm. per gram. These estimates of total area from projective area can scarcely claim an accuracy greater than ±5%.

The isotherms of a number of dyes in both emulsions were close approximations to the simplest Langmuir type; for five such dyes, the ratio of the saturation amounts of dye adsorbed per gram of silver halide in B and A, respectively, was 1.47 at 40°, with a mean deviation of ±0.03, while the ratio of the total surfaces on the assumption of the same shape factor for the two emulsions was 1.40. The agreement is as good as can be expected, considering the uncertainty in the estimates of the absolute surface areas of the emulsions.

Types of Adsorption Isotherms for Cyanine Dyes.[12]—Formula A shows a representative cyanine cation. The non-localization of the π-electrons in the conjugated chains of such structures is associated both with the intense visual absorption of these compounds, and also, because of the large amplitude of motion of electric charge through the conjugated

---

(5) E. P. Davey, *Trans. Faraday Soc.*, **36**, 323 (1940).

(6) A. E. Rabinowitch and S. V. Natanson, *J. Phys. Chem.* (*U. S. S. R.*), **11**, 434 (1938).

(7) The term "emulsion" is used in its normal photographic connotation, *viz.*, a suspension of silver halide grains in an aqueous gelatin medium.

(8) B. H. Carroll and W. West, "Fundamental Mechanisms of Photographic Sensitivity," edited by J. W. Mitchell, Butterworths Sci. Publications Ltd., London, 1951, p. 162.

(9) C. E. K. Mees, "The Theory of the Photographic Process," The Macmillan Co., New York, N. Y., 1942, pp. 975, 1070.

(10) W. West and B. H. Carroll, *J. Chem. Phys.*, **19**, 417 (1951).

(11) J. A. Leermakers, B. H. Carroll and C. J. Staud, *J. Chem. Phys.*, **5**, 878 (1937).

(12) For details on the structure and nomenclature of cyanine dyes, see reference 9, Chapter 24, pp. 992, 1003 *et seq.*

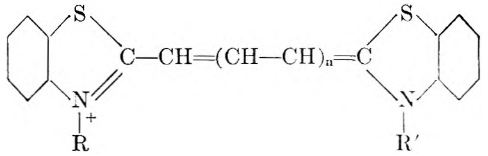

Formula A, n = 0, 1, 2, etc.

chain, with strong van der Waals forces[13]; these, on the one hand, tend to cause dimerization and further aggregation of the molecules in aqueous solution and, on the other, supplement electrostatic forces in causing adsorption at crystal surfaces.

In the dyes studied, the heterocyclic nuclei were benzoxazole, benzothiazole and quinoline; n was 0 (cyanine) or 1 (carbocyanine); the substituents on the N-atoms were alkyl or aryl groups, and other positions in the nuclei or in the methine chain were, on occasion, occupied by alkyl or aryl groups, or other substituents. The anions were bromide, iodide, p-toluenesulfonate or perchlorate; where different anions associated with the same dye cation were examined, no difference beyond experimental error was found in the isotherms in emulsion A, either at a pAg of about 8 or at the pAg corresponding approximately to equivalent concentrations of silver ion and bromide ion in solution.

The adsorption isotherms of more than thirty cyanine dyes in emulsions can be classified into three groups: (a) simple Langmuir isotherms with a well-defined saturation plateau indicating the formation of a monolayer, oriented edge-on to the surface; (b) isotherms exhibiting a low-adsorption "toe," merging, sometimes discontinuously, into a Langmuir branch with a saturation level indicating monolayer, edge-on adsorption; and (c) isotherms indicating polylayer adsorption, sometimes with second and subsequent layers differentiated from the first by a step rising from the monolayer plateau, sometimes undifferentiated in this way.

Table I

Dye Formulas

Thiacarbocyanines (only the cations of cyanine dyes are named and formulated): Positions not otherwise designated are occupied by H.

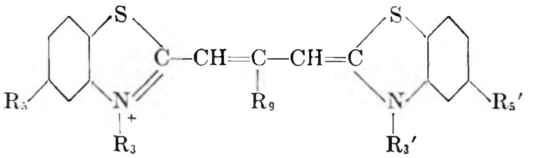

I, 3,3'-diethylthiacarbocyanine, $R_3 = R_3' = C_2H_6$

II, 3,3'-diethyl-9-methylthiacarbocyanine, $R_3 = R_3' = C_2H_5$; $R_9 = CH_3$

III, 5,5'-dichloro-3,3',9-triethylthiacarbocyanine, $R_3 = R_3' = R_9 = C_2H_5$; $R_5 = R_5' = Cl$

Thia-2'-cyanines

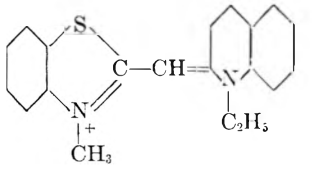

IV, 1'-ethyl-3-methylthia-2'-cyanine

2,2'-Cyanines

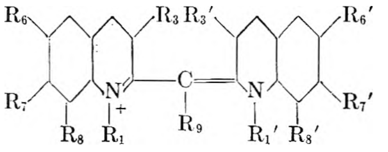

V, 1,1'-dimethyl-2,2'-cyanine, $R_1 = R_1' = CH_3$

VI, 1,1'-diethyl-2,2'-cyanine, $R_1 = R_1' = C_2H_5$

VII, 1,1'-Diethyl-6,6'-dimethyl-2,2'-cyanine, $R_1 = R_1' = C_2H_5$; $R_6 = R_6' = CH_3$

VIII, 1,1'-diethyl-7,7'-dimethyl-2,2'-cyanine, $R_1 = R_1' = C_2H_5$; $R_7 = R_7' = CH_3$

IX, 1,1'-diphenyl-2,2'-cyanine, $R_1 = R_1' = C_6H_5$

X, 1,1',3,3'-tetramethyl-2,2'-cyanine, $R_1 = R_1' = R_3 = R_3' = CH_3$

XI, 1,1'-diethyl-8,8'-dimethyl-2,2'-cyanine, $R_1 = R_1' = C_2H_5$; $R_8 = R_8' = CH_3$

XII, 1-ethyl-1',9-dimethyl-2,2'-cyanine, $R_1 = C_2H_5$; $R_1' = R_9 = CH_3$

XIII, 1,1',9-triethyl-2,2'-cyanine, $R_1 = R_1' = R_9 = C_2H_5$

Langmuir Isotherms.—Figure 1 shows the isotherms for the four cyanine dyes, 3,3'-diethylthiacarbocyanine iodide (I); 1'-ethyl-3-methylthia-2'-cyanine iodide (IV); 1,1'-dimethyl-2,2'-cyanine iodide (V), and the corresponding diethyl dye (VI).

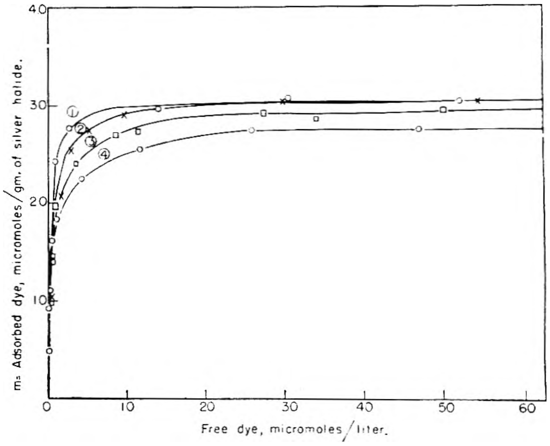

Fig. 1.—Typical Langmuir isotherms of cyanine dyes in emulsion A at 40°: (1) 3,3'-diethylthiacarbocyanine iodide (I); (2) 1'-ethyl-3-methylthia-2'-cyanine iodide (IV); (3) 1,1'-dimethyl-2,2'-cyanine iodide (V); (4) 1,1'-diethyl-2,2'-cyanine iodide (VI).

The abscissas represent the amount, m, of dye adsorbed, in micromoles per gram of silver halide, and the ordinates, the corresponding equilibrium concentration, c, of free dye, in micromoles per liter of liquid phase of the emulsion. The Langmuir relation

$$m/M = kc/(1 + kc)$$

applies to these curves, where M is the saturation amount of adsorbed dye and k is a constant, as is shown in Fig. 2 by the linearity of the plots of c/m against c. In this figure, the lines for dyes IV and V nearly coincide with that for dye I.

A scale drawing of dye V (1,1'-dimethyl-2,2'-cyanine iodide) is reproduced in Fig. 3. The area occupied per molecule of this dye at saturation, *i.e.*, the ratio of the total surface of the emulsion grains to the number of adsorbed dye molecules, is

---

[13] F. London, *J. Phys. Chem.*, **46**, 305 (1942).

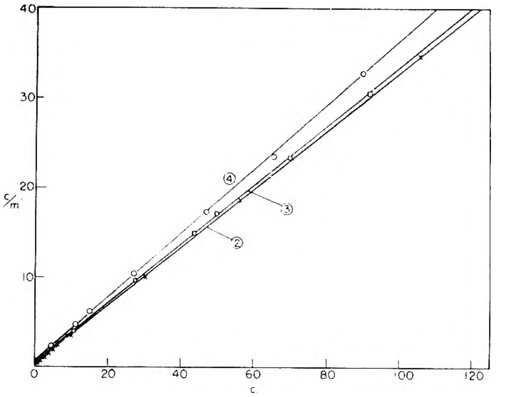

Fig. 2.—C/m vs. c in emulsion A at 40°: (2) 1′-ethyl-3-methylthia-2′-cyanine iodide (IV); (3) 1,1′-dimethyl-2,2′-cyanine iodide (V); (4) 1,1′-diethyl-2,2′-cyanine iodide (VI).

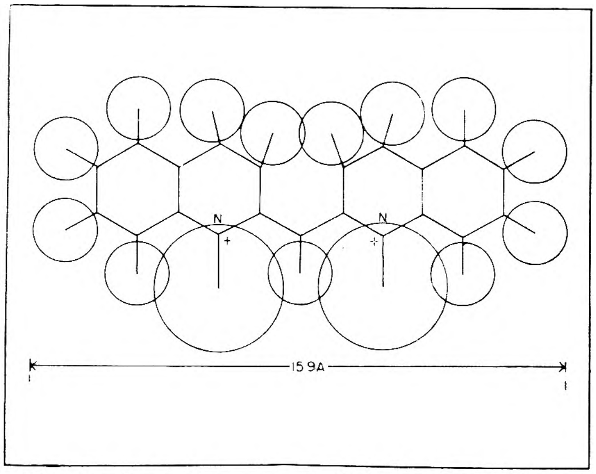

Fig. 3.—Scale drawing of 1,1′-dimethyl-2,2′-cyanine cation. Area of molecule: flat, 130 sq. Å.; edge-on, 70 sq. Å.; end-on, 35 sq. Å.

73.6 sq. Å. As is well known,[4,14] the conjugated double bond arrangement in methine and polymethine dyes tends to maintain the heterocyclic nuclei and the atoms in the connecting bridge in the same plane, unless the crowding of bulky substituents prevents the coplanar configuration.[4,15,16] The length of this cation is about 15.9 Å., the height about 8.1 Å., and its thickness will be at least the van der Waals thickness of the benzene ring, about 3.7 Å.

From a comparison of the observed area per molecule with the areas given in Fig. 3 for various orientations, it is clear that the only orientation consistent with a monolayer at saturation is the edge-on arrangement, with adjacent molecules parallel to each other and with their heterocyclic rings projecting out from the surface, in agreement with the conclusions of Sheppard, Lambert and Walker[4] based on the adsorption of certain thiacarbocyanines. The area for this molecule on emulsion grains, 73.6 Å.^{2}, is similar to that of the corresponding diethyl dye (VI) adsorbed on mica, for which Skerlak[17] gives the value 64 ± 12 Å.^{2} From the observed area and the estimated length of the molecule, the average intermolecular distance at saturation is found to be 4.63 Å., which is in excess of the van der Waals thickness of the nuclei. In Table II are collected data for a number of dyes whose isotherms exhibit Langmuir plateaus consistent with monolayer edge-on adsorption; for the most part, the average intermolecular distance at saturation lies between 4.5 and 5 Å. In the computation of intermolecular distances, any adsorbed anion furnished by the dye has been disregarded, since adsorption of anions such as halide, perchlorate or p-toluenesulfonate is probably small, most remaining as counter ions near the surface. The values of the internuclear distance computed in Table II from the saturation limits of the isotherms agree in general with the values deduced by Hoppe from X-ray diffraction,[18] for the interplanar distances in the aggregated forms of a number of 2,2′-cyanines in dried-down layers on glass deposited from solution in the presence of water or water vapor. Hoppe suggested that the observed interplanar distances, greater than the van der Waals thickness of the nuclei, indicated that the planes of adsorbed molecules were tilted at about 30° from the vertical.

TABLE II

AREAS PER MOLECULE AT SATURATION OF EMULSION A AND AVERAGE INTERMOLECULAR DISTANCES FOR DYES ADSORBED TO SILVER HALIDE IN PHOTOGRAPHIC EMULSIONS

Dyes	Area per molecule, sq. Å.	Length of molecule, Å.	Av. intermolecular distance, Å.	Type of absorption spectrum of adsorbed dye
2,2′-Cyanines				
1,1′-DiMe (V)	74	15.9	4.66	H, J
1,1′-DiEt (VI)	79	15.9	4.96	J
1,1′-Diphenyl (IX)	96	15.9	6.05	B
1,1′-DiEt-6,6′-diMe (VIII)	88	18.7	4.61	J
1,1-DiEt-7,7′-diMe (VIII)	97	18.7	5.20	B
1,1′-DiEt-8,8′-diMe (XI)	100	15.9	6.26	J
1,1′3,,3′-TetraMe (X)	95	15.9	5.98	J
Thia-2′-cyanines				
3-Et-1′-Me (IV)	73	15.9	4.60	J
3,1′-DiEt-6′-OMe	82	17.6	4.66	J
Oxacarbocyanines				
3,3′-DiMe (XIV)	91	18.0	5.06	B
3,3′-DiEt (XV)	87	18.0	4.90	B
3,3′-DiBu (XVI)	94	18.3	5.10^a	B
3,3′-Dihexyl (XVII)	106	23.3	4.56^a	B
3,3′,9-TriEt (XVIII)	93	18.0	5.17	B
3,3′,9-TriEt-5,5′-diphenyl (XX)	108	25.7	4.20	J
Thiacarbocyanines				
3,3′-DiEt (I)	76	18.1	4.20	B
3,3′-DiEt-9-Me (II)	79	18.1	4.36	J, H
3,3′,9-TriEt-5,5′-diCl (III)	105	20.7	5.06^b	J
Oxathiazolocarbocyanine				
3,3′-DiEt	91	19.3	4.71	B
Merocyanines				
Dye (XXI)	59	13.7	4.31	B
Dye (XXII)	59	14.0	4.23	B, H
Dye (XXIII)	70	17.0	4.13	B

[a] The carbon atom chain in the alkyl groups is assumed to be extended away from the center of the molecule, parallel to the plane of the nuclei, so as to permit closest intermolecular approach. [b] Calculated from the metastable monolayer saturation plateau (Fig. 7).

---

(14) G. Scheibe and L. Kandler, *Naturwissenschaften*, **26**, 412 (1938).

(15) L. G. S. Brooker, F. L. White, R. H. Sprague, S. G. Dent, Jr., and G. VanZandt, *Chem. Revs.*, **41**, 325 (1947).

(16) In the 2,2-cyanines, as drawn according to normal valence angles, there is some crowding of the H-atoms in the 3- and 3′-positions, but it seems likely that small accommodations of the angles in the critical region of the molecule will permit the existence of the planar structure.[17]

(17) T. Skerlak, *Kolloid. Z.*, **95**, 265 (1941).

(18) W. Hoppe, *ibid.*, **101**, 300 (1942); **109**, 21 (1944).

The absorption (or reflectance) spectra of adsorbed dye layers are important in connection with the structure of the layer. In general, the spectrum of an adsorbed dye layer on silver bromide passes through a sequence of changes with increasing coverage of the surface roughly parallel to those exhibited with increasing concentration of the dye in aqueous solution.[8] At very low coverage, the absorption spectrum is a relatively broad band displaced some 300 Å. bathochromically from the molecular spectrum in alcoholic or in very dilute aqueous solution. This spectrum presumably can be ascribed to the isolated adsorbed dye molecule, whose electronic levels are influenced by the surface environment, but not by interactions between dye molecules. With increasing concentration of adsorbed dye, a broad band appears hypsochromic to the molecular band, which appears analogous to the dimeric and polymeric bands hypsochromic to the molecular band seen in more concentrated aqueous solution. These are conveniently designated H-bands. At still higher coverages, for certain dyes only, a relatively sharp band appears at longer wave lengths than the molecular band. Some dyes exhibit in sufficiently concentrated aqueous solution, or on the addition of soluble salt to the aqueous solution, a still sharper band at nearly the same wave length as this sharp band on silver halide. This type of spectrum was first observed by Jelley[19] and by Scheibe[20] for 1,1′-diethyl-2,2′-cyanine chloride (VI) and certain similar dyes. The observations of Jelley, and particularly of Scheibe and his co-workers, have been interpreted as indicating that the sharp band, which has been termed a J-band, is associated with an aggregated structure in which strings of dye cations are lined up with their molecular planes parallel and with the long axis of the individual molecules perpendicular to the direction of the string; in fact, an arrangement similar to the edge-on orientation deduced for adsorbed layers. There seems little doubt that the sharp bands usually shown by adsorbed layers of those dyes which exhibit J-maxima in solution are of the same nature as the J-maxima; and many dyes, whose solubility in water is too low to allow the appearance of the J-band in solution, readily enter the J-state on adsorption to silver halides.[11] The shape and position of the J-band is normally reproduced in the spectral sensitivity curves of the dyed emulsions.[11,21] A similar tendency for adsorption on glass, quartz and mica to favor the appearance of the structure characterized by the J-band has been noted by Scheibe and co-workers.[14,22] The relatively thick films of 2,2′-cyanines on glass examined by Hoppe, already referred to, also exhibit J-bands. The dyes in Table II whose absorption band in the adsorbed state is of the J-type are so indicated in the last column.

The concentrations of adsorbed dye at which the spectral changes occur in the sequence of molecular band → H-aggregate → J-aggregate vary widely from dye to dye. Sometimes, as for 1,1′-diethyl-2,2′-cyanine iodide (VI), the J-state sets in at quite low coverages, and the molecular and H-bands are seen only over a very small range at low concentrations of adsorbed dye. On the other hand, for the corresponding 1,1′-dimethyl dye (V), the H-band dominates the spectrum in most emulsions. However, Table II shows that, irrespective of the nature of the spectrum, many cyanines can be adsorbed at saturation only in a packed edge-on arrangement, nor can any definite correlation be found between intermolecular distances at saturation and the nature of the absorption spectrum. Whatever may be the cause of the spectral differences between J-aggregates and H-aggregates, the intermolecular distance seems about the same for both, and some other requirement than the packed arrangement of parallel molecules seems necessary for the appearance of the J-band.

Förster[23] has made the suggestion, adopted in a modified form by Scheibe,[24] that the essential difference between the H-bands and the J-bands is in the electronic coupling between neighboring molecules of the aggregates, bands hypsochromic and bathochromic to the band of the unperturbed molecule arising according as neighboring electronic oscillators vibrate out of or in phase. The observed similarity in the packing of the saturated monolayers of dyes, irrespective of the nature of the absorption spectrum, is in accord with this type of explanation.

Some further remarks must be made concerning the dyes in Table II, whose absorption spectra are designated as B. For these dyes, the chief absorption maximum at saturation is a broad band at a wave length about 100 Å. longer than the molecular maximum in the adsorbed state; an H-maximum often also appears. Evidence presented later in this communication indicates that this maximum, in spite of its small shift from the maximum of the isolated adsorbed molecule, is associated with interaction between dye molecules, the upper and lower states apparently being affected about equally. The B-type of spectrum, like the H- and J-, is associated with a packed edge-on arrangement of the adsorbed molecules at saturation.

Cooperative Adsorption.—A form of isotherm frequently found for less tightly adsorbed cyanines is illustrated by those of the group of oxacarbocyanines in Fig. 4, and, in curve 7 of Fig. 5, by the isotherm for 1,1′,3,3′-tetramethyl-2,2′-cyanine iodide (X). The characteristic feature here is a "toe" in the curve denoting low adsorbability at low concentration of dye, followed by a branch indicative of higher adsorbability. This often suddenly springs up from the toe at a critical concentration of adsorbed dye, and attains a saturation level corresponding to monolayer edge-on adsorption; the rapidly ascending part of the isotherm is similar to the normal Langmuir curves exhibited by dyes like those in Fig. 1.

---

(19) E. E. Jelley, *Nature*, **138**, 1009 (1936).

(20) G. Scheibe, *Z. angew. Chem.*, **50**, 51 (1937).

(21) G. Schwarz, *Science et ind. phot.*, [2] **10**, 233 (1939).

(22) G. Scheibe, L. Kandler and H. Ecker, *Naturwissenschaften*, **25**, 75 (1937).

(23) T. Förster, *ibid.*, **33**, 166 (1946).

(24) G. Scheibe, *Z. Elektrochem.*, **52**, 283 (1948).

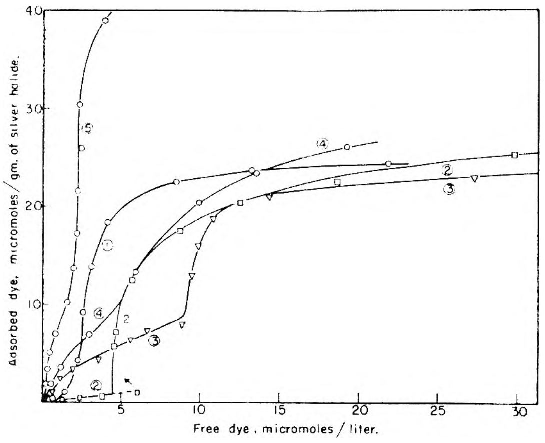

Fig. 4.—Adsorption isotherms of oxacarbocyanines in emulsion A at 40°: (1) 3,3′-dimethyloxacarbocyanine iodide (XIV); (2) 3,3′-diethyloxacarbocyanine iodide (XV); (3) 3,3′-di-*n*-butyloxacarbocyanine iodide (XVI); (4) 3,3′-di-*n*-hexyloxacarbocyanine perchlorate (XVII); (5) 9-ethyl-3,3′-dimethyloxacarbocyanine iodide (XIX).

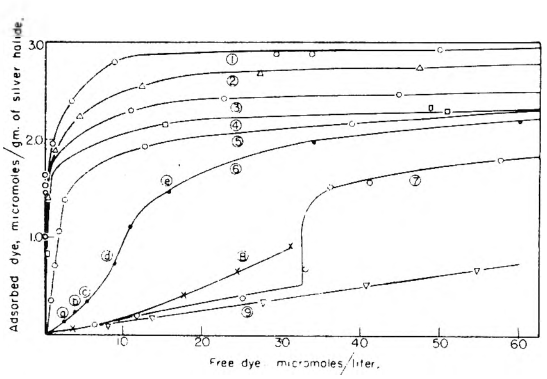

Fig. 5.—Adsorption isotherms of 2,2′-cyanines in emulsion A at 40°: (1) 1,1′-dimethyl-2,2′-cyanine iodide (V); (2) 1,1′-diethyl-2,2′-cyanine iodide (VI); (3) 1,1′-diethyl-6,6′-dimethyl-2,2′-cyanine iodide (VII); (4) 1,1′-diethyl-7,7′-dimethyl-2,2′-cyanine iodide (VIII); (5) 1,1′-diphenyl-2,2′-cyanine iodide (IX); (6) 1,1′-diethyl-8,8′-dimethyl-2,2′-cyanine iodide (XI); (7) 1,1′,3,3′-tetramethyl-2,2′-cyanine iodide (X); (8) 1-ethyl-1′,9-dimethyl-2,2′-cyanine iodide (XII); (9) 1,1′,9-triethyl-2,2′-cyanine perchlorate (XIII).

In isotherms of this sort, equilibrium is usually only slowly attained near the discontinuity—the adsorption tends to follow the toe beyond the discontinuity and to wander back slowly to equilibrium values on the other branch. This behavior resembles a phase change in which the new phase appears reluctantly, as in supersaturation or supercooling.

Moreover, as shown in Fig. 6, the adsorption discontinuity is accompanied by a sharp change in the absorption spectrum of the adsorbed layer. The figure refers to 1,1′-diethyl-8,8′-dimethyl-2,-2′-cyanine perchlorate (XI), the isotherm of which, in emulsion A, is curve 6 of Fig. 5. The reflectance spectra of the centrifuged grains corresponding to the points, a, b, c, d, e, in the isotherm, are represented by curves a-e in Fig. 6. The spectra were determined by a General Electric automatic spectrophotometer; minima of reflectance correspond to maxima of light absorption. The spectrum for the three lowest points, below the inflection point in the isotherm, is of the molecular type with maximum absorption at wave length 5560 Å., while a J-band at 5750 Å. appears on the high-concentration side of the inflection. Similarly, the discontinuity in the adsorption isotherm of 1,1′,3,3′-tetramethylcyanine iodide (X), (curve 7, Fig. 5) is accompanied by a sharp change from an absorption maximum of the molecular type at 5380 Å. to a J-maximum at 5760 Å. The isotherm of 3,3′-dimethyl-9-ethyloxacarbocyanine iodide (XIX), shown in curve 5 of Fig. 4, contains two inflection points, one of which, at the low concentration of 0.02 micromole of free dye per liter, is invisible at the scale of Fig. 4. This inflection point at low concentration is associated with a spectral change from a broad molecular band with a maximum at 5150 Å., at the low concentration side, to a J-band at 5600 Å. at the high concentration side. The second inflection point, visible in curve 5 of Fig. 4, represents the onset of polylayer adsorption, and is not accompanied by a spectral change. For 3,3′-diethyloxacarbocyanine iodide (XV) (Fig. 4, curve 2), the absorption spectrum changes in character at the discontinuity, although the change in wave length is merely from 5060 Å. at the low concentration side to 5160 Å. on the other, and the band at the higher concentrations lacks the characteristic sharpness of J-bands, which when they appear in oxacarbocyanines, have wave lengths about 5400–5600 A. Nevertheless, the change in shape and wave length of the absorption band of 3,3′-diethyloxacarbocyanine at the absorption discontinuity is quite distinct, and as for the other dyes mentioned, a change in the nature of the adsorbed layer at the discontinuity seems to occur. In general, the spectrum on the low concentration side of the discontinuity appears to be that of the isolated dye molecule, uninfluenced by interactions with other dye molecules, while, at the high concentration side, the spectrum is that of dye molecules in a state of mutual interaction. The interacting adsorbed state for many

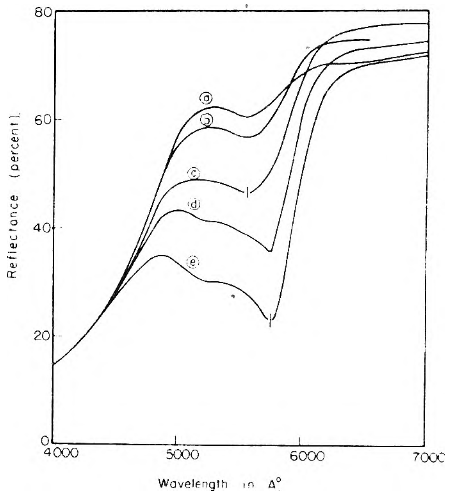

Fig. 6.—Spectral change accompanying onset of co-operative adsorption of 1,1′-diethyl-8,8′-dimethyl-2,2′-cyanine iodide (XI) in emulsion A at 40°. Reflectance spectra of centrifuged dyed grains. Curves a, b, c correspond to points a, b, c in the isotherm (Fig. 5, curve 6) below the inflection point; d and e to the corresponding points above the inflection point.

dyes is similar to the J-aggregate in solution, but the spectrum of the coöperative adsorbed state may also, as for 3,3′-diethyloxacarbocyanine and for the corresponding thiacarbocyanine, be only slightly displaced from the molecular band to form the type designated as B, in Table I. Caution should therefore be exercised in identifying absorption bands at high concentrations of adsorbed dye with the band of the non-coöperative molecule merely because the wave lengths are not very different.

We are thus led to the picture that low concentrations of cyanine dyes are adsorbed as isolated molecules, and, since adsorption is conditioned partly by van der Waals forces emanating from the ring structures in the molecule, it is probable, as Davey suggested[5] that the first isolated molecules lie flat on the surface. As the molecules approach each other with increasing concentration, lateral interactions come into play, and ultimately cause the flat molecules to stand on edge and be pulled in toward one another in a packed edge-on array. At the critical concentration, which for a given dye depends on the temperature, the nature of the solid adsorbant, the gelatin content, and *p*Ag of the emulsion, the fitting into the new coöperative structure requires some time, allowing the continuation of the low concentration branch of the isotherm in a metastable state of the system; but once the coöperative layer has started, further molecules from solution are readily incorporated and the isotherm rises steeply to a limiting monolayer plateau.

Polylayer Adsorption.—Figure 7 shows the isotherms of 5,5′-dichloro-3,3′-9-triethylthiacarbocyanine iodide (III) after holding times of 3, 24 and 48 hours. A monolayer corresponding to an area of 105 sq. Å. per molecule and an intermolecular distance of 5.06 Å., *i.e.*, to edge-on adsorption, is rapidly formed, but slow deposition of dye with the formation of a second and further layers occurs. There is no indication of a saturation level for the additional layers in the range of concentrations covered, and ultimately differentiation between the first and subsequent layers is lost. The absorption spectrum of the dyed grains is the same for coverage by one or more layers, the main feature being a strong J-band at about 6350 Å. This suggests that the second and subsequent layers are also held edge-on; the adsorbed dye seems to assume a layer structure with the orientation of the molecules in subsequent layers substantially that of the J-aggregate, which differs from the arrangement in the normal crystal. The polylayer films of cyanine dyes on silver halide resemble the relatively thick films dried down from alcoholic solution on glass in the presence of water vapor, which may also show J-bands.[18]

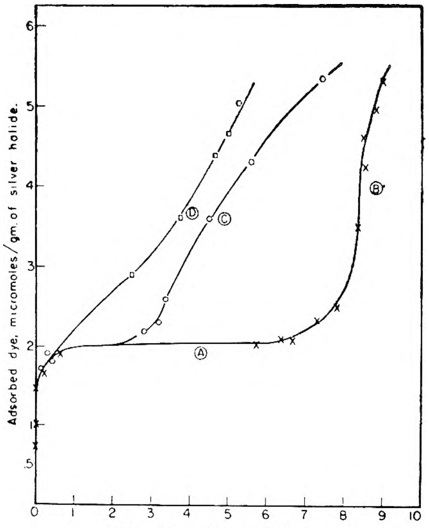

Fig. 7.—Polylayer adsorption of 5,5′-dichloro-3,3′,9-triethylthiacarbocyanine bromide (III) in emulsion A at 40°: curves A and B after 3 hours of equilibration; C, after 24 hours; D, after 48 hours.

In some dyes, the second layer begins to form before the first is complete, and the isotherm lacks steps discriminating between the layers. An example is 9-ethyl-3,3′-dimethyloxacarbocyanine iodide (XIX), curve 5, Fig. 4, in which the upper part of the isotherm represents a polylayer branch springing up before completion of the monolayer.

Effect of Substituents on Adsorption of Cyanine Dyes.—Curves 1–4 in Fig. 4 illustrate the 40° isotherms in emulsion A of oxacarbocyanines with various alkyl substituents on the nitrogen atoms.

Table III

Formulas of Oxacarbocyanines

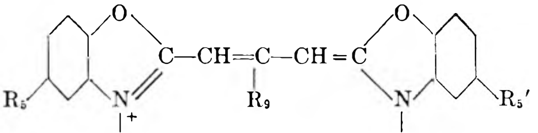

XIV, 3,3′-Dimethyloxacarbocyanine, $R_3 = R_3' = CH_3$

XV, 3,3′-Diethyloxacarbocyanine, $R_3 = R_3' = C_2H_5$

XVI, 3,3′-Di-*n*-butyloxacarbocyanine, $R_3 = R_3' = n\text{-}C_4H_9$

XVII, 3,3′-Di-*n*-hexyloxacarbocyanine, $R_3 = R_3' = n\text{-}C_6H_{13}$

XVIII, 3,3′,9-Triethyloxacarbocyanine, $R_3 = R_3' = CH_3$; $R_9 = C_2H_5$

XIX, 9-Ethyl-3,3′-dimethyloxacarbocyanine, $R_3 = R_3' = CH_3$; $R_9 = C_2H_5$

XX, 3,3′,9-Triethyl-5,5′-diphenyloxacarbocyanine, $R_3 = R_3' = R_9 = C_2H_5$; $R_5 = R_5' = C_6H_5$

Dyes XIV to XVII show the discontinuity representing the transition from random to coöperative adsorption, with a decreasing tendency toward coöperation in the order: methyl > ethyl > *n*-butyl. The dihexyl dye is more adsorbable than the dibutyl, a fact probably connected with the lower solubility of the former.

At the higher concentrations of dye, on the coöperative branch of the isotherm, most of the dye is rapidly adsorbed, but the last amounts of the dibutyl and dihexyl dyes are taken up slowly, complete equilibrium requiring about 24 hours for the dibutyl dye and over 48 hours for the dihexyl. Slow equilibration seems to be associated with large groups on the nitrogen atoms. The slowness cannot be attributed to slow diffusion to the grain surface, for comparative experiments on the rates of diffusion of dimethyl (XIV) and dihexyloxacarbocyanine (XVII) in gelatin solutions of the same composition as in the emulsion eliminate this explanation, and the slow process must be the attachment of the dye to the coöperative layer.

The adjustment of the large alkyl groups on the N atoms to the configuration allowing greatest interaction between adjacent adsorbed molecules might well require some time, especially if the alkyl groups are held to the surface. If, then, the conclusion is correct that in the coöperative layer the dye molecules are held edge-on, it seems probable from these considerations of rate that at least one of the N atoms in the dye molecule must be directed toward the surface.

Effect of Non-planarity on Adsorption.—The isotherms of a number of 2,2′-cyanines in emulsion A, illustrated in Fig. 5, divided themselves into two groups, one set of normal Langmuir curves (1–5) for the dyes containing only methyl, ethyl or phenyl on the nitrogen atoms, and also for those containing methyl groups on the 6,6′- and 7,7′-positions, in addition to N-ethyl. Coöperative interaction begins for these dyes with the first additions to the surface, the dye appearing to be adsorbed, even at low concentrations, as islands of coöperative aggregate. The types of absorption spectra exhibited by the saturated monolayers of these dyes are indicated in Table II, and it will be noted that they are not all of the J-type.

Curves 6–9 of Fig. 5 apply to 2,2′-cyanines containing alkyl groups in the 3,3′-(X) or 8,8′-(XI) positions in the nuclei, and in the 9-position in the methine bridge (XII) and (XIII). The dyes with alkyl substitution in the 3- and 9-positions differ from those in the first group in that, as discussed by Brooker and his coworkers,[15] the crowding on the rest of the molecule by large groups in these positions prevents a coplanar configuration of the nuclei. Figures 8 and 9 illustrate this crowding for the "extended" structure of the cations, and similar drawings for other configurations show that no planar structure can accommodate the alkyl groups without interpenetration of the van der Waals spheres of influence. These dyes are therefore forced to assume a non-planar configuration of the nuclei, which become twisted about the methine bridge, with large effects on the absorption spectra,[15] adsorption and optical sensitization.

In dye XI, carrying methyl groups on the 8,8′-positions adjacent to the N atoms of the quinoline nuclei, the crowding of the 8-methyl on the 1-ethyl group does not necessarily force the two nuclei from coplanarity, but causes distortion from normal valence angles about the region of crowding. This type of crowding has been discussed by Brooker, *et al.*,[15] for the 8,8′-substituted 2,2′-carbocyanines.

It is found that non-planar dyes are invariably much more poorly adsorbed than planar dyes of the same class, the difference in adsorbability between crowded and related planar dyes shown in Fig. 5 being typical. This, no doubt, is partly attributable to the greater distance from the surface which a non-planar configuration imposes on some of the atoms in the dye molecule; moreover, non-planarity, by restricting the freedom of motion of the π-electrons in the conjugated band systems, will diminish the van der Waals forces, which are particularly large when the full effect of resonance is in play.[13] Both the forces which cause adhesion to the surface and the lateral interactions which lead to the coöperative branch of the isotherm are therefore diminished in the non-planar dye. In 1,1′,3,3′-tetramethyl-2,2′-cyanine (X), the structure in which the nuclear planes are twisted about the methine bridge still permits close packing in a form of edge-on orientation, and, at sufficiently large dye concentrations, coöperative adsorption sets in with a rapid rise of the isotherm to a saturation plateau. The area per molecule at saturation is 97 Å.^{2}, considerably larger than for planar 2,2′-cyanines of the same length (74 Å.^{2} for the 1,1′-dimethyl; 79 Å.^{2} for the 1,1′-diethyl dye (Table II), although it is uncertain whether this actually represents a greater thickness of the non-planar dye or whether it indicates the existence

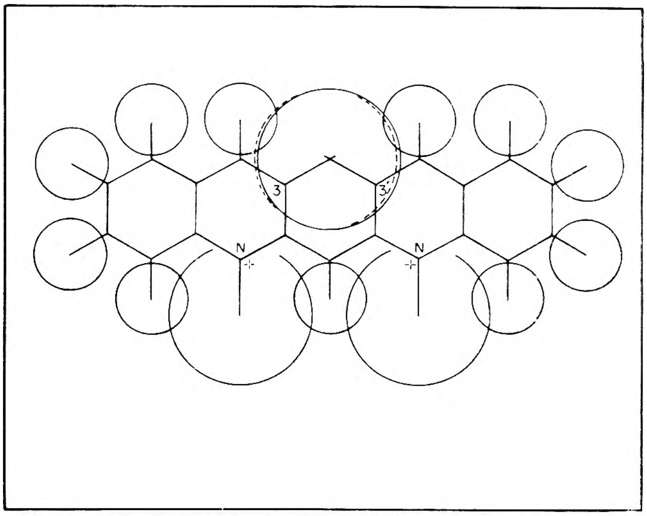

Fig. 8.—Scale drawing of 1,1′,3,3′-tetramethyl-2,2′-cyanine (X), showing overlap of spheres of influence of the 3- and 3′-methyl groups in a planar configuration.

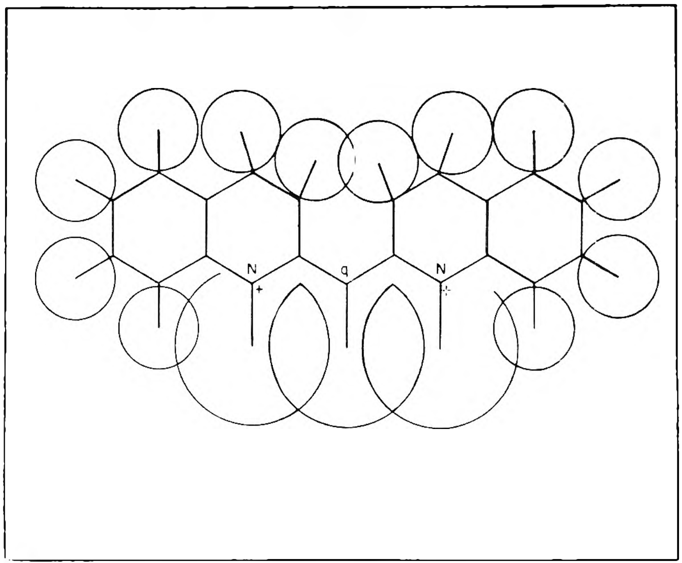

Fig. 9.—Scale drawing of 9-alkyl-2,2′-cyanines (XII, XIII) showing crowding in a planar configuration.

of adsorptive sites efficient toward the planar dyes but inefficient toward the non-planar.

Apart from the dyes in which the heterocyclic nuclei are not coplanar, the least adsorbable of the 2,2′-cyanines listed in Fig. 5 contain phenyl groups on the nitrogen atoms (IX) or methyl groups on the adjacent 8-position, crowding on alkyl groups on the nitrogen atoms (XI). It seems probable, therefore, that the 2,2′-cyanines are held with the edge containing the N atoms presented toward the surface, as Sheppard, *et al.*, suggested on general electrostatic grounds,[3,4] and, in accord with the conclusion drawn in a previous paragraph of this communication, from the rates of adsorption of oxacarbocyanines with large alkyl groups on the nitrogen atoms.

Influence of Gelatin on Adsorption of Cyanines.—Both the rate of adsorption[4] and the equilibrium between the dye and the surface depend on the gelatin content of the emulsion. Gelatin tends to depress the rate and, at the lower concentrations of added dye, to diminish the area covered at equilibrium by a given amount of dye.

Figure 10 shows the isotherm at 40° for the non-planar dye, 1,1′,3,3′-tetramethyl-2,2′-cyanine iodide (X), in grains of the same type (emulsion A) suspended in 7% gelatin aqueous medium and in an aqueous solution containing about one-twentieth of the normal gelatin, other conditions being constant. The toe nearly vanishes in the suspension of low gelatin content, and the adsorption of dye is much increased, although the saturation plateau is the same for both suspensions. Apparently the gelatin enters into adsorptive competition with dye, although the common saturation limit suggests that all the gelatin can ultimately be displaced from the surface at sufficiently high concentration of dye.

If dyed grains in the low-gelatin suspension in condition A (Fig. 10) are centrifuged and resuspended in the 7% gelatin medium, dye is lost by the grain until, after about 48 hours, the equilibrium distribution between surface and solution for the high-gelatin medium is reached (B, Fig. 10). The isotherm in 7% gelatin therefore represents a complete equilibrium, reached from both sides.

Merocyanines.—Merocyanines form a class of non-ionized dyes and those discussed in this communication contain basic heterocyclic nuclei, such as benzothiazole, linked by a conjugated bond system to heterocyclic rings, such as rhodanine or pyrazolone. The color is associated with resonance of the amide type involving the nitrogen atom and the carbonyl oxygen atom of the two nuclei.[25] Although not ionized, these dyes have high dipole moments; they are usually very sparingly soluble in water, but a few containing the thiazoline or thiazole nuclei are sufficiently soluble in aqueous gelatin to permit following the isotherm without great trouble from precipitation. Some merocyanines rendered more soluble in water by the addition of sulfonic acid or carboxymethyl groups were also examined.

Typical merocyanines examined are formulated in Table IV.

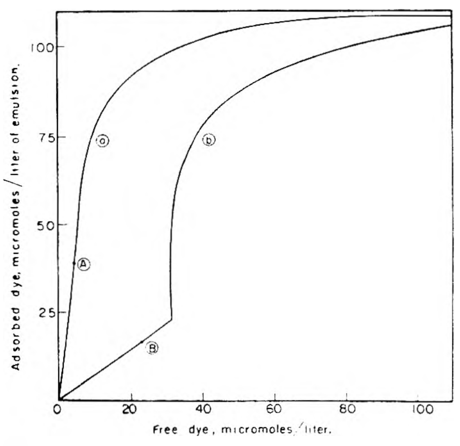

Fig. 10.—Effect of gelation on isotherm of 1,1′,3,3′-tetramethyl-2,2′-cyanine iodide: (a) 0.3% gelatin; (b) 7% gelatin; temp., 40°.

Table IV

Merocyanines

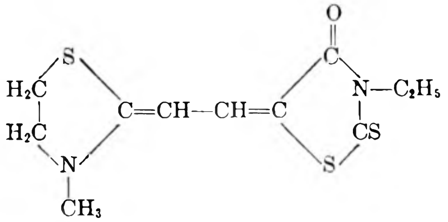

XXI, 3-ethyl-5-[(3-methyl-2-thiazolinylidene)-ethylidene]-rhodanine

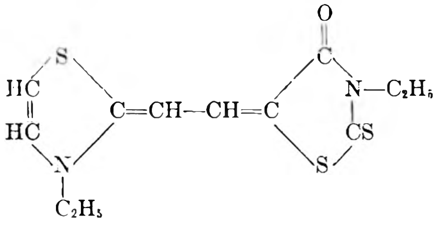

XXII, 3-ethyl-5-[(3-ethyl-2(3)-thiazolylidene)-ethylidene]-rhodanine

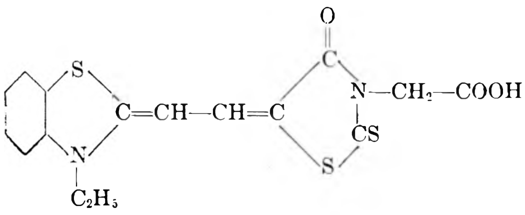

XXIII, 3-carboxymethyl-5-[(3-ethyl-2(3)-benzothiazolylidene)-ethylidene]-rhodanine

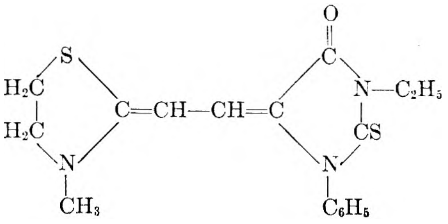

XXIV, 3-ethyl-5-[(3-methyl-2-thiazolinylidene)-ethylidene]-1-phenyl-2-thiohydantoin

---

[25] L. G. S. Brooker, G. H. Keyes, R. H. Sprague, R. H. VanDyke, E. VanLare, G. VanZandt and F. L. White, *J. Am. Chem. Soc.*, **73**, 5326 (1951).

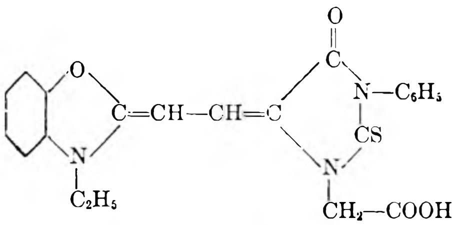

XXV, 1-carboxymethyl-5-[(3-ethyl-2(1)-benzoxazolylidene)-ethylidene]-3-phenyl-2-thiohydantoin

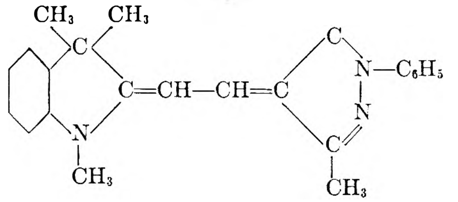

XXVI, 4-[(1,3,3′-trimethyl-2-indolenylidene)-ethylidene]-3-methyl-1-phenyl-5-pyrazolone

The rhodanine merocyanines, XXI, XXII and XXIII, showed simple Langmuir isotherms (Fig. 11, curves 1 and 2), indicating an area per molecule at saturation consistent with edge-on orientation in a monolayer, with an average internuclear distance about 4.3 A., comparable with the values for the cyanine dyes (Table II).

The absorption spectrum of these rhodanine merocyanines in the adsorbed state is not of the J-type, another example of the possibility of edge-on orientation without the appearance of this type of band.

Merocyanines containing the thiohydantoin nucleus, represented in XXIII and XXIV, do not exhibit saturation limits in adsorption (curves 4, 5, Fig. 11), and usually conform well to the Freundlich equation, $m = kc^{1/n}$.

The isotherm of the merocyanine dye, XXVI, in Fig. 11, curve 6, is an extreme example of the type with a coöperative discontinuity. A critical concentration must be attained before dye is measurably adsorbed at all, when a Langmuir isotherm suddenly springs up to attain a saturation value corresponding to coverage of only a small fraction of the surface. The onset of coöperative adsorption in this dye is accompanied by the appearance of a J-absorption band.

Effect of Silver Ion Concentration on Adsorption of Cyanines and Merocyanines.—Sheppard and his co-workers[3,4] and Leermakers, Carroll and Staud[11] found that the adsorption of cyanine dyes to silver halide particles in suspension was diminished with increasing concentration of silver ion, and Sheppard, in particular, concluded from this fact that the adsorptive forces were essentially the electrostatic attraction between the dye cation and the bromide ions in the surface, the organophilic part of the molecule setting itself away from the surface. As Sheppard, Lambert and Keenan[3] themselves point out, however, very considerable quantities of pinacyanol (1,1′-diethyl-2,2′-carbocyanine iodide) are adsorbed by suspensions of silver bromide at silver ion concentrations at which the solid behaves as the "silver body," in the sense of Fajans and Frankenburger.[26] This type of behavior, in fact, is general with cyanine dyes on silver bromide. Although there is an undoubted tendency, varying with the individual dye, for adsorption to be diminished at the higher concentrations of silver ion, these dyes, unlike adsorption indicators, exhibit no sharp change in adsorption at the silver ion concentration at which the solid particle of adsorbant changes the sign of its charge.

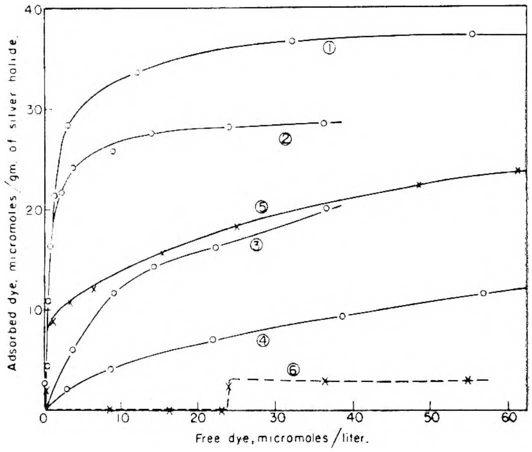

Fig. 11.—Adsorption isotherms of merocyanines at 40°: (1) dye XXI in emulsion A; (2) dye XXII in emulsion A; (3) dye XXIV in emulsion A; (4) dye XXV in emulsion A; (5) dye XXV in emulsion B; (6) dye XXVI in emulsion A.

For pinacyanol, Sheppard and Keenan suggested that complex formation between silver ion and the dye was connected with the adsorption to silver bromide at relatively high concentrations of silver ion, but for other cyanines, *e.g.*, 3,3′-diethylthiacarbocyanine, there is, on treatment of dye solutions with silver nitrate solution, neither spectroscopic nor potentiometric evidence of the formation of complexes. It seems therefore in better accord with the general facts to attribute the adsorption of cyanine dyes to silver bromide at relatively high silver ion concentrations to non-specific van der Waals forces, which supplement the electrostatic forces.

Figure 12 illustrates the effect of silver ion concentration on the adsorption of 3,3′-diethylthiacarbocyanine iodide and of the corresponding oxacarbocyanine in emulsion A at 40°. The adsorption is indicated as the percentage of a given amount of dye added to the emulsion which is adsorbed to the surface. For 3,3′-diethylthiacarbocyanine iodide (curve 1) practically the whole of the dye added (82 micromoles per liter of emulsion) is adsorbed at *p*Ag above 6; at *p*Ag values between 5 and 6, adsorption begins to decrease but at *p*Ag 4, 90% of the dye is still adsorbed; a rapid fall in adsorbability occurs below this value of *p*Ag, and about *p*Ag 3 in the emulsion little dye is adsorbed (*cf.* ref. 11). The oxacarbocyanine, added at 87 micromoles per liter (curve 2) is 90% adsorbed at *p*Ag 8.5, and is distinctly less adsorbed at *p*Ag 6, below which a more rapid fall in adsorbability takes place. The smaller amount added (curve 3) is practically unadsorbed at *p*Ag 4.

The shape of the complete isotherm for diethylthiacarbocyanine iodide is little changed between *p*Ag 6 and 9, and the saturation value is constant.

---

[26] K. Fajans and W. Frankenburger, *Z. physik. Chem.*, **106**, 255 (1933).

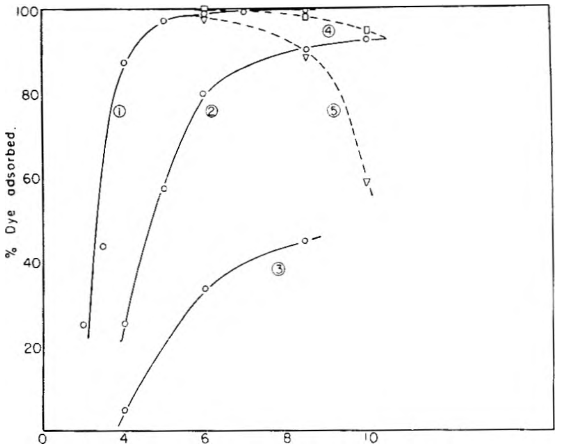

Fig. 12.—Effect of silver ion concentration on adsorption of cyanines and merocyanines in emulsion A at 40°: (1) 3,3'-diethylthiacarbocyanine iodide (I), 82 micromoles per liter added; (2) 3,3'-diethyloxacarbocyanine iodide (XIV), 87 micromoles per liter added; (3) 3,3'-diethyloxacarbocyanine iodide, 4.4 micromoles per liter added; (4) merocyanine (XXII) 106 micromoles per liter added; (5) merocyanine (XXIV) 59 micromoles per liter added.

At *p*Ag 5 in emulsion A, the isotherm is of the type showing a low adsorption toe, followed by a cooperative discontinuity, the isotherm now resembling that for diethyloxacarbocyanine at the normal emulsion *p*Ag (curve 2, Fig. 4); the saturation value is the same as at higher *p*Ag. As the *p*Ag is decreased, the toe extends to higher concentrations of free dye, and the saturation plateau, although retaining its quality of saturation, sinks to lower levels, as if only a fraction of the surface is able to retain adsorbed dye.

Merocyanines containing the rhodanine and thiohydantoin nuclei are affected by silver ion in the opposite way to the cyanines; the adsorption is increased by increasing the silver ion concentration (curves 4, 5, Fig. 12, for dyes XXII and XXIII, respectively). The addition of silver nitrate to acetone solutions of these dyes causes bathochromic displacement of the absorption band, and, since this behavior with silver is most pronounced for merocyanines containing the $C{=}S$ group and absent for many merocyanines without it, it seems probable that some kind of sulfur–silver ion linkage is formed. The effect of silver ion in facilitating adsorption of rhodanine and thiohydantoin merocyanines would then suggest that forces between the double-bound S atom of the dye and silver ions of the surface are important.

Dye XXVI, which contains no sulfur atom in the molecule, and whose isotherm is the anomalous curve, 6, of Fig. 11, is adsorbed to a greater extent as the bromide ion is increased. Saturation of the surface by this dye occurs long before complete coverage of the surface; hence the area per molecule gives no information on the orientation of the molecules. The J-band in the absorption spectrum of this dye adsorbed to silver halide, however, suggests that it is adsorbed in close-packed molecular aggregates which must be scattered as islands over the surface. The increased adsorption at high bromide ion concentrations then suggests that the nitrogen atom of the pseudoindole nucleus, near the positive end of the molecular dipole, is directed toward the surface, and the oxygen atom of the pyrazolone nucleus, the negative end of the dipole, away from the surface.

Heat of Adsorption of Dyes in Emulsion.—The isosteric heats of adsorption of some sensitizing dyes in emulsions have been determined from the 40° and 60° isotherms by means of the Clapeyron–Clausius equation. Illustrative pairs of isotherms for 3,3'-dimethyloxacarbocyanine iodide (XIV) and for the merocyanine (XXIV) are shown in Fig. 13. Table V gives some results.

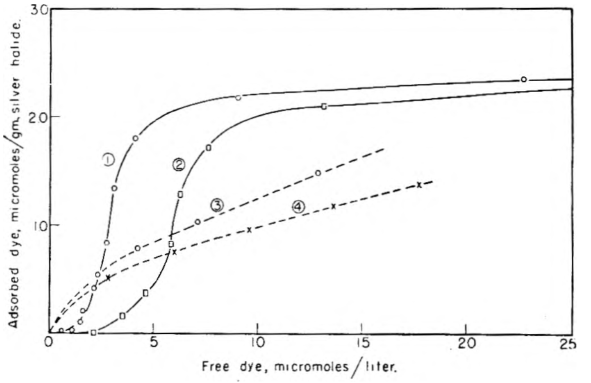

Fig. 13.—Temperature coefficient of adsorption of dyes in emulsion A: (1) 3,3'-dimethyloxacarbocyanine iodide at 40°; (2) 3,3'-dimethyloxacarbocyanine iodide at 60°; (3) merocyanine XXIV at 40°; (4) merocyanine XXIV at 60°.

Table V

Heats of Adsorption of Sensitizing Dyes in Emulsions

Dye	Heat of adsorption, cal. per mole	Fraction of surface covered, %	Emulsion
1,1'-DiEt-2,2'-cyanine iodide (VI)	12,000	45	A
	9,000	76	A
1,1',3,3'-TetraMe-2,2'-cyanine iodide (X)	7,100	11–20	A
	12,700	20–30	Same grains as A suspended in very dil. gelatin soln.
3,3'-DiMe-oxacarbocyanine iodide (XIV)	9,800	30	A
	7,200	10	B
	6,600	30	B
3,3'-DiEt-oxacarbocyanine iodide (XV)	12,000	10	A
	9,700	50	A
	8,100	av. 10–50	B
Merocyanine (XXI)	8,500	50–75	A
Merocyanine (XXIV)	4,220	*ca.* 50	A
	8,300	*ca.* 50	B

As has been frequently observed in other systems, the heat of adsorption is greatest for the first additions of dye to the surface. The heats for planar cyanine dyes in emulsion A are about 10,000 to 12,000 cal. per mole at low coverage of the surface, decreasing to 8,000 or 9,000 cal. as more dye is added. The most probable explanation seems to be adsorption of the first quantities of dye added at the most active adsorptive sites in the surface. The heat of adsorption also depends on the type of grain, being, for example, lower for oxacarbocyanines in the chlorobromide emulsion, B, than in the bromoiodide emulsion, A, while with the merocyanine, XXIV, the heat is greater in the chlorobromide. The non-planar dye 1,1',3,3'-tetramethyl-2,2'-cyanine iodide (X), shows a distinctly lower heat in emulsion A than its planar relative, 1,1′-diethyl-2,2′-cyanine iodide (VI), correlated with the generally lower adsorption of the non-planar dye. The heat term as measured from the temperature coefficient of adsorption in these emulsions is, of course, a complex quantity, including terms for the desorption of gelatin, and, in fact, the heat of adsorption of the non-planar dye (X) was found to be considerably greater in a suspension of the same grains as in emulsion A in a very dilute gelatin solution than in the 7% concentration usually used in these experiments.

Some of the dyes in Table V show coöperative discontinuities in their isotherms, and the lateral interactions in the coöperative state might have been expected to cause a higher heat of adsorption than for the toe, instead of the lower heat observed. If, however, the toe corresponds to a flat and the other branch to edge-on orientation, part of the lateral interaction would be compensated for by diminished van der Waals interaction with the surface, and, in addition, it seems that the energy of coöperative interaction is masked by the lower activity of the surfaces sites involved in holding the coöperating molecules at the higher coverages.

Some Miscellaneous Dyes.—Figure 14 shows the 40° isotherms in emulsion A of a few miscellaneous dyes other than cyanines and merocyanines. Methylene blue, a photographic desensitizer, shows a Langmuir isotherm with a saturation plateau corresponding to an area of 88 Å.,[2] too low for a flat orientation. Pinakryptol green, another desensitizer, is only feebly adsorbed. Erythrosin and congo red sensitizers are feebly adsorbed, compared with sensitizing cyanines; eosin still less; and fluorescein scarcely at all in these emulsions.

Part II. Relations between Dye Adsorption and Sensitization

Adsorbability of a dye in itself has long been known to be no criterion of its sensitizing power, nor indeed would one expect adsorption to be the only requirement for the effective transfer of energy from a dye to silver halide. No general correlation between dye adsorption and sensitization is to be expected, but questions arise concerning possible correlations between adsorption and sensitization characteristics (a) of a single dye as functions of the concentration of dye in the emulsion, (b) of the members of a chemically similar group of dyes, in which the transfer efficiency as determined by the general chemical structure might be constant, (c) of a single dye as influenced by addenda which are known to affect the sensitization, as in the phenomenon of supersensitization. It turns out that well-marked correlations can often be found between the adsorption and sensitization characteristics of a single dye, but that, even within a restricted chemical group of sensitizers, relative adsorbability is no certain guide to relative sensitizing efficiency, and that supersensitization cannot be explained as the result of changes in the adsorption of the sensitizer effected by the supersensitizer.

(a) **Adsorption–Sensitization Relations in Individual Dyes.**—A well-marked correlation between sensitization and adsorption in a given dye is illustrated by sensitizers whose adsorption isotherm shows the discontinuities attributed to the onset of coöperative adsorption before the completion of the first layer. For example, emulsions dyed with the oxacarbocyanines of Fig. 4 exhibit changes in absorption spectra and in spectral sensitivity, at the point corresponding to the discontinuity in the isotherm, which might therefore be described as conditioned by the change in adsorption. Again, the merocyanine, XXVI (curve 6, Fig. 11), exhibits a critical concentration below which it practically does not sensitize and above which it sensitizes, with a J-maximum, which agrees precisely with the critical concentration necessary for appreciable adsorption. This critical concentration depends on the solvent, methyl alcohol or acetone, in which the dye is added to the emulsion, although the saturation limit does not depend on the solvent.

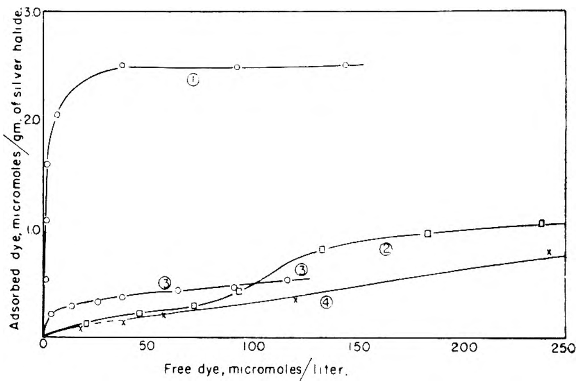

Fig. 14.—Adsorption isotherms of some miscellaneous dyes: (1) methylene blue; (2) capri blue; (3) congo red; (4) erythrosin, in emulsion A at 40°.

The parallelism between the adsorption and sensitization as functions of concentration of sensitizers in general does not extend throughout the whole concentration range to the establishment of the close-packed monolayer. As was pointed out by Sheppard, Lambert, Keenan and Walker[3,4] optical sensitization attains a maximum at dye concentrations decidedly below the saturation value for adsorption. In emulsions A and B, optimum sensitization is attained when the surface is about one-third to one-half covered with dye in edge-on orientation. Spence and Carroll[27] have shown that the main reason for a maximum in the sensitization–concentration function is a desensitization by the dye, acting independently of its optical sensitization.

(b) **Adsorption–Sensitization Relations among Dyes of Similar Chemical Structure.**—No detailed parallelism is found between the adsorption and sensitization of the members of series of dyes, such as the N-alkyloxacarbocyanines illustrated in Fig. 4, or the 2,2′-cyanines illustrated in curves 1–5 of Fig. 5. In the oxacarbocyanines, the adsorption of the 3,3′-dimethyl dye compound is quite considerably greater than that of the 3,3′-diethyl dye, while the latter, added to the emulsion at the same concentration as the dimethyl dye, confers the greater sensitivity. Similarly, while there is no

---

(27) J. Spence and B. H. Carroll, This Journal, **52**, 1090 (1948).

great difference in the adsorbability of 1,1′-dimethyl- and 1,1′-diethyl-2,2′-cyanines, the latter is the more efficient sensitizer. Comparing the two oxacarbocyanines, a greater intrinsic efficiency of sensitization of diethyloxacarbocyanine more than compensates for the deficiency in the amount of this dye adsorbed, and, in general, adsorbability and efficiency of sensitization, even within a restricted family of dyes, are not related in any simple way. The quantum efficiency of a sensitizer is determined by an expression of the form

$$\phi = k_s[s]/(k_f + k_d + k_s[s])$$

where the k's are, respectively, the velocity constants for sensitization (k_s), fluorescence (k_f), and the sum (k_d), of the velocity constants for all internal and external deactivation processes, and $[s]$ is the "active mass" of the sensitized substrate. It seems that, within a group of chemically similar dyes, substituents affect the relative values of these constants in a manner not parallel to their effects on the simpler process of adsorption.

Interesting comparisons can be made between the adsorption and sensitization of non-planar dyes in their relation to planar dyes of the same class. The relatively low adsorbability of non-planar dyes has already been referred to and is illustrated for 2,2′-cyanines in Fig. 5, curves 6–9. The sensitization of non-planar dyes is, in general, much lower than that of planar dyes of similar chemical structure, as first shown in a few examples by Sheppard, Lambert and Walker[28] and since confirmed for a number of non-planar dyes prepared under the direction of Dr. L. G. S. Brooker, of these laboratories. There is therefore a qualitative parallelism between low adsorption and low sensitization in non-planar dyes, but quantitatively, it is quite impossible to account for the deficiency in sensitization by the deficiency in adsorption. For example, the sensitization of the non-planar 2,2′-cyanine iodide (X) is only hundredths as large as that of the corresponding planar dye, 1,1′-diethyl-2,2′-cyanine iodide (VI), when added to the emulsion at the same concentration, 4×10^{-5} molar; the non-polar dye is then about 40% adsorbed, while the planar dye is practically completely adsorbed. Allowing for some decreased absorption of light by the adsorbed non-planar dye, the sensitization of this dye, if determined by the adsorption and light-absorption relations alone, would be not less than 20% of that of the planar dye, instead of nearly zero. This behavior is general; non-planar dyes are invariably poorly adsorbed and poor sensitizers, but the loss in sensitization, compared with the corresponding planar dye, is always much greater than can be attributed to the diminution in adsorption.[29]

The distorted configuration of non-planar dyes probably increases the separation between some of the chromophoric atoms and the surface, but experimental and theoretical considerations make it unlikely that the probability of a sensitizing transfer can fall off very rapidly in a distance of a few atomic diameters, and a rapid internal deactivation somehow associated with non-planarity seems a more probable reason for the inefficiency of non-planar dyes as sensitizers.

(c) **Adsorption and Supersensitization.**—In supersensitization, an enhancement of the sensitization produced by certain sensitizers is caused by the presence in the adsorbed layer of certain other substances, which may be colorless, or may be dyes absorbing in a different spectral region from that of the sensitizer.[8,10] A typical example of the phenomenon is afforded by 1,1′-diethyl-2,2′-cyanine iodide (VI). The quantum efficiency of sensitization of this dye at 575 mμ, relative to that for light absorbed by the silver halide, is increased from 0.05 in certain emulsions to nearly unity by the addition of a small amount of the merocyanine dye (XXVII), which itself sensitizes somewhat feebly in the blue-green region of the spectrum.

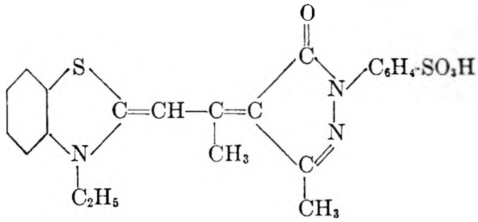

XXVII, 1-(*p*-Sulfophenyl)-3-methyl-4-[(3-ethylbenzothiazolylidene)-isopropylidene]-5-pyrazolone

It is clear from the isotherm of the sensitizer in this combination, curve 2 of Fig. 5, that the supersensitization observed cannot be attributed to any increase in the gross amount of adsorbed dye. Actually, there is a slight displacement of the sensitizer from the surface by the supersensitizer at the concentration for optimum sensitization, increasing with the amount of supersensitizer. For this sensitizer–supersensitizer combination, the change in adsorption of the sensitizer caused by the presence of the supersensitizer seems to have nothing to do with the increased efficiency of sensitization.

The adsorption of the supersensitizer in this combination is significantly increased by the presence of the sensitizer. Figure 15, curve 1, shows the adsorption of the merocyanine dye alone in emulsion B at 40° (in which emulsion the supersensitization effect is great, as it is in A), and curve 2 is the isotherm for the merocyanine in the presence of a constant amount of the sensitizer, 44 micromoles per liter being added to the emulsion. The supersensitizer at low concentration is adsorbed to a greater extent in the presence of the cyanine dye, but at higher concentrations, the merocyanine is less adsorbed in the presence of the more tightly bound cyanine. This particular merocyanine contains a sulfonic acid group on the pyrazolone nucleus, and the increased adsorption at low concentrations caused by the basic cyanine dye may be caused by interionic attraction.

---

(28) S. E. Sheppard, R. H. Lambert and R. D. Walker, *J. Chem. Phys.*, **9**, 96 (1941).

(29) The non-planarity concerned in suppressing optical sensitization is that involving the atoms in the resonating chain; substituents, like phenyl, can be introduced in a different plane from that of the heterocyclic nuclei and methine chain without seriously inhibiting sensitization or coöperative adsorption, so long as they do not crowd on atoms in the chromophoric chain. In erythrosin, the central carboxyphenyl group is displaced from the plane of the atoms constituting the chromophore, but, although it is very poorly adsorbed (Fig. 14, curve 4), the sensitizing efficiency of what dye is adsorbed appears to be relatively high.

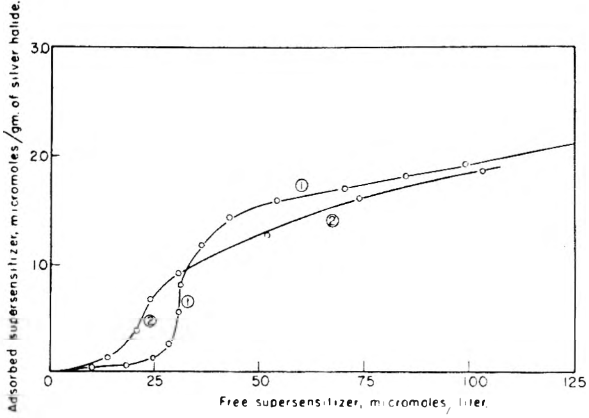

Fig. 15.—Effect of a sensitizer on the adsorption of a supersensitizer: (1) isotherm of merocyanine XXVII alone; (2) isotherm of XXVII in presence of 44 micromoles per liter of the sensitizer, 1,1′-diethyl-2,2′-cyanine iodide (VI), in emulsion B at 40°.

One of the most remarkable examples of supersensitization is the conversion of certain non-planar cyanines, alone almost without sensitizing properties, into moderate sensitizers by the addition of appropriate supersensitizers, of the same general nature as are effective for the corresponding planar dyes. Such a combination is 1,1′,3,3′-tetramethyl-2,2′-cyanine iodide (X) and the merocyanine (XXVII) just discussed, which sensitizes in the absorption band of the cyanine with an efficiency some hundreds of times greater than that of this dye alone. Here there is a considerable increase in the adsorption of the non-planar dye as a result of the presence of the supersensitizer (Fig. 16); the low adsorption toe nearly disappears, and coöperative adsorption begins at low concentrations of added cyanine. When the non-planar dye at a concentration of 44 micromoles per liter is added to the emulsion alone, it assumes a condition, A, in which about 40% is adsorbed, probably in flat orientation; in the presence of an added quantity of supersensitizer of 44 micromoles per liter, the cyanine assumes a condition, B, in which about 80% is adsorbed in the coöperative state (as is shown also by the appearance of the J-band in the presence of the supersensitizer). The coöperative state in itself is not the cause of sensitization, for dye in a condition, C, on the coöperative branch of the isotherm without supersensitizer is as inefficient in sensitization as in condition A. It is clear, however, that the increased sensitization in the presence of the supersensitizer is far too great to be attributed to a mere doubling in the amount of adsorbed dye.

In this combination, the adsorption of the supersensitizer is increased by the addition of the non-planar dye over a wide concentration range—interionic attractions cause mutual increase in adsorption.

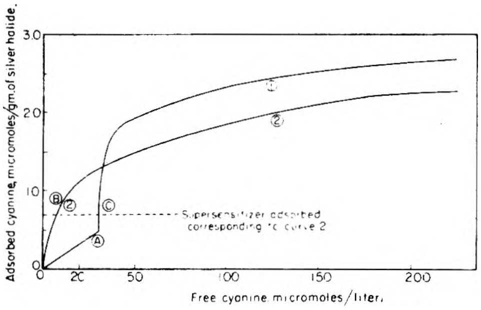

Fig. 16.—Effect of a supersensitizer on the adsorption of a non-planar cyanine: (1) 1,1′,3,3′-tetramethyl-2,2′-cyanine iodide (X) alone; (2) (X) in presence of supersensitizer (XXVII), in emulsion A at 40°.

With the object of detecting any effect of the supersensitizer on the strength of the adsorption forces holding the non-planar dye to the surface, careful estimates of the heat of adsorption of this dye with and without the supersensitizer were made from the 40° and 60° isotherms. To eliminate to some degree the complication of the presence of gelatin, these measurements were carried out on grains of the same sort as in emulsion A, but suspended in an aqueous medium of low gelatin content (about 0.3%). At this low gelatin content, the isotherm loses the toe characteristic for this dye in normal emulsions and assumes a simple Langmuir form (Fig. 10, curve a). The heat of adsorption for about 80% coverage of the surface by the non-planar dye alone was 12,700 cal. per mole, with a mean deviation of ±900 cal., and for the same amount of adsorbed cyanine in the presence of 44 micromoles per liter of added merocyanine, the heat was 9,500 cal. per mole ±1,100 cal. Both of these values are higher than the 7,500 cal. in normal A emulsion, presumably because less energy was expended in displacing gelatin from the surface. The supersensitizer certainly does not increase the heat of adsorption of the non-planar dye—the observed decrease seems real, and perhaps may be attributed to the greater number of adsorptive sites engaged in the presence of the supersensitizer, with a consequent increase in the number of less active sites holding the non-planar dye.

These results on the degree and heats of adsorption of sensitizers in the presence of supersensitizers seems to make it certain that supersensitization is not caused by any effect of the supersensitizer on the geometrical disposition of the sensitizing dye toward the silver halide surface. The essential reason for the increase in sensitization efficiency in the most typical examples of this phenomenon seems to be connected with an effect of the supersensitizer in interrupting the propagation of energy throughout the adsorbed dye layer, as is discussed in detail elsewhere.[10]

Acknowledgments.—We wish to acknowledge the assistance of Mr. E. E. Richardson in obtaining spectrophotometric curves and of Mr. H. Gunther in preliminary experiments.

THE SOLUBILITIES OF OLEIC AND LINOLEIC ACIDS IN COMMON ORGANIC SOLVENTS[1]

BY C. W. HOERR AND H. J. HARWOOD

Research Division of Armour and Company

Received February 16, 1952

Oleic and linoleic acids were prepared by combination of crystallization and distillation procedures, giving careful consideration to the problems involved in the removal of the naturally occurring impurities. The solubilities of these highly purified acids were determined in a variety of common organic solvents over wide ranges of temperature and concentration. Factors influencing the solubility were evaluated by comparing the curves in different solvents on a molecularly equivalent basis. It was found that the fundamental solubility behavior of oleic and linoleic acids differs little from that of stearic acid. The internal pressures, polarities, molar volumes, hydrogen-bonding tendencies, and heats of fusion estimated from the slopes of the solubility curves of oleic and linoleic acid are consistent with the values calculated from other observations.

The only quantitative solubility data of oleic and linoleic acids are those determined by Foreman and Brown[2] and by Singleton[3] in several common organic solvents at a few temperatures between −25 and −70°. Despite these meager data, oleic acid has probably received more attention regarding its preparation in a pure state than any other higher aliphatic compound. Although numerous investigators have claimed the preparation of highly purified oleic acid, their corroborative evidence in all but a very few instances fails to withstand critical evaluation. Unfortunately, the vast majority of investigators neglected to determine the freezing points of their samples, relying upon neutralization equivalents, iodine numbers, thiocyanogen values and melting points (usually capillary) as criteria of purity. Failure to consider the experimental error involved in these determinations and the substantial influence of the saturated and more highly unsaturated homologs upon the physical properties of oleic acid has been responsible for many doubtful claims of purity.

The earlier work on the preparation of oleic acid has been summarized sufficiently by Ralston.[4] The more recent investigations have been reviewed quite thoroughly by Smith[5] and by Brown.[6,7] The earlier work was, in general, based upon the differential solubilities of the metal salts of the saturated and unsaturated fatty acids in ethanol or acetone.[8–13] Subsequent investigators found that stepwise precipitation of the fatty acids yielded oleic acid of a quality at least as high as, if not higher than, that obtained by the metal-salt procedures.[5,6,14,15] The more recent work of Stewart and Wheeler[16] and that of Brown[2,17] involves a combination of vacuum distillation and fractional crystallization of the methyl esters.

Most investigators have been fully aware of the difficulty of removing the last few per cent. of stearic acid from an oleic acid preparation, and Hartsuch[15] concluded that oleic acid exceeding a purity of 98% had not yet been obtained. This observation should be amended to refer only to preparations involving solvent crystallization of the fatty acids without additional treatment. The reason for the failure to remove the remaining 2% of stearic acid by this procedure, apparently overlooked by previous investigators, can readily be understood by consideration of Smith's curves[5] for the binary system oleic–stearic acid showing a eutectic composition consisting of 98% oleic acid. It is for this reason that fractional distillation is combined with crystallization to remove the final amounts of impurities. Whereas Smith employed the ester distillation prior to the fractional crystallization, in the present investigation the oleic acid obtained by crystallization from acetone was subjected directly to careful fractionation *in vacuo*, thus avoiding any further complications which might be introduced by esterification and subsequent conversion to the acid. The quality of the final product appeared to be equal to, or better than, the best reported in the literature.

In contrast to the extensive research on oleic acid, there are relatively few reports on the purification of linoleic acid, and the claims regarding the purity of the products are far more modest. With the exception of the work of Brown,[18] who purified linoleic acid directly by low-temperature fractional crystallization, all other investigations employed the bromination process. Other work by Brown[19] demonstrated quite conclusively that the latter procedure resulted in mixtures of isomeric linoleic acids from which it was extremely difficult to isolate the desired 9,12-octadecadienoic acid. Although a number of refractive indices reported for linoleic acid are quite consistent, the respective melting points reported are so low as to suggest

---

[1] For detailed paper (or extended version or material supplementary to this article) order Document 3619 from American Documentation Institute, 1719 N. Street, N. W., Washington 6, D. C., remitting $1.00 for microfilm (images 1 inch high on standard 35 mm. motion picture film) or $1.35 for photocopies (6 × 8 inches) readable without optical aid.

[2] H. D. Foreman and J. B. Brown, *Oil and Soap*, **21**, 183 (1944).

[3] W. S. Singleton, *J. Am. Oil Chem. Soc.*, **25**, 15 (1948); **26**, 332 (1949).

[4] A. W. Ralston, "Fatty Acids and Their Derivatives," John Wiley and Sons, Inc., New York, N. Y., 1948, pp. 104–110.

[5] J. C. Smith, *J. Chem. Soc.*, 974 (1939).

[6] J. B. Brown and G. Y. Shinowara, *J. Am. Chem. Soc.*, **59**, 6 (1937).

[7] J. B. Brown, *Chem. Revs.*, **29**, 333 (1941).

[8] E. Twitchell, *J. Ind. Eng. Chem.*, **13**, 806 (1921).

[9] E. Raymond, *Chimie & industrie*, 523 (1929).

[10] S. H. Bertram, *Rec. trav. chim.*, **46**, 397 (1927).

[11] H. W. Scheffers, *ibid.*, **46**, 293 (1927).

[12] L. Keffler and J. H. McLean, *J. Soc. Chem. Ind.*, **54**, 362 (1935).

[13] J. H. Skellon, *ibid.*, **50**, 131 (1931).

[14] J. B. Brown and G. C. Stoner, *J. Am. Chem. Soc.*, **59**, 3 (1937).

[15] P. J. Hartsuch, *ibid.*, **61**, 1142 (1939).

[16] H. W. Stewart and D. H. Wheeler, *Oil and Soap*, **18**, 69 (1941).

[17] R. C. Millican and J. B. Brown, *J. Biol. Chem.*, **154**, 437 (1944).

[18] J. B. Brown and J. Frankel, *J. Am. Chem. Soc.*, **60**, 54 (1938).

[19] N. L. Matthews, M. E. Brode and J. B. Brown, *ibid.*, **63**, 1064 (1941).

that the products were mixtures of isomers. Therefore, in the present investigation the unsaturated acids of soya oil were recrystallized repeatedly from several solvents without resort to the bromination procedure. The final product appeared to be of a purity equal to the best reported, though no claims are made relative to its absolute purity.

This paper presents the solubility of oleic acid in 23 common organic solvents from −40° to the melting point of the acid and the solubility of linoleic acid in 14 solvents from −50° to the melting point of the acid, or to the temperatures at which the immiscible liquid phases became homogeneous.

Experimental

Preparation of Oleic Acid.—About one kg. of high quality olive oil was saponified by means of excess aqueous sodium hydroxide and the fatty acids were recovered by acidification in the usual manner. Oleic acid was obtained from this mixture by crystallization from 6% solution in acetone. The solution was cooled twice to −20°, filtered each time, and both precipitates were discarded. The filtrate was then cooled to −60° and filtered, the filtrate being discarded. The precipitate was recrystallized twice in the same manner at −60°, the filtrate being discarded each time. The final precipitate was stripped of solvent under reduced pressure, yielding about 150 g. of material having the following constants: freezing point, 12.2°, iodine number, 85.4 (calcd. 89.9), and refractive index, 1.4582, *t*, 20°. On the basis of Smith's diagrams,[6] this material apparently consisted of 95% oleic acid, the eutectic mixture with palmitic acid, as would be expected of the procedure employed.

This impure acid was carefully fractionated *in vacuo* in a Stedman packed column, the distillate being collected in fifteen 10-cc. fractions. Fractions 10 to 13, inclusive, were combined to yield 40 g. of oleic acid which was used for the solubility determinations. The physical constants of this sample are listed in Table I. The iodine number and neutralization equivalent have been omitted since they agreed with the calculated values, but are not sufficiently precise to be of great value in estimating high purity.

Table I

Physical Constants of Oleic Acid

	F.p., °C.	M.p., °C. α-Form	M.p., °C. β-Form	Refractive index n^t_D	t, °C.
		This investigation			
	13.38	13.38	16.30	1.4599	20
				1.4564	30
		Reference values			
5	13.34	13.36	16.25	1.4616	15
				1.4597	20
6	...	...	...	1.4585	20
9	...	13	16	.....	..
10	13.2	13.2	16	1.45823	20
				1.44179	70
11	...	12	15.4	1.46140	15
				1.45298	40
				1.44399	70
13	11.8–12.2	13–14	...	1.4610	20
16	13.2	13.4	16.2	.....	..
20	...	13.5–14	...	1.4611– 1.4620	20

Preparation of Linoleic Acid.—About 1.2 kg. of Neo-Fat No. 3-R[21] was separated by stepwise fractional crystallization from 10% solution in acetone. The temperature of the solution was lowered successively to −10, −20, −33, −50, −60 and −70°, the precipitates being removed by filtration at each temperature and discarded. After the sixth filtration, the solvent was stripped from the filtrate under reduced pressure, yielding about 125 g. of material freezing at −7.0° and possessing an iodine number of 171 (calcd. 181.0). This material was then recrystallized three times from 10% solution in Skellysolve B at −60°, the filtrate being discarded after each filtration. The final precipitate was freed of solvent by stripping under reduced pressure, and the material was vacuum distilled rapidly through a short Vigreux column. The middle cut (about 25 g.) was taken as the final product for use in the solubility determinations. The physical constants of this sample are listed in Table II.

Table II

Physical Constants of Linoleic Acid

	F.p., °C.	M.p., °C.	Refractive index n^t_D	t, °C.	Iodine no.
			This investigation		
	−5.3	−5.2	1.4703	20	180
			1.4664	30	181.0 calcd
			Reference values		
15	−7.2	−6.5	....	..	...
18	...	−6.8	1.4699	20	...
19	...	−5.2 to −5.0	1.4699	20	...
22	...	−8 to −7	....	..	...
23	...	−12 to −1	1.4715	11.5	...
			1.4683	21.5	...
24	...	−9 to −8	....	..	...

Experimental Procedures.—Freezing and melting points were determined by immersing a calibrated thermometer directly in a 5-g. sample of acid. The temperatures thus obtained were reproducible within ±0.01° and are considered accurate within ±0.02°.

The solubilities of oleic and linoleic acids were determined by weighing 2–5 g. portions of the acids into 2 × 15 cm. Pyrex test-tubes which were fitted with a Nichrome stirrer and a thermocouple well, the test-tube being inserted into a larger tube which served as an air-bath. An iron-constantan thermocouple was used in conjunction with a Leeds and Northrup potentiometer for measuring temperatures. Upon successive additions of weighed amounts of solvent, the solubilities were determined by measuring the temperatures at which crystals precipitated and dissolved upon alternately cooling and heating the systems in an acetone–Dry Ice-bath or water-bath as required. The solution temperatures thus obtained were reproducible within ±0.05° and are considered accurate within ±0.1°.

The solvents used in this investigation were of the best grade available and were dried by means of the customary drying agents and freshly distilled before using. The ethanol was commercial "absolute" diluted to 95.0% by weight with conductivity water, the composition being determined by comparing its density with the values in the "International Critical Tables."

Results

The solution temperatures of a sufficient number of known concentrations of oleic and linoleic acids in the various solvents were determined[1] in order to establish the liquidus curves of the systems in the temperature ranges investigated. By plotting the curves on a relatively large scale on 50-cm. cross-section paper, the solubilities at various desired temperatures could readily be obtained with reasonable accuracy. These solubilities are listed in Tables III and IV as g. acid per 100 g. solvent at a variety of temperatures. The values given are considered accurate within ±1%.

In order to compare these solubilities with those in the literature, corresponding values have been listed in Table V. The literature values have been converted to g. acid per 100 g. solvent so that corresponding solubilities would be on the same basis. The results are in generally good agreement, despite several inexplicable discrepancies. The solubility of oleic acid in furfural (Table III) contradicts a report[25] that this system is miscible at 0° as well as at 25 and 40°.

Oleic and linoleic acids form eutectics with some of the solvents in the temperature ranges investigated. These eutectic compositions and melting points are listed in the footnotes to Tables III and IV.

---

(20) D. Holde and K. Rietz, *Ber.*, **57B**, 99 (1924).

(21) A product of Armour and Company, Chemical Division, Chicago, Ill. Neo-Fat No. 3-R consists of approximately 60% linoleic acid and 40% oleic acid with perhaps 1–2% saturated acids.

(22) D. Holde and R. Gentner, *Ber.*, **58**, 1067 (1925).

(23) W. C. Smit, *Rec. trav. chim.*, **49**, 539 (1930).

(24) J. W. McCutcheon, *Can. J. Research*, **16B**, 158 (1938).

(25) F. Trimble, *Ind. Eng. Chem.*, **33**, 660 (1941).

TABLE III

SOLUBILITY OF OLEIC ACID IN VARIOUS ORGANIC SOLVENTS

Solvent	g. oleic acid per 100 g. solvent						
	−40.0°	−30.0°	−20.0°	−10.0°	0.0°	10.0°	20.0°
n-Hexane	0.1	1.2	9.1	44.4	160	720	∞
Benzene^a	Eutectic system		..	..	253	910	∞
Cyclohexane^b	Eutectic system		..	80	233	870	∞
Carbon tetrachloride^c	Eutectic	..	24.6	68	160	590	∞
Chloroform	11.5	23.3	46.0	92	205	760	∞
o-Xylene^d	Eutectic	..	30.5	88	250	1100	∞
Diethyl ether	1.2	4.4	17.9	60	195	870	∞
Chlorobenzene	2.5	6.2	27.0	85	220	900	∞
1,2-Dichloroethane	..	<0.1	1.3	26.1	130	670	∞
Nitrobenzene^e	Eutectic system		..	..	220	1100	∞
Dioxane^f	Eutectic system		..	..	237	1120	∞
Furfural^g	..	0.1	0.3	1.3	4.7	14.5	27.0
Ethyl acetate	1.6	4.5	12.2	44.0	185	750	∞
n-Butyl acetate	2.8	6.4	14.8	48.0	200	770	∞
Acetone	0.5	1.4	5.1	27.4	159	870	∞
2-Butanone	1.0	2.6	8.6	33.5	170	880	∞
Methanol	0.3	0.9	4.0	31.6	250	1820	∞
95.0% ethanol	0.7	2.2	9.5	47.5	235	1470	∞
2-Propanol	1.1	3.2	11.5	55.0	226	1160	∞
n-Butanol	1.3	4.0	15.2	56.5	100	950	∞
Nitromethane^h	0.1	0.2	0.4	0.6	0.8	1.0	1.1
Nitroethane^i	.2	.8	1.3	2.2	3.4	8.7	14.3
Acetonitrile^j	.1	.3	0.7	1.1	1.8	7.7	9.1

^{a} Eutectic at 59.7 wt. % oleic acid, −9.2°. ^{b} Eutectic at 38.9 wt. % oleic acid, −12.1°. ^{c} Eutectic at 9.4 wt. % oleic acid, −25.6°. ^{d} Eutectic at 6.0 wt. % oleic acid, −31.0°. ^{e} Eutectic at 58.5 wt. % oleic acid, 0.0°. ^{f} Eutectic at 61.6 wt. % oleic acid, −3.3°. ^{g} Miscible above 26.2°. ^{h} Miscible above 94.5°. ^{i} Miscible above 31.7°. ^{j} Miscible above 61.0°.

TABLE IV

SOLUBILITY OF LINOLEIC ACID IN VARIOUS ORGANIC SOLVENTS

Solvent	g. linoleic acid per 100 g. solvent							
	−50.0°	−40.0°	−30.0°	−20.0°	−10.0°	0.0°	10.0°	20.0°
n-Hexane	3.0	14.3	53	170	990	∞	∞	∞
Benzene^a	Eutectic system		..	320	1250	∞	∞	∞
Cyclohexane^b	Eutectic system		..	275	1210	∞	∞	∞
Carbon tetrachloride^c	Eutectic	..	70	160	600	∞	∞	∞
Chloroform	19.0	40.0	88	210	770	∞	∞	∞
Ethyl acetate	5.6	14.7	58	200	1300	∞	∞	∞
Acetone	3.3	8.6	27.2	147	1200	∞	∞	∞
2-Butanone	4.6	10.6	37.0	185	1220	∞	∞	∞
Methanol	3.3	9.9	48.1	233	1850	∞	∞	∞
95.0% ethanol	4.5	11.1	42.5	208	1150	∞	∞	∞
2-Propanol	6.0	11.7	45.2	203	1080	∞	∞	∞
n-Butanol	8.0	18.9	56	180	870	∞	∞	∞
Nitroethane^d	..	<0.1	0.4	2.1	8.3	34.2	∞	∞
Acetonitrile^e	..	<0.1	0.2	0.4	4.9	7.5	11.2	17.7

^{a} Eutectic at 74.6 wt. % linoleic acid, −21.2°. ^{b} Eutectic at 51.8 wt. % linoleic acid, −28.3°. ^{c} Eutectic at 31.9 wt. % linoleic acid, −35.3°. ^{d} Miscible above 1.5°. ^{e} Miscible above 39.5.

The solubilities of oleic acid listed in Table III refer to those of the form most stable in each of the systems. As would be expected of a dimorphic material, oleic acid exhibits two solubility curves in some solvents, as illustrated by the benzene system in Fig. 1. Upon cooling such a system, the solute precipitates in a transparent, unstable, crystalline form, which, if the temperature is raised rapidly, redissolves at the temperature at which precipitation occurred. If, however, the precipitate is held for an interval of time at or below its precipitation temperature, the material transforms to a more opaque, stable crystalline form which, upon heating dissolves at temperatures somewhat above those at which precipitation occurred. In the case of oleic acid, the transformation occurs relatively rapidly and only portions of the unstable curves in regions of higher concentration were observed with any degree of certainty in most of the non-polar and slightly polar solvents. Such polar solvents as the alcohols and ketones appear to promote the precipitation of only the higher-melting form of oleic acid. Such solutions could not be cooled below the liquidus curves of the opaque form without precipitation. Such polar solvents as acetonitrile and the nitroparaffins exhibit the opposite behavior, promoting the precipitation of only the lower-melting transparent form of oleic acid. These solvents appear to prevent the transformation to the higher-melting opaque form. Precipitated samples maintained at low temperatures for long intervals of time failed to transform and always redissolved at temperatures on the liquidus curves of the transparent form. This behavior demonstrates the specific influence of the solvent in determining the crystal form of the solute upon precipitation. This phenomenon has been observed in this Laboratory during investigations relative to the polymorphic behavior of some of the long-chain nitrogen compounds,[26] and has been en-

---

(26) In preparation for publication.

TABLE V

COMPARISON OF SOLUBILITIES

Acid	Solvent	g. acid per 100 g. solvent			
		−50°	−40°	−30°	−20°
Oleic	Hexane[a]	...	0.1	1.2	9.05
		0.104[2]	.485[2]	1.19[2]	..
		...	.36[3]	1.96[3]	9.90[3]
	Diethyl ether	...	1.2	4.4	..
		...	4.57[3]	...	..
	Acetone	...	0.5	1.4	5.0
		.189[2]	.519[2]	1.44[2]	..
		...	.66[3]	2.09[3]	5.93[3]
	Methanol	...	.3	0.9	4.1
		.089[2]	.330[2]	0.713[2]	..
Linoleic	Hexane[a]	3.0	...	...	..
		1.73[2]	...	...	..
	Acetone	3.3	...	...	..
		5.04[2]	...	...	..
	Methanol	3.3	...	...	..
		2.58[2]	...	...	..

[a] Foreman and Brown[2] and Singleton[3] used commercial Skellysolve B, whereas in this investigation purified n-hexane was employed.

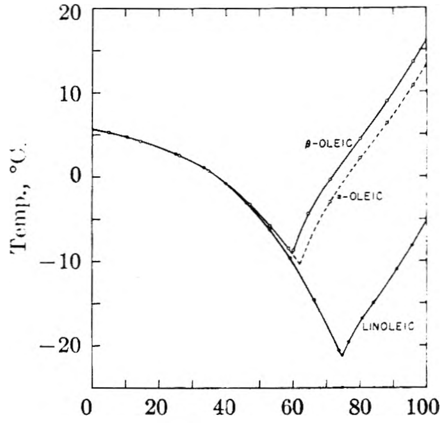

Fig. 1.—Liquidus curves of oleic and linoleic acids with anhydrous benzene.

countered in X-ray studies of saturated fatty acids.[27]

Discussion

Factors influencing solubility can properly be evaluated only if reliable quantitative data are established systematically on an equivalent basis. The solubilities of oleic and linoleic acids are shown in Figs. 2–5, inclusive, plotted as the logarithm of the mole fraction of acid *vs.* reciprocal of the absolute temperature. This method has been used extensively by Hildebrand[28] in his studies of solubilities of a wide variety of non-electrolytes, and has been applied by Bailey[29] to the correlation of fatty acid solubilities. The ideal solubilities were calculated from the heats of fusion of the solutes. The value used for the heat of fusion of oleic acid, 7.6 kcal. per mole, was estimated by Bailey[29] from Smith's data[5] on the binary system oleic–palmitic acid. Although there is no value for the heat of fusion of linoleic acid in the literature, this value was computed from a large-scale plot of the data reported by Stewart and Wheeler[16] for the binary system oleic–linoleic acid. The heat of fusion of linoleic acid, calculated from the temperature of the liquidus curve at 0.96 mole fraction of linoleic acid, is estimated to be 6.8 ± 0.2 kcal. per mole.

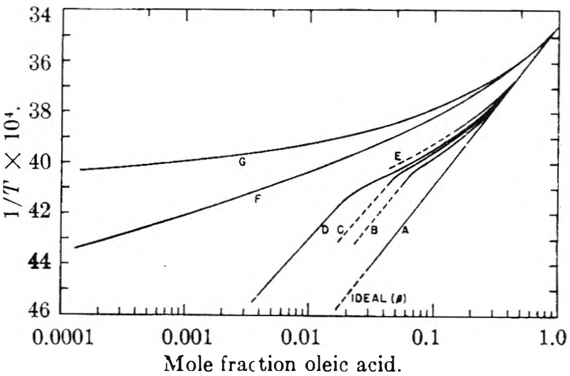

Fig. 2.—Solubilities of oleic acid in several non-polar and slightly polar solvents: A, chloroform; B, carbon tetrachloride; C, o-xylene; D, chlorobenzene; E, benzene; F, n-hexane; and G, 1,2-dichloroethane.

As would be anticipated, the fundamental solubility behavior of oleic and linoleic acids differs little from that of stearic acid.[29] All the curves of oleic and linoleic acids occur in the same order as do those of stearic acid, particularly in the lower concentration ranges. Percentagewise, the unsaturated acids deviate to a greater extent from their respective ideal solubilities than stearic acid, the deviations of the former being relatively greater with increased polarity of the solvents. In general, the solubility of oleic acid differs from its ideal by relatively greater increments in all solvents than does that of linoleic acid. Whereas liquid–liquid miscibility is exhibited by stearic acid in all the solvents investigated with the exception of nitromethane, the unsaturated acids form immiscible liquid systems over considerable concentration ranges in the very highly polar solvents employed.

By comparing the order of the curves in Figs. 2–5 in the lower concentration ranges with the order of the internal pressures of the solvents listed in Table VI, it will be noted that there is fairly good correlation. Solvents possessing relative internal pressures either higher or lower than 1.4–1.6 times that of hexane result in positive

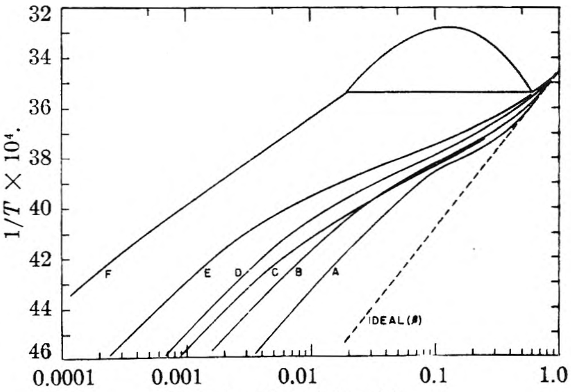

Fig. 3.—Solubilities of oleic acid in several moderately polar and highly polar solvents: A, butyl acetate; B, ethyl acetate; C, diethyl ether; D, 2-butanone; E, acetone; and F, nitroethane.

---

[27] A. W. Ralston, "Fatty Acids and Their Derivatives," John Wiley and Sons, Inc., New York, N. Y., 1948, p. 335.

[28] J. H. Hildebrand, "The Solubility of Non-Electrolytes," 2nd Ed., Reinhold Publishing Corp., New York, N. Y., 1936; J. H. Hildebrand and R. L. Scott, *ibid.*, 3rd ed., 1950.

[29] A. E. Bailey, "Melting and Solidification of Fats," Interscience Publishers, Inc., New York, N. Y., 1950, Chap. V.

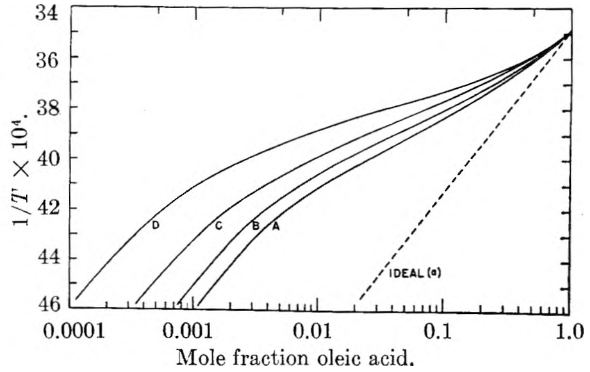

Fig. 4.—Solubilities of oleic acid in the lower alcohols: A, *n*-butanol; B, 2-propanol; C, 95.0% ethanol; and D, methanol.

deviations roughly proportionate to the amount by which their values differ from this range. Thus, oleic and linoleic acids appear to possess relative internal pressures of this general magnitude.

Table VI

Relative Internal Pressures of Solvents[28]

Solvent	Rel. int. press.[a]	Solvent	Rel. int. press.[a]
Hexane	1.00	Chloroform	1.6
Diethyl ether	1.1	Butanol	1.7
Cyclohexane	1.2	Acetone	1.7
Butyl acetate	1.2	Nitroethane	2.2
Ethyl acetate	1.4	Ethanol	2.3
CCl_4	1.5	Acetonitrile	2.6
2-Butanone	1.5	Methanol	3.2
Benzene	1.6		

[a] These values were computed by dividing the respective absolute values[28] by that of hexane, the lowest of this series.

On the basis of the relatively wider divergences of these acids from their respective ideal curves at the lower concentrations in comparison with those of stearic acid, particularly in the non-polar and slightly polar solvents, it would be inferred that the internal pressures of the unsaturated acids are appreciably higher than that of stearic acid, that of oleic acid being the highest of the three.

The relatively long transitional segments of the unsaturated acid curves, and their gradual approach to linearity at the lower concentrations, demonstrate the effect of considerable differences in the molar volumes of the solutes and solvents, the respective differences being greater than in the case of stearic acid. This behavior indicates that the molar volumes of oleic and linoleic acids are somewhat larger than that of stearic acid. This conclusion is confirmed by calculation of the molar volumes from the densities of the acids,[4] the density of stearic acid being extrapolated to the lower temperatures for comparison. This computation gives 297, 318 and 321 cc. per mole at 20° for stearic, oleic and linoleic acids, respectively. The molar volumes of some representative solvents, for example, are 41, 74, 75, 81, 98 and 133 cc. per mole for methanol, acetone, butanol, chloroform, ethyl acetate and butyl acetate, respectively.

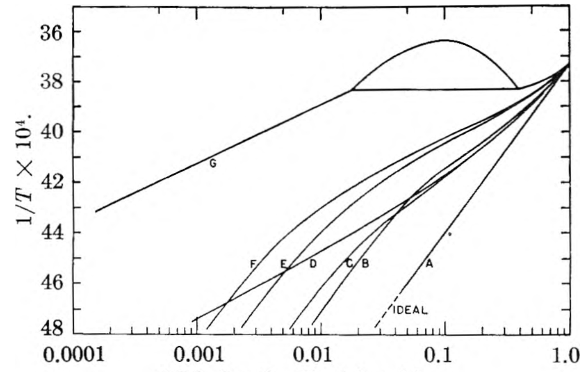

Fig. 5.—Solubilities of linoleic acid in several organic solvents: A, chloroform; B, *n*-butanol; C, ethyl acetate; D, *n*-hexane; E, acetone; F, methanol; and G, nitroethane.

The proportionately greater deviations from ideality of oleic acid in the moderately polar and highly polar solvents in comparison with those of stearic and linoleic acids indicate that oleic acid is somewhat less polar. This is verified by a report[30] of the dipole moments of these acids, the values being 1.506, 1.452 and 1.512 × 10^{-18} e.s.u. for stearic, oleic and linoleic acids, respectively. Despite the fact that these absolute values may be questionable,[31] their general interrelation seems consistent with the solubility measurements.

Hydrogen bonding between solvent and solute molecules is evidenced by the fact that many of the solubilities of oleic and linoleic acids are greater than would be anticipated on the basis of differences in internal pressures and polarities alone. Despite the well-known tendencies of the lower alcohols to form strong hydrogen-bonded networks of molecules in their liquid state, the carboxyl hydrogen atom of the unsaturated acids is evidently sufficiently active to compete with the bonding tendencies of the hydroxyl groups of the alcohols. The solubilities of these acids in methanol and ethanol, for example, are considerably greater than they theoretically should be in solvents possessing such high internal pressures. From the limited solubilities in the nitroparaffins and in acetonitrile, on the other hand, it appears that the carboxyl hydrogen of oleic and linoleic acids is insufficiently potent to disrupt the highly polar fields of nitrogen-containing solvent molecules. Hydrogen bonding characteristics of stearic acid[29] are almost identical with those of these unsaturated acids.

The solubility of the fatty acids in chloroform is unique. In this solvent, the unsaturated acids, as well as all the high molecular weight saturated acids,[29] exhibit apparently ideal solutions over wide ranges of concentration. It is oddly coincidental that all the factors affecting solubility should exist in such an exact equilibrium in these systems as to bring about this apparent ideality, irrespective of chain length or degree of unsaturation. Estimation of the heats of fusion of the unsaturated acids based upon their chloroform solubilities confirms the value calculated for oleic acid by Bailey[29] and that for linoleic acid from the binary systems,[16] the value obtained for oleic acid being 7.6 ± 0.1 kcal. per mole and that for linoleic acid being 6.9 ± 0.1 kcal. per mole.

---

(30) M. P. Volarovich and N. H. Stepanenko, *J. Exptl. and Theoret. Phys.* (*U.S.S.R.*), **10**, 817 (1940).

(31) Reference 27, p. 352.

The authors are indebted to Mr. R. S. Sedgwick for the preliminary crystallization of linoleic acid and to Dr. W. O. Pool for the careful fractionation of oleic acid.

MAGNETIC PROPERTIES OF ADSORBED VAPORS

By W. O. Milligan and Harry B. Whitehurst[1]

The Rice Institute, Houston, Texas

Received February 22, 1952

Adsorption isotherms have been obtained at 25° on silica gel, using water, *n*-propyl alcohol, acetic acid, salicylaldehyde and *n*-heptane as adsorbates. At each point on the isotherms, the magnetic susceptibility of the adsorption complex was measured, using the Faraday method. At high pressures, near saturation, the observed diamagnetic susceptibilities of the adsorbed material corresponded to the susceptibilities of the bulk liquids, except in the case of salicylaldehyde where less than two layers were adsorbed. When less than a monolayer had been adsorbed, the susceptibilities differed from bulk liquid values except in the case of *n*-heptane. An increase was observed for water and *n*-propyl alcohol, and a decrease for acetic acid.

Introduction

Previous investigations of magnetic susceptibility changes during the course of adsorption have followed changes in the properties of the adsorbent, or changes due to chemical interaction between the adsorbent and the adsorbate.[1–6] Investigations of the processes of physical adsorption by following changes in magnetic susceptibility can be achieved by choosing adsorbents which do not react with the adsorbates, and vapors which show changes in their magnetic properties depending on their physical state.

The diamagnetic suceptibility of liquid water varies with temperature[7] and should be different in the vapor and liquid phases. This variation in susceptibility is probably due to changes in hydrogen bonds, although the exact nature of the effect has been the subject of some discussion.[8–11] It is known that the diamagnetic susceptibility of water increases with increasing temperature, and is greater than that of ice. If the susceptibility of water is dependent upon hydrogen bond formation, interruption of the bonds would lead to an increase in diamagnetism.

Recently, Rumpf and Séguin have compared the magnetic susceptibility of salicylaldehyde and *p*-hydroxybenzaldehyde.[12] They have concluded that the difference in magnetic susceptibility may be due in part to internal hydrogen bonds. Freymann and Freymann[13] have investigated the absorption of microwaves by water vapor adsorbed on silica gel. Their measurement show that the adsorbed water retains its liquid character at temperatures as low as −90°. It has been pointed out by these authors that the apparent disassociation of hydrogen bonds in the adsorbed water causes the freezing point to correspond to that which would be predicted by extrapolation from the freezing points of H_2Te, H_2Se and H_2S.

The experiments described below were carried out to determine whether or not there is a difference in magnetic susceptibility of adsorbed gases and their corresponding bulk liquids. Silica gel was used as the adsorbent, and the vapors adsorbed were water, *n*-propyl alcohol, acetic acid, salicylaldehyde and *n*-heptane, at 25°.

Apparatus.—The instrument constructed at the Rice Institute for simultaneous measurements of magnetic susceptibility and adsorption is similar in many respects to instruments previously constructed for the gravimetric measurement of adsorption only. One of these instruments has been described elsewhere.[14] The incorporation of an electromagnet with suitably shaped pole faces allowed simultaneous determination of magnetic susceptibility by Faraday's method. Details of the construction of the apparatus are to be published.

Results

The equation relating the force exerted by an

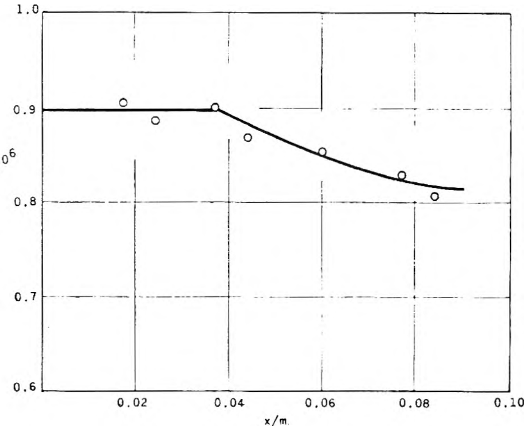

Fig. 1.—Apparent magnetic susceptibility of adsorbed *n*-propyl alcohol.

---

(1) M. H. Dilke, D. D. Eley and E. B. Maxted, *Nature*, **161**, 804 (1948).

(2) M. Goldsmith, *J. Chem. Phys.*, **18**, 523 (1950).

(3) R. Juza, R. Langheim and H. Hahn, *Z. angew. Chem.*, **51**, 354 (1938).

(4) R. Juza, H. Lubbe and L. Heinlein, *Z. anorg. Chem.*, **258**, 105 (1949).

(5) L. H. Reyerson and J. E. Wertz, This Journal, **53**, 234 (1949).

(6) F. Simon, *Z. Elektrochem.*, **34**, 528 (1928).

(7) H. Auer, *Ann. Physik*, **18**, 593 (1933).

(8) S. V. Anantakrishnan and F. S. Varadachari, *Proc. Ind. Acad. Sci.*, **20A**, 128 (1944).

(9) W. R. Angus and W. K. Hill, *Trans. Faraday Soc.*, **36**, 923 (1940).

(10) C. M. French, *ibid.*, **43**, 356 (1947).

(11) K. Lonsdale, *Nature*, **164**, 101 (1949).

(12) P. Rumpf and M. Séguin, *Bull. soc. chim. France*, 366 (1949).

(13) M. Freymann and R. Freymann, *Compt. rend.*, **232**, 1096 (1951).

(14) W. O. Milligan, Warren C. Simpson, Gordon L. Bushey, Henry H. Rachford, Jr., and Arthur L. Draper, *Anal. Chem.*, **23**, 739 (1951).

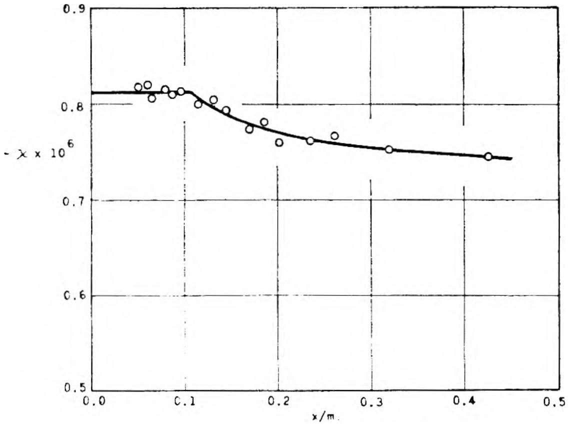

Fig. 2.—Apparent magnetic susceptibility of adsorbed water.

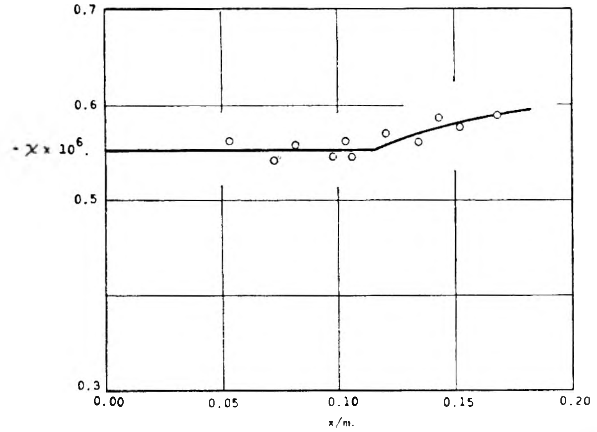

Fig. 3.—Apparent magnetic susceptibility of adsorbed salicylaldehyde.

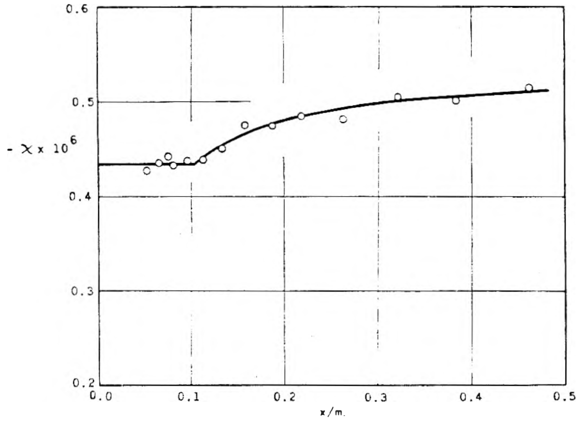

Fig. 4.—Apparent magnetic susceptibility of adsorbed acetic acid.

inhomogeneous magnetic field upon a sample may be written as

$$F = m\chi H \frac{\mathrm{d}H}{\mathrm{d}x}$$

where

F = force exerted on the sample
m = mass of sample
χ = magnetic susceptibility
H = magnetic field strength
$\mathrm{d}H/\mathrm{d}x$ = gradient of the magnetic field

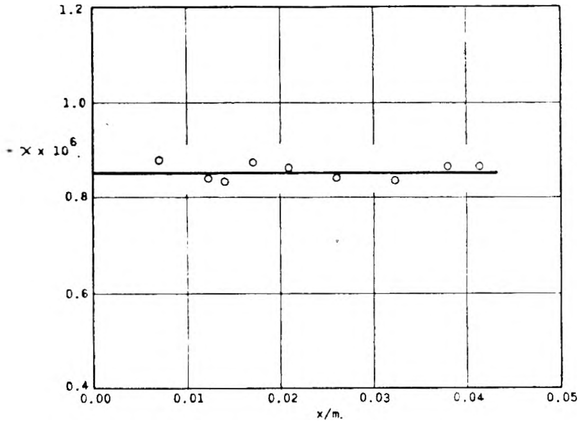

Fig. 5.—Apparent magnetic susceptibility of adsorbed *n*-heptane.

In the Faraday method, the magnetic field is designed to have an effective gradient only in the vertical direction; F may then be measured as an apparent loss or gain in weight resulting from the application of the magnetic field. If the sample occupies the same place in the magnetic field during each observation, $H\mathrm{d}H/\mathrm{d}x$ will remain a constant throughout the experiment. Calculations of the magnetic susceptibility of the adsorbed phase are based on the assumption that the susceptibility of the silica gel remains constant throughout the course of the experiment. The force exerted by the magnetic field on the sample with no adsorbed gas may be determined at the beginning

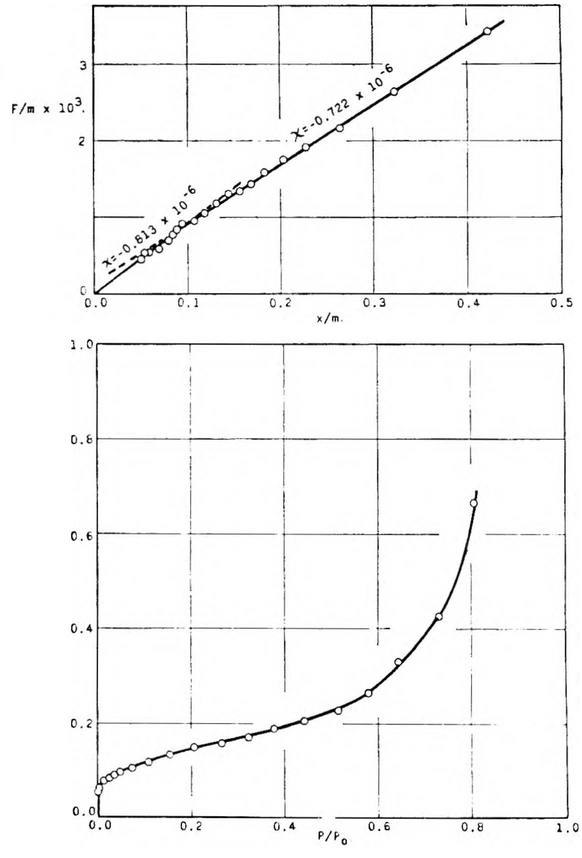

Fig. 6.—Upper drawing: force exerted by the magnetic field on adsorbed water. Lower drawing: adsorption isotherm for water on silica gel.

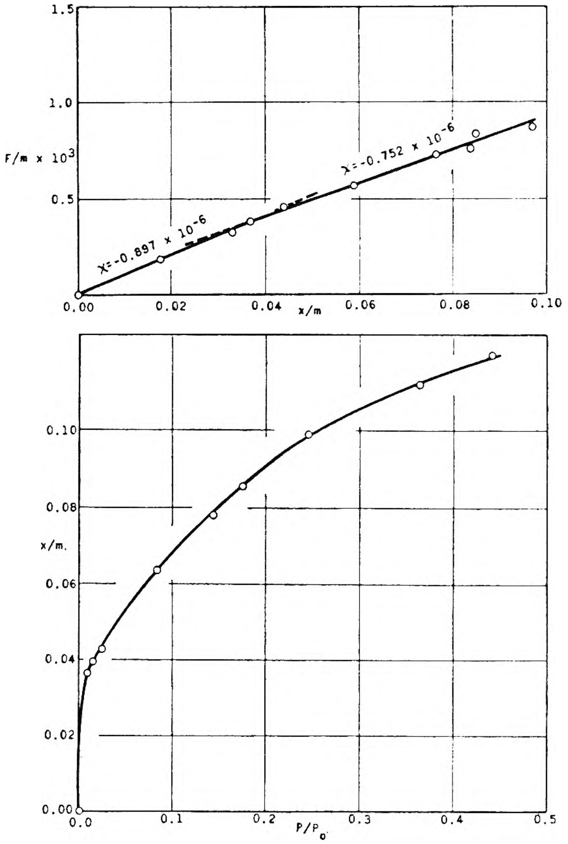

Fig. 7.—Upper drawing: force exerted by the magnetic field on adsorbed *n*-propyl alcohol. Lower drawing: adsorption isotherm for *n*-propyl alcohol on silica gel.

of the experiment, or by extrapolation if water vapor is the adsorbate, and applied as a correction factor. Thus, in the above equation, F becomes the difference between the force exerted at zero adsorption and the force exerted at any particular point along the isotherm. Similarly, m becomes the mass of the adsorbed vapor at that point. In order to determine any differences in magnetic susceptibility of successive increments of adsorbed vapor, the apparent loss in weight due to the magnetic field may be plotted as a function of the weight of gas adsorbed. The slope of the resultant line will be proportional to the magnetic susceptibility of any given adsorption increment.

Calculations of adsorption were made on the basis of "dry sample weight" of silica gel. A portion of the silica gel used in the experiments was taken at the same time the sample was placed in the apparatus and ignited to dryness at 1000°. The loss in weight upon ignition determined the amount of water present in the sample initially. Before each experiment the sample was evacuated to a pressure of 10^{-6} mm. All of the water is not given off under the reduced pressure at 25°. In the case of the organic sorbates, it was assumed that there was no residual adsorption at the beginning of each experiment, and the residual water was not considered as a part of the sample weight. Outgassing of the sample by heat treatment was not attempted, since irreversible changes in the silica gel occur under such conditions.

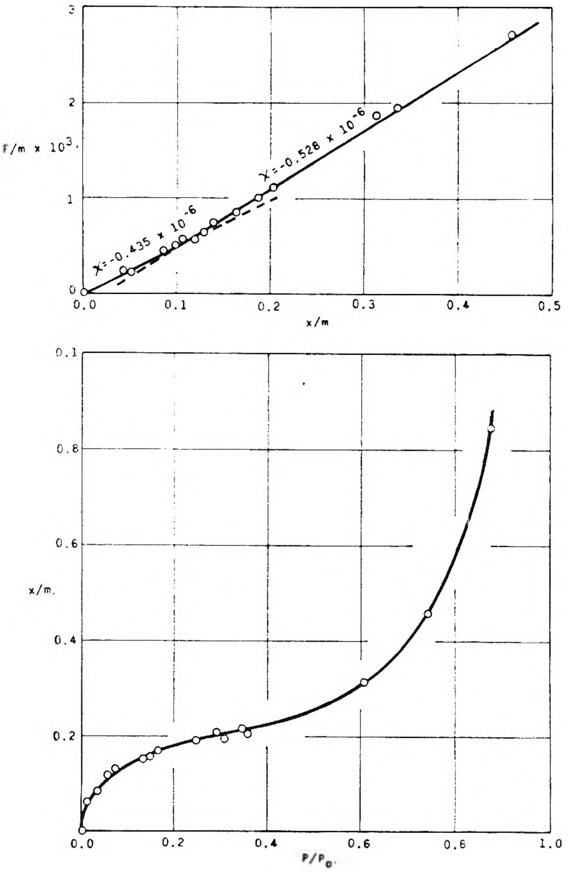

Fig. 8.—Upper drawing: force exerted by the magnetic field on adsorbed acetic acid. Lower drawing: adsorption, isotherm for acetic acid on silica gel.

It was found that the apparent magnetic susceptibility of the sample and the adsorbed vapor was a function of the amount of adsorption only, although hysteresis in the adsorption isotherm was observed. Plots of the apparent magnetic susceptibility as a function of adsorption are shown in Figs. 1–5. The units of adsorption are x/m where x = weight of adsorbed vapor and m = sample weight.

In Figs. 6–10, F/m is plotted as a function x/m. These figures also include the adsorption branch of the corresponding isotherms. The points in the first plot appear to fall into two straight lines, with the exception of that for *n*-heptane. The slopes of the straight line portions have been multiplied by a proportionality constant to give values for magnetic susceptibility. These values are given in Table I, where χ_1 is the susceptibility calculated from the slope of the lower portion of the graph, and χ_2 from the slope of the higher. Values for the diamagnetic susceptibility of the bulk liquids are given as χ. When the values for magnetic susceptibility obtained from the slopes in Figs. 6–10 are compared, it is found that χ_2 is less than χ_1, for water and *n*-propyl alcohol. The opposite is true for acetic acid and salicylaldehyde, while *n*-heptane exhibits the same susceptibility throughout the entire experiment.

With the exception of salicylaldehyde, the magnetic susceptibilities of the second and higher layers correspond closely to values given in the literature for the bulk liquids. The first layer

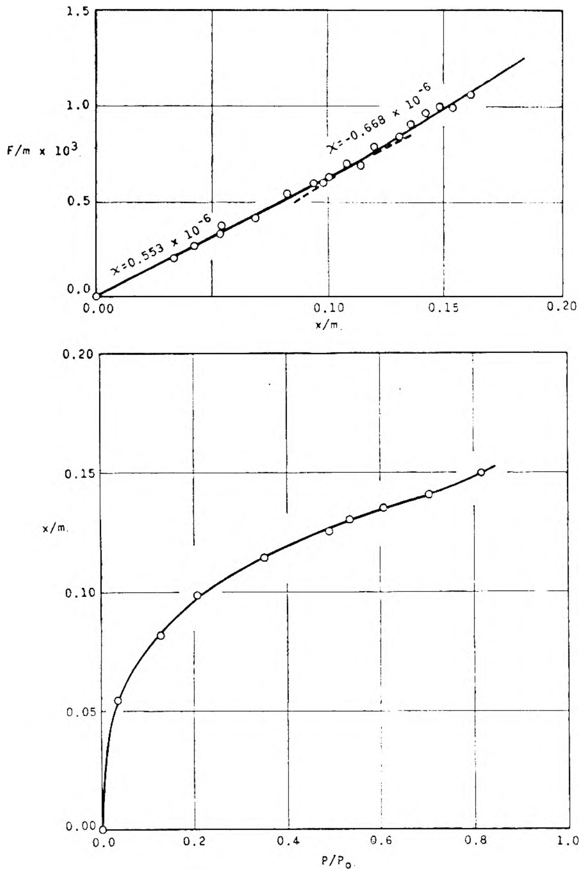

Fig. 9.—Upper drawing: force exerted by the magnetic field on adsorbed salicylaldehyde. Lower drawing: adsorption isotherm for salicylaldehyde on silica gel.

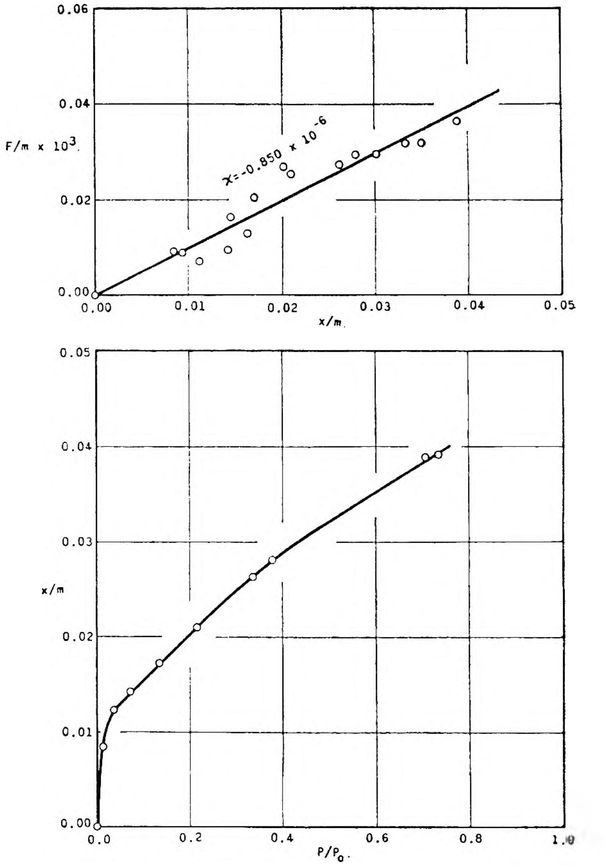

Fig. 10.—Upper drawing: force exerted by the magnetic field on adsorbed n-heptane. Lower drawing: adsorption isotherm for n-heptane on silica gel.

value for salicylaldehyde (-0.553×10^{-6}) is slightly greater than the values reported by Rumpf and Séguin[12] for freshly distilled salicylaldehyde (-0.527×10^{-6}) and for the product after several days of standing (-0.539×10^{-6}). In the present investigation, salicylaldehyde is the only compound which did not show completion of a second monolayer. The highest value observed for θ was 1.4.

The value of x/m corresponding to the completion of a monolayer of adsorbate molecules on the surface of the adsorbent was calculated from the equation of Brunauer, Emmett and Teller. The values for the different absorbates are given in Table I as q_m. The values of x/m occurring at the intersection of the straight line portions of the graphs 7 to 11 are also given in Table I as q. It may be seen that the two values correspond closely.

TABLE I

Adsorbate	$-\chi_1 \times 10^6$	$-\chi_2 \times 10^6$	$-\chi \times 10^6$	q_m	q
Water	0.813	0.722	0.722	0.107	0.106
n-Propyl alcohol	.897	.752	.752	.039	.038
Acetic acid	.435	.528	.529	.103	.104
Salicylaldehyde	.553	.668	.539	.113	.115
n-Heptane	...	.850	.851	.016	...

Discussion

It has been assumed that the magnetic susceptibility of the "dry" silica gel remains constant throughout the course of the experiment. When organic vapors were adsorbed, it was also assumed that the water in the gel had a constant magnetic susceptibility. Although these assumptions may not be strictly valid, some speculations may be advanced concerning the nature of the magnetic susceptibility changes observed. The influence which hydrogen bonds might have upon magnetic susceptibility has been discussed by Anantakrishnan and Varadachari.[8] Since a decrease in temperature lowers the diamagnetic susceptibility of bulk water, it may be assumed that the formation of hydrogen bonds causes a decrease in the diamagnetic susceptibility of water.

It appears from the above results that the water vapor adsorbed in amounts corresponding to less than monolayer coverage, the water molecules are separated on the surface of the gel in a manner which does not allow the formation of hydrogen bonds, or that the mechanism of adsorption precludes the formation of such bonds. The same conditions appear to be present in the case of n-propyl alcohol. The first molecules adsorbed do not regain the susceptibility of bulk water even after formation of several layers, indicating that it is probably the process of adsorption which prevents the formation of hydrogen bonds in the first layer.

The hydrogen bonds in acetic acid and the chelate bonds in salicylaldehyde differ from those in alcohols and water in that the bonds complete the formation of a molecular ring in each case. Acetic acid is known to exist as a dimer even in the vapor phase. The formation of such ring structures should cause an increase in diamagnetic susceptibility. It is known that aromatic compounds and organic molecules containing saturated rings show a diamagnetic susceptibility larger than would be expected from a simple rule of additivity. The total result of chelation upon magnetic susceptibility is the result of several effects. Ring formation is accompanied by hydrogen bonding, and possibly by the introduction of some strain. Angus and Hill[9] conducted experiments with salicylic acid and benzoic acid in solution with different solvents. These investigators found that for salicylic acid in chloroform and ethyl acetate and for benzoic acid in benzene, the diamagnetic susceptibility of the solute decreased with increasing concentration. The opposite was true for benzoic acid in ethyl acetate. It was concluded that the over-all result of ring formation due to hydrogen bonding was a decrease in susceptibility. Angus[15] has since stated that these interpretations may have been untimely. Rumpf and Séguin[12] have compared meta and para isomers of compounds capable of chelation in the ortho form, and have found that the ortho form has the lower susceptibility. The difference may be due in part to hydrogen bonds, and strain introduced by ring closure may also contribute. In any event, the factors tending to decrease the magnetic susceptibility upon chelation are predominant in the bulk liquids. If the magnetic susceptibility of the silica gel remains constant, the results shown in Table I indicate that the first layer of adsorbed acetic acid molecules have a smaller susceptibility than the bulk liquid. This situation would result if the effect of the ring structure is greater than that due to strain and hydrogen bonding, or if the latter effects are comparable for molecules in the bulk liquid and in the first adsorption layer.

For salicylaldehyde, the first layer of adsorbed molecules has a susceptibility slightly greater than that of the bulk liquid. This would seem to indicate that the isolated molecules are comparable to the meta or para isomers of the compound. The rather large increase in susceptibility shown by the first portion of the second layer may be due to a configuration of molecules in which large intermolecular orbitals are established. The low extent to which the second layer is covered may also introduce some error in the interpretation of the data.

Acknowledgment.—The authors wish to express their appreciation to the Humble Oil and Refining Company which made these studies possible by establishing a fellowship program at the Rice Institute.

---

[15] W. R. Angus and D. V. Tilston, *Trans. Faraday Soc.*, **43**, 221 (1947).

PARTICLE GROWTH IN THE AQUEOUS POLYMERIZATION OF VINYL ACETATE[1]

BY W. J. PRIEST

Kodak Research Laboratories, Eastman Kodak Co., Kodak Park Works, Rochester, N. Y.

Received March 22, 1952

Latices produced by the polymerization of vinyl acetate in water have been examined by means of electron-microscopic observations. Particles produced in the absence of surfactants are large, of the order 0.1–1.0 micron in diameter. The size distribution of these particles is quite narrow. A mechanism for particle-size development by interparticle combination during polymerization has been proposed, based on measurements of relative size and size distribution. Factors influencing particle size and growth have been investigated. Conclusions pertaining to the stabilization of latices of the vinyl acetate type are presented, based on these data. Less detailed examination of the latices from other slightly water-soluble monomers polymerized in "self-stabilized" systems indicates that the mechanism given for growth of particles of vinyl acetate latices is general.

Introduction

Emulsion polymerization systems in which latex particles originate by initiation in micelles have been studied at length.[2] Comparatively little information is available in regard to non-micellar systems which may also lead to latices.

In the latter types of system, rapid rates of polymerization and well-dispersed latices may be obtained for monomers which have appreciable water-solubility if the polymer particles which separate from the initial polymerization mixture are capable of being stabilized at diameters of about a micron or below. Non-micelle-forming stabilizers which may be employed are numerous, including a variety of water-soluble polymeric materials.

In preliminary work with aqueous vinyl acetate latices stabilized with polymethacrylic acid/salt,[3] it was noted that the product contained unusually large particles of relatively narrow size distribution. Inasmuch as these particles were larger by several orders of magnitude than those obtained in most surfactant-stabilized latices, it is evident that there are important differences in the growth mechanisms in the two types.

The best method for measuring particle growth in a latex polymerization would be based on a series of particle-size measurements taken at various stages of a single polymerization run. However,

---

[1] Communication No. 1481 from the Kodak Research Laboratories.

[2] W. D. Harkins, *J. Polymer Sci.*, **5**, 217 (1950).

[3] This notation is used because the polyacids were always used at such a pH that they were partly neutralized.

it was not convenient to isolate samples of polymer formed in the initial stages of polymerization, because the particles existing under these conditions are highly swollen with monomer and during preparation for electron microscope measurements tend to fuse or to flatten out on deposition. Moreover, as will be shown below, interparticle combination occurs among such swollen particles, so that the size upon observation is a function of the time and methods of handling during the process of preparation for size measurement. For these reasons, the measurements of particle size in this study were all conducted on completely polymerized latex systems.

Experimental

Materials. Vinyl Acetate.—Commercial vinyl acetate was freed from inhibitor by distillation through a 2-ft. fractionating column.

Other Monomers.—Samples were purified by scrubbing with alkali, where possible, followed by distillation; otherwise by distillation alone.

Polymethacrylic Acid.—Methacrylic acid was polymerized in 10% aqueous solution with potassium persulfate catalyst at 100°.

Method of Polymerization.—The emulsions were made in capped bottles tumbled at 15 r.p.m. in a thermostat. Since the bottles were normally filled nearly to capacity, and in each case contained about the same amount of free space, no effort was made to sweep out air in any of the experiments. Under these conditions, the induction periods at 50° were fairly short. All polymerizations were run substantially to completion.

Electron Micrographs.—For the electron micrographs, the samples were diluted to about the same solids content, and portions were evaporated on collodion screens prior to gold shadowing. The technique used in preparation of the samples is given by Wyckoff.[4]

Measurements.—The size measurements were made by means of a traveling microscope from the electron micrograph enlargements. In all the runs except those in series 1 (see below), 10 particles were counted and their sizes averaged. For each of the experiments in series 1, the measurements were made on 100 particles.

Results

1. Size vs. Phase Ratio: Vinyl Acetate Emulsion Polymerization. a. Self-stabilized.—Table I gives size data for terminal particles obtained by polymerization of vinyl acetate in water containing initiator only.

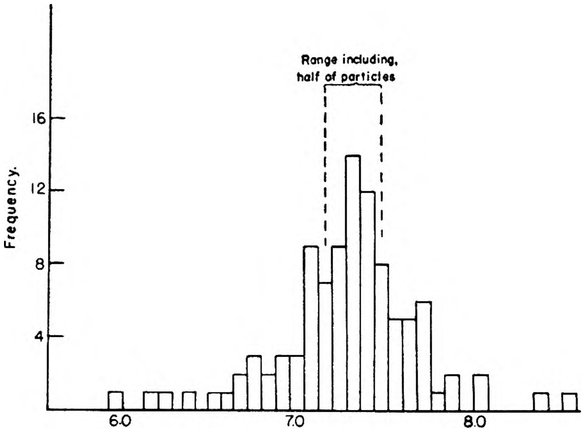

Fig. 1.—Particle size distribution in a "self-stabilized" polyvinyl acetate, latex sample 1C.

Table I

Size *vs.* Ratio of Vinyl Acetate to Aqueous Phase
Temperature, 51°; initiator concentration (potassium persulfate), 2.5 × 10^{-3} mole/liter

Sample	Phase ratio monomer/water	Average particle size (of 100 particles in cc.)	Dispersion,[a] %
1A	0.023	3.14×10^{-15}	21.2
1B	.058	3.61×10^{-14}	20.5
1C	.144	7.40×10^{-14}	4.1

[a] Dispersion: Minimum range of size which includes one-half of the total number of particles, divided by the average particle size; expressed here in terms of volume.

Figure 1 shows the distribution of sizes in a typical polyvinyl acetate sample (1C).

b. **Polymethacrylic Acid/Salt Stabilizer.**—Another series of polymerizations at different phase ratios was conducted under the following conditions: temperature, 51°; initiator concentration (potassium persulfate), 4.6 × 10^{-3} mole/liter; stabilizer concentration (polymethacrylic acid/salt), 0.625% (wt.).

Figure 2 shows a plot of the number of particles per gram of polymer *vs.* relative amounts of vinyl acetate employed in this series of polymerizations.

2. **Particle Size *vs.* Amount of Initiator.**—The effect of initiator concentration on particle size is shown in Table II.

Table II

Particle Size *vs.* Persulfate Initiator Concentration
Temperature, 51°; vinyl acetate/water, 0.058; added stabilizer, none

Sample	Concentration of initiator, mole $K_2S_2O_8$/liter	Average particle size (cc.)
2A	4.62×10^{-4}	2.15×10^{-14}
1B	2.5×10^{-3}	3.61×10^{-14}
2B	1.16×10^{-2}	2.18×10^{-14}

3. **Particle Size *vs.* Temperature of Polymerization.**—Results for polymerization at two temperatures are shown in Table III.

Table III

Particle Size *vs.* Temperature
Vinyl acetate/water, 0.058; potassium persulfate concentration, 2.5 × 10^{-3} mole/liter; added stabilizer, none

Sample	Temperature (°C.)	Particle size (cc.)
1B	51	3.6×10^{-14}
3A	70	1.15×10^{-14}

4. **Effect of Added Electrolytes.**—Polymerizations were run using various levels of sodium chloride in the aqueous phase, employing (a) no added stabilizer and (b) polymethacrylic acid/salt.

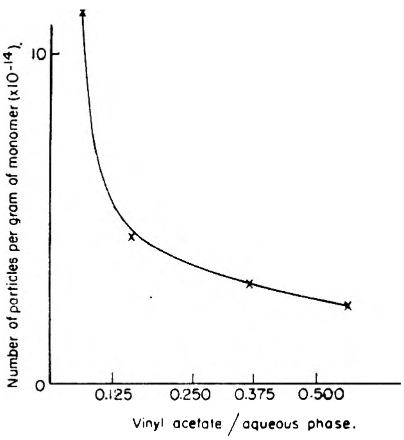

Fig. 2.—Number of particles formed in polymethacrylic acid/salt-stabilized vinyl acetate polymerizations for various values of phase ratio.

---

[4] R. W. G. Wyckoff, "Electron Microscopy. Technique and Applications," Interscience Publishers, Inc., New York, N. Y., 1949.

a. **No Added Stabilizer.**—Data are summarized in Table IV.

TABLE IV

EFFECT OF ADDED SALT ON PARTICLE SIZE, SELF-STABILIZED

Temperature, 51°; initiator concentration (potassium persulfate), 3.45 × 10^{-3} mole/liter; vinyl acetate/water, 0.058

Sample	Sodium chloride concentration, mole/liter	Particle size (cc.)
4A	0.107	1.48×10^{-12}
4B	.064	5.2×10^{-13}
4C	.021	6.44×10^{-14}
1B	None	3.61×10^{-14}

b. **Polymethacrylic Acid/Salt Stabilizer.**—Table V shows sizes of particles obtained when vinyl acetate was polymerized in an emulsion system containing polymethacrylic acid/salt with various amounts of added electrolyte.

TABLE V

EFFECT OF ADDED SALT ON PARTICLE SIZE, STABILIZED

Temperature, 51°; initiator concentration (potassium persulfate), 4.6 × 10^{-3} mole/liter; stabilizer (polymethacrylic acid/salt), 1.25% (wt.) vinyl acetate/water, 0.347

Sample	Sodium chloride concentration, mole/liter	Particle size (cc.)
4G	1.50	1.10×10^{-13}
4F	0.96	7.24×10^{-14}
4E	0.43	8.60×10^{-14}
4D	..	6.34×10^{-14}

5. **Effect of Added Polymerization Inhibitor.**—The introduction of inhibitors into the vinyl acetate polymerization increases the period of induction during which there is no apparent reaction. The inhibitors used in these experiments were of two types: (a) phenolic and (b) unsaturated. In both types, active free radicals are swept from the system and replaced by more inert types which disappear, in general, by reactions leading to low molecular weight products. The latices formed under these conditions begin to form at times of heating substantially in excess of those obtained when inhibitor is absent. Table VI shows the effect of various inhibitors on the particle size of vinyl acetate latices.

TABLE VI

EFFECT OF INHIBITORS ON PARTICLE SIZE

Temperature, 51°; initiator concentration (potassium persulfate), 4.6 × 10^{-3} mole/liter; vinyl acetate water, 0.058

Sample	Inhibitor type	Moles inhibitor/moles vinyl acetate	Particle size (cc.)
6A	Hydroquinone	8.9×10^{-4}	1.01×10^{-16}
6B	Hydroquinone	8.9×10^{-5}	7.18×10^{-16}
6C	Styrene	3.0×10^{-2}	1.11×10^{-15}
6D	β-Naphthol	1.2×10^{-4}	1.13×10^{-14}

6. **Effect of Size of Added Surfactant.**—Vinyl acetate was polymerized in emulsion systems containing different levels of sodium lauryl sulfonate. Size data are shown in Table VII.

TABLE VII

EFFECT OF SURFACTANT ON PARTICLE SIZE

Polymerization temperature, 51°; initiator concentration (potassium persulfate), 2.5 × 10^{-3} mole/liter; vinyl acetate/water, 0.058

Sample	Sodium lauryl sulfonate, mole/liter	Average particle size (cc.)
7A	4.6×10^{-2}	2.0×10^{-17}
7B	1.15×10^{-2}	3.1×10^{-17}
7C	3.7×10^{-3}	1.8×10^{-16}
7D	1.38×10^{-3}	6.5×10^{-16}

Emulsion Polymerization of Other Monomers.—Several monomers other than vinyl acetate were polymerized under conditions similar to those prevailing for sample 1A, Table I.

Critical Micelle Concentration in Sodium Lauryl Sulfonate.—In order to determine whether the sizes of latex particles of vinyl acetate obtained in the systems in which sodium lauryl sulfonate was employed were in any way connected with initiation of polymerization in micelles, a series of measurements of critical micelle concentrations was made in the range of sodium lauryl sulfonate concentrations employed in the polymerizations. These measurements were made by means of the dye adsorption method[5] using pinacyanol dye. In making the measurements, the initial polymerization mixtures were duplicated as closely as possible. It was found that the persulfate oxidized the dye; hence, potassium sulfate was substituted in equal weight. The results of these measurements are summarized in Table VIII.

TABLE VIII

CRITICAL MICELLE CONCENTRATIONS IN SODIUM LAURYL SULFONATE–POTASSIUM SULFATE SOLUTIONS

Sample	Solution titrated Sodium lauryl sulfonate, mole/liter	Potassium sulfate, mole/liter	Measured critical micelle concentration
A	1.15×10^{-2}	4×10^{-3}	6.5×10^{-3}
B	3.7×10^{-3}	4×10^{-3}	No micelles found

In further experiments it was found that the critical micelle concentration was substantially unchanged by the addition of vinyl acetate monomer to saturation. While these measurements were made at temperatures some 25° less than those employed in the polymerization, it is not likely that the values for critical micelle concentration are significantly different at temperatures 25° higher.[6]

Discussion

The general features exhibited by multicomponent systems in which polymerization occurs leading to dispersions of polymer insoluble in the polymerization medium are well known, particularly when the suspending fluid is water or aqueous mixtures. Such polymerizations may be initiated either in solution or in micelles leading to particles which separate from the aqueous medium in the form of small droplets which are kept from coagulating by the presence of suitable stabilizers. It has been shown that the major locus of polymerization is the swollen polymer droplet.[2] The monomer in these continues to polymerize, actuated by free radicals which are produced in the aqueous phase and which diffuse into the droplets. The monomers dealt with in this study have sufficient solubilities in water that their solution polymerization at saturation occurs at a fairly rapid rate. When water-soluble polymerization initiators are decomposed in solutions of such monomers, polymerization in solution is the initial process. While the aqueous phase is not an important locus of polymerization in respect to the relative quantities of monomer converted to polymer, the species formed in this phase are of importance in their influence on the nature of the latices formed at high conversion. Some of these factors will be discussed below.

In emulsion polymerizations in which the monomer is solubilized in micelles, the number of primary particles is established by the number of micelles present at the outset.[7] For polymerizations which begin as solution processes and in which the polymer is not soluble in the solvent, it is not possible to estimate with certainty the number of primary particles. With the growth of a given polymer chain, a point is reached at which the polymer is

---

(5) M. L. Corrin and W. D. Harkins, *J. Am. Chem. Soc.*, **69**, 679 (1947).

(6) H. B. Klevens, *J. Colloid Sci.*, **2**, 301 (1947).

(7) W. V. Smith and R. H. Ewart, *J. Chem. Phys.*, **16**, 592 (1948).

no longer soluble and should separate from solution. With such a model, the number of primary particles would be sensibly equivalent to the number of chains initiated in solution. Since solution polymerization continues to occur throughout the whole range of conversion to monomer, new particles should form at an approximately constant rate so long as monomer concentration is maintained at saturation. This is in contrast to the micellar systems, in which no further primary particles are produced when micelles disappear from solution, owing to depletion of surfactants by adsorption on polymer particles. The maximum number of primary particles to be developed in a solution polymerization leading to a latex is equal to the number of polymer chains long enough to give water-insolubility formed throughout the course of the polymerization. The number actually produced may be reduced by supersaturation effects and also by combination of incompletely developed chains with polymer droplets before the former are adequately stabilized.

The number of particles actually found at the completion of an emulsion polymerization is the total number of primary particles less the reduction caused by coalescence during the course of reaction. The tendency toward coalescence of particles is evidently related to the quantity and efficiency of the material employed as an emulsion stabilizer. Of those stabilizers examined in this study, the most efficient, from the standpoint of limiting interparticle coalescence, were the surfactant types exemplified by sodium lauryl sulfonate. In Table VII, composition 7C has a concentration of sodium lauryl sulfonate below the critical micelle concentration, but the number of particles obtained in this milieu is several times greater than that obtained with less effective stabilizer systems.

In vinyl acetate polymerization mixtures to which no stabilizers have been added, the latex particles which appear are doubtless prevented from coagulating by adsorption of small quantities of sulfated species produced during the induction period, together with additional sulfate groups derived from the initiator in the course of initiation of chains of polymer in the particles.[8,9] The ultimate particle size in mixtures employing the same ratio of monomer to water is presumably a function of the relative number of sulfate groups per particle. By increasing the temperature at which polymerization is conducted, the average polymer chain length is shortened and the relative number of sulfate end-groups is increased. Thus, the decrease in particle size with increase in temperature noted in Table III is to be expected. A similar decrease in particle size should be noted as the concentration of catalyst is increased. This is masked, however (Table II), by the change in electrolyte level which acts in opposition.

The data summarized in Table VI show that very much smaller particles are obtained when inhibitors are present at the beginning of polymerization. This is attributed to the adsorption on the particles of charged substances formed by interaction of the persulfate and inhibiting materials while the latter are being removed from the system during the induction period. Among these materials is considerable low polymer with sulfate end-groups. These polymers resemble surfactants of the sodium lauryl sulfonate type, and the increase in the number of particles obtained is a measure of the amount of charged molecules available for sorption when insoluble particles begin to separate.

Colloid stabilizers such as polyacrylic or polymethacrylic acid/salt do not stabilize large surfaces. The number of particles obtained when these are used is comparable in magnitude to that found in systems in which no stabilizer is added. Electrostatic repulsion is evidently of minor importance in the action of these substances, since uncharged colloids such as polyvinyl alcohol find extensive application[10] in polyvinyl acetate latex manufacture. Water-soluble colloids may act by enveloping the particles in a hull of water-soluble material which minimizes contact of the interior of the droplets on collision. It is not known whether these materials are selectively adsorbed on the polymer particles or whether they may be actually chemically combined.

The final number of particles formed in a vinyl acetate emulsion polymerization depends on conditions employed in the polymerization. Thus, from Fig. 2, representing the particle counts from a group of polymerizations in which only the initial vinyl acetate–aqueous phase ratios were varied, it is seen that the number of particles per unit weight of polymer decreases as more vinyl acetate monomer is employed. In all of these experiments, the composition of the aqueous phase at the outset of polymerization was the same, since saturation with respect to vinyl acetate prevailed. The character of nucleation must therefore be identical in each experiment. It follows that growth by interparticle fusion must occur under the conditions employed in these experiments.

The number of particles at various stages of a vinyl acetate emulsion polymerization is variable and may be represented by a curve of the form shown in Fig. 3. At the outset of reaction represented by the first portion of the ascending branch

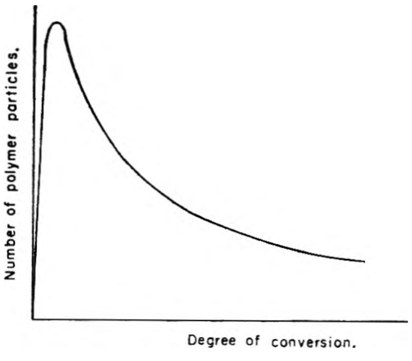

Fig. 3.—Form of curve showing change in number of particles with degree of conversion in a typical persulfate-initiated vinyl acetate polymerization conducted in absence of stabilizer.

---

[8] P. D. Bartlett and K. Nozaki, *J. Polymer Sci.*, **3**, 216 (1948).

[9] J. M. Willis, *Ind. Eng. Chem.*, **41**, 2272 (1949).

[10] N. Platzer, *Mod. Plastics*, **28**, 95 (1951)

of the curve, the polymer particles are formed at a uniform rate. As the concentration of centers increases, the rate of particle combination becomes greater, and at the maximum portion of the curve has become sufficiently high that the rate of production of centers from polymerization in the aqueous phase is balanced by their rate of removal by combination.

If the primary particles are single molecules of polymer, the portion of Fig. 3 containing the maximum likely occurs in the very early stages of polymerization, since, in the absence of supersaturation, the primary particle size would be of the order of 10^{-20} cc.[11] Unfortunately, neither the relative numbers nor lengths of polymerization chains which start in the aqueous phase and the swollen monomer particles, respectively, are known, so that calculation of the primary particle size from the final size is not possible. Under the conditions of maximum stabilization (see Table VII), the final particle size obtained from a phase ratio of 0.058 appears to approach about 10^{-17} cc. If it is assumed that there is little interparticle combination under these conditions, and if single polymer molecules are the primary nuclei, each particle increases in size by a factor of about 10^3 during the polymerization period. On the basis of these assumptions, almost all of the polymerization (99.9%) occurs within the swollen polymer droplets, and a maximum of 0.1% may be identified with primary particles.

Some additional conclusions pertaining to the mechanism of particle growth can be deduced from the distribution of particle size obtained by frequency counts of the final product polymer particles. The final particle size obtained in a well-stabilized system uncomplicated by the presence of surfactant micelles may be estimated by interpolation of the data in Table VII to be no larger than about 10^{-16} cc. In the comparable case in which the polymerization was conducted in the absence of stabilizer (sample 1B), the average final particle size was 3.6×10^{-14} cc. In the self-stabilized polymerization, the number of particles has accordingly decreased during the course of the reaction by a factor of at least 360. The sequence of combinations representing such a process may be written as

$$\begin{array}{l} m_1 + m_1 \longrightarrow m_2 \quad k_{1,1} \\ m_1 + m_2 \longrightarrow m_3 \quad k_{1,2} \\ \hdashline m_x + m_y \longrightarrow m_{x+y} \quad k_{x,y} \end{array}$$

where m_1, m_2, ---m_x, ---m_y are particles containing multiples of primary particles m_1, corresponding to the subscripts, and $k_{1,1}$, $k_{1,2}$, $k_{x,y}$ are the rate "constants" for the processes of combination.

If all of the rate constants, k, are assumed to have the same value, then the distribution of sizes resulting from the interactions in a system originally composed of n identical particles, m_1, may be calculated. The distribution function obtained in a process of this type is

$$\pi_x = xp^{x-1}(1-p)^2$$

where x represents the size of the particles produced by intercombination in multiples of m_1, and p the total number of combinations which have occurred divided by the total number possible. Curve A of Fig. 4 is the calculated final distribution which results from the intercombination of n identical particles of size 10^{-16} cc. to an average size of 3.6×10^{-14} cc., according to the sequence of reactions shown and in which all of the rate constants are equivalent. Curve B is the distribution obtained experimentally in sample 1B, Table I. A comparison of these plots shows that the distribution found has much less spread than that calculated using the simple set of assumptions given above. Moreover, the spread in size distribution tends to decrease as phase ratios are increased, to give larger average sizes (Table I). Thus, the particle size distribution obtained from polymerizations employing high ratios of monomer to aqueous phase is remarkably narrow (Fig. 1).

In order that better correspondence of the calculated and observed functions be attained, it is necessary to conclude that the rate constants for the intercombination process in the vinyl acetate system decrease as the particles become larger. In the polymerization of vinyl acetate conducted in the absence of added stabilizer and initiated by persulfate, the polymer droplets are presumably kept from rapid coalescence by the presence of negative charges localized in the polymer at the sulfate end-groups. The number of these end-groups associated with a droplet chosen at random increases as the amount of polymer in the droplet increases; hence larger particles should be better stabilized than those which are smaller. This provides a reasonable explanation for the indicated decrease with particle size in the specific rate "constant" necessary to the interpretation of the data. While the effects of stabilizers on the growth behavior of latex particles in the vinyl acetate system emerge as the dominant factor in the limitation of coalescence, other properties of the particles may

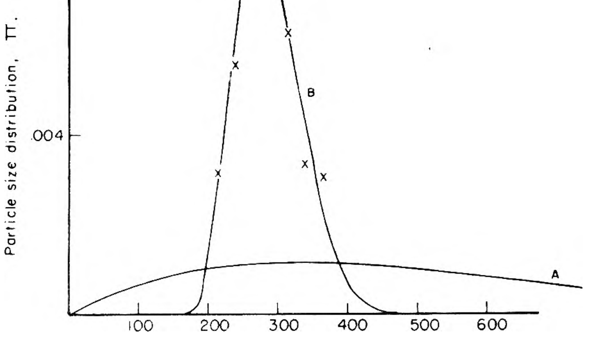

Fig. 4.—Comparison of distribution functions observed (B) and calculated for simplified model (A).

---

[11] A polymerization, in which the components were similar to those of sample 1A, Table I, was carried to the point where haze was just beginning to form, short-stopped, and the polymer isolated. The intrinsic viscosity of this sample was 0.55, whence the molecular weight calculated from Wagner's formula [R. H. Wagner, *J. Polymer Sci.*, **2**, 29 (1947)] is 4600.

also be of importance. One of these is the degree of swelling of the polymer droplets, which is variable throughout the course of conversion of monomer to polymer. It is reasonable to expect that the more highly swollen the droplets, the more probable is the fusion on collision. The data taken in this study offer no means for separation of effects of the latter types. For this reason, it is unprofitable to derive a more sophisticated relationship between particle size and the rate "constants" for particle combination.

A tendency toward greater stability of larger particles has been reported for butadiene–styrene latex systems in which the stabilizers are not adequate to prevent interparticle combination during polymerization.[12] In this study it was found that the larger particles under certain conditions would sweep up the smaller particles. However, where stabilization in similar systems is efficient, there is no evidence of a change in the number of particles with degree of monomer conversion.[13]

For vinyl acetate polymerization employing no stabilizer, the dielectric environment is seen to exert a large effect on the ultimate particle size and presumably on the combination during polymerization of the polymer droplets (Table IV). This is the expected result if it is assumed that the particles are stabilized by electrostatic charges, since these charges become effectively screened in the presence of electrolytes.

The effect of electrolytes is much less marked (Table V) when a polyacid/salt stabilizer is employed in the production of vinyl acetate latices. In this mode of stabilization, the particles are doubtless kept from agglomerating by envelopes of polyacid/salt which present a hydrophilic surface to the suspending phase and inhibit fusion of the interior portions of the droplets, except under conditions of relatively high distortion from spherical shape.

While the mechanism of large-particle development by intercombination of polymer droplets has been examined only for polyvinyl acetate, it appears likely that the mechanism is quite general in all systems where the stabilizer available is not efficient or is not present in sufficient amount to cover the large area of interface present in latex systems of small particle size. In all of the examples examined in this study, the particle sizes are large compared to latices of the same materials prepared in the presence of surfactants, and in no case is there evidence of the existence of many very small particles.

Acknowledgments.—The author wishes to express his thanks to Messrs. R. Davis and J. F. Hamilton, of the Physics Division, for the electron-microscopic work and for some of the particle counts; to Mr. J. F. Wright, of the Chemistry Division, for the measurements of micelle concentration; and to Dr. M. L. Huggins, of the Chemistry Division, for helpful discussions of the material.

---

[12] C. E. Rhines and J. McGavack, *Rubber Age*, **63**, 599 (1948).

[13] W. Smith, *J. Am. Chem. Soc.*, **70**, 3695 (1948).

THE CATALYTIC ACTIVITY OF REDUCED NICKEL MOLYBDATE AND REDUCED NICKEL CHROMATE[1]

By J. Rooley, C. S. Rohrer and O. W. Brown

Department of Chemistry, Indiana University, Bloomington, Indiana

Received March 31, 1952

Reduced nickel molybdate and reduced nickel chromate were studied as catalysts for the vapor phase reduction of 1-nitropropane. The reduced nickel molybdate is a very good catalyst for this reduction, giving yields of propylamine as high as 94.8%. Using the reduced nickel chromate as a catalyst, propylamine is the primary product, giving yields up to 70.6%. Small amounts of propionamide are also produced, the yield increasing with an increase in the reaction temperature to approximately 8% at 240°. The activity of this catalyst is very sensitive to the time and temperature at which the nickel chromate salt is reduced.

Metals and their oxides have been classified in the order of their activities as catalysts in many reactions. Numerous additional investigations have been made as to the effect of various addition agents on the activity and structure of these catalysts.

One of the most intimate and homogeneous alterations to be affected in structure or interatomic distances should be made by the addition of a nonmetallic oxide to the metallic oxide catalyst such that a salt is formed. Yet there have been few studies on these compounds or the reduced metals obtained from these compounds as catalysts for the vapor phase reduction of organic nitro compounds to their respective amines with hydrogen. It is hoped that the series will lead to a better understanding of the effect of these anions in modifying the activity of a catalyst and aid in predicting the behavior of an untried catalyst. Nickel molybdate and nickel chromate have been used as aromatization catalysts for hydrocarbons.[2] The chromate has been used to dehydrogenate and cyclize paraffin hydrocarbons[3] and to selectively hydrogenate butadiene to butylene in the gas phase.[4] The only catalyst reported for the reduc-

---

[1] Contribution No. 556 from the Department of Chemistry at Indiana University.

[2] Standard Oil Development Co., British Patent 594,569 (Nov. 13, 1947).

[3] A. Holter and A. C. Welty, U. S. Patent 2,392,738 (June 28, 1946).

[4] G. Natta, R. Rigamonti and P. Tone, *Chem. and Industria* (*Milan*), **29**, 235 (1947).

tion of nitropropane with hydrogen is reduced nickel tungstate.[5]

Apparatus.—A vertical type aluminum block furnace, electrically heated, thermally controlled and containing a 35-mm. Pyrex glass reaction tube was employed. Temperature was recorded by means of 2 thermocouples extending one inch into the catalyst bed from either end and a third extending well into the metal block. Feed was from above, controlled by the delivery of 2.00 ml. of 1-nitropropane under a variable head of mercury through a calibrated capillary tube. Hydrogen was measured in liters per hour through a calibrated flow meter.

Reduced Nickel Molybdate Catalyst.—The nickel molybdate catalyst was prepared by slowly adding a boiling solution, 90 g. of nickel nitrate hexahydrate in 500 ml. of water, to a boiling solution, 125 g. of sodium molybdate dihydrate in 500 ml. of water, to give a pale green nickel molybdate precipitate. An excess of the anion was used in an effort to prevent the formation of any nickel hydroxide whose presence would probably give a catalyst with abnormally high activity. X-ray diffraction studies gave no evidence of such in the precipitate. The freshly precipitated salt was washed until no trace of the nitrate ion was detectable and was then dried for 24 hours at 110°. Twenty grams of this salt was placed in the furnace, heated to a temperature of 405° and held there for one hour with 17 liters of hydrogen per hour flowing over the catalyst.

X-Ray powder diffraction patterns show that the most prominent line appearing for the reduced catalyst corresponds to the *d*-value of the strongest line in the pattern for metallic nickel. The second and third strongest lines recorded for metallic nickel also appear in lesser intensities for the reduced catalyst giving a strong indication that this catalyst is to some extent metallic nickel. This confirms the findings of Woodman, Taylor and Turkevich[6] which through measurements of magnetic susceptibilities on this catalyst, prepared in a slightly different manner, indicated the presence of some dispersed nickel. The X-ray diffraction patterns gave no evidence for the presence of metallic molybdenum, and it is assumed that the anion is present in some partially reduced state.

The optimum temperature found for the reduction of the nitro compound is seen in Fig. 1 to be 145°. The operating conditions for the construction of this curve were 10 ml. per hour of nitropropane and a fivefold excess of hydrogen flowing over the catalyst.

TABLE I

Catalyst, 20 g. of nickel molybdate on 4 g. of asbestos reduced; furnace temperature, 145°

	Nitropropane, g. per hr.	Hydrogen in % excess	Amine in % converted
A	6	500	86.2
	8	500	88.9
	9	500	93.2
	10	500	94.8
	11	500	93.0
	12	500	90.4
	14	500	87.8
B	10	300	89.8
	10	400	90.6
	10	500	94.8
	10	550	93.6
	10	600	92.9
	10	700	91.1

The rate of feed giving maximum yields was 10 ml. per hour of nitropropane, Table IA, and the optimum rate of flow of hydrogen was approximately 500% excess of nitropropane, Table IB.

This catalyst is seen to be an excellent one for the reduction of nitropropane to propylamine. It is of interest to note the 500% excess of hydrogen found for this reaction is the same value found when nickel tungstate was used as the catalyst.

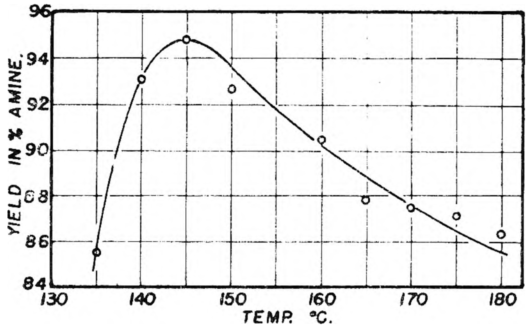

Fig. 1.—Conversion % *vs.* °C. for the reduced nickel molybdate catalyst.

Reduced Nickel Chromate Catalyst.—The catalyst was prepared by slowly adding a boiling solution, 100 g. of nickel nitrate dihydrate in 500 ml. of water, to a boiling solution of 145 g. of sodium chromate decahydrate in 500 ml. of water. The precipitate formed was washed repeatedly until traces of the nitrate ion could be no longer detected. The moist salt was then dried in an oven for 24 hours at 110°. Twenty grams of the nickel chromate on 4 g. of shredded asbestos was placed in the furnace for reduction. Table II shows effects of the temperature, for reduction of this catalyst, on the yield of propylamine as recorded in the treatment of our original catalyst. A reduction temperature of 500° for a duration of approximately 10 hours was finally determined to give the catalyst of maximum activity.

TABLE II

Catalyst, nickel chromate; rate of hydrogen during reduction and heating, 17 liters per hour; rate of hydrogen during reduction of nitropropane, 250% of theory; rate of nitropropane, 10 ml. per hour; furnace temperature for the reduction of the nitropropane, 165°

Procedure in reducing the catalyst	Yield of 1st run in % converted	Average yield in % converted
Reduced at 405° for 1 hr.	56.7	54.0
Additional heating, 1.5 hours at 405°	79.0	57.9
Additional heating, 13 hours at 405°	85.5	66.8
Additional heating, 14 hours at 450°	87.6	62.7
Additional heating, 10 hours at 500°	90.1	70.6
Additional heating, 10 hours at 550°	72.8	55.1

Another point of interest is that in every case the yields of amine for the first run of nitropropane over the newly treated catalyst was appreciably higher than those obtained after several experiments where the yields became constant.

X-Ray powder diffraction measurements on the reduced nickel chromate show the three most prominent lines correspond to the *d*-values for the three most prominent lines of

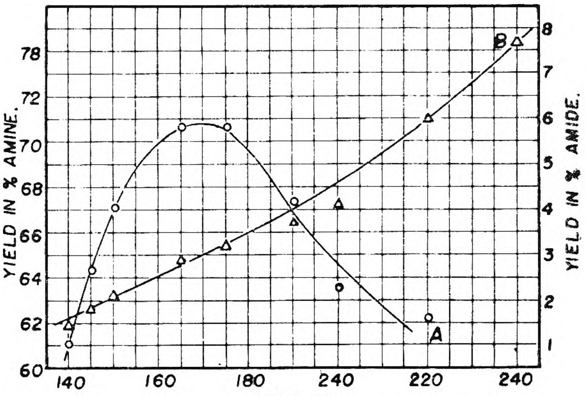

Fig. 2.—Conversion % *vs.* °C. for the reduced nickel chromate catalyst: A, % propyl amine; B, % propionamide.

---

[5] C. S. Rohrer, J. Rooley and O. W. Brown, THIS JOURNAL, **55**, 211 (1951).

[6] J. F. Woodman, H. S. Taylor and J. Turkevich, *J. Am. Chem. Soc.*, **62**, 1397 (1940).

metallic nickel. This again strongly indicates the catalyst contains considerable amounts of dispersed nickel. Since none of the *d*-values correspond to those reported for chromium, it is again assumed the anion is present in some partially reduced state. So far as can be determined by electron micrograph the size and shape of the particles are not changed by reduction, however they take on the appearance of being considerably more porous.

The primary products of the reduction of 1-nitropropane was *n*-propylamine with some propionamide. The optimum temperature for the production of the amine is seen from Fig. 2, curve A, to be from 165 to 175°, and the amide yield is seen to continually increase from 1.4% at 140° to 8% at 240° in Fig. 2, curve B. No attempt was made to increase the yield of the amide by further increase in temperature. The other variables show little or no effect on the yields of propionamide and all the experiments conducted at 165° gave approximately 2.6%.

Feed of approximately 10 ml. of nitropropane per hour gives the best yields, Table IIIA. The ratio of hydrogen to nitropropane giving the best yield is 250%, Table IIIB.

TABLE III

Catalyst, 20 g. nickel chromate on 4 g. asbestos reduced; furnace temperature, 165°

	Nitropropane, g. per hr.	Hydrogen in % theory	Amine in % converted
A	8	250	62.1
	9	250	66.8
	10	250	70.6
	12	250	61.6
B	10	200	67.5
	10	250	70.6
	10	300	67.1
	10	450	65.0
	10	500	64.7
	10	550	64.1
	10	600	59.7

BLOOMINGTON, INDIANA

THE EXTENT OF THE PHOTOCHEMICAL REDUCTION OF PHOSPHOTUNGSTIC ACID

BY LYMAN CHALKLEY

Received April 18, 1952

Phosphotungstic acid, $H_3PW_{12}O_{40}$, has been reduced by *i*-propyl alcohol under the influence of sunlight to a black product which precipitated silver from silver nitrate solution, while undergoing oxidation to the starting material. One molecule of $H_3PW_{12}O_{40}$ after reduction precipitated one atom of silver from solution. Thus the reduced acid was in a state of oxidation equivalent to $H_4PW_{12}O_{40}$.

Background

Like tungstic and molybdic acids,[1] silicotungstic and the 9 and 12 series phosphotungstic acids are photosensitive in presence of suitable reducing agents. Phosphomolybdic acid is also photosensitive. Rindl[2] reported the photosensitivity of "phosphotungstic acid" and concluded it to be due to a reaction of tungstic acid in dissociative equilibrium with the phosphotungstic acid. On the basis of preliminary experiments he postulated the formation of a blue tungsten oxide, W_5O_{14}. Rindl's identification of the oxide was tentative and based upon widely divergent analytical results.

Discussion

It was observed that the color produced on photoreduction of the 12 series phosphotungstic acid, and also silicotungstic acid, was not the same as that produced by the reduction of tungstic acid. The product from tungstic acid is greener and of higher chroma ("brighter") than that from silicotungstic and the 12 series phosphotungstic acids. This observation threw doubt on Rindl's hypothesis as applied to the 12 series acids and led to a reexamination of the nature of the reduction product.

The reduced acid is reoxidized by air and by various other oxidizing agents. Thus there is a reciprocal relationship, $H_3PW_{12}O_{40}$ + reducing agent + light → reduced acid, and reduced acid + oxidizing agent → $H_3PW_{12}O_{40}$, and the degree of reduction could be determined by measurement of the consumption of either the reducing agent or of the oxidizing agent required for the reverse process. Vasil'eva,[3] working with tungstic acid, and Rindl[2] with a phosphotungstic acid measured the quantity of oxidizing agent. The same approach has been followed in the present work but milder oxidizing agents have been used. For the problem is to oxidize the reduced tungsten compound without oxidizing the organic substances present.

In preliminary experiments gaseous oxygen was used as the agent. These experiments were made under conditions that did not permit of precise results and tended to give high readings of the oxygen consumed. Nevertheless they showed that the photochemical process stopped after two or three days exposure to sunlight. The highest oxygen consumption obtained was one atom of oxygen to 15 atoms of tungsten, indicating that W_5O_{14} was not the end-product of the reduction.

To attain greater precision, silver nitrate was used to oxidize the reduced phosphotungstic acid, and the precipitated silver was collected and determined. These determinations, like those made with O_2, indicated that the photochemical process terminated in a stable state after the action of sunlight for two to three days.

The results by this method were much more consistent than in the experiments with gaseous oxygen. Expressed in terms of atoms of tungsten in the form of reduced 12 series phosphotungstic acid required to reduce one silver ion, five determinations gave 10.9, 11.1, 11.8, 11.8 and 11.6 atoms of tungsten per atom of silver. The median was 11.6 and the average 11.4.

While not as precise as might be desired, these figures were sufficiently consistent to indicate a

---

(1) Mellor, "Comprehensive Treatise on Inorganic Chemistry," 11, 537, 755 (1931).

(2) M. Rindl, *S. African J. Sci.*, 11, 362 (1916).

(3) A. Vasil'eva, *J. Russ. Phys. Chem. Soc.*, 44, 819 (1912); *C. A.*, 6, 2886 (1912).

strong probability that one molecule of reduced $H_3PW_{12}O_{40}$ (and possibly also a reduced 11 series phosphotungstate ion) required one silver ion for reoxidation to the original $H_3PW_{12}O_{40}$. If it were postulated that the reduced acid were derived from an oxide of tungsten that had a discrete existence apart from the complex in a heteropoly acid, the oxide would have the composition $W_{23}O_{68}$, or $W_{24}O_{71}$.

What has been demonstrated is that an intensely black, water-soluble, photochemically reduced phosphotungstic acid exists which has the following stoichiometric relationship (or close to it) to the parent acid

$$H_3PW_{12}O_{40} + H + \text{Light} \longrightarrow H_4PW_{12}O_{40} \text{ or } H_2PW_{12}O_{39} + H_2O$$

or some equivalent.

Experimental Part

Use of Gaseous Oxygen to Oxidize the Reduced Acid.—In the outer bulb of what was essentially a double Hempel gas pipet made of Pyrex was placed a solution of 5 g. of 12 series phosphotungstic acid, 10 g. of glucose in 100 ml. of *N*/100 hydrochloric acid. The outlet from this bulb to the air was further protected by a thin rubber bulb. The inner, or gas absorption, bulb of the pipet was charged with a solution of 1.00 g. of Merck and Co., Inc., "Reagent" phosphotungstic acid said to have the formula "approximately $P_2O_5 \cdot 24WO_3 \cdot 25H_2O$." (The lack of precision in the results obtainable in this apparatus made the exact analysis of this starting product unnecessary), and 5 g. of glucose in 100 ml. of *N*/100 HCl. The apparatus was swept out with nitrogen to leave an atmosphere of nitrogen in the free space between the liquid in the two bulbs. The apparatus was then exposed to direct sunlight in the summer and fall of 1950 at Washington, D. C., until the color no longer seemed to deepen, though an exact colorimetric control was not employed. This state was reached after exposure to bright sunlight for 2.5 days, and measurement of oxygen consumption by the solution after a 2.5-day exposure showed as much oxygen consumed as after a 17-day exposure.

After the light exposure the pipet was removed to a dark room and air, or oxygen, introduced into the absorption bulb from a buret in which water was used as the fluid. Contact was maintained until the color of the solution had faded to a very pale gray. If this point was exceeded, no sharp end-point was possible because just about as much oxygen would dissolve in 100 ml. of water as was reduced by the reduction product from 1 g. of phosphotungstic acid.

The rate of oxidation of the reduced acid was very slow. When air was employed about two weeks were required, and when the gas was pure oxygen 2 to 3 days were required for oxidation.

THE RESULTS OBTAINED

Expt. No.	Gas used	Days of exposure to sun and daylight	Ml. of O_2 consumed (at 0° and 760 mm.)	Atoms of W per atom of O (to nearest whole number)
1	Air	2.5	2.61	17
2	O_2	12	3.3	Ran past end-point
3	O_2	17	2.48	18
4	O_2	>10	2.92	15

The gas was kept under pressure during the time of reaction. The long time required made possible diffusion of air or oxygen through the water in the buret, and losses through rubber connections and the stopcock, to give high results. And it had not been shown that oxygen would not react slowly with the oxidized glucose. However, these results did indicate that the photoreduction stopped long before a W_5O_{14} oxide could be reached.

The gas absorption method could probably be refined to give precise results. The rate of oxidation of the reduced acid can be increased by increasing the acidity of the solution and can be enormously accelerated by use of other solvents, such as acetic acid; the concentration of the absorbant solution could be increased; and the apparatus could be designed to measure small volume differences over long periods of reaction. However, the silver nitrate reduction method appeared to promise more rapid progress.

Analysis by Reduction of Silver Nitrate.—When a solution of photochemically reduced phosphotungstic acid was mixed at room temperature with a solution of silver nitrate metallic silver was immediately precipitated, and the reduced acid was quantitatively oxidized to the colorless phosphotungstic acid. The metallic silver could be collected, dissolved in nitric acid and titrated with thiocyanate. This was the procedure employed in the following work.

Weighed amounts of sodium tungstate that analyzed 70.55% WO_3 were placed in Pyrex tubes closed at one end. The sample was dissolved in 2.05 ml. of 1.55% aqueous phosphoric acid per gram of sodium tungstate plus an equal amount of water, and then converted into $H_3PW_{12}O_{40}$ (or its sodium salt) by addition of 13.4 ml. of *N*/1 × 1.02 sulfuric acid per gram of sodium tungstate. These proportions allowed an excess of phosphoric acid, and a little over 2 molecules of sulfuric acid per molecule of sodium tungstate. Sodium tungstate was used as the starting product rather than phosphotungstic acid so as to control the conditions under which the phosphotungstic acid was formed, and because there were standard methods for analysis of sodium tungstate. Approximately 0.1 volume of isopropyl alcohol was added, most of the air exhausted, and the tubes sealed and exposed on a roof to sunlight and daylight. The tubes were of such size that the liquid occupied $^1/_2$ to $^3/_4$ their volume, and thus presented a large area of solution to irradiation when the tubes were laid on their sides during exposure.

After exposure the sealed tip of the tube was broken under a solution made from 8 ml. of *N*/10 $AgNO_3$ per gram of sodium tungstate used, and sufficient water to fill the free space in the tube. When the tip was broken the silver nitrate solution was forced into the exhausted tube by atmospheric pressure. Silver was immediately precipitated and the black color of the reduced phosphotungstic acid vanished. The silver was formed as a colloidal suspension and did not produce a mirror. The precipitated silver was coagulated in the first experiments by boiling the reaction mixture, and was then collected on a porous alumina or fritted glass crucible, and washed with a salt solution to prevent further dispersion and passage through the filter. The washed precipitate was dissolved in nitric acid and titrated with *N*/20 KSCN.

Preliminary experiments were made to learn if the photoreaction stopped at a definite limit, and to determine how much exposure was necessary to reach this limit if it existed. Exposures of 1, 4.5 and 40 days resulted in sufficient reduced phosphotungstic acid to precipitate 0.0220, 0.0297 and 0.0294 g. of Ag, respectively, per gram of sodium tungstate in the sample. These results confirmed the earlier conclusions from the experiments in the gas analysis apparatus that the reaction did reach a definite limit, and that the required outdoor exposure in the vicinity of Washington was less than a week of normally good weather in February and March, when the experiments were made.

The first attempts to determine the precise amount of silver precipitated by a given weight of tungsten as reduced phosphotungstic acid produced by exposures of 39, 40 and 23 days gave 0.0301, 0.0294 and 0.0276 g. of Ag per gram of $Na_2WO_4 \cdot 2H_2O$ used. The difference between the highest and lowest of these figures was over 8% and therefore require a re-examination of the procedure being used for sources of error.

The mixture of silver nitrate, phosphotungstic acid and *i*-propyl alcohol produced by addition of the silver nitrate to the photoreaction solution was itself photosensitive and precipitated a significant amount of silver on exposure for a couple of hours to sunlight. In this reaction the phosphotungstic acid acted as a catalyst for the reduction of silver nitrate by *i*-propyl alcohol. However, in the dimly lit laboratory where the analytical work was carried out, standing for more than three days did not result in the precipitation of a weighable amount of silver.

Some samples of *i*-propyl alcohol were found to reduce silver nitrate solution on heating in a closed tube on a water-bath for an hour. All three samples of 91% *i*-propyl alcohol in the laboratory at the time had this ability to a greater or lesser extent. However, the absolute *i*-propyl alcohol that had been used in the photochemical experiments reduced only a trace of silver nitrate on an hour of heating, and could hardly have been the source of the divergent results.

However, there seemed to be a relation between the time the photochemical reaction mixtures had been heated and the yield of silver obtained—the longer the heating the higher the result. In the series above the reaction mixture of Expt. 1 was boiled for about 20 minutes, that of Expt. 2 for 10 minutes, while that of Expt. 3 was treated with $MgSO_4$, quickly heated almost to boiling and then removed from the flame.

Acetone, formed in the photochemical reduction of phosphotungstic acid by *i*-propyl alcohol, did not reduce silver nitrate solution on heating for an hour in a boiling water-bath, but a sample of acetone that had been stored in a colorless glass stoppered bottle for several years and had become slightly yellow was found to reduce silver nitrate solution quickly on heating. Apparently acetone is itself converted by light into a substance that will reduce silver nitrate on heating. In the reaction under study acetone was formed during a prolonged exposure to direct sunlight and therefore its photochemical product with reducing properties could not be avoided, and would introduce an error causing high results if the reaction mixture were heated.

To try to reduce this error the following process was used on two more samples exposed for 12 days in March and April, 1952. The silver nitrate solution was boiled to expel oxygen and cooled just before mixing with the photochemical reaction product. (This precaution was probably unnecessary because of the enormous difference in speed of reduction of O_2 and $AgNO_3$.) The silver suspension was transferred to a flask, treated with 0.2 its volume of 10% $MgSO_4 \cdot 7H_2O$ and let stand in the dark at room temperature for 4.5 hours (Expt. 4) or 22 hours (Expt. 5), and filtered through a "fine" Pyrex fritted glass Gooch crucible. The precipitate was washed first with 2% magnesium sulfate and after most of the phosphotungstic acid had been removed, with 2% KNO_3 solution until the filtrate gave no cloud when tested with a few drops of $N/1$ HCl. The tube in which the light exposure had been carried out, the flask in which the reaction mixture had stood, and the stirring rod used to transfer the solution were cleaned with concentrated HNO_3 to collect any adherent silver, and the precipitate on the filter dissolved in HNO_3. All of the nitric acid solutions were combined, boiled to remove N_2O_4, cooled and titrated with $N/20$ KSCN. The results of the three experiments recorded above and of the two new ones gave 0.0301, 0.0294, 0.0276, 0.0278 and 0.0282 g. of Ag per gram of $Na_2WO_4 \cdot 2H_2O$ in the sample. The weight of $Na_2WO_4 \cdot 2H_2O$ used in a sample varied from 3.3052 to 4.4458 g. The amounts of silver obtained corresponded to 10.9, 11.1, 11.8, 11.8 and 11.6 atoms of tungsten per atom of precipitated silver.

The procedure could probably be standardized to give more consistent results, but such an effort might well obscure rather than eliminate a source of error still indicated by the nearly 2% difference in results between experiments 4 and 5. This error, while relatively small from the standpoint of general conclusions from the work, should not be ignored, and indicates the need for study to elucidate further the chemical relationships.

Washington, D. C.

LINEAR POLYMETAPHOSPHATES—QUATERNARY AMMONIUM SALTS

By R. K. Iler

Grasselli Chemicals Department, Experimental Station, E. I. du Pont de Nemours and Company, Inc., Wilmington, Delaware

Received April 18, 1952

The quaternary ammonium salts of linear high molecular weight polymetaphosphoric acid represent a new class of organo-inorganic, film-forming polymers. Film-forming properties become pronounced at a degree of polymerization of the metaphosphate above 130; a degree of polymerization of 1000 has been readily attained. The physical properties of these polymers are improved by cross-linking with minor proportions of polyvalent metal cations. These products are prepared from inorganic linear polymetaphosphates, *e.g.*, the potassium and lead salts. An ion-exchange method may be used in the preparation of the water-soluble tetramethylammonium polymetaphosphate, while simple metathesis and precipitation may be employed in the case of the insoluble derivatives such as cetyl trimethylammonium polymetaphosphate. The polymers can be oriented by cold drawing. In the case of a long chain quaternary ammonium salt, the X-ray diffraction pattern indicates that the side chains lie at right angles to the metaphosphate polymer chains which are oriented in the direction of drawing.

Soluble linear polymetaphosphates,[1] such as the mixed sodium–potassium salt derived from potassium metaphosphate, behave as linear polymers,[2] and form clear, continuous, and initially coherent though subsequently brittle films when dried on a smooth surface such as glass. It was therefore of interest to investigate the behavior of similar linear polymetaphosphates in which the cation is organic rather than inorganic, *e.g.*, the quaternary ammonium polymetaphosphates, since the latter polymers might be internally plasticized. The precipitation of cetylpyridinium bromide from an aqueous solution of glassy sodium metaphosphate ("Calgon") has been described by Powney[3] and by Steigmann.[4] However, these products were of low average molecular weight; as has been shown by Van Wazer,[5] such metaphosphates consist of mixtures of short and long metaphosphate chains. Also, as will be shown, the quaternary ammonium salts derived from a sodium metaphosphate glass exhibit the weak, soft and gummy characteristics of a relatively low molecular weight polymer, in contrast with the hard, firm polymers derived from the high molecular weight, crystalline KPO_3.[6]

Water-soluble Quaternary Ammonium Polymetaphosphates.—The lower aliphatic quaternary ammonium polymetaphosphates have been prepared from KPO_3 either by ion exchange with the quaternary ammonium salt of an ion-exchange resin or by neutralizing polymetaphosphoric acid obtained by treating KPO_3 with the hydrogen form of an ion-exchange resin. Films of tetramethylammonium polymetaphosphate are firm when dry, but under ordinary atmospheric conditions absorb water and act as a very viscous fluid

---

(1) Since the "linear polymetaphosphates" possess end-groups, they do not precisely conform to the formula for a "metaphosphate" and are therefore, strictly speaking, "polyphosphates."

(2) (a) H. Malmgren and O. Lamm, *Z. anorg. Chem.*, **B252**, 256 (1944); (b) R. Pfanstiel and R. K. Iler, paper in preparation.

(3) J. Powney, *Nature*, **152**, 76 (1943).

(4) A. Steigmann, *J. Soc. Chem. Ind.*, **66**, 353 (1947).

(5) John R. Van Wazer, *J. Am. Chem. Soc.*, **72**, 639, 647, 655, 966 (1950).

(6) M. T. Goebel and R. K. Iler (du Pont), U. S. Patent 2,592,273.

unless cross-linked with minor amounts of metal ions.

The partially cross-linked tetramethylammonium polymetaphosphate can be cold-drawn and gives an X-ray diffraction pattern characteristic of an oriented polymer. The oriented polymer is strong and flexible, but still quite soluble in water.

Experimental

Preparation of Tetramethylammonium Polymetaphosphate.—Four hundred grams of pure KH_2PO_4 (Baker C.P.) in a three-inch diameter platinum dish was placed in a muffle at 675° and held at this temperature for 40 minutes, removed, quickly cooled and pulverized. The loss in weight was 13.7% (theoretical 13.25%). A sample of this KPO_3 was converted to the soluble sodium–potassium salt for estimation of molecular weight as follows: Ten grams of pulverized KPO_3 was suspended in 500 ml. of distilled water and 70 g. of air-dried cation-exchange resin in the sodium form ("Dowex 50") was then stirred in and agitation continued for 30 minutes while maintaining the *p*H at 8 to 9 by addition of sodium hydroxide. The resin was then removed from the clear viscous solution by filtration through glass cloth. As measured at an equivalent KPO_3 concentration of 1%, the specific viscosity (25°) was 102, corresponding to a degree of polymerization of about 2000.[2a]

Fifty grams of KPO_3 (0.425 *M*) was suspended in 2450 g. of CO_2-free distilled water at 25°, the *p*H adjusted to 8 by addition of $(CH_3)_4NOH$. Separately, the tetramethylammonium salt of a cation-exchange resin ("Nalcite HCR") was prepared by neutralizing the hydrogen form of the resin with excess of the quaternary ammonium base; the capacity of the resin in the wet-drained state was determined to be about 1.4 milliequivalents per ml., or 3 milliequivalents per gram of air-dried resin. Five hundred and seventy-five grams of the air-dried quaternary ammonium resin (about 1.5 equivalents), 133.5 g. of air-dried resin in the calcium form, and 33.4 g. in the magnesium form were added to the KPO_3 suspension and the mixture was stirred slowly for 65 minutes. The *p*H was kept between 8 and 9 by the addition of free base. The solution was then separated from the resin by filtration through glass wool, aged 16 hours at 5-10°, evaporated to a volume of 1 liter, under vacuum at 35°, and cast in 6″ × 6″ glass cells, previously greased lightly with silicone stopcock grease. Drying was carried out at room temperature in a current of air.

The resulting films were strong, pliable and non-hygroscopic, but dissolved readily in water. The polymer could be cold-drawn under conditions of high humidity. The tensile strength of the oriented polymer ranged from 3000 to 4000 lb. per sq. in., based on cross-section at break. When dried over P_2O_5, the polymer became hard and rather brittle.

Analysis indicated that the proportions of cations in the polymer were (based on total cations analyzed): tetramethylammonium, 60%[a]; potassium, 20%; calcium, 16%; magnesium, 4% = 100% total.

Another series of samples containing different ratios of sodium, potassium and tetramethylammonium ions was prepared from polymetaphosphoric acid as follows: Twenty grams of pulverized KPO_3 was suspended in 1980 ml. of CO_2-free distilled water at 3°, 192.5 g. of air-dried cation-exchange resin in the hydrogen form was added, and the mixture stirred for 20 minutes while keeping the mixture at about 3°. The viscous solution was decanted from the resin and run through a column of the hydrogen resin, previously chilled with ice-water. The presence of polymetaphosphoric acid in samples of the effluent was detected by adding a long chain quaternary ammonium salt ("Hyamine 1622") which gives an immediate precipitate with polymetaphosphate ions. With a flow rate of about 30 ml./min., the effluent was collected and kept at 0°. Titration of a sample of the composite effluent with 0.1 *N* NaOH indicated a concentration of polymetaphosphoric acid equivalent to 0.54% $NaPO_3$, corresponding to 0.122% Na and 0.164% P. (Analysis of the neutralized solution gave 0.128% Na, 0.169% P and 0.003% K.)

Portions of the solution of polymetaphosphoric acid were neutralized to *p*H 7.5 with 1 *N* solutions of $(CH_3)_4NOH$, KOH, NaOH and mixtures of these; the results are given in Table I.

TABLE I

	Proportions of equivalents of cations[a]	Concentration of polymer, milli-equiv./liter	Specific viscosity, 25°	Film appearance (air-dried)
(A)	98.5% $(CH_3)_4N^+$ 1.5% K^+	80	5.26	Very tacky, hygroscopic, soft, not orientable
		16	2.08	
		4	1.24	
(B)	100% K			Opaque, white, very brittle
(C)	98.5% Na 1.5% K			Clear, very brittle
(D)	49.3% $(CH_3)_4N^+$ 50.7% K	80	3.71	Clear, firm, flexible, slightly tacky, brittle when very dry
		13	1.73	
		4	0.83	
(E)	49.3% $(CH_3)_4N^+$ 1.5% K 49.2% Na	80	3.53	Same as (D)
		16	1.56	
		4	0.85	
(F)	24.6% $(CH_3)_4N^+$ 75.4% K	80	2.31	Clear, strong when wet, very brittle when dry
		16	1.04	
		4	0.54	
(G)	49.3% $(CH_3)_4N^+$ 50.7% K	80	2.21	Same as (D)
		16	1.07	
		4	0.61	
(H)	73.8% $(CH_3)_4N^+$ 26.2% K	80	2.32	Soft, tacky, flexible, hygroscopic
		16	0.90	
		4	0.57	

[a] Based on total cations analyzed.

All the films were water-soluble. Samples (D) and (E) were prepared by mixing the neutralized solutions (A) and (B) and (A) and (C), respectively, while (F), (G), and (H) were prepared by neutralizing the acid with a suitable mixture of the bases. By extrapolation of curves of log specific viscosity *versus* log concentration, to 85 milliequivalents per liter (corresponding to 1% KPO_3), the degree of polymerization of the polymer in the neutralized solutions is roughly estimated as (A) 1700; (D) and (E), 1300; (F), (G) and (H) 1000. This downward trend indicates the hydrolysis and degradation of the stock solution of polymetaphosphoric acid which was stored at 3° during the several hours required for the experiments. Solutions of the acid which were permitted to be degraded until the viscosity of the neutralized solution indicated a degree of polymerization less than about 130, gave tetramethylammonium salts which were only viscous oils upon drying in air, the film-forming character having been lost.

The tetramethylammonium polymetaphosphate has also been prepared from crystalline lead metaphosphate, which appears to be a linear inorganic polymer. As has been shown by Warschauer,[7] anhydrous crystalline lead metaphosphate can react with a solution of sodium sulfide to obtain lead sulfide and a viscous solution of sodium polymetaphosphate. A film of tetramethylammonium polymetaphosphate was prepared *via* the lead salt as follows: Pure lead oxide (PbO) and phosphoric acid in the ratio of $PbO:P_2O_5$, 1:1, were heated together in a platinum dish for 18 hours at 110°, then at 650° for 16 hours, cooled to 500°; the resulting clear glass was removed from the furnace, cooled and pulverized and reheated at 540° for 30 minutes, which caused complete crystallization to lead metaphosphate (m.p. 660°). Separately 7.4 ml. of a 1.1 *N* tetramethylammonium hydroxide was saturated with hydrogen sulfide and then an additional 0.8 ml. of the base was added to raise the *p*H to 10. Three and one-half grams of finely powdered crystalline lead metaphosphate was then added, with vigorous stirring, together with 2.2 ml. of the 1.1 *N* base to maintain the *p*H around 9. Stirring was continued for 25 minutes; the solution became very viscous and lead sulfide appeared as a black precipitate. The latter was removed by centrifuging and the clear viscous solution was cast on greased glass, and dried to give a film very similar to that prepared from KPO_3. Since no cross-linking ions were present, the film was hygroscopic and tacky in moist air but hard and coherent in a dry atmosphere.

Stability of Tetramethylammonium Polymetaphosphate and Effect of Foreign Cations.—It has

---

(7) Warschauer, *Anorg. Chem.*, **36**, 137 (1903).

been shown by B. Ingelman and H. Malmgren[8] that polymetaphosphate is most stable at *p*H 7 to 9.5, the rate of hydrolysis being practically independent of the *p*H within this range. It was therefore of interest to obtain some idea of the stability of the tetramethylammonium salt within this range. The following solutions containing polymetaphosphate equivalent to 1% KPO_3 were prepared by ion exchange and aged at 90°, keeping the *p*H between 8 and 9 by addition of small amounts of tetramethylammonium hydroxide as required. The initial degree of polymerization, based on the viscosity of the corresponding sodium–potassium salt, was about 1150.

TABLE II

STABILITY OF METAPHOSPHATE SOLUTIONS

	Approximate cation distribution					Specific viscosity after indicated time			
	$(CH_3)_4N^+$	K	Na	Mg	Ca	0 min.	27 min.	54 min.	104 min.
(a)	100	..	..	..	..	710	89	42	17
(b)	60	40	..	..	..	87	59	49	32
(c)	60	20	..	..	20	38	9	5	2
(d)	65	35	..	..	..	100	41	29	18
(e)	65	25	..	..	10	53	21	14	8
(f)	0	50	50	..	..	34	15	10	6
(g)	69	10	..	3.5	17	33	9	5	3

It is evident from (a), (b) and (c) that the initial viscosity is a function of the type of cations present, the quaternary ammonium ion giving much the highest viscosity, potassium and sodium lowering the viscosity greatly, and calcium having the greatest depressant effect. However, in regard to the rate of hydrolysis as indicated by decrease in viscosity, a comparison of (a) and (d) suggests that potassium has a stabilizing effect as compared to tetramethylammonium ion. A comparison of (d) and (e) shows that the viscosity is approximately halved by the replacement of Ca^{++} for K^+, but the ratio of viscosities is about constant during degradation, showing that the effect of Ca^{++} is about the same as K^+, as far as the rate of degradation is concerned. Compositions (c) and (g) are about equal in regard to relative stability, indicating that Mg^{++} has no adverse effect as compared with Ca^{++}. Finally, the sodium–potassium salt (f), free from quaternary ammonium ions, shows the lowest rate of degradation.

The hypothesis is advanced that, in accordance with Van Wazer's observations regarding complex ion formation,[5] the metal cations form soluble complexes with the polymetaphosphate, while the quaternary ammonium ion cannot. Consequently, in the presence of the quaternary ammonium ion the ionic charge on the polymetaphosphate chain remains high, the chain remains outstretched, giving higher viscosity, but decreasing the stability toward hydrolytic cleavage. It is visualized that a strain is imposed upon the mid-region of the chain due to the mutual repulsion of the negative charges along the chain. The chain is therefore more readily cleaved by hydrolysis in the mid-section, especially in the case of the quaternary ammonium salt where the charge on the chain is highest. This picture also may explain why, as reported by Malmgren,[8,9] cleavage of the polymetaphosphate chain does not give many orthophosphate ions split from the chain ends, although this might also be explained by the stability of the pyrophosphate ion.

The sample of pure tetramethylammonium polymetaphosphate spectroscopically free from metal cations (a) was prepared as follows: A purified tetramethylammonium salt of HCR resin was prepared by extracting a sample of the ion-exchange resin with HCl to remove traces of metal ions, washing and neutralizing with the base. Then 5 g. of pure KPO_3, 495 g. of H_2O, 50 g. of air-dried resin were stirred together and the *p*H maintained at 8.0 by addition of $(CH_3)_4NOH$. The resulting solution was passed four times very slowly (8 hours per pass) through fresh columns (55 × 1.5 cm.) of quaternary ammonium resin. The resulting solution, which was 1.12 *N*, was diluted to 1.0 *N* for stability tests.

Oriented Polymer.—The tetramethyl polymetaphosphate film (g) described above, containing metal cations, showed typical cold-drawing behavior when humidified. A quarter-inch wide strip of the film was stretched about fourfold and compared with unstretched material by X-ray diffraction. A diffuse but measurable pattern, characteristic of an oriented polymer, was obtained. A spacing of 4.7 ± 0.1 Å, in the direction of drawing was identified. Since on single fibers of KPO_3 a repeating distance of 4.55 Å. along the fiber axis was separately established, it is probable that the metaphosphate chains run parallel to the direction of drawing of the film. Copper radiation with nickel filter, with a film distance of 7.0 cm., was employed.

Water-insoluble Long-chain Substituted Quaternary Ammonium Polymetaphosphates.—Long-chain quaternary ammonium ions such as cetyltrimethylammonium polymetaphosphate are readily precipitated as gummy or waxy solids which are hydrophobic and relatively insoluble in water. The hardness and strength of these polymeric materials is markedly increased by the introduction of polyvalent metal ions such as Mg^{++}. Although the polymers can be oriented, the oriented polymers are considerably weaker than the tetramethylammonium salts. X-Ray patterns indicate that in the oriented polymer the long hydrocarbon chains are probably oriented at right angles to the direction of the metaphosphate chains which are parallel to the direction of orientation.

Experimental

Cetyl Trimethylammonium Polymetaphosphate. (A).—To five hundred ml. of a 0.085 *M* solution of the previously described sodium–potassium polymetaphosphate (0.0425 mole) in a Waring Blendor was added 125 ml. of a 0.339 *M* solution of cetyltrimethylammonium bromide (CETAB—0.0245 mole, Eastman Kodak), over a period of about 5 minutes at a temperature which increased from 25 to 35°. The very gummy precipitate was washed by kneading in 200 ml. of distilled water, adding NaOH to maintain the *p*H between 7 and 9. Excess water was squeezed from the polymer, which was then spread in thin sheets and air-dried.

	Analysis, %
Phosphorus	6.4, 6.5
Nitrogen	3.24, 3.29
Carbon	55.43, 55.14
Hydrogen	11.54, 11.64
Bromine	1.48, 1.34
K	0.086
Na	0.41

	Approx. composition, %
Quaternary metaphosphate	76
Quaternary bromide	9
Water and other salts	15

(**B**).—For comparison, a corresponding polymer was prepared from glassy $NaPO_3$, or Graham salt. The latter was made by heating $NaH_2PO_4 \cdot H_2O$ (Baker and Adamson) to 725° for 70 minutes and quenching the melt between stain

---

[8] B. Ingelman and H. Malmgren, *Acta Chem. Scand.*, 1, 422 (1947).

[9] H. Malmgren, *Acta Chem. Scand.*, 2, 147 (see p. 161) (1948).

less steel plates previously cooled with Dry Ice. The clear glass was dissolved to give a 1% solution in water; this gave a relative viscosity of 1.22 at 25° or a specific viscosity of 0.22. This would correspond to a degree of polymerization of about 50, based on the data obtained on linear KPO$_3$,[2a] but an end-group titration indicated a degree of polymerization of 220. These data are of the same order of magnitude as those reported by Van Wazer, who has shown that Graham's salt is highly heterogeneous in regard to molecular weight. The corresponding cetyltrimethylammonium polymetaphosphate was prepared by mixing 100 ml. of 0.2 *N* solution of Graham salt with 66 ml. of 0.33 *N* solution of CETAB. Complete flocculation occurred at once, but the precipitate was much less coherent than that prepared from the high molecular weight polymetaphosphate. When partially dry, the material was a soft curd, which coalesced to a dark, soft, grease-like mass.

	Analysis, %	Approx. composition, %	
Phosphorus	6.79, 6.42	Quaternary metaphosphate	78
Nitrogen	3.17, 3.40	Quaternary bromide	7
Carbon	53.3, 53.7	Sodium bromide	3
Hydrogen	10.59, 10.77	Water, etc.	12
Bromine	4.70, 4.65		
Sodium	2.13		

(C) **Mixed Magnesium Cetyltrimethylammonium Polymetaphosphate Polymer.**—Exactly the same technique and quantities of solution were employed as in (A), except that 0.86 ml. of 1.0 *M* MgCl$_2$ solution was added to the metaphosphate solution before adding the quaternary ammonium salt. This corresponds to 2 magnesium ions per 100 PO$_3^-$ units. The product was much firmer than in the absence of Mg^{++} ions.

	Analysis, %	Approx. composition, %	
Phosphorus	6.45, 6.20	Quaternary metaphosphate	75
Nitrogen	3.30, 3.32	Quaternary bromide	11
Carbon	55.81, 55.82	H$_2$O	11
Hydrogen	11.51, 11.74	Found Mg per 100 PO$_3^-$ =	3.5
Magnesium	0.18, 0.16		
Bromine	1.78, 1.81		

During the addition of the cetyltrimethylammonium bromide (CETAB), it was noted that the end-point of precipitation could be readily observed, since the reaction medium became clear, the precipitate being completely coagulated. As excess of the organic cation is added, the solution becomes very foamy and the precipitate begins to be dispersed. In a series of runs in which still more MgCl$_2$ was added, the amount of quaternary ammonium salt required for complete precipitation of 0.0425 equivalent of (PO$_3^-$) decreased.

TABLE III

Equivalent of Mg^{++}	Equivalent of CETAB	Total equiv.	Mg^{++} ions per 100 PO$_3^-$ units
0	0.0425	0.0425	0
.0068	.0364	.0432	8
.0136	.0283	.0419	16
.0203	.0223	.0426	24

The magnesium ions combine with the metaphosphate ions forming a soluble complex, and are not displaced by the organic cations, since all the Mg is found in the polymers. When 0.0068 equivalent of Mg^{++} was employed, the precipitate was leathery and short; larger amounts of Mg^{++} giving 0.020 equivalent of Mg^{++} (24 Mg/100 PO$_3^-$), gave hard, brittle polymers.

Oriented Polymer.—Freshly prepared laurylpyridinium polymetaphosphate was prepared by adding 0.0535 mole of laurylpyridinium chloride, dissolved in water to a total volume of 150 to 500 ml. of a solution containing 0.0535 equivalent of sodium–potassium metaphosphate prepared by solubilizing KPO$_3$ by means of the sodium salt of an ion-exchange resin, as previously described. The insoluble polymer collected on the stirring rod was washed by kneading in several charges of distilled water. The polymer was spread in a 1/8" thick sheet on a glass plate to dry in air for two days, and then strips were cut from the resulting leathery sheet and oriented by drawing from 2- to 3-fold in length. Comparison of the X-ray patterns of the drawn with the undrawn polymer showed development of an interference corresponding to a spacing of 4.6 Å. in the direction of elongation, characteristic of the metaphosphate chain. However, at right angles to this, spacings of 39, 19, 15, 12.9 and 10.9 Å were noted. This suggests that the lauryl and pyridine groups may be oriented roughly at right angles to the drawing direction. The relatively low tensile strength of the oriented polymer is understandable when it is considered that the principal bonding forces between the polymetaphosphate chains therefore arise only from the van der Waals forces between the hydrocarbon chains which project at right angles from the metaphosphate chains.

Additional Types of Quaternary Ammonium Polymetaphosphates.—The following water-insoluble polymers were prepared from KPO$_3$, solubilized by ion exchange with the sodium salt of an ion-exchange resin as previously described. A solution of the quaternary ammonium bromide or chloride was added in stoichiometric amount to the metaphosphate solution in a Waring Blendor, and the gummy precipitate collected from the walls and stirrer blades, washed with water and pressed to thick films which were then air-dried.

Dimethyldi-*n*-octadecylammonium polymetaphosphate was an extremely tacky, water-repellent wax which adhered strongly to metal, glass, and to the fingers. The *n*-octadecyldimethylbenzylammonium compound dried to a crumbly, waxy mass which dissolved in chloroform, giving a viscous solution which dried to a coherent, continuous water-repellent coating on glass and other surfaces. The polymer softened to a viscous mass at 90°, from which films could be pressed. The diisobutylphenoxyethoxyethyldimethylbenzylammonium salt was an elastic, transparent solid which could be pressed to flexible films.

In addition to cross-linking cetyltrimethylammonium polymetaphosphate with magnesium ions as previously described, cross-linking with other polyvalent metal ions was also briefly investigated. Cross-linking with barium equivalent to 20% of the metaphosphate ions gave a non-tacky, flexible mass which could be cold drawn by stretching up to fourfold in length, to give an opaque, rope-like solid with a fiber structure which could be split readily in the direction of stretching. Without barium, the polymer could be stretched indefinitely by continuous application of tension, and it remained soft, tacky, and very flexible. Cross-linking with chromium, nickel and cadmium (from the chlorides) to the extent of 20% of the amount equivalent to metaphosphate ions, gave products of similar physical properties. Aluminum appeared to be somewhat more effective, as little as ten equivalent per cent. (or only 3.3 Al atoms per 100 PO$_3^-$ units) gave a firm solid which could not be stretched more than 20% of its length without breaking.

Water-soluble polymers were also prepared by the method employed for the tetramethylammonium salt. Benzyltrimethylammonium polymetaphosphate, cross-linked with 26 equivalent per cent. of magnesium ions, was a non-tacky, rather strong and elastic solid as compared with the soft hygroscopic mass obtained without introducing magnesium. Both polymers were, however, soluble in water; the cross-linking effect of magnesium appears to be exerted only in the case of the air-dried polymer and not in the presence of water.

Tetraethanolammonium, phenyltrimethylammonium and tetraethylammonium polymetaphosphates were prepared with and without cross-linking metal ions, having about the same properties as the tetramethylammonium salt except that they exhibited different degrees of hygroscopicity and qualitatively appeared to be more rubbery and had less strength. Introduction of magnesium ions made the resulting films less tacky, stronger, and less hygroscopic, but did not make the films insoluble in water.

Acknowledgments.—The author is indebted to Dr. M. C. Paulson and Dr. R. Pfanstiel, who carried out the preparation and study of most of the polymers herein described, to Dr. L. F. Beste and Dr. E. H. Wittbecker who checked certain of the preparations, to Dr. E. P. Meibohm and Dr. J. Grandine for the X-ray work, to K. W. Greenan and R. E. Lawrence for chemical analyses, and to Dr. M. T. Goebel for advice and guidance in initiating and carrying out this investigation.

IONIC EQUILIBRIA IN AQUEOUS AND MIXED SOLVENT SOLUTIONS OF SILVER ACETATE AND SILVER MONOCHLOROACETATE

By F. H. MacDougall and Leo E. Topol[1]

School of Chemistry, University of Minnesota, Minneapolis

Received April 18, 1952

The electromotive force of cells containing silver acetate and sodium acetate in one half-cell and silver nitrate and sodium nitrate in the other half-cell has been measured at 25°, using as solvents 10, 20 and 30% ethanol–water and 10, 20 and 30% acetone–water mixtures. A similar study has been made with silver monochloroacetate in water, and 10, 20 and 30% ethanol–water mixtures. In unsaturated solutions of silver acetate and silver chloroacetate equilibrium constants for the following equilibria have been determined: $AgA \rightleftarrows Ag^+ + A^-$; $AgA_2^- \rightleftarrows Ag^+ + 2A^-$. The relation between the value of an equilibrium constant and the dielectric constant of the medium is given by the simple Born theory more satisfactorily than one might well expect. The activity-product constants obtained in previous studies of the solubility of silver acetate in various solvents have been corrected by making use of the dissociation constants obtained by means of the electromotive force measurements.

Introduction

In our earlier work in this field,[2-5] measurements were made of the solubility of silver acetate in water and in mixed solvents in the presence of added electrolytes, including acetates and silver salts. Evidence was obtained leading to the view that in these solutions complex ions of the form AgA_2^- and Ag_2A^+ were formed. Estimates were made of the dissociation constants of these ions. Values of the activity product, $K_1 = a_{Ag^+}a_{Ag^-}$ were also obtained on the assumption that in the solutions investigated silver acetate was virtually completely dissociated.

More recently, electromotive force measurements were made of appropriate cells.[6,7] These measurements soon led to the conclusion that in 0.05 *M* silver acetate in aqueous solution the silver acetate is roughly 85% dissociated. This work also enabled us to obtain a more accurate estimate of K_2, the dissociation constant of the complex ion AgA_2^-. In the present investigation, electromotive force studies have been extended to solutions of silver acetate in water–ethanol and water–acetone mixtures and to solutions of silver monochloroacetate in mixtures of water and ethanol.

Preparation of Silver Electrodes and of Solutions.—In this connection, it must suffice to refer to the paper by MacDougall and Peterson.[6,7] Our silver electrodes were found to agree within less than 0.04 millivolt. It should be added that solutions of silver monochloroacetate undergo a slow hydrolysis forming chloride ion. The rate of hydrolysis increases with the temperature and decreases with increasing per cent. of alcohol. This type of hydrolysis has been frequently investigated.[8] Because of the occurrence of this hydrolysis, our results with chloroacetate solutions are probably less trustworthy than those with acetate solutions.

The compositions of the water–alcohol and water–acetone mixtures were calculated from the densities measured at 25°.[9,10] The dielectric constants, *D* were interpolated from the values given by Åkerlof.[11]

The Experimental Method.—All of the cells investigated were of the type

$$\mathrm{Ag}\ \left|\ \begin{array}{c}\mathrm{AgA}(c_1)\\ \mathrm{NaA}(c_2)\end{array}\ \right|\ \begin{array}{c}\mathrm{KNO_3}\\ \text{saturated}\end{array}\ \left|\ \begin{array}{c}\mathrm{AgNO_3}(c_1')\\ \mathrm{NaNO_3}(c_2')\end{array}\ \right|\ \mathrm{Ag}$$

where the symbol A denotes either the acetate or the chloroacetate radical and where *c* is the molarity. In any given cell, the concentrations c_1 and c_1' on the one hand and the concentrations c_2 and c_2' on the other hand were made as nearly equal as possible.

The cells used were similar to those employed by MacDougall and Peterson.[6] The potentiometer was a Leeds and Northrup Type K-2 and the galvanometer was of the wall-type. The temperature of the water-bath was maintained at 25.00 ± 0.02°. Electromotive measurements were made at hourly intervals. Readings become constant after two to four hours and remained so for periods ranging from two hours to eight days.

Experimental Data.—Table I gives the results obtained in the measurement of the electromotive force at 25° of the cells which contained silver acetate in 10% ethanol.[12]

Table I

Electromotive Force Data of Silver Acetate at 25° in 10% Ethanol

Solvent = 9.23% ethanol; d_0 = 0.98159; *D* = 73.24

Cell	c AgA	c_2 NaA	c_1' AgNO$_3$	c_2' NaNO$_3$	Density	*E*, volt
1	0.008352	0.7178	0.008346	0.7173	1.0133	0.03705
2	.01389	.1025	.01388	.1026	0.9890	.00142
3	.01389	.4105	.01388	.4105	1.0011	.02600
4	.01116	.1434	.01116	.1434	0.9894	.01350
5	.01116	.5535	.01116	.5534	1.0068	1.03125
6	.1104	.02044	.01104	.02044	0.9840	0.00393
7	.005500	.1434	.005504	.1434	.9895	.01303
8	.005500	.1025	.005504	.1026	.9869	.01030
9	.004592	.8559	.004590	.8559	1.0187	.04160
10	.008247	.2056	.008249	.2055	0.9925	.01665
11	.02206	.04109	.02206	.04111	0.9875	.00655

Theory

In order to be able to make a quantitative in-

---

[1] This paper is based on a thesis presented by Leo E. Topol to the Graduate School of the University of Minnesota in partial fulfillment of the requirements for the degree of doctor of philosophy.

[2] F. H. MacDougall, *J. Am. Chem. Soc.*, **52**, 1390 (1930); F. H. MacDougall and J. Rehner, Jr., *ibid.*, **56**, 368 (1934); F. H. MacDougall and C. E. Bartsch, This Journal, **40**, 649 (1936).

[3] E. Larsson and B. Adell, *Z. anorg. allgem. Chem.*, **196**, 354 (1931).

[4] F. H. MacDougall and W. D. Larson, This Journal, **41**, 417 (1937).

[5] F. H. MacDougall and M. Allen, *ibid.*, **46**, 730 (1942); **49**, 245 (1945); F. H. MacDougall, *ibid.*, **46**, 738 (1942).

[6] F. H. MacDougall and S. Peterson, *ibid.*, **51**, 1346 (1947).

[7] J. V. Parker, C. Hirayama and F. H. MacDougall, *ibid.*, **53**, 912 (1949).

[8] H. M. Dawson and E. R. Pycock, *J. Chem. Soc.*, 778 (1934); 153 (1936); H. M. Dawson, E. R. Pycock and G. F. Smith, *ibid.*, 317 (1945); W. A. Drushel and C. S. Simpson, *J. Am. Chem. Soc.*, **39**, 2435 (1917); S. Matsuura, *Bull. Chem. Soc. Japan*, **8**, 113 (1933); L. B. Nannings, *Rec. trav. chim.*, **69**, 76 (1950); G. Senter, *Proc. Chem. Soc.*, **23**, 60 (1907); *J. Chem. Soc.*, **91**, 460 (1907); G. Senter and H. Wood *ibid.*, **109**, I. 681 (1916); G. F. Smith, *ibid.*, 521 (1943); A. Tian, *Bull. soc. chim.*, [5] **1**, 115 (1934).

[9] "International Critical Tables," Vol. III, McGraw-Hill Book Co., Inc., New York, N. Y., 1929, p. 116.

[10] *Ibid.*, p. 112.

[11] G. Åkerlof, *J. Am. Chem. Soc.*, **54**, 4125 (1932).

[12] Detailed data with respect to the other types of cells may be obtained in mimeographed form on application to the Division of Physical Chemistry of the University of Minnesota.

terpretation of our experimental results, we have been compelled to introduce a number of simplifying assumptions. It would be, for instance, very difficult, if not impossible, to make an accurate estimate of the liquid junction potentials in our cells. Accordingly, we make the following assumptions: (1) The use of a saturated solution of potassium nitrate between the half-cells reduces the resultant liquid-junction potential to zero. (2) The activity coefficient of undissociated silver acetate or of undissociated silver chloroacetate is unity. (3) The activity coefficients of all univalent ions, not only in a given solution, but in all solutions of the same ionic strength, are equal. (4) $AgNO_3$ and $NaNO_3$ are assumed to be completely ionized in the solvents we have used.

On the basis of assumption 1, the electromotive force of any of our cells is given by the equation

$$E = \frac{RT}{F} \ln \frac{a'}{a}$$

where a' and a are the activities of silver ion in the nitrate and acetate (or chloroacetate) solutions, respectively. Moreover, since the two half-cells are prepared so as to have equal ionic strengths, it follows from assumptions 3 and 4 that the expression for the electromotive force of any cell may be written

$$E = \frac{RT}{F} \ln \frac{c_1'}{c_{Ag^+}} \qquad (1)$$

where c_1' is the concentration of $AgNO_3$ and c_{Ag^+} is the concentration of Ag^+ in the other half-cell.

The equilibria that are of chief interest are indicated in the following scheme, with the corresponding equilibrium constants

I $AgA\text{(dissolved)} \rightleftarrows Ag^+ + A^-$; K_i
II $AgA_2^- \rightleftarrows Ag^+ + 2A^-$; K_2
III $AgA\text{(solid)} \rightleftarrows Ag^+ + A^-$; K_1

In our solutions the concentration of Ag_2A^+ is negligibly small. Let C_s and C_a be the total (analytical) concentrations of silver and acetate in a given solution. Then

$$C_s = C_{Ag^+} + C_{AgA} + C_{AgA_2^-} \qquad (2)$$

$$C_a = C_{A^-} + C_{AgA} + 2C_{AgA_2^-} \qquad (3)$$

From (2) and (3), we find

$$C_{A^-} = C_a - C_s + C_{Ag^+} - C_{AgA_2^-} \qquad (4)$$

Since $C_{AgA_2^-}$ is usually less than 1% of C_{A^-}, it follows that $C_{AgA_2^-}$ can be neglected in calculating C_{A^-} from equations (4) and (1).

Equation (2) can be easily transformed into

$$\frac{1}{K'} = \frac{C_s - C_{Ag^+}}{\gamma^2 C_{Ag^+} C_{A^-}} = \frac{1}{K_i} + \frac{C_{A^-}}{K_2} \qquad (5)$$

an equation which defines the quantity K' (see also Leden).[13] Equation (5) predicts that on plotting $1/K'$ against C_{A^-}, one should obtain a straight line with an intercept equal to $1/K_i$ on the $C_{A^-} = 0$ axis and with a slope equal to $1/K_2$.

Previous work on solubility had shown that the experimental data could be satisfactorily reproduced by a Debye equation of the form

$$\log \gamma^2 = -\frac{2BS^{1/2}}{1 + AS^{1/2}} \qquad (6)$$

where S is the ionic strength, B is equal to $354.37/D^{3/2}$ at 25° and A is equal to $2.912 \times 10^8 \times$ ("average ionic diameter")$/D^{1/2} \simeq 1.00$.

Using $A = 1.00$, equation (6) was applied to each set of solutions used in the earlier solubility measurements, to calculate the values of γ. An approximate value of K_i was employed to correct for the incomplete ionization of the silver acetate. The results so obtained were used in equation (5) to get a set of K_i and K_2 values. These new values of K_i and K_2 were then used to find a more satisfactory value of A. If this value of A differed by 0.10 or more from unity, it was used in equation (6) to get better values of γ which led to a new set of K_i and K_2 by means of equation (5). Figures 1 to 4 show the result of plotting $1/K'$ against C_{A^-}. Finally for each set of solutions, the best values of K_i and K_2 were obtained by the method of least squares. The results obtained are summarized in Table II in which we have included the constants

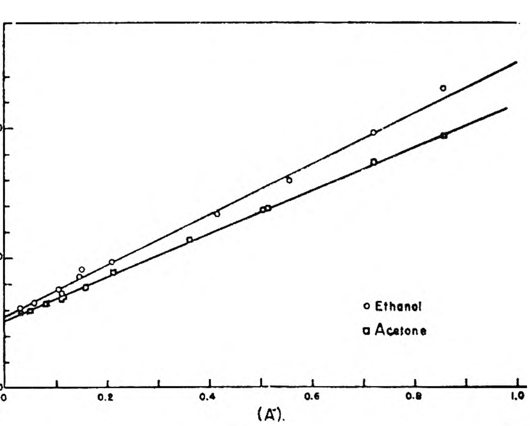

Fig. 1.—The function $1/k'$ *versus* concentration of A^- for silver acetate in 10% ethanol-water and 10% acetone-water mixtures.

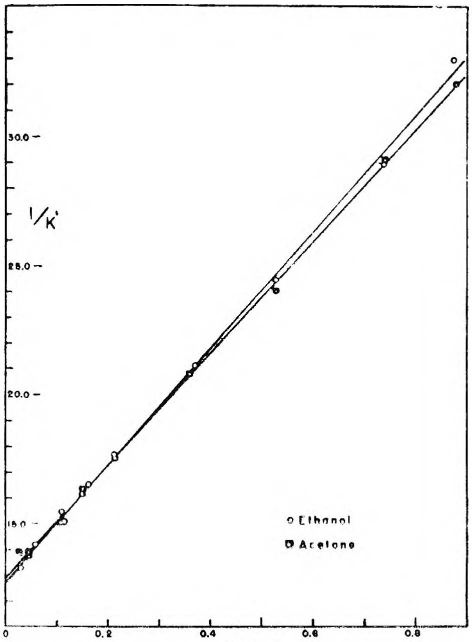

Fig. 2.—The function $1/k'$ *versus* concentration of A^- for silver acetate in 20% ethanol-water and 20% acetone-water mixtures.

---

[13] I. Leden, *Svensk Kem. Tid.*, **58**, 129 (1946).

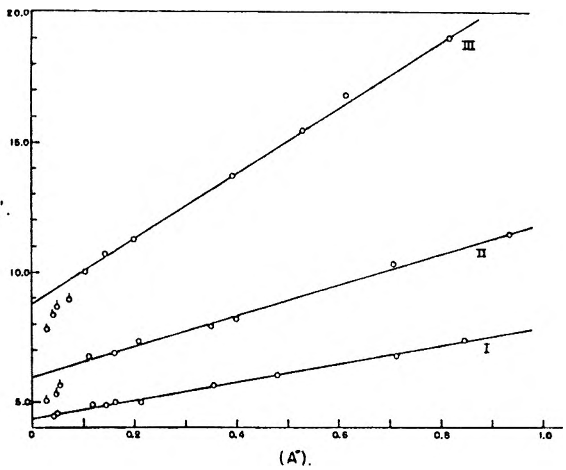

Fig. 3.—The function $1/k'$ *versus* concentration of A^- for silver monochloroacetate in water (I), 10% (II) and 20% (III) ethanol–water mixtures.

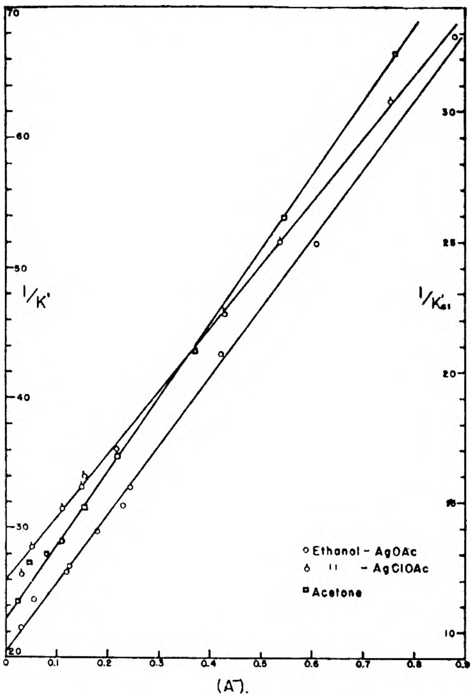

Fig. 4.—The function $1/k'$ *versus* concentration of A^- for silver acetate and chloroacetate in 30% ethanol–water and for silver acetate in 30% acetone–water.

obtained by MacDougall and Peterson[6] in their study of aqueous solutions of silver acetate. It should be remarked that during the computations it became clear that the listed values of K_2 are subject to greater uncertainties than are the listed K_i values.

Activity Product of Silver Acetate and Silver Chloroacetate.—We have used the values of the dissociation constants of AgA and AgA_2^- to correct values of $K_i = a_{Ag^+} \times a_{A^-} = \gamma^2 C_{Ag^+} C_{A^-}$ obtained previously from solubility measurements in various solvents on the assumption that silver acetate and silver chloroacetate were completely ionized. The necessary calculations are tedious but not difficult and will not be reproduced here. We give in Table III the final results.

Table II

Equilibrium Constants

Solvent	D	A	K_i	K_2
Silver Acetate at 25°				
Water	78.54	1.00	0.186	0.230
9.25% ethanol	73.24	1.00	0.130	0.100
19.97% ethanol	67.01	0.90	.0786	.0443
29.93% ethanol	61.09	0.85	.0488	.0190
9.95% acetone	73.05	1.10	0.132	0.119
20.10% acetone	66.92	1.00	.0775	.0461
30.11% acetone	60.97	1.00	.0436	.0177
Silver Monochloroacetate at 25°				
Water	78.54	1.00	0.229	0.292
9.23% ethanol	73.24	1.00	.168	.170
21.81% ethanol	65.89	1.00	.114	.0786
31.23% ethanol	60.29	1.00	.0833	.0415

Table III

Activity Product Constant K_i

Solvent	D	A	$K_i \times 10^4$ mole²liter⁻²
Silver Acetate			
Water	78.54	1.00	19.5
9.17% ethanol	73.27	1.00	10.9
20.37% ethanol	66.78	0.90	4.97
30.02% ethanol	61.04	0.85	2.41
10.35% acetone	72.80	1.10	10.1
20.50% acetone	66.70	1.00	4.36
28.25% acetone	62.11	0.95	1.96
Silver Monochloroacetate			
Water	78.54	0.95	25.9

Comparison with Work of Other Investigators.—P. B. Davies and C. B. Monk have recently published[14] a report on the dissociation of silver acetate in water and in mixed solvents. Their experimental work consisted in the measurement of the solubility of silver bromate in various solvents in the presence of sodium acetate and a small amount of acetic acid. They assumed for aqueous solutions a value of 0.5 for the dissociation constant of silver bromate from analogy with that obtained (0.6) by Monk for silver perchlorate. They used 3.8 as the dissociation constant for sodium bromate. Apparently sodium acetate was assumed to be completely ionized. For other solvents, these dissociation constants were assumed to change from solvent to solvent in the same way as the dissociation constant of silver acetate. It may be added that Davies and Monk did not take into account the formation of the complex ion AgA_2^-.

In Table IV we give a comparison of our results for K_i with those obtained by Davies and Monk for comparable solutions. In the case of one acetone-water mixture, Davies and Monk seem to have made an error in either the percentage composition or the dielectric constant. For the mixture which they state to be 26.1% acetone they give a dielectric constant of 60.5, which, according to Åkerlof's results, would be the value for a mixture of slightly more than 30% acetone. We have therefore compared their value of K_i for this mix-

---

(14) P. B. Davis and C. B. Monk, *J. Chem. Soc.*, 2718 (1951).

ture with the one we obtained for a 30.11% solution.

TABLE IV

DISSOCIATION CONSTANT, K_i, OF SILVER ACETATE AT 25°

Solvent	This work	Davies and Monk
Water	0.186	0.235
29.93% ethanol	.0488	.053
20.1% acetone	.0775	.092
30.11% acetone	.0436	.053 (26.1%?)

In view of the uncertainties in the calculated values of K_i, the agreement between the two sets of values is fairly satisfactory. It is seen that the values obtained by Davies and Monk are from 10 to 20% higher than ours.

Equilibrium Constants and Dielectric Constant.—The theory of Born[15] in its simplest form leads to the following relation between the equilibrium constant, K, of a reaction, and the dielectric constant D of the medium at 25°

$$\log K = \text{constant} - \frac{121.6}{D} \Sigma \frac{\nu_i z_i^2}{r_i} \tag{7}$$

where ν_i is the coefficient of a substance in the chemical equation, taken as negative or positive according as the corresponding substance is on the left or the right hand side of the equation as it is usually written, $z_i\epsilon$ is the electric charge on the molecule (or ion) and r_i is its radius. On plotting the logarithms of the various equilibrium constants, K_i, K_2 and K_1, against $1/D$, it is found that the points lie pretty satisfactorily on straight lines that are given by the analytical expressions in the following section.

Mixtures containing silver acetate

$$\log K_i = 1.448 - 171.1/D \tag{8}$$
$$\log K_2 = 3.25 - 307/D \tag{9}$$
$$\log K_1 = 0.652 - 264/D \text{ (water-ethanol)} \tag{10}$$
$$\log K_1 = 1.02 - 293/D \text{ (water-acetone)} \tag{11}$$

Mixtures containing silver chloroacetate

$$\log K_i = 0.791 - 113.6/D \tag{12}$$
$$\log K_2 = 2.24 - 219/D \tag{13}$$

If we define a mean radius, $\bar{r}$, for the two ions, Ag^+ and A^-, by means of the relation

$$\frac{2}{\bar{r}} = \frac{1}{r_{Ag^+}} + \frac{1}{r_{A^+}} \tag{14}$$

we find on comparing equations 8, 10 and 11 with 7, for silver and acetate ions

$$\bar{r} = 1.43 \text{ Å. from equation 8}$$
$$= 0.93 \text{ Å. from equation 10}$$
$$= 0.83 \text{ Å. from equation 11}$$

Similarly on comparing equations 12 and 7, we find, for silver and chloroacetate ions

$$\bar{r} = 2.14 \text{ Å. from equation (12)}$$

From equations 7, 9 and 13, we obtain

$$\frac{1}{r_{Ag^+}} + \frac{2}{r_{A^-}} - \frac{1}{r_{AgA_2^-}} = 2.52 \text{ (A = acetate radical)},$$
$$= 1.80 \text{ (A = chloroacetate radical)}.$$

Two remarks may be made about these calculated radii: First, they are of a reasonable order of magnitude. Second, the fact that the solubility product data give smaller values than are obtained from the dissociation constants is something that has been previously observed.[4]

---

[15] M. Born, *Z. Physik*, **1**, 45 (1920).

D-FRUCTOSE-WATER PHASE DIAGRAM

By FRANK E. YOUNG, FRANCIS T. JONES AND HAROLD J. LEWIS

Western Regional Research Laboratory,[1] *Albany, California*

Received April 19, 1952

The D-fructose-water system has been studied between −30 and +40°. Well defined crystalline phases studied include anhydrous D-fructose, stable above +21.4°; D-fructose hemihydrate, stable between +21.4 and +19.9°; D-fructose dihydrate, stable below +19.9°; and ice. In addition, solubility data are given for a crystalline phase, found during this investigation, which appears to be a metastable form of D-fructose dihydrate. A D-fructose gel, also discovered during this investigation, is described and the approximate range of solution concentrations in which it can exist has been determined between −20 and +10°.

Despite the widespread occurrence of D-fructose (levulose) in honey (in which it is the major constituent[2]) and in fruit and invert sugar, very little is known about phase relationships in the D-fructose-water system. Previous work on this system appears to be confined to approximate measurements of the solubility of anhydrous D-fructose at three temperatures[3] and to several measurements of the freezing points of dilute D-fructose solutions.[4] No previous measurements of the solubility of D-fructose hemihydrate appear to have been made at any temperature, although it was first reported in 1888.[5]

This paper reports measurements of the freezing points of D-fructose solutions and the solubilities of anhydrous D-fructose, D-fructose hemihydrate and D-fructose dihydrate. The discovery of a gel which forms in concentrated D-fructose solutions at low temperatures is also reported. These measurements were made as part of the investigation being carried out at this Laboratory of phase equilibria

---

[1] Bureau of Agricultural and Industrial Chemistry, Agricultural Research Administration, U. S. Department of Agriculture. Presented at American Chemical Society meeting, March 30–April 3, 1952, Milwaukee, Wisconsin. Article not copyrighted.

[2] R. F. Jackson and C. G. Silsbee, *Natl. Bur. Standards Technologic Papers*, **18**, 295 (1924) (No. 259).

[3] R. F. Jackson, C. G. Silsbee and M. J. Proffitt, *Natl. Bur. Standards Scientific Papers*, **20**, 587 (1926) (No. 519).

[4] H. C. Jones and F. H. Getman, *Am. Chem. J.*, **32**, 308 (1904); E. H. Loomis, *Z. physik. Chem.*, **37**, 414 (1901); R. A. Abegg, *ibid.*, **15**, 222 (1894).

[5] M. Hönig and L. Jesser, *Monatsh.*, **9**, 563 (1888).

of basic importance in the freezing preservation of foods. The preparation and properties of D-fructose hemihydrate[6] and D-fructose dihydrate[7] have recently been described.

Experimental

Solubility measurements were made on solutions prepared from distilled water and D-fructose (levulose) which contained less than 0.05% ash, less than 0.1% moisture and gave $[\alpha]_D^{20}$ −92.15°. (Isbell and Pigman[8] gave −92.4° for pure D-fructose under the same conditions.) The solubilities measured were not changed by increasing the ratio of solid phase to solution, which indicates that any impurities present did not affect the results. After the discovery of D-fructose dihydrate[7] most measurements were made on solutions of D-fructose dihydrate which had been purified by crystallization from aqueous solutions of anhydrous D-fructose. These measurements were in good agreement with those made on solutions prepared from the anhydrous material.

Solubilities of the crystalline phases (with a few exceptions discussed later) were measured refractometrically on solutions which had been allowed to come to equilibrium in a constant-temperature bath controlled to ±0.03°. Ample time was allowed for thermal mutarotation before the refractive index of a solution was measured. Refractive indices were converted to D-fructose concentrations by the table of Jackson and Mathews.[9] Solubilities determined with solutions which were initially oversaturated agreed within ±0.1% with those found for initially undersaturated solutions. Bath temperatures were measured on thermometers which had been certified recently by the National Bureau of Standards. The results obtained by warming curves were found to be unreliable because of the slow approach to equilibrium encountered with all of the solid phases in this system.

The behavior of the gel made it necessary to determine its apparent solubility in a different way. This was done by tumbling a D-fructose solution containing a small lump of gel in a bath, the temperature of which was raised about 1/2° each day until the highest temperature was found at which the gel was still visible. The solution was analyzed refractometrically.

Results and Discussion

The data obtained in this investigation are shown in the phase diagram (Fig. 1). The concentrations of D-fructose solutions at equilibrium with the various solid phases given in Table I were read from this diagram. Because it was possible to follow several of the curves into the regions where the corresponding solid phases were metastable, solid lines have been used for all well-defined curves in both stable and metastable regions. Broken lines represent portions of the curves which are less certain because of difficulties in making measurements or in reaching equilibrium.

Equilibrium between solid and solution was reached slowly and difficulties were sometimes encountered in obtaining equilibrium between the solution and a metastable phase before a more stable phase appeared. This was true to some extent of all solid phases in this investigation.

TABLE I

Temp., °C.	Concn., Wt. %	Temp., °C.	Concn., Wt. %
(a) Ice		(b) D-Fructose dihydrate	
0.0	0.0	21.3[b]	83.3
− 1.3	10.0	20.0	79.7
− 2.7	20.0	15.0	71.1
− 4.75	30.0	10.0	64.9
− 7.65	40.0	+ 5.0	59.1
−12.3	50.0	0.0	54.05
−19.35	60.0	− 5.0	49.1
−30.4	69.2	− 9.7[a]	44.7
(c) D-Fructose hemihydrate		(d) Anhydrous D-fructose	
27.9	82.05	39.4	84.3
20.0	79.4	30.0	81.9
10.0	75.95	20.0	79.4
0.0	72.55	10.0	77.0
−10.35	69.05	0.0	74.7
		− 3.85	73.7
(e) Gel		(f) Metastable crystalline phase	
+10	78	16.3	73.6
5	74.5	+15.0	71.85
0	72	10.0	65.6
− 5	69	5.0	59.85
−10	67	0.0	54.8
−15	65	− 5.0	49.85
−20	62.5	− 7.35	47.55

[a] Eutectic of ice and D-fructose dihydrate. [b] Melting point of D-fructose dihydrate.

Ice.—Points on the ice curve AE (Fig. 1) and in Table Ia were obtained without difficulty although D-fructose dihydrate crystallized spontaneously during several of the measurements below −15°, and the gel appeared once during measurements at −20.4°. In contrast to the behavior observed in the sucrose–water system,[10] ice was surprisingly slow in coming to equilibrium; consequently neither heating nor cooling curves could be used in the determination of the ice line.

The point on the ice curve at −30.4° was obtained by allowing a solution from which ice had crystallized at −40° to stand at −30.4° for several days. During this time, most of the ice melted leaving a few well defined flakes of ice scattered through the solution. Analysis showed that the solution contained 69.2% D-fructose. This value is evidently close to the equilibrium concentration for ice at −30.4°, as the concentration decreased only to 69.1%, when all ice was melted.

Anhydrous D-Fructose.—The solubilities for anhydrous D-fructose (Table Id and curve EH, Fig. 1) obtained in this investigation are in good agreement with the approximate results of Jackson, Silsbee and Proffitt.[3] Their work, however, was not carried below +20°. As the temperature is lowered below 20°, the tendency for anhydrous D-fructose to change into the hemihydrate increases. For this reason we were unable to obtain the anhydrous D-fructose–ice eutectic or to extend the solubility curve of the anhydrous solid below −3.9°.

D-Fructose Hemihydrate.—The solubilities of D-fructose hemihydrate at various temperatures are given in Table Ic and curve DJ (Fig. 1). Although this curve indicates that D-fructose hemihydrate is the stable phase only in the range from +19.9 to +21.4°, its transformation to anhydrous D-fructose is quite slow in the vicinity of room temperature

---

(6) F. E. Young, F. T. Jones and D. R. Black, *J. Am. Chem. Soc.*, **74**, 5798 (1952).

(7) F. E. Young, F. T. Jones and H. J. Lewis, *J. Phys. Chem.*, **56**, 738 (1952).

(8) H. S. Isbell and W. W. Pigman, *J. Research Natl. Bur. Standards*, **20**, 773 (1938) (RP 1104).

(9) R. F. Jackson and J. A. Mathews, *ibid.*, **8**, 412 (1932) (RP 426).

(10) F. E. Young and F. T. Jones, THIS JOURNAL, **53**, 1334 (1949).

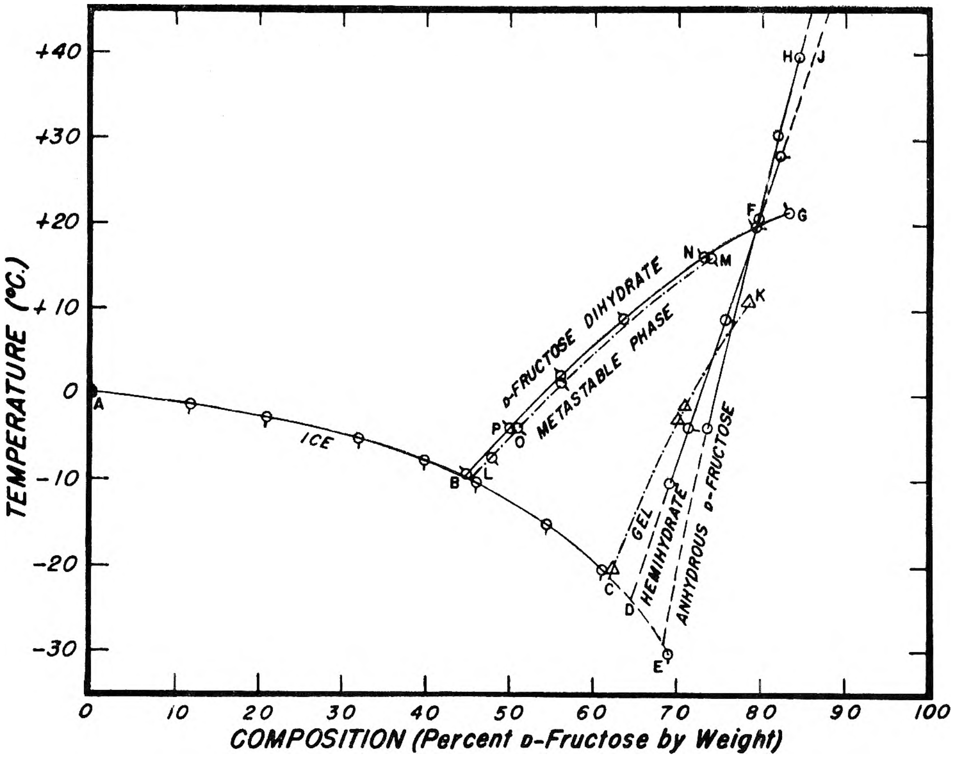

Fig. 1.—D-Fructose–water phase diagram: ♀, ice; ○, anhydrous D-fructose; ○-, D-fructose hemihydrate; ბ, D-fructose dihydrate; ᑫ, metastable phase; Δ, gel.

(up to about +27°), and it frequently has formed spontaneously at +24 to 26° in concentrated solutions such as the solution formed by melting D-fructose dihydrate (83.3% fructose). In some cases, it has formed under these conditions even in solutions seeded with anhydrous D-fructose.

Below +19.9°, D-fructose hemihydrate will usually change to the dihydrate if it is crushed or vigorously stirred in a saturated solution. Once the transformation has been initiated it proceeds rapidly. In some cases, it has been essentially complete in one hour.

D-Fructose Dihydrate.—As shown by curve BG (Fig. 1) and Table Ib, D-fructose dihydrate is the stable phase below +19.9° and 79.4% D-fructose. As compared with the solubility of anhydrous D-fructose, the solubility of D-fructose dihydrate decreases much more rapidly with decreasing temperature and is much lower at −9.7° (the D-fructose dihydrate–ice eutectic temperature). These properties suggest that D-fructose may advantageously be purified by crystallization as D-fructose dihydrate instead of anhydrous D-fructose. The ease and rapidity with which the dihydrate may be crystallized and the greater fluidity of the more dilute mother liquor at −9.7° are further advantages. Preliminary experiments indicate that this method of purification of D-fructose is feasible.

If a solution of D-fructose containing less than 44.7% D-fructose is stored a few degrees below the dihydrate–ice eutectic temperature (−9.7°), ice will crystallize and float at the surface, thereby raising the concentration to approximately that given by the ice curve (AE, Fig. 1) for the temperature used. As may be seen from the phase diagram (Fig. 1), the resulting solution is oversaturated with respect to D-fructose dihydrate. Crystallization of the latter usually requires seeding and when crystals form, they settle to the bottom of the bottle. Since ice crystallizes more rapidly than the dihydrate, the solution remains oversaturated with the dihydrate. As a result, the two layers continue to grow until they are almost in contact. This behavior makes it possible to recover D-fructose from solutions containing as little as 10–15% D-fructose without the risk of decomposition which may occur during evaporation at higher temperatures.

Occasionally large, opaque, prismatic aggregates (apparently coarsely crystallized D-fructose dihydrate–ice eutectic) form in the ice layer. If the ice layer is carefully melted, the dihydrate crystals held in the aggregates are released and fall to the dihydrate layer. As these opaque aggregates usually form only on long standing after considerable ice has crystallized, they may largely be avoided by straining the ice out from time to time.

Below about −18°, a fine-grained D-fructose dihydrate–ice eutectic forms rapidly and a clean separation into two layers is not easily obtained.

The melting point of D-fructose dihydrate (G, Fig. 1), +21.3°, was determined in a thermostatically regulated bath with ample time for attainment of mutarotatory equilibrium.[7]

Metastable Crystalline Phase (Curve LM, Fig. 1).—The first solubilities obtained by measurements at −3.9° (from undersaturation only) and at +16.3° (from both under and oversaturation) fell on curve LM (at points O and M). After several days at M, the concentration of the initially undersaturated solution at +16.3° dropped suddenly to point N on curve BG. The concentration of the corresponding initially oversaturated sample, however, remained at M for three weeks. When it was seeded with crystals from the solution at N, its concentration dropped suddenly to N. The original crystals, with which points O and M were obtained, apparently changed in storage at +1° because all subsequent measurements in which they were used as the solid phase gave solubilities on curve BG. Later, solubilities on curve

LM at +1.4 and −7.4° were obtained when crystals which had formed spontaneously from hemihydrate during storage at +1° were used. It is not likely that curve LM was caused by impurities, because the solubility of the stable phase at −3.9° was not affected by the amount of excess solid phase. No differences were observed microscopically in the crystals giving the two curves, and all analyses gave values close to theoretical for the dihydrate. Although more work is necessary to establish the identity of this phase, its behavior and close similarity to fructose dihydrate suggest that it is a metastable polymorph of the dihydrate. Solubilities of this phase taken from curve LM (Fig. 1) are given in Table If.

Gel.—An unusual feature of this system is the D-fructose gel which was discovered during measurements of the solubility of D-fructose hemihydrate. This gel is colorless, transparent, and slightly elastic, and shows no tendency toward stickiness or viscous flow. Birefringence varies from faint in some samples to strong in others and also varies from region to region in a given sample. On long aging below 0°, the gel becomes increasingly milky with a bluish tint (by reflected light), again with variations from one region to another. The initially rigid gel appears to become more rigid with aging, but this has not been confirmed by quantitative measurements.

This gel has formed spontaneously in solutions ranging from 63% and higher D-fructose concentration at −20° to 70% and higher at −3°. It has also grown at higher temperatures in solutions on the right of the gel line CK (Fig. 1) which were "seeded" with a small lump of gel. Solutions which were highly "supersaturated" have gelled completely after they were seeded. In solutions which were less "supersaturated," lumps of gel have grown larger without causing gelation of the entire solution.

The gel is probably most easily obtained by slowly tumbling a solution containing over 68% D-fructose at about −20°. In about three days of continued tumbling, the entire solution will usually gel. Agitation appears to be necessary for gelation to occur. No gel has formed in unagitated, unseeded D-fructose solutions stored at −23° for more than a year. The previous history of the solution does not appear to affect its gelling behavior; gelation does not appear to take place in the solution obtained by melting a gel at a temperature slightly above the gel curve (CK, Fig. 1) any more readily than in freshly prepared solutions. In "seeded" agitated solutions, gelation may take place in 24 hours or less. Impurities in the fructose also appear to have no effect. Gelation has taken place equally readily in solutions in which these impurities were concentrated and in highly purified solutions.

The gel curve (CK in Fig. 1) indicates that the gel should change to hemihydrate above about +2°. This transformation took place so readily above about +10° that it was difficult to make measurements at higher temperatures. Below +2° the reverse change, hemihydrate to gel, which would be expected, has not been observed even with both phases in contact. Instead, the gel has changed to hemihydrate occasionally even at −23°. This change occurred more frequently when the gel was cut or otherwise disturbed.

At lower temperatures, particularly below −10°, the gel has occasionally formed in solutions containing the hemihydrate. In such cases, the gel appeared to form independently of the hemihydrate, and not as a result of transformation from the hemihydrate.

Attempts to determine points on the gel curve (CK, Fig. 1) by the method used for crystalline phases in this investigation gave variable and usually unreproducible results. One difficulty was the extremely long time required for the gel to reach equilibrium. In addition, when a lump of gel in an undersaturated solution was cut into smaller pieces to accelerate the approach to equilibrium, the solution concentration sometimes suddenly increased to $^1/_2$ to 1% above the value which had been obtained from the oversaturated side, and the concentration continued to rise slowly for several weeks. Because of this behavior, curve CK and the data in Table Ie must obviously be regarded only as a useful approximation of the limits of gel existence.

Acknowledgments.—The authors wish to thank Dr. Fred Stitt for suggestions and criticisms.

ALBANY, CALIFORNIA

HOT ATOM CHEMISTRY. PHOTONUCLEAR PREPARATION OF COBALT-58, COBALT-58m[1]

BY DARLEANE CHRISTIAN HOFFMAN AND DON S. MARTIN, JR.

Iowa State College, Ames, Iowa

Received April 21, 1952

Samples of $K_3[Co(C_2O_4)_3]\cdot 3H_2O$ were irradiated in the X-ray beam of the 68-Mev. synchrotron. The Szilard–Chalmers process appeared to be nearly 100% effective in ejecting the radioactive cobalt atoms from the complex. The 9.2 hr. Co^{58m} and 72 d Co^{58} formed during the irradiation were separated from the complex in high specific activity by adsorption on IRC-50 cation exchange resin. The total saturation yield for Co^{58} and Co^{58m} was found to be 8.6 relative to C^{11}. A solution of the complex was prepared from the active cobalt separated by adsorption on the resin. A method utilizing the chemical decomposition of the complex, occurring in the isomeric transition of Co^{58m} to Co^{58} by the emission of conversion electrons, was employed to calculate the ratio of the rates of formation of the two isomers. The ratio of the photonuclear rate of formation of Co^{58} to that of Co^{58m} was found to be 0.61 ± 0.04.

Introduction

The Szilard–Chalmers reaction has been used extensively to obtain high specific activities of isotopes produced in neutron bombardments. A review of this field has been given by Barnes, Burgus and Miskel.[1b] A similar process can be used to obtain high specific activities from photonuclear reactions if appropriate complexes are irradiated with high energy X-rays. In order to produce a high specific activity of Co^{58} and Co^{58m}, the complex compound $K_3[Co(C_2O_4)_3]\cdot 3H_2O$ was irradiated in the 70 Mev. X-ray beam of the Iowa State College synchrotron. This complex was chosen for several reasons. First, it is one of the complexes whose optical isomers have been resolved. Therefore, the central cobalt atom would not be expected to undergo exchange with other cobalt species. Second, the target cobalt is in an anion. The active atoms, which are ejected from the complex and will be expected to exist finally as Co^{++} in aqueous solution, can be separated from the target by the adsorption on a cation exchange resin. Such a separation is efficient, rapid and should not necessitate the addition of inactive cobalt carrier. Third, the preparation of this complex is simple and rapid. Retention of activity in oxalato complexes has not been investigated for neutron bombardments. However very high recoil energies are involved in photonuclear processes, and retention was found to be negligible within the limits of experimental error in the following experiments with this complex.

Strauch[2] originally identified Co^{58m}. He observed the emission of 17 and 24 kev. conversion electrons for a 24.9 ± 1.0 kev. γ-ray with an 8.8 hr/half-life to form the well established 72 d Co^{58}. The K to L conversion coefficient ratio was found to be 1.9 ± 0.2. He also determined the rate of formation of Co^{58m} relative to that of Co^{58} to be 1.7 when manganese is bombarded with α-particles. This calculation was based on data obtained by observation of the growth of the continuous positron spectrum of the 72 d activity. The 8.8 hr activity was also found in cobalt fractions from nickel and cobalt bombarded with 18 Mev. deuterons and fast neutrons, and from deuterons on copper. The identity of the Co^{58m} is therefore well established. It is of interest to determine if similar yield ratios of isomers are obtained in photonuclear reactions since agreement would imply the formation of similar excited nuclei. The method used by Strauch could not be applied because of low intensities. Indeed, characterization of the activities for the photonuclear reactions would have been impracticable without the application of "hot atom" techniques to give enriched samples.

In this investigation the nuclear isomers of Co^{58} have been separated and their relative rates of formation from the photonuclear process in Co^{59} were calculated. The rate of formation of Co^{58m} relative to that of Co^{58} was based on the principle that decay of Co^{58m} to Co^{58} by the emission of conversion electrons would cause dissociation of the trioxalato complex in which Co^{58m} was originally present. Therefore, the complex ion, $[Co(C_2O_4)_3]^{\equiv}$, was prepared in solution from activity separated by the original Szilard–Chalmers process. After a period of time the activity present as cobalt(II) was separated from the complex and the amount of the activity in the complex and in the separated cobalt(II) was determined. From these data it was possible to calculate the relative rates of formation of the two isomers.

The ratio of the rate of formation of Co^{58m} to that of C^{11} was determined by comparison of the absolute disintegration rate of Co^{58m} with that of the C^{11} formed in a portion of the complex during the same irradiation by (γ,n) reactions on the oxalate carbon.

Experimental

Ion Exchange Resin Separation.—Amberlite IRC-50 cation exchange resin manufactured by the Rohm and Haas Company was used in the separation of the cobalt(II) activity from the irradiated cobalt complex. The effectiveness of the resin separation was determined by performing tracer experiments using Co^{60}. Co^{60} activity in the form of cobalt(II) chloride containing very little carrier was added to solutions containing 0.5 g. of complex per 20 ml. of water. To these, 0.25 g. of IRC-50 cation exchange resin in the potassium form was added for each 20 ml. of solution. Samples were taken before and after shaking the solution with the resin for varying periods of time. It was found that after 15 minutes only 2–3% additional activity could be removed from the solutions by extended treatment with resin. Therefore, in all separations the resin in the potassium form was shaken with the solutions for the standard period of 15 minutes. For a solution originally in the pH range 3.1 to 5.8, the resin separation was accompanied

---

[1] Contribution No. 201 from the Institute for Atomic Research and Department of Chemistry, Iowa State College, Ames, Iowa. Work performed in the Ames Laboratory of the Atomic Energy Commission.

[1b] J. W. Barnes, W. H. Burgus and J. A. Miskel, "Radioactivity Applied to Chemistry," A. C. Wahl and N. A. Bonner, Editors, John Wiley and Sons, Inc., New York, N. Y., 1951, p. 244.

[2] K. Strauch, *Phys. Rev.*, **79**, 487 (1950).

by a pH change to a value of 6.5–9.5. In seven experiments, a separation of 96.4 ± 1.7% was obtained. In case the final pH values exceeded 9.5, decomposition of the complex was observed and the separation efficiency decreased. This decrease in separation efficiency may be due to the formation of a precipitate of cobalt(III) hydroxide which either carries or exchanges with the active cobalt(II). At final pH values below 6.5, the capacity of the resin was low due to reversion of the resin to the hydrogen form. The presence of ammonia also reduced the efficiency of the separation.

These experiments also indicate that little exchange can occur between cobalt(II) and the trioxalatocobaltate(III). In some cases the solutions were allowed to stand for 19 hr. in the dark at 25° at a pH of 3.5–4.5. At the end of this period 98% of the activity was separated by the cation exchange resin indicating negligible exchange had occurred in this period. Decomposition of the complex occurs on long standing at pH values above 6. Similar experiments in which the solutions remained for 19 hr. at pH of 6–7 gave separations of 80–82%.

It was found that quantitative removal of the cobalt(II) activity on the resin could be accomplished in a few minutes by heating the resin with two 10-ml. portions of 6 N HCl.

Electrodeposition.—Cobalt counting samples were prepared by electroplating the cobalt activity on platinum discs 2.5 cm. in diameter. A micro-electrodeposition cell manufactured by Tracerlab, Inc., was used with a rotating anode. The completeness of the deposition was tested using Co^{60} as tracer. It was found that at least 99% of the Co^{60} activity, in solutions with a volume of 5–10 ml. and containing 0.5–3.0 mg. of cobalt carrier, was deposited in 15 minutes with a current of about 1.5 amperes. The solution of $CoCl_2$ was made approximately 15 M in ammonia, and 0.3–0.4 g. of NH_4Cl and 0.2–0.3 g. of hydrazine dihydrochloride were added. (The hydrazine dihydrochloride prevented formation of cobalt(III).)

In the first experiments a rotating platinum anode was used. However, in blank runs a serious increase in sample weight of about 0.2 mg. was noted. Brophy[3] has reported similar high results using platinum anodes and attributed the weight increase to deposition on the cathode of platinum which had been dissolved from the anode by the action of chlorine evolved during the electrolysis. Our results verified this since when graphite anodes were used, no increase in weight was observed in the blank runs. Graphite electrodes $^3/_{16}$ inch in diameter, and manufactured for spectroscopic arc analyses were used as the rotating anodes.

Preparation of Complex.—The complex compound, $K_3[Co(C_2O_4)_3]\cdot 3H_2O$, was prepared by a lead dioxide oxidation of an oxalate solution of cobalt(II) according to the procedure of Bailar and Jones.[4] Solutions of the complex are unstable toward prolonged exposure to sunlight, heating or alkali. Crystals of the compound are much more stable.

To determine the relative rate of formation of Co^{58m} to that of Co^{58}, it was necessary to prepare the complex ion, $[Co(C_2O_4)_3]^{≡}$, from the cobalt activity separated by the Szilard–Chalmers process. Since 1–3% of the complex was found to decompose during the irradiations, the amount of cobalt present to be converted to the complex could be estimated. The preparation was carried out by addition of a small excess of all reagents to ensure as complete conversion as possible. Instead of crystallizing the complex compound, it was allowed to remain in solution. A resin separation was then performed to remove any cobalt(II) not converted to the complex. The conversion of Co^{II} to complex was found to be about 40%.

To test the separation efficiency under these conditions, Co^{60} as cobalt(II) was added to a solution of the complex and a resin separation was then performed. The average efficiency for five such separations was 97.5 ± 0.6%, about the same as was found previously. After the separation the pH of the solution was adjusted to 4.5 with a small amount of HCl, and the solution was stored in the dark at room temperature. About 19–20 hours later, more Co^{60} as cobalt(II) was added and another resin separation was performed. A separation of 97% was obtained which is in agreement with the other experiments.

Irradiations.—Samples to be irradiated were contained in test-tubes of 1-cm. diameter. The test-tubes were held close to the synchrotron doughnut in a plastic holder which was carefully aligned in the X-ray beam. Only one sample was irradiated at a time and all irradiations were at the maximum energy of the 70 Mev. synchrotron. The intensity of the beam was monitored by an ionization chamber and plotted by a recording milliammeter. All of the samples used for yield determinations were irradiated at a nearly constant beam intensity. For comparison of the Co^{58m} and C^{11} yields, 1–1.5-g. samples of $K_3[Co(C_2O_4)_3]\cdot 3H_2O$ crystals were irradiated for one hour. In the determination of the yield of Co^{58} relative to the yield of Co^{58m}, it was necessary to irradiate 4–5-g. samples of the complex in order to obtain sufficient activity.

Measurements.—C^{11} samples were prepared simply by spreading a weighed amount of the irradiated $K_3[Co(C_2O_4)_3]\cdot 3H_2O$ crystals evenly over a 2.5-cm. diameter circle of scotch tape mounted on cardboard. The samples were then covered with scotch tape and the decays followed for nine to ten half-lives with an end-window G–M tube. All cobalt samples were electroplated on platinum as previously described and were counted with a windowless, gas flow G–M counter manufactured by the N. Wood Co. The samples were inserted into the counter chamber to detect the very low energy electrons of the Co^{58m}. All samples were compared with a Co^{60} absolute beta standard calibrated by the coincidence method. The Co^{60} standards had been prepared by electrodeposition on platinum in the same manner as the Co^{58} samples. From the comparison of the beta counting rates of C^{11} and the standard with the appropriate corrections for absorption in counter window, air and sample covering, for self-absorption and for back-scattering,[5] the disintegration rate of C^{11} was calculated. In the windowless counter, back-scattering by platinum was found to be independent of the maximum β-ray energies in the energy range 0.07 to 1.7 Mev.[6] For the Co^{58}, Co^{58m} samples therefore only a correction for self-absorption was used.

To determine this correction, a number of the usual counting samples were prepared from different fractions of a sample of the Co^{58m} activity. These samples with different thicknesses all had the same actual specific activity in terms of disintegration rate per unit mass. The observed specific activity in terms of counting rate per unit mass for these samples was plotted as a function of sample thickness in Fig. 1. It is to be noted that such a function decreases with sample thickness but does not give a sharp break at the thickness corresponding to the range of a given electron component. However, the first very steep portion of the curve undoubtedly represents absorption of the Auger electrons associated with the cobalt K X-rays and emitted following the internal conversion process. These electrons have an energy of about 6 kev. and an estimated range of 0.07 mg./cm.^{2}. The dashed line extrapolation to zero sample and the remainder of the curve indicate the self-absorption of the 17 and 24 kev. electrons which have ranges of 0.6 and 1.1 mg./cm.^{2}, respectively. Auger electrons are, of course, emitted in coincidence with the conversion electrons. The contribution of the Auger electron component of 20–25% at zero sample thickness is consistent with the conclusion from the back-scattering experiments that thin β-emitters mounted on platinum in the windowless counters give counting rates of 75–80% of the actual disintegration rates. The comparison of counting rates with those of a Co^{60} standard using the self-absorption correction gave the disintegration rate of Co^{58m} at the time of observation.

By extrapolation of the decay curve to the end of irradiation the saturation disintegration rate or the rate of formation, R, for the synchrotron irradiation could be calculated for each radioactive isotope. The formation rates or yield ratios were calculated on an atomic basis. Therefore, the C^{11} rates of formation were divided by six before comparison with those of Co^{58m} because of the six carbon atoms for each cobalt atom in the complex.

---

[3] D. H. Brophy, *Ind. Eng. Chem., Anal. Ed.*, **3**, 363 (1931).

[4] J. C. Bailar, Jr., and E. M. Jones, "Inorganic Syntheses," Vol. I, H. S. Booth, Editor-in-Chief, McGraw-Hill Book Co., Inc., New York, N. Y., 1939, p. 37.

[5] D. W. Engelkemeir, J. A. Seiler, E. P. Steinberg and L. Winsberg, "Radiochemical Studies: The Fission Products," National Nuclear Energy Series, IV, Vol. 9, McGraw-Hill Book Co., Inc., New York, N. Y., 1951, p. 56.

[6] Darleane Christian Hoffman, Wayne W. Dunning and Don S. Martin, Jr., *Nucleonics*, **10**, No. 5, 40 (1952).

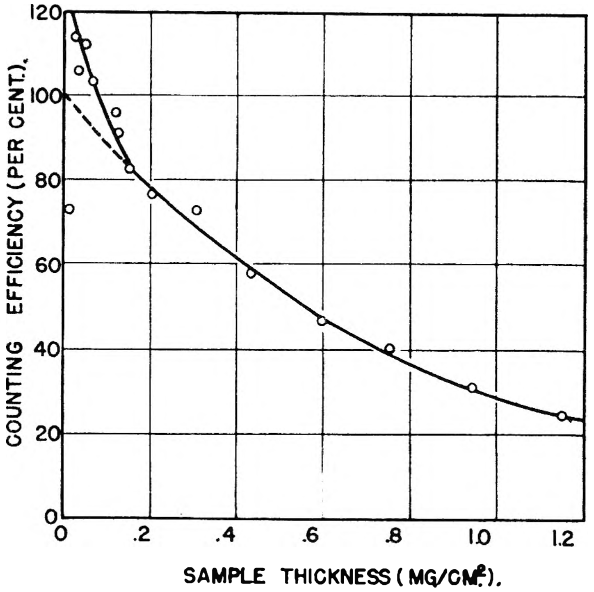

Fig. 1.—Self-absorption curve for Co^{58m} in the windowless counter. Ordinate gives counting rate per unit mass of sample expressed in terms of the efficiency of the conversion electrons using the extrapolation indicated by the dashed curve.

Calculations and Results

Activities Produced.—In the cobalt yield samples an activity with a half-life of 9.2 ± 0.2 hr (Fig. 2) was found together with a very low intensity of a longer component. By following the decay of the activity produced in a 30.1-hour irradiation, the long component showed a half-life of 72 ± 4.0 d (Fig. 3). From magnetic deflection experiments it was found to emit positrons. These two periods were attributed to Co^{58m} and Co^{58}, respectively. Apparently 270 d Co^{57} which would form by a $(\gamma,2n)$ reaction was not present in detectable amounts. A half-life of 20.5 min., in agreement with reported values, was found for the C^{11} counted as a yield standard.

The effectiveness of the Szilard–Chalmers process was tested by several experiments in which the complex was decomposed after the ion exchange resin removal of the ejected cobalt atoms. Samples of the cobalt from the complex were electroplated and the intensity of 72 d activity compared with that in the separated samples. Even with the large corrections for self absorption in the sample it was evident that not more than 3 ± 1% of the total 72 d activity had remained in the complex fraction. In view of the efficiency of the ion exchange separation, retention of activity by the complex during irradiation was below the limit of detection by these methods. Apparently, if a recoiling Co^{58}, Co^{58m} atom collides and transfers most of its kinetic energy to a Co^{59} atom, the coördination of oxalate ligands around the radioactive cobalt, necessary for retention of radioactivity as a complex anion, is not accomplished.

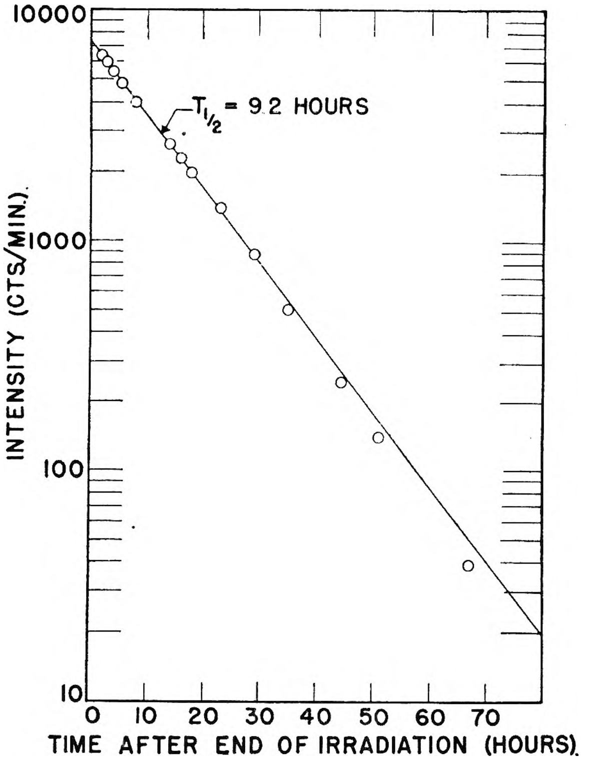

Fig. 2.—Short-lived component (Co^{58m}) formed in a 1.0 hr irradiation of Co with a 70 Mev. maximum beam energy.

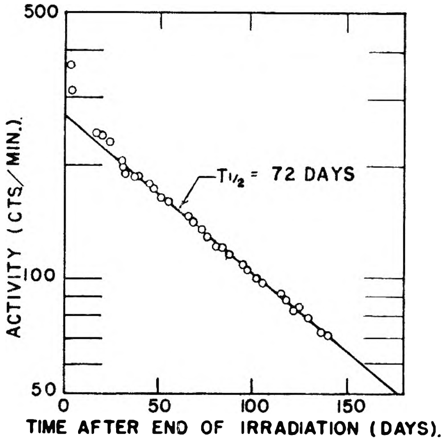

Fig. 3.—Decay curve of the activity prepared by a 30.1 hr irradiation of Co with a 70 Mev. maximum beam energy.

From the weight of cobalt in the counting samples separated from the complex, the decomposition of the complex which had occurred during the irradiation or other treatment was measurable. With the best samples this decomposition amounted to about 1% for irradiations of a few hours and was probably induced primarily by the radiation of the X-ray beam. Enrichment factors of 30–100 were commonly obtained.

Relative Rate of Formation of Co^{58} Isomers.—A direct method, in which the growth of the 72-day activity is followed, could not be utilized with the intensities available. The possibility was considered of using a thin absorber to remove the 17,24 kev. conversion electron component so the growth of positron activity might be observed. It was estimated that with reasonable irradiation times a total growth of about 50 counts/min. over an original activity of 50 counts/min. and background of 40 counts/min. could be achieved. However, the estimated cobalt K X-rays associated with the 9.2h conversion electrons would originally give a greater contribution to the counting rate, and hence the growth would be obscured.

Consequently, a chemical separation procedure was used to evaluate the relative formation of the two isomers. A solution of $[Co(C_2O_4)_3]^{=}$ was prepared from the separated Co^{58}, Co^{58m} activity and allowed to stand for a period of time. Initially, all Co^{II} was removed by the ion exchange separation. It was necessary to assume that each isomeric transition resulted in the decomposition of the complex ion so the daughter isomer would exist as Co^{II}. The Co^{II} was separated from the complex by the ion exchange procedure at the end of the standing period. A counting sample was prepared from each fraction, *i.e.*, the resin fraction or the Co^{II}, and the complex fraction or the $[Co(C_2O_4)_3]^{=}$. After the Co^{58m} had decayed to a negligible level, the counting rate in each fraction which was due to Co^{58} was determined. If the complex were chemically stable, the counting ratio would give the fraction of the Co^{58} which formed by the decay of Co^{58m} during the standing period. From this value the yield ratio can be computed. In the following treatment

Subscripts "1" and "2" refer to Co^{58m} and Co^{58}, respectively

Subscripts "r" and "c" refer to the ion exchange resin fraction and the complex fraction, respectively λ is a radioactive decay constant

T is the period of irradiation

t' is the period between the end of irradiation and the first ion exchange separation of Co^{II} (the start of the standing period)

t'' is the time interval between the initial and the final ion exchange procedures (the standing period)

N represents a number of atoms

R represents a rate of formation of radioactive atoms in a steady synchrotron irradiation

The equations which give the number of atoms of Co^{58} in each fraction are

$$N_{2r} = \frac{R_1\,(1 - e^{-\lambda_1 T})e^{-\lambda_1 t'}\,(e^{-\lambda_2 t''} - e^{-\lambda_1 t''})}{\lambda_1 - \lambda_2} \qquad (1)$$

$$N_{2c} = \left[\frac{(R_1 + R_2)\,(1 - e^{-\lambda_2 T})e^{-\lambda_2 t'}}{\lambda_2} + \frac{R_1\,(e^{-\lambda_1 T} - e^{-\lambda_2 T})e^{-\lambda_2 t'}}{(\lambda_1 - \lambda_2)} + \frac{R_1\,(1 - e^{-\lambda_1 T})(e^{-\lambda_1 t'} - e^{\lambda_2 t'})}{(\lambda_2 - \lambda_1)}\right] e^{-\lambda_2 t''} + \frac{R_1\,(1 - e^{-\lambda_1 T})e^{-\lambda_1(t'+t'')}}{\lambda_1} \qquad (2)$$

Absolute values of N_{2c} and N_{2r} were not required. The ratio N_{2c}/N_{2r} was computed from the counting rate ratio of the two fractions after the decay of Co^{58m}. From values of this ratio and the other quantities in equations (1) and (2), which are known, the yield ratio, R_2/R_1 was calculated. The results are given in Table I. The uncertainties in the ratios were based on the standard deviations due to the statistical fluctuation in the counting rates.

By counting the cobalt samples immediately after the final separation, any 9.2 hr activity present in them could be detected. The presence of 9.2 hr activity in the resin sample would be a measure of the decomposition of the complex which had occurred. A correction was made for the observed decomposition which is listed in Table I. A correction was applied in the first two cases of Table I for the incomplete removal of Co^{II} in the initial ion exchange separation (separation efficiency 97.5%). No correction was necessary in the third experiment since the ion exchange separation was repeated immediately. In each case a correction for the efficiency of the ion exchange separation at the end of the standing period was applied.

Table I

Determinations of Isomeric Yield Ratios

Irradiation time, T, hr.		t', hr.	t'', hr.	N_c/N_r (cor)	Sample thickness, mg./cm.^{2} Complex fraction	Resin fraction	Decomposition, %	Yield ratio $\frac{R_2(Co^{58})}{R_1(Co^{58m})}$
	1.0	5.65	19.03	2.46	0.17	0.34	7.3	0.72 ± 0.19
On	0.65							
Off	.13	2.93	21.47	1.35	.13	.09	12.4	.69 ± .11
On	.27							
	1.0	2.10	21.20	1.405	.52	.49	3.8	.59 ± .05

Since the critical ratio of counting rates involved the same activity, only a correction for self-absorption was needed. Self-absorption corrections were interpolated from a self-absorption curve given by Graf, Comar and Whitney[7] for the 0.26 Mev. beta of Ca^{45} counted in a windowless G-M counter. For sample thicknesses under 2 mg./cm.^{2}, the correction may be nearly independent of energy since the radiation being absorbed is probably the very soft radiation due to back-scattering. Interpolations for the corrections were necessarily approximate and may account for some of the variation in the calculated R_2/R_1 values. In the first and second experiments (Table I) the sample thicknesses were different and corrections were applied. In the third experiment no correction was necessary since the counting samples were fairly thick and within a few per cent. of equal weight.

Because of the low intensities produced by the synchrotron irradiations, the uncertainty introduced into the results by the statistical fluctuation of counting rates was large. The third determination was the most satisfactory both on a basis of intensity and of the decomposition which occurred during the standing period. The individual values were consistent with respect to their standard deviations. An average value for R_2/R_1, obtained by weighting each value in proportion to its $1/\sigma^2$, was 0.61 ± 0.04 (the rate of formation of Co^{58} to that of Co^{58m} for the (γ,n) reaction).

This value agrees within experimental error with 0.59 found by Strauch for the formation of these isomers by α-particle bombardment of manganese. In both cases the isotopes had been prepared by bombardments well above the threshold energies; accordingly, the formation of equivalent excited product nuclei would be expected which would lead to identical isomer yield ratios.

The ratio determined by our method is very sensitive to the fraction of complex ions which are decomposed by the isomeric transition of the central Co^{58m} atoms. If this decomposition were incomplete, the results would be too high. Decomposition would not be expected to result from

---

[7] W. L. Graf, C. L. Comar and I. B. Whitney, *Nucleonics*, 9, No. 4, 22 (1951).

the γ-ray photon recoil at such low energies. However, Strauch has proposed that the transition is of the type $\lambda = 4$, for which internal conversion coefficients are very high, and the photon emission is a negligible fraction. Ionization of an atom occurring in isomeric transitions is amplified by the ejection of additional Auger electrons.[8] For the isomeric transition of Br^{80} in an organic compound, it has been reported that although separation is nearly complete in the gas phase, a considerable fraction of the activity was retained by the organic fraction in experiments with condensed phases.[9,10] However, in the case of the trioxalatocobaltate(III) complex the loss of electrons accompanying the isomeric transition of the cobalt might logically lead to the oxidation of the oxalate. With loss of the ligand essential to the stability of cobalt(III), a rapid reduction to the cobalt(II) state would result in zero retention by the complex of the daughter activity.

The results of these experiments are therefore consistent with the logical conclusions that: (1) the yield ratio of the photonuclear and the heavy particle processes are identical, (2) the retention of daughter activity by the complex in the isomeric transition was negligible. The possibility is not excluded, of course, that the variation in one of the above quantities might be by coincidence exactly cancelled by a variation in the other.

Yield of Co^{58m} Relative to C^{11}.—From six yield determinations, an average value of 5.4 ± 0.7 was obtained for the rate of formation of Co^{58m} relative to that of C^{11}. The tentative value reported earlier[11] was estimated before the back-scattering and self-absorption corrections for the conversion electrons, described in this paper, were completely worked out. The yield ratio relative to C^{11} for the combined Co^{58} and Co^{58m} was then 8.6. This value can be compared with those reported by other investigators for elements in this range of atomic numbers. For the reactions $Ni^{58}(\gamma,n)$ Ni^{57} and $Cu^{63}(\gamma,n)$ Cu^{62} relative to the reaction C^{12} (γ,n) C^{11}, Perlman and Friedlander[12,13] reported values of 2.7 and 14.3, respectively.

Acknowledgments.—The authors wish to express their appreciation to Dr. L. J. Laslett, Dr. D. J. Zaffarano and their assistants for providing the synchrotron irradiations and to Richard A. Lorenz for his assistance in obtaining counting data.

---

[8] E. P. Cooper, *Phys. Rev.*, **61**, 1 (1942).

[9] D. DeVault and W. F. Libby, *J. Am. Chem. Soc.*, **63**, 3216 (1941).

[10] W. H. Hamill and J. A. Young, *J. Chem. Phys.*, **17**, 215 (1945).

[11] D. Christian and D. S. Martin, Jr., *Phys. Rev.*, **80**, 1110 (1950).

[12] M. L. Perlman and G. Friedlander, *Phys. Rev.*, **74**, 442 (1948).

[13] M. L. Perlman, *ibid.*, **75**, 988 (1949).

THE PROBABILITY FACTOR IN BIMOLECULAR REACTIONS. I. UNCOMPLICATED ION-DIPOLE SYSTEMS

BY H. KACSER*

The Queen's University, Belfast, N. Ireland

Received May 1, 1951

An equation for the "effective shape" of a polar molecule in the field of an ion is developed. By presenting regions with varying energy barriers, this shape determines the success of reactive approaches from any given direction. If the energy surface deviates appreciably from spherical symmetry there will be favored directions which make the major contribution to the reaction rate. This will be reflected in the deviation of the non-exponential factor of the Arrhenius equation from the calculated frequency factor based on collisions over the total solid angle. When applied to experimental data the treatment yields the approach distance of reacting molecules and gives information concerning the steric course of the reaction.

The introduction of the concept of the probability factor into the collision theory of bimolecular reactions, though theoretically sound, did nothing more than give a quantitative measure of the deviation from the theoretically calculated rate. The formulation of the rate equation based on statistical mechanics associates this probability with the entropy of activation but leaves matters in essentially the same state of uncertainty.

There have been a number of attempts[1–4] to relate various electrical and steric considerations to this deviation term. Except in the case of ion–ion interaction, however, it is not possible to predict the magnitude of the probability factor from the known parameters of the reacting species.

Differences in the rates of certain homologous compounds have been related[5,6] to the change in activation energy due to change in "steric hindrance." From the results it is, however, clear that a not inconsiderable part of the change in the rate is due to the temperature independent factor. The special case of a series of systems showing identical activation energies has been related[7,8] to the number of possible configurations in the activated complex. The assumption of this treatment, namely, a single direction of approach, and its neglect of electrostatic and solvent influences, restricts its usefulness considerably, but principally it is a comparative method and therefore gives no information concerning the absolute magnitude of the A factor for a single reaction.

---

* Institute of Animal Genetics, The University, Edinburgh, Scotland.

[1] Hinshelwood and Winkler, *J. Chem. Soc.*, 371 (1936).

[2] Christiansen, *Z. physik. Chem.*, **113**, 35 (1924).

[3] Scatchard, *Chem. Revs.*, **10**, 229 (1932).

[4] Moelwyn-Hughes, "Kinetics of Reactions in Solution," Oxford University Press, New York, N. Y., 1947

[5] A. G. Evans, *Trans. Faraday Soc.*, **42**, 719 (1946).

[6] Hughes and Ingold, *J. Chem. Soc.*, 173 (1946).

[7] Bauer and Magat, *J. chim. phys.*, **47**, 922 (1950).

[8] Ivanhoff and Magat, *ibid.*, **47**, 914 (1950).

The Rate Equation for Anisotropic Reactants.—The formulation of the classical rate equation based on the kinetic theory is given by

$$k = Ze^{-E/RT} \tag{1}$$

where

$$Z = \frac{N_0}{1000}r^2\left\{8\pi RT\left(\frac{1}{m_A} + \frac{1}{m_B}\right)\right\}^{1/2} \tag{2}$$

The assumption of incompressibility of reactants, implicit in the kinetic theory, may not be valid for the fraction of high energy collisions constituting the kinetic expression. The substitution of average molecular radii, $(r_A + r_B)$, for r, determined by non-kinetic methods, is therefore not justified. Instead r should represent the "approach distance" without any assumption as to what experimental value should be used or how it may be determined. But even with this modification equation (1) will be true only for molecules which are spherically symmetrical in the gross structural sense as well as isotropic from a reaction point of view, since it is only under these conditions that all approaches may be regarded as geometrically identical. If, however, we are dealing with molecules which are unsymmetrical and reactively anisotropic, insofar as interaction depends on specified groups at definite portions of the molecule, then the relative orientation of the molecules toward one another and toward the direction of approach become important. The presence of a dipole or of "bulky" groups will make approach to a certain portion of the molecule more difficult but will never prevent it completely. There will be some molecules with such high energy that approach from even the most unfavorable direction will be successful, provided no secondary reaction takes place. This is equivalent to saying that the activation energy varies with direction of approach.

$$E = \mathrm{f}(\theta,\varphi) \tag{3}$$

In some cases the polar nature of certain groups will constitute the major directional variation, in others the "van der Waals envelope" may be taken as a measure of the obstacles of approach to a specific point.

If we wish to formulate the rate equation for such a model we may proceed by defining any direction in terms of two angles θ and φ. The solid angle $d\omega$ or "sector" is

$$d\omega = \sin\theta d\theta d\varphi \tag{4}$$

If we take the number of A molecules, n_A, approaching one B molecule per sec. as Z_{A1}, then the number of "approaches" toward B per sector per sec. is

$$Z^{\omega}_{A1} = \frac{Z_{A1}d\omega}{4\pi} \tag{5}$$

If we assume the activation energy to vary with direction, then the number of "successful approaches" per sector per sec. is

$$Z^{\omega*}_{A1} = \frac{Z_{A1}\,d\omega}{4\pi}e^{-\mathrm{f}(\theta,\varphi)/RT} \tag{6}$$

For the total solid angle and the total number of approaches between A and B we obtain

$$Z^*_{AB} = \frac{Z_{AB}}{4\pi}\int_0^{\pi}\int_0^{2\pi}e^{-\mathrm{f}(\theta,\varphi)/RT}\sin\theta d\theta d\varphi \tag{7}$$

Since the activation energy is a joint property of both molecules we may consider it residing in one molecular species only. We can choose this as B which is then considered as a point whose chance of reaction depends on its speed and direction of approach toward another point A.

If the energy surface has axial symmetry $\mathrm{f}(\theta,\varphi)$ is independent of φ and equation (7) reduces to

$$Z^*_{AB} = \frac{Z_{AB}}{2}\int_0^{\pi}e^{-\mathrm{f}(\theta)/RT}\sin\theta d\theta \tag{8}$$

For spherical symmetry $\mathrm{f}(\theta)$ is independent of θ and we obtain

$$Z^*_{AB} = Z_{AB}e^{-C/RT} \tag{9}$$

which is of course the classical equation.

The Form of the Function $\mathrm{f}(\theta,\varphi)$: Uncomplicated Ion–Dipole Systems.—Reactions between ions and polar molecules are particularly suitable since the former are spherically symmetrical and we are not without some information concerning the spatial disposition of groups and dipoles in the latter. The energy of interaction between a charged particle and a dipole is a function of the direction of the line joining the charge and the center of the dipole and the direction of the polar axis. We therefore have a case where the energy of interaction varies with the direction of approach. The energy of interaction in very dilute solution may be given[9] by

$$E_e = \frac{N_0\mu_A z_B\epsilon\cos\theta}{D'r^2} \tag{10}$$

where N_0 = Avogadro constant, μ_A = dipole moment of the molecule, z_B = the valency of the ion, ϵ unit electric charge, θ the angle which the line of approach makes with the polar axis, r = the distance between the centers of the dipole and the ion and D' is a function of the dielectric constant D of the medium. This function may be taken as $\frac{3D}{D+2}$ as the influence of the medium when it is surrounding the reacting species in contact with one another or, for "reacting collisions," may be taken as unity (*cf.* ref. 10).

It is usual (*e.g.*, ref. 2, 3, and 4) to give the rate equation for such a reaction by an equation of the form

$$k = Ze^{-(E+E_c)/RT} \tag{11}$$

where E is an energy term representing the non-electrostatic forces. Substituting equation (10) in (11) we have

$$k = Ze^{-\left(E + \frac{N_0\mu_A z_B\epsilon\cos\theta}{D'r^2}\right)/RT} \tag{12}$$

But the substitution of (10) into what is in effect an integrated equation, (11), is not admissible in view of the angular variation of E_e. If we assume that the ion–dipole interaction is the only cause of the directional variation in the activation energy, we may apply equation (8). By rearrangement of the energy function of (12) we obtain

$$\mathrm{f}(\theta) = E/RT\left(1 + \frac{N_0\mu_A z_B\epsilon}{E\,D'\,r^2}\cos\theta\right) \tag{13}$$

---

[9] Moelwyn-Hughes, "Physical Chemistry," Cambridge University Press, New York, N. Y., 1940, p. 98.

Substituted into an equation of the form (8) we may write the rate equation

$$k = \frac{Z}{2}\int_0^\pi e^{-c(1+a\cos\theta)}\sin\theta \mathrm{d}\theta \qquad (14)$$

where

$$c = E/RT \qquad (15)$$

$$a = \frac{N_0\mu_A z_B \epsilon}{E D' r^2} \qquad (16)$$

On integration equation (14) gives

$$k = \frac{Z}{2ca}\{e^{-c(1-a)} - e^{-c(1+a)}\} \qquad (17)$$

The function

$$R = c(1 + a\cos\theta) \qquad (18)$$

for $0 \leq a \leq 1$ has the following properties. Along the axis of symmetry the value of R for $\theta = 0$ is $c(1 + a)$; for $\theta = \pi$ it is $c(1 - a)$.

Resubstituting for c and a in equation (17) and writing

$$E'_e = \frac{N_0\mu_A z_B\epsilon}{D' r^2} \qquad (19)$$

we obtain

$$k = \frac{Z}{2E'_e/RT}\{e^{-(E-E'_e)/RT} - e^{-(E+E'_e)/RT}\} \qquad (20)$$

or rearranged

$$k = \frac{Z(1 - e^{-2E'_e/RT})}{2E'_e/RT}e^{-(E-E'_e)/RT} \qquad (21)$$

When $2E'_e$ is appreciably greater than RT, equation (21) reduces to

$$k = Z\frac{RT}{2E'_e}e^{-(E-E'_e)/RT} \qquad (22)$$

The Relation to the Arrhenius Parameters.—Since the experimental determination of the activation energy is given by

$$E_A = RT^2\frac{\mathrm{d}\ln k}{\mathrm{d}T} \qquad (23)$$

we have on differentiating ln k of equation (22) with respect to T

$$E_A = \frac{3}{2}RT + E - RT^2\frac{\mathrm{d}\ln E'_e}{\mathrm{d}T} + RT^2\frac{\mathrm{d}E'_e/RT}{\mathrm{d}T} \qquad (24)$$

Depending on what function of D' in E_e is used, there will be differences in the last two terms.

(a) For $D' = 1$, *i.e.*, $\mathrm{d}D/\mathrm{d}T = 0$, we have

$$E_A = \frac{3}{2}RT + E - E'_e \qquad (25)$$

(b) For $D' = 3D/(D + 2)$, we have

$$E_A = \frac{2}{3}RT + E - \frac{2LRT^2}{D + 2} - E'_e\left(1 - \frac{2LT}{D + 2}\right) \qquad (26)$$

where L is a constant for the solvent given by

$$D = ce^{-LT} \qquad (27)$$

The two terms involving L are small for all solvents and their effect compared with the other terms may be neglected. In any case, neither the accuracy of the available results nor the range of temperature usually covered justifies such a refined analysis. Equation (25) may therefore be used for either forms of D' under consideration and different values will only arise from the value of D' determining the magnitude of E'_e.

From equation (25)

$$E - E'_e = E_A - \frac{3}{2}RT = E_r \qquad (28)$$

and equation (22) we may determine the A factor of the Arrhenius equation from its definition

$$A = k_t/e^{-E_A/RT} \qquad (29)$$

We obtain

$$A = Z\frac{RT}{2E'_e}e^{3/2} \qquad (30)$$

Substituting (2) and (19) in (30) we obtain

$$A = \frac{N_0 r^2\left\{8\pi RT\left(\frac{1}{m_A} + \frac{1}{m_B}\right)\right\}^{1/2} RTr^2D'e^{3/2}}{1000 \times 2 \times N_0\mu_A z_B\epsilon} \qquad (31)$$

We therefore derive an expression for r, the only parameter not directly ascertainable.

$$r = \left\{\frac{2000 A \mu_A z_B\epsilon}{RTD'\left\{8\pi RT\left(\frac{1}{m_A} + \frac{1}{m_B}\right)\right\}^{1/2}e^{3/2}}\right\}^{1/4} \qquad (32)$$

It will be noted that the value of r so calculated, involving as it does the experimental parameter A, is the average distance of the centers for all those approaches which result in reaction. Substituted in equation (2) we obtain Z_r, the maximum possible number of such approaches. However, only the fraction $e^{-(E-E_e')/RT}$ possesses sufficient energy to penetrate to that distance. This is further reduced by the factor $RT/2E'_e$ which we may provisionally designate by P_r.

It is thus seen that Z_r is not the "collision frequency" as ordinarily understood which uses an average distance $(r_A + r_B)$ determined from X-ray, viscosity and other non-kinetic data. The "reaction distance" r stands in the same relationship to $(r_A + r_B)$ as does the activation energy to the average energy of the system. The value of $(r_A + r_B)$ and the derived collision frequency Z_{AV} have, in fact, for reaction kinetics little significance. They are ground state quantities.

It will further be noted that as r increases, the term E'_e decreases and therefore the term a (equation (16)) tends to zero. This is the condition for the equation for a spherical energy surface (Fig. 1). The rate equation, therefore, tends to

$$k \approx Ze^{-E/RT} \qquad (33)$$

Put in another way we may say that if reaction is possible at large distances, the direction of approach is irrelevant. The term

$$P_r = RT/2E'_e \qquad (34)$$

may be interpreted in terms of the "steric" and "orientation" parts of the usual probability factor (*cf.* ref. 1).

$$P = p \times s \times o \qquad (35)$$

Its magnitude is determined by E'_e which is seen to be (equation (19)) the electrostatic energy at $\theta = 0$

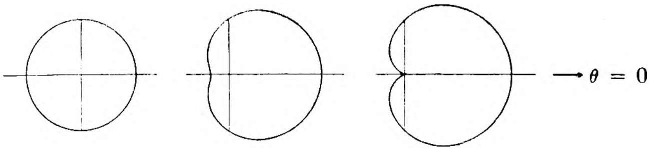

a = 0 a < 1 a = 1

Fig. 1.

TABLE I

No.	Dipole	Ion	Solvent	A	E_A (cal.)	Ref.
1	CH_3Br	I^-	(a) H_2O	1.68×10^{10}	18260 ± 130	13
			(b) CH_3OH	2.26×10^{10}	18250 ± 250	14
			(c) $(CH_3)_2CO$	2.24×10^{11}	16080 ± 800	15
				1.15×10^{10}	14340 ± 1200	16
2	CH_3I	Br^-	(a) H_2O	6.02×10^{9}	19310 ± 750	13
			(b) CH_3OH	3.91×10^{11}	21400 ± 1000	14
			(c) $(CH_3)_2CO$	2.83×10^{11}	16150 ± 1500	15
3	(a) CH_3Cl	OH^-	H_2O	4.11×10^{12}	24280 ± 120	17
	(b) CH_3Br			1.04×10^{13}	23000 ± 150	17
	(c) CH_3I			1.24×10^{12}	22220 ± 230	17
4	(a) CH_3Cl	$S_2O_3^{--}$	H_2O	1.01×10^{12}	20520	17
	(b) CH_3Br			6.28×10^{12}	19540	17
	(c) CH_3I			2.01×10^{12}	18880	17

which is the direction of greatest repulsion. The appearance of E_e' in the integrated equation both in the exponential term and in P_r may be interpreted as meaning that the electrostatic contribution not only influences the necessary minimum approach energy but determines the effective fraction of all such possible approaches. This is a reflection of the fact that, from a kinetic point of view, the "effective shape" of a molecule is determined by the force fields of both partners in reaction and that this shape determines the probability that any particular orientation of approach will result in reaction.

Application to Experimental Results.—The above equations are directly applicable to reactions where no other factors contribute to the directional variation of the interaction energy and where the seat of reaction lies close to the center of the dipole. Such a case is represented by the reaction

$$CH_3X + Y^- \longrightarrow CH_3Y + X^- \qquad (36)$$

where Y^- is an ion which must show no serious deviation from spherical symmetry. The application is restricted to methyl compounds for two reasons. (1) The introduction of larger groups in place of one or two of the hydrogens, even if they did not constitute dipoles of significant magnitude, would create an unsymmetrical van der Waals envelope invalidating the assumption that E is invariant with respect to θ and φ. (2) Reactive approaches from directions within the solid angle bounded by the three hydrogen valences involve the energy of inversion of these valency angles, while approaches from all other directions leave the dispositions of valences untouched. Only when the energy of inversion is negligible compared with E are the conditions for the present treatment fulfilled. We may assume that in methyl compounds this is the case (*cf.* ref. 5, 10, 11). The dipole moment of the molecule is overwhelmingly determined by the C^+–X^- structure (see, *e.g.*, the very small changes in the moment for the series of alkyl halides[12]) so that we may neglect the C–H dipole contributions. Furthermore reaction takes place at the C-atom which must lie very close to the center of the dipole. Reaction (36) therefore represents a suitable case for analysis.

Data are available for the systems given in Table I.

Equations 2, 19, 25, 28, 32 and 34 were used in evaluating r, Z_r, P_r, E_e', E and E_r with the following extra-kinetic parameters:

Dipole	$\mu_A \times 10^{18}$	Solvent	$D^{20°}$	
CH_3Cl	1.86	H_2O	80.0	
CH_3Br	1.79	CH_3OH	32.5	$T = 293°$
CH_3I	1.62	$(CH_3)_2CO$	31.0	

There are two sets of results in Table II according to the choice of D'. (a) $D' = 1$; (b) $D' = \dfrac{3D}{D+2}$.

It is not possible to decide between the alternative formulations (a) and (b) without making assumptions concerning the magnitude of E or until more precise and comparable data for the variation of k with D are available. On general grounds, however, it seems unlikely that the solvent has no effect on the reaction and we shall therefore assume formulation (b) to give more nearly the correct values.

Before discussing the structural significance of the values in Table II it is best to consider how the magnitude of r (and the other parameters dependent on it) are affected by the experimental errors. These errors arise from the determination of k and E_A of which the latter carries the more serious uncertainty.

An error of 600 cal. (*cf.* Table I) at $T = 293°$ results in the derived magnitude of A being in error by a factor of 2.72 or 0.37 for +ve. or −ve. ΔE_A, respectively. Equation (32) shows that this in turn produces factors of 1.28 and 0.78, respectively, in the magnitude of r. Taking this at, say, 3 Å., the limits are 2.33 and 3.85 Å.—a total uncertainty of 1.52 Å. Even with the smaller errors recorded in Table I the lower limit for the uncertainty is about 0.75 Å., while a large error (±1000 cal.) at 10 Å. gives a total uncertainty of 8.8 Å. In spite of this sensitivity of the analytical procedure, the range of r values for each formulation of each of the systems lies within reasonable limits. We may therefore accept the order of magnitude of

---

(10) Ogg and Polanyi, *Trans. Faraday Soc.*, **31**, 604 (1935).

(11) Baughan and Polanyi, *ibid.*, **37**, 648 (1941).

(12) *Trans. Faraday Soc.*, **30**, Appendix (1934).

(13) Moelwyn-Hughes, *J. Chem. Soc.*, 779 (1938).

(14) Moelwyn-Hughes, *Trans. Faraday Soc.*, **35**, 368 (1939).

(15) A. G. Evans and Hamann, *ibid.*, **47**, 30 (1951).

(16) Moelwyn-Hughes, *ibid.*, **45**, 167 (1949).

(17) Moelwyn-Hughes, *Proc. Roy. Soc.* (*London*), **A196**, 540 (1949).

TABLE II

Dipole	Ion	Solvent	D'	r(Å.)	Z_r	P_r	E_e'	E	E_r
CH_3Br	I^-	(a) H_2O	a	3.97	1.01×10^{11}	3.75×10^{-2}	7820	23200	17380
			b	3.04	5.92×10^{10}	6.40×10^{-2}	4580	21960	17380
		(b) CH_3OH	a	4.27	1.18×10^{11}	4.34×10^{-2}	6760	24130	17370
			b	3.30	6.99×10^{10}	7.28×10^{-2}	4020	21390	17370
		(c) $(CH_3)_2CO$	a	7.58	3.70×10^{11}	1.36×10^{-1}	2150	17350	15200
			b	5.85	2.20×10^{10}	2.29×10^{-1}	1280	16480	15200
			a	3.61	8.40×10^{10}	3.10×10^{-2}	9450	22910	13460
			b	2.79	5.00×10^{10}	5.19×10^{-2}	5650	19110	13460
CH_3I	Br^-	(a) H_2O	a	3.00	5.94×10^{10}	2.31×10^{-2}	12500	30930	18430
			b	2.29	3.48×10^{10}	3.99×10^{-2}	7320	2875	18430
		(b) CH_3OH	a	8.50	4.65×10^{11}	1.88×10^{-1}	1550	22120	20520
			b	6.56	2.76×10^{11}	3.16×10^{-1}	922	21440	20520
		(c) $(CH_3)_2CO$	a	7.85	3.95×10^{11}	1.61×10^{-1}	1820	17090	15270
			b	6.03	2.34×10^{11}	2.68×10^{-1}	1090	16360	15270
(a) CH_3Cl	OH^-	H_2O	a	13.2	2.32×10^{12}	3.98×10^{-1}	740	24140	23400
			b	10.1	1.36×10^{12}	6.75×10^{-1}	430	23830	23400
(b) CH_3Br			a	16.8	3.50×10^{12}	6.65×10^{-1}	440	22560	22120
			b	12.8	2.04×10^{12}	>1	260	22380	22120
(c) CH_3I			a	9.66	1.14×10^{12}	2.44×10^{-1}	1200	22540	21340
			b	7.38	6.63×10^{11}	4.17×10^{-1}	700	22040	21340
(a) CH_3Cl	$S_2O_3^{--}$	H_2O	a	12.6	1.27×10^{12}	1.81×10^{-1}	1620	21260	19640
			b	9.60	7.42×10^{11}	3.08×10^{-1}	950	20590	19640
(b) CH_3Br			a	21.0	2.92×10^{12}	5.25×10^{-1}	560	19220	18660
			b	16.1	1.71×10^{12}	9.00×10^{-1}	330	18990	18660
(c) CH_3I			a	15.5	1.44×10^{12}	3.15×10^{-1}	930	18930	18000
			b	11.9	8.39×10^{11}	5.38×10^{-1}	540	18540	18000

these values. Such questions as differences in solvent and substituent influences, however, cannot be significantly discussed.

Systems 1 and 2.—An inspection of the E_e' values shows that the assumption

$$1 - e^{-2E_e'/RT} \approx 1$$

leading to equation (22) is justified. A possible exception is 2b, giving 0.956, but its relation to the other reactions makes it certain that experimental errors account for the deviation. This being so, it is clear from our analysis that reaction will take place mainly along the direction represented by $\theta = \pi$ in our model, which is the direction of minimum energy, $(E - E_e')$. Since E_e' is of reasonable size, directions other than in close proximity to this line will present much greater barriers with consequent few transitions.

Substitution is, therefore, invariably accompanied by nearly 100% inversion of the hydrogen valences. This, of course, has been the *assumption* of many theoretical treatments and the *induction* from experiments with more complex, optically active compounds (see, *e.g.*, ref. 18–21). The present paper demonstrates this as a necessary consequence of the kinetic analysis.

Systems 3 and 4.—The E_e' values here are all small and equation (22) is therefore not applicable. The calculations have nevertheless been carried out for comparison. The analysis using the unsimplified equation (21) is rigorously not possible and in any case would produce results differing very little from those using the classical equation. The latter gives values very similar to the (a) formulations of Table II. (There is of course no (b) formulation for the classical equation.)

From the above we reach the somewhat surprising conclusion that these systems do not show exclusive inversion. Collisions from all directions are roughly equally successful which would tend to about 25% inversion and 75% retention of configuration (Fig. 2).

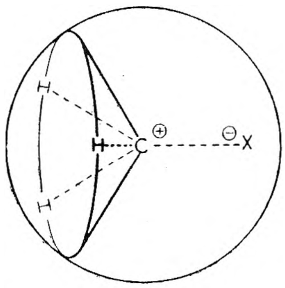

Fig. 2.

This striking difference in the behavior of the hydroxyl ion (system 3) compared with the halides is parallel to their respective conductances and ionic mobilities (OH^- about 3 times Cl^-, Br^- and Cl^-). An explanation for this has been advanced[22] which postulates a Grotthus type of chain. The OH^- ion owing to its strong solvation with water molecules loses some of its identity and under certain circumstances (electric field or dipole) the solvation complex can release OH^- ions from its periphery. According to this view the OH^- ion would be capable of acting at a distance equal to the solvation shell diameter although the charge center remains substantially in the center of the complex

---

(18) Bergmann, Polanyi and Szabo, *Trans. Faraday Soc.*, **32**, 843 (1936).

(19) Cowdrey, Hughes, Ingold, Mastermann and Scott, *J. Chem. Soc.*, 1252 (1937).

(20) Hughes, *Trans. Faraday Soc.*, **34**, 186 (1938).

(21) Olson and Long, *J. Am. Chem. Soc.*, **56**, 1294 (1934).

[22] Huggins, *ibid.*, **53**, 3190 (1931).

up to the moment of reaction. The large reaction distance and small electrostatic contribution in system 3 may thus find an explanation. Of the halogens it appears that only the F^- ion has any substantial solvation[23] but data for F^- substitution are not available to check this interesting correlation between electrolytic and kinetic behavior of ions.

The thiosulfate ion is strictly not spherically symmetrical but the double charge may be regarded as "smearing out" any such deviations. This double charge increases r by a factor of 1.2. The effective diameter of the $S_2O_3^{--}$ ion is not known but is certainly large so that the order of magnitude of the values recorded for system 4 is not unexpected.

From the magnitude of r, the distance between ion and dipole center, we can arrive at a figure for d, the distance between the approaching ion and the C-atom at the moment of reaction. The vagueness of the concept "center of the dipole" makes a definite calculation difficult. We may, however, make the reasonable assumption (*cf.* ref. 10) that the center of the dipole lies close to the point of contact of the covalent radii of the atoms responsible for the dipole, *i.e.*, at 0.77 Å. from the carbon center. Neglecting the slight variation of d/r for small angles, we may subtract this figure from the values of r and obtain the true kinetic reaction distance. Systems 1 and 2 only are given since for reasons discussed above it is not possible to give a precise structural significance to the values in the other systems.

Table III

Distance	Br...C	I...C
d (H_2O)	1.42	2.27
d (CH_3OH)	5.79	2.53
d ($(CH_3)_2CO$)	5.26	5.08
		2.02
Transition state	2.34	2.55
Electron diffraction	1.91	2.10
Microwave	1.939	2.144

The distances so calculated may be compared with the average internuclear separation of the final products from electron diffraction studies[24] and from microwave values[25,26] as well as with the values of the transition state distance estimated on theoretical grounds from non-kinetic data.[10]

The divergence of the d values is considerable and the uncertainties of these experimentally difficult reactions makes it unprofitable to discuss the recorded differences. The advantage of the present method lies not in the values so obtained but in the fact that it yields such a value without the rigid assumption of a single direction of approach. It also yields without further assumptions a value for the deviation term. The variation of reaction distance and activation energy with the total solid angle may produce preferential reaction in one direction. Kinetic analysis will detect this by a low probability factor. In other cases no serious directional differences arise with a consequent value of $P_r \approx 1$.

[23] Bernal and Fowler, *J. Chem. Phys.*, **1**, 515 (1933).

[24] L. Pauling, "Nature of the Chemical Bond," Cornell University Press, Ithaca N. Y., 1945, p. 167.

[25] Simmons, *Phys. Rev.*, **76**, 686 (1949).

[26] Simmons and Swan, *ibid.*, **80**, 289 (1950).

SOLUBILITY OF FLUORIDES OF METALS IN LIQUID HYDROGEN FLUORIDE

By Albert W. Jache[1] and George H. Cady

Department of Chemistry and Chemical Engineering, University of Washington, Seattle, Washington

Received May 27, 1952

Solubilities of the fluorides of a number of metals in liquid hydrogen fluoride have been measured over a temperature range from about −25° to approximately 12°. In general the values found are in accord with the qualitative information available in the past. Many of the solubilities are of the same order of magnitude as those of the corresponding hydroxides when dissolved in water; however, it appears that in general the fluorides are more soluble. Some fluorides are much more soluble in hydrogen fluoride than the corresponding bases are in water. For example, the value for silver(I) fluoride is 3×10^4 times that for silver oxide.

In spite of the fact that it is well known that liquid hydrogen fluoride resembles water by being a highly polar polymerized solvent for electrolytes, it is still true that only a limited amount of quantitative information about its solutions is to be found in the literature. For example, in recent reviews both Simons[2a] and Jander[2b] give qualitative information regarding the solubilities of many substances but report only a few quantitative values. The purpose of the present paper is to increase the number of quantitative data and to compare the solubilities of fluorides in hydrogen fluoride with the solubilities of hydroxides in water.

Experimental

Preparation of Fluorides.—Hydrogen fluoride was prepared by a method similar to that of Simons.[3] A solution containing hydrogen fluoride and potassium fluoride in a ratio of about three moles to one was obtained by absorbing commercial hydrogen fluoride in molten KHF_2. Traces of water and other impurities were removed by an electrolytic decomposition which was continued until fluorine had been liberated at the anode for two hours or more. Hydro-

---

[1] This paper represents part of a thesis submitted by A. W. Jache to the Graduate School, University of Washington, in partial fulfillment of the requirements for the Ph.D. degree.

[2] (a) J. H. Simons, "Fluorine Chemistry," Academic Press, New York, N. Y., 1950, pp. 225–292; (b) Jander, "Die Chemie in Wasserahnlichen Losungsmitteln," Springer-Verlag, Berlin, 1949, pp. 1–37.

[3] J. H. Simons, "Inorganic Syntheses," Vol. 1, McGraw-Hill Book Co., Inc., New York, N. Y., 1939, p. 134.

gen fluoride was then distilled from the mixture through a vertical 60-cm. length of copper tubing packed with small copper ribbon. The condensed liquid was collected in a polyethylene bottle. Later it was distilled from this bottle through a system, made of polyethylene, into the bottle to be used in a solubility measurement. Liquid prepared in this manner was found to have a specific electrical conductivity of about 7×10^{-4} ohm^{-1} cm.$^{-1}$. This indicates a rather high degree of purity but not as high as that attained by Fredenhagen and Krefft.[4]

In the table, the second column indicates by letters the means used to obtain the metal fluorides. The letters a, b, c, etc., stand for the methods now to be described. (a) These fluorides were commercial chemicals or were obtained as research samples from chemical manufacturers. Each fluoride was placed in the bottle to be used for the solubility measurements and was then washed three to five times by decantation with liquid hydrogen fluoride. This washing procedure served to remove water from the sample, to convert impurities such as carbonates, chlorides, oxides, etc., to fluorides and to dissolve any traces of impurities more soluble than the fluoride being studied. It was used with all of the fluorides discussed in this paper except silver(I) fluoride and thallium(I) fluoride. (b) These fluorides were prepared by the action of liquid hydrogen fluoride upon carbonates of the metals. (c) Fluorides indicated by this letter were produced by the action of liquid hydrogen fluoride upon nitrates of the metals. (d) Cerium fluoride was precipitated from an aqueous solution of the nitrate. The solid was washed with water and then with hydrogen fluoride. (e) Fluorides of lithium and calcium were formed by the action of hydrogen fluoride upon the metals. After the metal had all dissolved its salt was washed by decantation several times with hydrogen fluoride. (f) Aluminum fluoride was obtained by dissolving the metal in aqueous hydrofluoric acid. The salt was washed in the usual manner with hydrogen fluoride. (g) Mercury(I) fluoride was formed by the action of hydrogen fluoride upon mercury(I) oxide. (h) Bismuth(III) fluoride was prepared by reaction of bismuth hydroxide with hydrogen fluoride. (i) Iron(II) fluoride was obtained from iron(II) chloride and hydrogen fluoride. (j) Thallium(I) fluoride was prepared by dissolving metallic thallium in aqueous hydrofluoric acid. This process required a long time even though the sticks of thallium were wrapped with platinum wire to serve as a catalyst. The resulting solution was evaporated to dryness. Hydrogen fluoride was then added and was later evaporated away. The salt obtained by this process was found to contain 8.48% fluorine (theor., 8.51%). (k) Thallium(III) fluoride was formed by passing fluorine, diluted with nitrogen, through a solution of thallium(I) fluoride in hydrogen fluoride. As the fluorine passed, thallium(III) fluoride precipitated. Even though a large excess of fluorine was used, much of the thallium(I) fluoride failed to react. The precipitated thallium(III) fluoride was washed twice by decantation with liquid hydrogen fluoride. Finally it was again suspended in hydrogen fluoride in the solubility bottle and was again treated with dilute fluorine. (l) Silver(I) fluoride was made by the action of liquid hydrogen fluoride upon silver carbonate and upon silver oxide. The solvent was evaporated away. The solid was again dissolved in hydrogen fluoride and the solvent was again evaporated away; fluorine content found 15.2% (theor. = 15.0%). (m) Silver(II) fluoride was prepared from silver(I) fluoride using the same type of procedure as that described for thallium(III) fluoride.

Preparation, Sampling and Analysis of Solutions.—Vessels made from polyethylene plastic were employed in these studies. This material is resistant to attack and is convenient to use because tubing can be fused together and apparatus can be assembled in much the same manner as glass apparatus. The suitability of the plastic was shown by allowing a 270-ml. bottle to stand filled with liquid hydrogen fluoride for four days. The dry bottle weighed about 33 g. and the treatment with hydrogen fluoride caused it to increase in weight 16 mg. There was a slight darkening of color. A second treatment with hydrogen fluoride caused the bottle to increase in weight by only one milligram. All bottles used in this research were pretreated for several days with liquid hydrogen fluoride. When a ten-gram sample of hydrogen fluoride which had stood in a bottle for a week was evaporated to dryness in a platinum crucible, the residue remaining weighed not over 0.1 mg. As the result of continued use, the bottles darkened in color somewhat.

Solubility bottles were made from 270-ml. bottles. Two pieces of 12 mm. (i.d.) tubing were sealed to each bottle to serve as inlet and outlet for gases. These tubes could be closed with Teflon (polytetrafluoroethylene) stoppers. The bottle was punctured near the top with a needle which left a hole of about 0.5 mm. diameter. This hole was opened when a sample was to be taken; at other times it was kept closed with a piece of polyethylene cemented in place with a waxy form of poly-(chlorotrifluoroethylene).

Sampling bottles had volumes of about 70 ml. Each bottle was attached to a no. 20 hypodermic needle by means of a Teflon adapter. The only opening in the sampling apparatus was the hole in the needle.

A solution was prepared by washing an excess of the metal fluoride to be studied with hydrogen fluoride. Several decantations were made as indicated under method (a) for obtaining fluorides. Finally, the solubility bottle was about two-thirds filled with liquid hydrogen fluoride. In most cases diluted fluorine was bubbled through the solution for an hour or more to react with any water which might have been present. This step was omitted when one of the following fluorides was present: mercury(I), silver(I), thallium(I), cerium(III), lead(II), antimony(III), bismuth(III), iron(II), cobalt(II) and nickel(II). The bottle was then closed with Teflon stoppers and it was placed in a low frequency shaker in an air thermostat.

At approximately daily intervals samples of the clear supernatant solution were withdrawn into sampling bottles. First, the solid was allowed to settle in the solution; then the sampling bottle, which had been cooled to the temperature of the solution, was squeezed, and the hypodermic needle was inserted through the tiny hole in the wall of the solubility bottle. As the sampling bottle expanded to its original size a sample of liquid flowed in through the needle. The hole in the solubility bottle was then covered at once, and the sampler needle was capped with a piece of polyethylene plastic. The size of the sample was determined by weighing the sampling bottle before and after discharging the sample for analysis.

Usually the sample was analyzed simply by evaporating it to dryness in a platinum crucible and weighing the residual metal fluoride. Normally the fluoride was dried in the atmosphere at 110° before weighing. Sodium fluoride was heated to redness, however, to drive off all hydrogen fluoride. In the cases which follow other analytical methods were used: (1) Silver(I) fluoride was determined by discharging the solution into hydrochloric acid. The silver chloride so formed was weighed. (2) Silver(II) fluoride was usually determined by discharging the solution into a mixture of aqueous potassium iodide and ice. The iodine so formed was titrated with sodium thiosulfate. A comparison of this method with the one usually used for other salts indicated that the two were in agreement within the limits of accuracy. (3) Mercury(I) fluoride solutions were analyzed by the procedure used for silver(I) fluoride. (4) Mercury(II) fluoride obtained by evaporation of the solvent was converted to the oxide and weighed as such. (5) Solutions containing thallium(I) fluoride were added to a mixture of ice and water. Potassium iodide was then added and the weight of the precipitated thallous iodide was determined. (6) Thallium(III) fluoride was determined by the method used for silver(I) fluoride. In the one case tested, this method agreed substantially with the method usually employed for other salts. (7) Solutions of manganese(III) fluoride were analyzed by precipitating manganese dioxide. This was dried and then weighed. (8) Since solid iron(III) fluoride was very hygroscopic it was converted to ferric oxide and weighed as such.

Analysis of the Solid Phase.—After the solubility determinations for a salt had all been made, the cap was removed from the solubility bottle and some of the solid phase was removed on a spatula. This slurry was placed on an 80-mesh copper gauze filter and liquid was quickly removed by centrifugation. The solid was then weighed in a platinum crucible and in most cases it was dried at 110° to remove hydrogen fluoride. Loss in weight upon drying corresponded to hydrogen fluoride driven off. For some of the salts the special analytical procedures described in the preceding paragraph were used.

---

[4] K. Fredenhagen and O. T. Krefft, *Z. Elektrochem.*, 35, 670 (1929).

Table I

Solubility of Fluorides in Hydrogen Fluoride

Salt	Preparation method	Solubility in g. unsolvated salt per 100 g. of hydrogen fluoride						Composition of solid (not dried), moles HF per mole salt	Solubility ratio	Former solubility rating
		°C.	Solubility	°C.	Solubility	°C.	Solubility			
LiF	a, c	12.2	10.3 ± 0.1	− 3.3	10.3 ± 0.1	−23.0	10.3 ± 0.1	1.09	0.74	S
NaF	a	11.0	30.1 ± 0.1	− 9.8	25.1 ± 0.1	−24.3	22.1 ± 0.1	4.10	0.25	S
KF	Ref. 6	8	(36.5)	−45	(27.2)			4	0.30	S
RbF	Ref. 7	20	(110)						0.5	S
CsF	Ref. 8	10	(199)	−16	(177)			3	0.64	S
NH_4F	Ref. 5	17	(32.6)					5		S
CuF_2	b	12.4	0.010 ± 0.005	− 8.3	0.008 ± 0.004	−23.1	0.010 ± 0.004	0.28	32	I
AgF	l	11.9	83.2 ± 0.8	− 9.8	43.8 ± 0.1	−25.0	27.2 ± 0.7	1.94	3×10^{1}	S
AgF_2	m	11.5	0.048 ± 0.006	− 8.9	0.030 ± 0.002	−25.2	0.024 ± 0.001	0.0		
BeF_2	c	11.2	0.015 ± 0.004	− 5.1	0.013 ± 0.003	−24.2	0.014 ± 0.002	0.03	1.6×10^{3}	SS
MgF_2	b	12.2	0.025 ± 0.003	− 3.3	0.025 ± 0.004	−23.0	0.033 ± 0.002	0.25	8.7	SS
CaF_2	b, c	12.2	0.817 ± 0.015	− 3.3	1.061 ± 0.005	−23.0	1.444 ± 0.004	1.86	6.8	SS
SrF_2	a	12.2	14.83 ± 0.09	− 3.3	14.63 ± 0.01	−23.0	14.43 ± 0.01	3.22	16.5	SS
BaF_2	a	12.2	5.60 ± 0.12	− 3.3	4.74 ± 0.04	−23.0	3.61 ± 0.01	5.95	1.15	SS
ZnF_2	b	14.2	0.024 ± 0.002	− 4.4	0.019 ± 0.002	−23.0	0.016 ± 0.002	0.05	1.1×10^{2}	I
CdF_2	b	14.2	0.201 ± 0.009	− 4.4	0.198 ± 0.001	−23.2	0.189 ± 0.001	0.07	75	I
HgF_2	a	11.9	0.54 ± 0.01	− 7.8	0.62 ± 0.01	−25.2	0.61 ± 0.01	0.01	10	I
Hg_2F_2	g	11.8	0.877 ± 0.005	− 4.5	0.81 ± 0.02	−22.5	0.79 ± 0.02	0.00		..
AlF_3	f	11.2	≦0.002	− 5.1	≦0.003	−24.2	≦0.004	0.22	1.2	I
TlF_3	k	11.5	0.081 ± 0.003	− 8.9	0.029 ± 0.005	−25.2	0.027 ± 0.003	1.04		..
TlF	j	11.9	580 ± 45	− 7.8	450 ± 50	−25.2	305 ± 15	1.92	8.5	S
CeF_3	d	11.9	≦0.043	− 7.8	≦0.037	−25.2	≦0.041	0.53		I
CeF_4	a	11.9	0.10 ± 0.01	− 9.8	0.10 ± 0.01	−23.8	0.106 ± 0.006	0.03		..
ZrF_4	c	12.4	0.009 ± 0.002	− 8.3	0.015 ± 0.003	−23.1	0.023 ± 0.002	1.00		..
ThF_4	c	11.8	≦0.006	− 4.5	≦0.002	−22.5	≦0.001	0.84		..
PbF_2	b	12.4	2.62 ± 0.09	− 8.3	3.56 ± 0.04	−23.1	3.67 ± 0.01	2.23	2.3×10^{2}	I
SbF_3	a	11.9	0.536 ± 0.005	− 9.8	0.285 ± 0.010	−23.8	0.191 ± 0.003	0.13		..
BiF_3	h	12.4	0.010 ± 0.002	− 8.3	0.011 ± 0.003	−23.1	0.010 ± 0.002	0.16	6.5	I
MnF_3	a	11.5	0.164 ± 0.004	− 7.8	0.147 ± 0.010	−25.2	0.134 ± 0.003	0.11		..
FeF_3	a	11.9	0.008 ± 0.002	− 7.8	0.003 ± 0.002	−25.2	≦0.001	0.60	5×10^{2}	I
FeF_2	i	11.8	0.006 ± 0.002	− 4.5	0.005 ± 0.002	−22.5	0.005 ± 0.002	0.32	80	I
CoF_3	a	11.9	0.257 ± 0.003	− 9.8	0.264 ± 0.015	−23.8	0.272 ± 0.016	0.35	7.7×10^{2}	..
CoF_2	b	14.2	0.036 ± 0.002	− 4.4	0.033 ± 0.002	−23.2	0.040 ± 0.003	0.38		I
NiF_2	b	11.9	0.037 ± 0.002	− 9.7	0.040 ± 0.002	−25.0	0.035 ± 0.002	0.25	27	I

Results

For each salt the solubility was determined at three different temperatures. A run was continued at one temperature until the concentration of solute in each bottle remained constant for about three days or more. Daily analyses were made using samples of solution weighing about 10 g. The solubility values are listed in Table I together with an indication of the apparent precision of the measurement.

The meaning of the table may be clear by considering the row for lithium fluoride. This salt was obtained in two ways. A commercial sample was used and another sample prepared from lithium metal and hydrogen fluoride was also tested. Both samples had the same solubility. At 12.2° and also at −3.3° and −23.0° the experimental values for the solubility ranged between 10.2 and 10.4 g. of LiF per 100 g. of hydrogen fluoride. This uncertainty in the analysis is represented in the table by reporting the solubility to be 10.3 ± 0.1. The ±0.1 is not the probable error; it represents the precision of the analyses or, in the case of low solubilities, the limit of accuracy which could be reached with the balance. The larger of these two limits is the one recorded in the table for each solubility value. In the column marked "Composition of solid" the value 1.09 means that the centrifuged sample of lithium fluoride as removed from the solubility bottle lost weight upon drying corresponding to 1.09 moles of HF per mole of LiF. This is an indication, but not a proof, that the solid in the bottle was LiF·HF. Values in this column may fail to represent the true composition of the solid phase for two reasons: (1) an appreciable weight of liquid might remain on the solid even after centrifugation, thereby giving too high a value; (2) hydrogen fluoride might be lost from the solid before the sample could be weighed, thereby giving too low a value. In spite of these experimental difficulties, many of the values appear to be clear in meaning regarding the composition of the solid phase. For example: some of the solid phases apparently were LiF·HF, NaF·4HF, AgF·2HF, AgF_2, BeF_2, MgF_2, CaF_2·2HF, SrF_2·3HF, BaF_2·6HF, ZnF_2, etc.

Data in the table for NH_4F,[5] KF,[6] RbF[7] and CsF[8] have been selected from the literature and the refer-

---

[5] O. Ruff and L. Staub, *Z. anorg. allgem. Chem.*, **212**, 399 (1933).

[6] G. H. Cady, *J. Am. Chem. Soc.*, **56**, 1431 (1934).

[7] K. R. Webb and E. B. R. Prideaux, *J. Chem. Soc.*, 111 (1939).

[8] R. V. Winsor and G. H. Cady, *J. Am. Chem. Soc.*, **70**, 1500 (1948).

ences are listed in the column labeled "Preparative method." These solubilities were not determined in this research, but they are included to permit the tabulation of these fluorides.

Discussion

In the table, the column giving former solubility ratings uses the system of notation employed by Simons.[1] The letter S means soluble probably over 1%, while SS means slightly soluble, and I stands for insoluble. Much of the information used by Simons in the preparation of his table was obtained from a paper by Fredenhagen.[9] Although there is a general agreement between the present research and these qualitative ratings, there are some fluorides which are actually more soluble than the ratings indicate. A majority of the few quantitative solubilities, now reported in the literature, for salts studied in this research are lower than the values in the table. Lithium fluoride has, according to Fredenhagen,[5] a solubility of 2.6 g. per 100 cc. of solution at 18° while its solubility as given by Bond and Stowe[10] is close to 0.044 mole of LiF per mole of HF over a temperature range from 0 to 40°. This corresponds to 5.7 g. of LiF per 100 g. of hydrogen fluoride and is considerably less than the value, 10.3, found in this research. Bond and Stowe[10] found the solubilities of calcium fluoride, zinc fluoride and magnesium fluoride at 0° to be less than 0.01%. Fredenhagen's[9] solubility of silver(I) fluoride at $-15°$ is 33 g. of the salt per 100 cc. of solution. While this may be in rather good agreement with data in the table, one cannot be certain, because the density of the solution is not known.

A sample of commercial hydrated ferric fluoride was found to be very soluble. Repeated washing of the solid by liquid hydrogen fluoride yielded anhydrous ferric fluoride of low solubility. Perhaps the influence of a little water upon the solubility of this salt is the result of the formation of fluoride ions by the reaction $H_2O + HF = H_3O^+ + F^-$. Fluoride ions so formed may dissolve ferric fluoride due to the formation of complex ions such as FeF_6^{---}. Hydrated chromic fluoride was also found to be very soluble, but the action of hydrogen fluoride did not yield a satisfactory anhydrous salt.

Since one may regard the metal fluorides as bases in the hydrogen fluoride system of compounds, it is of interest to compare their solubilities in hydrogen fluoride with the solubilities of the corresponding hydroxides in water. This is done in the table in the "solubility ratio" column. This quantity is defined by the equation

$$\text{solubility ratio} = (C_M)_{HF}/(C_M)_{H_2O}$$

in which $(C_M)_{HF}$ is the concentration of the metal in gram atoms per 100 g. of hydrogen fluoride in a solution saturated with the fluoride of the metal at 10°, and $(C_M)_{H_2O}$ is the concentration of the metal in gram atoms per 100 g. of water in a solution saturated with the hydroxide of the metal at 25°. When calculating values for this ratio, solubilities of the hydroxides were taken from Seidell.[11] Solubilities for the oxides rather than the hydroxides were used for the elements silver(I), mercury(II) and lead(II), and a few of the solubilities were taken at 18 or 20° rather than at 25°.

It is apparent that the fluorides, in their solubilities, are much like the corresponding hydroxides. Thus, the fluorides of the alkali and alkaline earth elements are soluble, and the solubility increases as one goes to elements of higher atomic weight in one of the families. Strontium fluoride is out of line, but its high solubility as compared to that of barium fluoride is probably due to the difference in degree of solvation of the solid phases of the two substances. One here compares the solubilities of $SrF_2 \cdot 3HF$ and $BaF_2 \cdot 6HF$. Probably $BaF_2 \cdot 3HF$ would be more soluble than $SrF_2 \cdot 3HF$. Fluorides of the subgroup elements of group two are less soluble than the alkaline earth fluorides. There is a decrease in solubility in the order: sodium fluoride, magnesium fluoride, aluminum fluoride. The expected type of behavior is shown by silver, mercury, thallium and iron in that the lower valence fluorides are more soluble than those in which the metal has its higher valence.

By contrast, the higher valence fluorides of cerium and cobalt are the more soluble.

Several of the fluorides, particularly silver(I) fluoride, are relatively much more soluble than the corresponding hydroxides and none are strikingly less soluble. Perhaps this means that on the whole, fluorides are more basic in hydrogen fluoride than hydroxides are in water.

Acknowledgment.—This research was performed under contract with the Office of Naval Research, U. S. Navy Department. The authors are grateful to the Whitemarsh Research Laboratories of the Pennsylvania Salt Manufacturing Co. for analyzed samples of mercury(II) fluoride, cerium(IV) fluoride, manganese(III) fluoride, cobalt(III) fluoride and iron(III) fluoride.

---

(9) K. Fredenhagen, *et al.*, *Z. physik. Chem.*, **A164**, 176 (1933).

(10) P. A. Bond and V. M. Stowe, *J. Am. Chem. Soc.*, **53**, 30 (1931).

(11) Seidell, "Solubilities of Inorganic and Metal Organic Compounds," D. Van Nostrand Co., Inc., New York, N. Y., 1940, 3rd ed.

ADDITIONS AND CORRECTIONS

Reino Hakala. The Periodic Law in Mathematical Form.

Page 180. In col. 2, line 8 (equation), the last part should read "($0 \leqq l \leqq n - 1$)."

Page 181. Col. 2, line 5 of second paragraph, read "... degree $< n$ is." Near end of col., first line of the last equation should have $-$ (minus sign) at the end of the line.—REINO HAKALA.

Hiroshi Fujita. On the Distribution of Liquid Ascending in a Filter Paper.

Page 629. In Fig. 6, the ordinate legend should be a_L, and the arrows should have a_L^* at the end.—HIROSHI FUJITA.

Hugo Fricke. Kinetics of Thermal Denaturation of X-Rayed Egg Albumin.

Page 789. In col. 2, line 14, for "$.090 \times 10^{-6}$" read "1.90×10^{-6}."—HUGO FRICKE.

Author Index to Volume LVI, 1952

Adamson, A. W. Electron transfer processes and oxidn.-redn. reacns. of hexacyanoferrate(III) ion in aq. soln., 858; see Grossman, J. J., 97.

Adler, I., and Steigman, J. Adsorption of UX_1 and Ra E by an Aquadag coated Geiger–Mueller tube... 493

Alexander, S. See Clarke, J. T., 100.

Allen, A. O., Hochanadel, C. J., Ghormley, J. A., and Davis, T. W. Decompn. of H_2O and aq. solns. under mixed fast neutron and γ-radiation... 575

Amis, E. S. See Broach, W. J., 189.

Amundson, N. R. See Edeskuty, F. J., 148; Kasten, P. R., 683; Lapidus, L., 373, 984.

Anderson, R., Schnizlein, J. G., Toole, R. C., and O'Brien, T. D. Viscosity, d., and crit. consts. of OF_2... 473

Anderson, R. B. See Hall, W. K., 688.

Anderson, R. B., and Emmett, P. H. Surface complexes on C blacks (I) high temp. evacuation studies, 753; (II) adsorption of NH_3, C_2H_2, C_4H_{10}, CH_3NH_2 and H_2O vapor... 756

Anderson, R. D., and Taylor, H. A. Prepn. and some phys. consts. of $CdMe_2$, 161; photolysis of $CdMe_2$... 498

Argersinger, W. J., Jr. See Reynolds, C. A., 417.

Argersinger, W. J., Jr., and Davidson, A. W. Exptl. factors and activity coeffs. in ion exchange equil... 92

Arnikar, H. J. Production of Joshi effect under direct current excitation... 457

Audrieth, L. F. See Osterheld, R. K., 38.

BAIN, O. See Giguère, P. A., 340.

Baker, H. R., Shafrin, E. G., and Zisman, W. A. Adsorption of hydrophobic monolayers of carboxylic acids... 405

Band, W., and Emery, E. B. Approximate adsorption isotherms for a mixt. of 2 isotopes... 384

Bard, R. J. See Bartell, F. E., 532.

Bartell, F. E. See Donahue, D. J., 480.

Bartell, F. E., and Bard, R. J. Effect of atmospheric gases on interfacial tension between Hg and several different liquids... 532

Bartell, F. E., and Bjorklund, C. W. Hysteresis of contact angles—study of interfacial contact angles in mercury–benzene–water system... 453

Bartell, F. E., and Donahue, D. J. Preferential capillary adsorption of water from solns. of alcs. by silica gel... 665

Basolo, F., Bergmann, J. G., and Pearson, R. G. Mechanism of subsn. reacns. in complex ions (I) kinetics of aquation and hydrolysis of some C-subsd. acetatopentamminecobalt(III) ions... 22

Bauer, S. H. Remarks on structures of volatile fluorides... 343

le Beau, D. S. See Hauser, E. A., 136.

Becker, E. I. See Schachat, R. E., 722.

Becker, E. W., and Beyrich, W. Effect of isotopic subsn. on collision properties of CO_2 mol... 911

Beckett, R. J., and Croft, R. C. Structure of graphite oxide... 929

Belcher, H. V. See Bestul, A. B., 432.

Bender, M., and Mouquin, H. Brownian movement and elec. effects... 272

Benesch, R. See Benesch, R. E., 648.

Benesch, R. E., and Benesch, R. Role of adsorption in redn. of org. Hg compds. at dropping Hg electrode 648

Bergmann, J. G. See Basolo, F., 22.

Bernstein, H. J. Phys. properties of mols. in relation to their structure (IV) bond distance relations in subsd. methanes and acyclic aliphatic hydrocarbons... 351

Bernstein, R. B. Enrichment of isotopes by difference in rates of irreversible isotopic reacns... 893

Bernstein, R. B., and Katz, J. J. Isotope exchange reacns. of F with halogen fluorides... 885

Bestul, A. B., Belcher, H. V., Quinn, F. A., Jr., and Bryant, C. B. Viscosities of 0.25 to 90% GR-S rubber solns... 432

Beyrich, W. See Becker, E. W., 911.

Bigeleisen, J. Effects of isotopic subsn. on rates of chem. reacns... 823

Bikerman, J. J. Mechanical destruction of young and old foam films... 164

Bjorklund, C. W. See Bartell, F. E., 453.

Bowden, S. T. See Fuge, E. T. J., 1013.

Briggs, D. R. See Colvin, J. R., 717.

Broach, W. J., Rowden, R. W., and Amis, E. S. Reacn. in acid soln. between tetrabromophenolsulfonphthalein and $AgNO_3$... 189

Brown, A. S., Robinson, R. U., Sirois, E. H., Thibault, H. G., McNeill, W., and Tofias, A. Crit. micelle concns. by a bubble pressure method... 701

Brown, G. L. See Fineman, M. N., 963.

Brown, M. J., and Foster, A. G. Sorption of amines by silica gels... 733

Brown, O. W. See Rohrer, C. S., 662; Rooley, J., 1082.

Bryant, C. B. See Bestul, A. B., 432.

Burbage, J. J., and Garrett, A. B. Phase rule studies in anhyd. $AlBr_3$... 730

Burkhard, R. K. See Klotz, I. M., 77.

Burton, M. Symposium on radiation chemistry—introduction, 545; see Manion, J. P., 560.

Burton, M., and Magee, J. L. Charge transfer in radiation chemistry of gases... 842

Buttner, F. H., Funk, E. R., and Udin, H. Adsorption of O on Ag... 657

deButz, E. H., Distribution of ions in solns. of weak electrolytes... 60

CADY, G. H. See Jache, A. W., 1106.

Cagle, F. W., Jr. See Eyring, H., 889.

Calvin, M. See Fry, A., 897, 901.

Carroll, B. H. See West, W., 1054.

Carter, P. R., and Davidson, N. Kinetics of oxidn. of Fe(II) by Br_2... 877

Cartledge, G. H. Review of "Phase Transformation in Solids" (Smoluchowski, Mayer, Weyl)... 288

Chalkley, L. Extent of photochem. redn. of phosphotungstic acid... 1084

Chalvet, O., and Daudel, R. Bond length calcn. in conjugated mols... 365

Chrisman, C. H., Jr. See Fox, H. W., 284.

Christena, R. C. See Rohrer, C. S., 662.

Cimino, A., and Parravano, G. Production of Ni_3C by decompn. of n-hexane on metallic Ni... 706

Clarke, J. T., Marinsky, J. A., Juda, W., Rosenberg, N. W., and Alexander, S. Electrochem. properties of a permionic anion membrane... 100

Cohen, M. Electron diffraction study of films formed by $NaNO_2$ soln. on Fe... 451

Collett, A. R. See Myers, R. T., 461.

Colvin, J. R., and Briggs, D. R. Electrophoretic analysis of protein interacn. (II) expl. of a boundary anomaly in system bovine serum albumin–Me orange 717

Conrad, C. M. See Tripp, V. W., 693.

Cook, E. L. See Hackerman, N., 524.

Cook, M. A. See Last, G. A., 637, 643.

Cook, M. A., and Talbot, E. L. Surface hydrolysis in Na lauryl sulfate solns. and its effect on surface tension and on adsorption at the solid–aq. soln. interface... 412

Coryell, C. D. See Spiegler, K. S., 106.

Costain, C. C., and Sutherland, G. B. B. M. Method of detg. potential barriers restricting inversion in NH_3, PH_3 and AsH_3 from vibrational force consts... 321

Coulson, C. A. Factors affecting bond lengths in conjugated and aromatic mols... 311

Courtney, W. G. See Duke, F. R., 19.

Cox, R. T. Statistical method of Gibbs in irreversible thermodynamics... 1030

Crawford, B., Jr. See Kirkwood, J. G., 1048.

Croft, R. C. See Beckett, R. J., 929.

Cutler, M. See Kimball, G. E., 57.

DALY, L. K. See Templeton, C. C., 215.
Daniels, F. See Morehead, F. F., Jr., 546; Schmitt, J. A., 917.
Daudel, R. See Chalvet, O., 365.
Davidson, A. W. See Argersinger, W. J., Jr., 92.
Davidson, N. See Carter, P. R., 877.
Davies, T. H. See Yosim, S., 599.
Davis, T. W. See Allen, A. O., 575; Doigan, P., 764.
Davis, W., Jr. See Steidlitz, M. E., 1010.
Dawson, L. R., and Griffith, E. J. Cryoscopic studies of solns. of KCl and NH_4Cl, and acetic, propionic and benzoic acids in formamide ... 281
DeLollis, N. J. Note on displacement pressure method for measuring affinity of liquids for solids ... 193
Delwaulle, M.-L. Study by Raman effect of Ge–H bond in $GeHX_3$ mols. and of mobility of halogen bond in halogenated derivs. of the C family ... 355
Dobay, D. G. See Wagner, G. H., 538.
Dodson, R. W. See Silverman, J., 846; Wolfgang, R. L., 872.
Doigan, P., and Davis, T. W. Photolysis of crystalline nitrates ... 764
Donahue, D. J. See Bartell, F. E., 665.
Donahue, D. J., and Bartell, F. E. Boundary tension at water–org. liquid interfaces ... 480
Donohue, J. H bond in org. crystals ... 502
Doty, P. See Oth, A., 43.
Doyle, G. J. See Volman, D. H., 182.
Draper, A. L. See Milligan, W. O., 123.
Duke, F. R. Disproportionation of MnO_4^{--}—MnO_2 as heterogeneous catalyst ... 882
Duke, F. R., and Courtney, W. G. Complexes in oxidn.-redn. reacns.—Cu(II)-cyanide reacn. ... 19
Dunning, H. N., and Washburn, E. R. Diffusion coeffs. and some related properties of Bu alcs. in aq. solns. ... 235
Durie, R. A., and Gaydon, A. G. Spectra and dissocn. energies of diatomic interhalogen mols. ... 316
Duval, J. E., and Kurbatov, M. H. Adsorption of Co and Ba ions by hyd. Fe_2O_3 at equil. ... 982

EDEN, M. See Kahler, H., 768.
Edeskuty, F. J., and Amundson, N. R. Mathematics of adsorption (IV) effect of intraparticle diffusion in agitated static systems ... 148
Edgell, W. F., and Riethof, T. R. Calcn. of vibrational frequencies of mols. with many atoms and little symmetry (I) simple derivs. of sym. mols. ... 326
Edwards, J. O. Reacn. of H_2O_2 with donor particles ... 279
Ellenbogen, E. See Oncley, J. L., 85.
Elving, P. J. See Loveland, J. W., 250, 255, 935, 941, 945.
El Wakkad, S. E. S., and Salem, T. M. Oxide film formation on surface of metallic Hg in aq. solns. and anomaly between its potential and that of the Hg-HgO electrode ... 621
Emery, E. B. See Band, W., 384.
Emmett, P. H. See Anderson, R. B., 753, 756; Kummer, J. T., 258.
Eyring, H., and Cagle, F. W., Jr. Significance of isotopic reacns. in rate theory ... 889
Eyring, H., and Smith, R. P. Some recent developments in reacn. rate theory ... 972

FINEMAN, M. N., Brown, G. L., and Myers, R. J. Foaming of non-ionic surface active agents ... 963
Foster, A. G. See Brown, M. J., 733.
Foster, J. F. See Zucker, D., 166.
Foster, J. F., and Zucker, D. Length of amylose–iodine complex as detd. by streaming dichroism, 170; streaming birefringence behavior of some subfractionated amylose prepns. ... 174
Fox, H. W., and Chrisman, C. H., Jr. Ring method of measuring surface tension for liquids of high d. and low surface tension ... 284
Francis, A. W. Structural colors in emulsions ... 510
Fricke, H. Kinetics of thermal denaturation of X-rayed egg albumin, 789, (corrn.) ... 1110
Frizzell, L. D. See Waldock, K. T., 654.
Fry, A., and Calvin, M. Isotope effect in decompn. of oxalic acid, 897; C^{14} isotope effect in decarboxylation of α-naphthyl- and phenylmalonic acids ... 901
Fuge, E. T. J., Bowden, S. T., and Jones, W. J. Some phys. properties of diacetone alc., mesityl oxide and Me isobutyl ketone ... 1013
Fujita, H. On the distribution of liq. ascending in a filter paper, 625, (corrn.) 1110; theory of percolation for the case of 2 solutes ... 949
Funk, E. R. See Buttner, F. H., 657.

GARNER, C. S. See Meier, D. J., 853.
Garrett, A. B. See Burbage, J. J., 730; Welsh, J. Y., 727.
Garrett, A. B., and Heiks, J. R. Dissoln. of metals over temp. range of 25–60° (II) dissoln. of Cd in HCl–MeOH–H_2O solns. ... 449
Gaydon, A. G. See Durie, R. A., 316.
Gemant, A. Cataphoresis study in hydrocarbon oil by radioactive and microscopic methods ... 238
Gevantman, L. H., and Williams, R. R., Jr. Detection and identification of free radicals in radiolysis of alkanes and alkyl iodides ... 569
Ghormley, J. A. See Allen, A. O., 575.
Ghormley, J. A., and Levy, H. A. Some observations of luminescence of alkali halide crystals subjected to ionizing radiation ... 548
Gierer, A., and Wirtz, K. Proton and deuteron transfer over H bridges as cause of conductivity effects ... 914
Gieseking, J. E. See Spencer, W. F., 751.
Giguère, P. A., and Bain, O. Force consts. in H and D peroxides ... 340
Gilchrist, A., and Sutton, L. E. Relations between length and reactivity in some C–halogen bonds ... 319
Gitlin, D. See Oncley, J. L., 85.
Glassman, I., and Harris, B. L. Collision diameters of some gases as functions of temp. ... 797
Gledhill, J. A., and Patterson, A., Jr. New method for measurement of high field conductance of electrolytes (Wien effect) ... 999
Glockler, G. Problem of bond energies ... 289
Gofman, J. W. See Trautman, R., 464.
Grad, H. Statistical mechanics of dynamical systems with integrals other than energy ... 1039
Gralén, N., and Lagermalm, G. Contribution to knowledge of some phys.-chem. properties of polystyrene ... 514
Grandine, J. D., 2nd. See Vold, R. D., 128.
Gregg, S. J., and Sing, K. S. W. Effect of heat treatment on surface properties of gibbsite (III) chem. nature of the products formed ... 388
Griffith, E. J. See Dawson, L. R., 281.
Grossman, J. J., and Adamson, A. W. Diffusion process for organolite exchangers ... 97
Guildner, L. A. See Thompson, J. B., 979.
Gunning, H. E. See Scott, R. J., 156.
Gurd, F. R. N. See Oncley, J. L., 85.
Gutmacher, R. G. See Kolthoff, I. M., 740.
Gyani, B. P. Factors governing hardness and transparency of alumina gels ... 762

HACKERMAN, N. See Powers, R. A., 187; Wang, H. L., 771.
Hackerman, N., and Cook, E. L. Dual adsorption of polar org. compds. on steel ... 524
Hagihara, H. Surface oxidn. of galena in relation to its flotation as revealed by electron diffraction, 610; mono- and multilayer adsorption of aq. xanthate on galena surfaces ... 616
Hakala, R. W. Periodic law in math. form, 178, (corrn.) 1110; calcn. of entropy and enthalpy changes from free-energy data ... 427
Harris, B. L. See Glassman, I., 797.
Harris, G. M. See Stranks, D. R., 906.
Hart, D. Periodicity of chem. thermodynamic functions ... 202
Hart, E. J. Radical pair yield of ionizing radiation in aq. solns. of formic acid ... 594
Harwood, H. J. See Hoerr, C. W., 1068.
Hauser, E. A., and le Beau, D. S. Surface structure and properties of colloidal SiO_2 and Al_2O_3 ... 136
Heiks, J. R. See Garrett, A. B., 449.
Henri, V. P., Maxwell, C. R., White, W. C., and Peterson, D. C. Chem. effects of α-particles on some C_6-hydrocarbons in vapor state ... 153

Herzfeld, S. H. Crit. concns. of K n-alkanecarboxylates as detd. by change in color and spectrum of pinacyanole, 953; effect of salt on crit. concns. of K n-alkanecarboxylates as detd. by change in color of pinacyanole . . . 959
Hickman, J. B. See Simons, J. H., 420.
Higuti, I., and Iwagami, Y. Calorimetric evidence for capillary condensation theory . . . 921
Higuti, I., and Shimizu, M. Studies on dielec. property of substances in the sorbed state (IV) freezing phenomenon of o-nitrophenol sorbed on silica gel . . . 198
Hill, T. L. Statistical thermodynamics of transition region between 2 phases (I) thermodynamics and quasithermodynamics . . . 526
Hindman, J. C. See Wehner, P., 10.
Hochanadel, C. J. Effects of Co γ-radiation on water and aq. solns., 587; see Allen, A. O., 575.
Hoerr, C. W., and Harwood, H. J. Solys. of oleic and linoleic acids in common org. solvents . . . 1068
Hoffman, D. C., and Martin, D. S., Jr. Hot atom chemistry—photonuclear prepn. of Co-58, Co-58m 1007
Holleran, E. M., and Hulburt, H. M. Relation among kinetic theory cross-section integrals and new relations involving transport properties of gases . . . 1034
Holstein, T. Mobilities of positive ions in their parent gases . . . 832
Honig, J. M., and Reyerson, L. H. Adsorption of N, O and A on rutile at low temps.; applicability of concept of surface heterogeneity . . . 140
Hornbeck, J. A. Charge transfer and mobility of rare gas ions . . . 829
Hornig, H. C., and Libby, W. F. Catalysis of cerous–ceric electron exchange reacn. by fluoride . . . 869
Hough, E. W., Wood, B. B., Jr., and Rzasa, M. J. Adsorption at H_2O–He, –CH_3 and –N interfaces at pressures to 15,000 p.s.i.a. . . . 996
Hall, W. K., Tarn, W. H., and Anderson, R. B. Studies of Fischer–Tropsch synthesis (XIII) structural changes of a reduced Fe catalyst on reoxidn. and on formation of interstitial phases . . . 688
Hughes, V. L., and Vernon, A. A. Solys. of quaternary ammonium salts in certain org. solvents . . . 927
Hughes, W. L., Jr. See Morawetz, H., 64.
Hulburt, H. M. See Holleran, E. M., 1034.
Hurst, G. G. See Jonassen, H. B., 16.

ILER, R. K. Assocn. between polysilicic acid and polar org. compds., 673; polymn. of silicic acid: retarding effect of chromate ion, 678; polymn. of silicic acid: catalytic effect of fluoride, 680; linear polymetaphosphates—quaternary ammonium salts 1086
Irsa, A. P. See Thompson, S. O., 243.
Ivin, K. J., Wijnen, M. H. J., and Steacie, E. W. R. Reacns. of Et radicals . . . 967
Iwagami, Y. See Higuti, I., 921.

JACHE, A. W., and Cady, G. H. Solv. of fluorides of metals in liq. HF . . . 1106
Jonassen, H. B., Hurst, G. G., LeBlanc, R. B., and Meibohm, A. W. Inorg. complex compds. containing polydentate groups (VI) formation consts. of complex ions of diethylenetriamine and triethylenetetramine with divalent ions . . . 16
Jones, F. T. See Young, F. E., 738, 1093.
Jones, J. L. See Peterson, S., 491.
Jones, S. S., and Long, F. A. Complex ions from Fe and ethylenediaminetetraacetate: general properties and radioactive exchange . . . 25
Jones, W. J. See Fuge, E. T. J., 1013.
Juda, W. See Clarke, J. T., 100.

KACSER, H. Probability factor in bimol. reacns. (I) uncomplicated ion–dipole systems . . . 1101
Kahler, H., Lloyd, B. J., Jr., and Eden, M. Electron microscopic and other studies on a Cu–cystine complex . . . 768
Karush, F. Interacn. of optically isomeric dyes with bovine serum albumin . . . 70
Kasten, P. R., Lapidus, L., and Amundson, N. R. Mathematics of adsorption in beds (V) effect of intraparticle diffusion in flow systems in fixed beds . . . 683
Katz, J. J. See Bernstein, R. B., 885.
Kaufman, S., and Singleterry, C. R. Reacn. between t-amines and org. acids in non-polar solvents . . . 604
Kimball, G. E., Cutler, M., and Samelson, H. Theory of polyelectrolytes . . . 57
Kimpton, D. D., and Wall, F. T. Detn. of diffusion coeffs. from rates of evaporation . . . 715
Kirkwood, J. G., and Crawford, B., Jr. Macroscopic eqs. of transport . . . 1048
Klotz, I. M., Burkhard, R. K., and Urquhart, J. M. Binding of org. ions by proteins—comparison of bovine and human serum albumins . . . 77
Knabeschuh, L. H. See Peterson, S., 491.
Kobatake, Y. See Nagasawa, M., 1017.
Kobe, K. A., and Motsch, W. L. Solys. of Ca and Sr nitrates in monoalkyl ethers of ethylene glycol . . . 185
Kolthoff, I. M., and Gutmacher, R. G. Sorption of GR-S type of polymer on C black (III) sorption by commercial blacks . . . 740
Kottler, F. Logarithmico-normal distribution of particle sizes: homogeneity and heterogeneity . . . 442
Kressman, T. R. E. Ion exchange sepns. based on ionic size . . . 118
Kummer, J. T., and Emmett, P. H. H exchange reacns. over Fe synthetic NH_3 catalysts at −195° . . . 258
Kurbatov, M. H. See Duval, J. E., 982.
Kurbatov, M. H., and Wood, G. B. Rate of adsorption of Co^{++} on hydrous Fe_2O_3 . . . 698

LAGERMALM, G. See Gralén, N., 514.
Lapidus, L. See Kasten, P. R., 683.
Lapidus, L., and Amundson, N. R. Rate-detg. steps in radial adsorption analysis, 373; mathematics of adsorption in beds (VI) effect of longitudinal diffusion in ion exchange and chromatographic columns . . . 984
Last, G. A., and Cook, M. A. Collector-depressant equil. in flotation (I) inorg. depressants for metal sulfides, 637; (II) depressant action of tannic acid and quebracho . . . 643
Lazzell, C. L. See Myers, R. T., 461.
LeBlanc, R. B. See Jonassen, H. B., 16.
Lee, J. M. See Schweitzer, G. K., 195.
Levy, H. A. See Ghormley, J. A., 548.
Lewis, B. W. See Svirbely, W. J., 1006.
Lewis, H. J. See Young, F. E., 738, 1093.
Liang, S. C. Low vapor pressure measurement and thermal transpiration . . . 660
Libby, W. F. Theory of electron exchange reacns. in aq. soln., 863; see Hornig, H. C., 869.
Lima, F. W. On viscosity of binary liq. mixts. . . . 1052
Lind, S. C. Distribution of α-ray energy in radiation chemistry . . . 920
Lindsey, A. J. Vibrating micro-electrodes in polarography—relationship between diffusion current and frequency and amplitude of vibration . . . 439
Lloyd, B. J., Jr. See Kahler, H., 768.
Long, F. A. See Jones, S. S., 25.
Lorenz, P. B. Phenomenology of electro-osmosis and streaming potential . . . 775
Loveland, J. W., and Elving, P. J. Application of cathode-ray oscilloscope to polarographic phenomena (I) differential capacity of elec. double layer, 250; (II) surface charge d. of the elec. double layer, 255; (III) potentials of adsorption–desorption capacity peaks and surface charge d. relationships exhibited by alcs. at aq. saline soln.–Hg interfaces, 935; (IV) peak and min. capacities of adsorption–desorption processes exhibited by alcs. at aq. saline soln.–Hg interfaces, 941; (V) influence of frequency, concn. and structure of alcs. on film formation at aq. saline soln.–Hg interfaces . . . 945

MACDOUGALL, F. H., and Topol, L. E. Ionic equil. in aq. and mixed solvent solns. of Ag acetate and Ag monochloroacetate . . . 1090
Magee, J. L. Elementary processes in radiation chemistry (III) charge transfer mechanisms, 555; see Burton, M., 842.
Manion, J. P., and Burton, M. Radiolysis of hydrocarbon mixts. . . . 560
Mares, T. See Tripp, V. W., 693.
Marinsky, J. A. See Clarke, J. T., 100.

Martell, A. E., and Plumb, R. C. Complexes of various metals with ethylenediaminetetraacetic acid 993
Martin, D. S., Jr. See Hoffman, D. C., 1097.
Mason, D. M., Wilcox, O. W., and Sage, B. H. Viscosities of several liquids 1008
Mathur, H. B. See Mitra, R. P., 633.
Maxwell, C. R. See Henri, V. P., 153.
Mayer, J. E. See Smoluchowski, R., 288.
McLaren, A. D. See Schachat, R. E., 722.
McNeill, W. See Brown, A. S., 701.
Meibohm, A. W. See Jonassen, H. B., 16.
Meier, D. J., and Garner, C. S. Kinetics of Eu(II)-Eu(III) exchange reacn. 853
Merker, R. L., and Zisman, W. A. Competitive adsorption from soln. between hydrophobic and hydrophilic mols. and ions 399
Miller, G. H. See Zucker, D., 166.
Milligan, W. O., and Draper, A. L. Isobaric and isothermal studies in system soap–H_2O (II) 123
Milligan, W. O., and Vernon, L. W. Crystal structure of heavy metal orthovanadates 145
Milligan, W. O., and Whitehurst, H. B. Magnetic properties of adsorbed vapors 1073
Mitra, R. P., and Mathur, H. B. Titration curves of clay minerals attapulgite and nontronite 633
Mizushima, S., Morino, Y., and Shimanouchi, T. Some problems of internal rotation 324
Mod, R. R., and Skau, E. L. Binary f.-p. diagrams for acetamide with oleic and elaidic acids 1016
Morawetz, H., and Hughes, W. L., Jr. Interacn. of proteins with synthetic polyelectrolytes (I) complexing of bovine serum albumin 64
Morehead, F. F., Jr., and Daniels, F. Storage of radiation energy in crystalline LiF and metamict minerals 546
Morino, Y. See Mizushima, S., 324.
Motsch, W. L. See Kobe, K. A., 185.
Mouquin, H. See Bender, M., 272.
Mulliken, R. S. Magic formula, structure of bond energies and isovalent hybridization, 295; mol. compds. and their spectra (III) interacn. of electron donors and acceptors 801
Muschlitz, E. E., Jr., and Simons, J. H. Measurement of electron exchange in gases at low pressure 837
Myers, R. J. See Fineman, M. N., 963.
Myers, R. T., Collett, A. R., and Lazzell, C. L. Rate of saponification of acetate of unsatd. alcs. 461
Myerson, A. L. See Schmitt, J. A., 917.

NAGASAWA, M., and Kobatake, Y. Theory of membrane potential 1017
Narsimhan, G. On the dependence of average polymer mol. wt. on change in particle diameter of a homogeneous monomer emulsion 489
Nehls, J. W. See Schweitzer, G. K., 541, 692.

O'BRIEN, T. D. See Anderson, R., 473; Schnizlein, J. G., 233.
Olsen, S. R. Measurement of surface phosphate on hydroxylapatite and phosphate rock with radiophosphorus 630
Oncley, J. L., Ellenbogen, E., Gitlin, D., and Gurd, F. R. N. Protein–protein interacns. 85
Oriani, R. A. Irreversible phenomena in metallurgy 1025
Osterheld, R. K., and Audrieth, L. F. Polymn. and depolymn. phenomena in phosphate–metaphosphate systems at higher temps.—condensation reacns. involving KH orthophosphates 38
Oth, A., and Doty, P. Macro-ions (II) polymethacrylic acid 43

PARRAVANO, G. See Cimino, A., 706.
Patterson, A., Jr. See Gledhill, J. A., 999.
Pauling, L. Interat. distances and bond character in O acids and related substances, 361; College Chemistry (book review) 672
Pearson, R. G. See Basolo, F., 22.
Penner, S. S. On the kinetics of evaporation 475
Peterson, D. C. See Henri, V. P., 153.
Peterson, S., Jones, J. L., Schmitt, J. M., and Knabeschuh, L. H. Soly. of Ag propionate and Ag butyrate in aq. $NaNO_3$ 491
Pinkerton, R. C. Jacobian method for rapid evaluation of thermodynamic derivs., without use of tables 799
Plane, R. A., and Taube, H. Observations of kinetics of exchange of H_2O between $Cr(H_2O)_6^{+++}$ and solvent 33
Platt, J. R. Prediction of isomeric differences in paraffin properties 328
Plumb, R. C. See Martell, A. E., 993.
Powers, R. A., and Hackerman, N. Ni plating by chem. redn. (I) effect of the basis metal 187
Priest, W. J. Particle growth in aq. polymn. of vinyl acetate 1077

QUINN, F. A., JR. See Bestul, A. B., 432.

RAMAIAH, N. A. Study of Joshi effect in H_2O and D_2O vapor 218
Ramanathan, K. V. See Sastri, M. V. C., 220.
Reif, A. E. Study of reacns. of CO with coke, 778; mechanism of CO_2–C reacn. 785
Reyerson, L. H. See Honig, J. M., 140.
Reynolds, C. A., and Argersinger, W. J., Jr. Constitution and stability of complex ions from soly. minima 417
Riddiford, A. C. Temp. coeff. of heterogeneous reacns. 745
Riethof, T. R. See Edgell, W. F., 326.
Robertson, W. D. Pptn. of colloidal Fe_2O_3 by corrosion inhibitor ions 671
Robinson, R. U. See Brown, A. S., 701.
Rohrer, C. S. See Rooley, J., 1082.
Rohrer, C. S., Christena, R. C., and Brown, O. W. Catalytic activity of some reduced vanadate salts 662
Rollefson, G. K. Frequency factors of some bimol. reacns. 976
Rooley, J., Rohrer, C. S., and Brown, O. W. Catalytic activity of reduced Ni molybdate and reduced Ni chromate 1082
Rose, J. L., Jr. See Schweitzer, G. K., 428.
Rosen, F. D. See Steidlitz, M. E., 1010.
Rosenberg, N. W. See Clarke, J. T., 100.
Rowden, R. W. See Broach, W. J., 189.
Ruff, F. E. See Walling, C., 989.
Rzasa, M. J. See Hough, E. W., 996.

SAGE, B. H. See Mason, D. M., 1008.
Salem, T. M. See El Wakkad, S. E. S., 621.
Samelson, H. See Kimball, G. E., 57.
Sastri, M. V. C., and Ramanathan, K. V. Chemisorption of H on $ZnO–MoO_3$ catalyst—evidence of heterogeneity of the surface 220
Schachat, R. E., Becker, E. I., and McLaren, A. D. Enzyme models (II) kinetics of an artificial carboxylase catalysis 723
Schmitt, J. A., Myerson, A. L., and Daniels, F. Relative rates of hydrolysis of urea containing C^{14}, C^{13} and C^{12} 917
Schmitt, J. M. See Peterson, S., 491.
Schnizlein, J. G. See Anderson, R., 473.
Schnizlein, J. G., Sheard, J. L., Toole, R. C., and O'Brien, T. D. Prepn. and purification of OF_2 and detn. of its vapor pressure 233
Schott, H. See Vold, R. D., 128.
Schubert, J. Ion exchange studies of complex ions as a function of temp., ionic strength and presence of formaldehyde 113
Schweitzer, G. K., and Lee, J. M. Racemization rate studies on tris-(2,2′-dipyridyl)-Ni(II) chloride 195
Schweitzer, G. K., and Nehls, J. W. Variable in self-absorption of low-energy β-particles 541
Schweitzer, G. K., and Rose, J. L., Jr. Racemization rate studies on K tris-(oxalato)-chromate(III) 428
Schweitzer, G. K., Stein, B. R., and Nehls, J. W. Self-absorption phenomena in measurement of radioactivity of Ni^{63} 692
Scott, R. J., and Gunning, H. E. Polymn. of cyclopropane 156
Shafrin, E. G. See Baker, H. R., 405.
Sheard, J. L. See Schnizlein, J. G., 233.
Shiflett, C. H. See Steidlitz, M. E., 1010.
Shimanouchi, T. See Mizushima, S., 324.
Shimizu, M. See Higuti, I., 198.
Silverman, J., and Dodson, R. W. Exchange reacn.

between 2 oxidn. states of Fe in acid soln. 846
Simha, R., and Wall, L. A. Kinetics of chain depolymn. 707
Simons, J. H. See Muschlitz, E. E., Jr., 837.
Simons, J. H., and Hickman, J. B. Energy and vaporization of non-ionic, non-associated substances 420
Sing, K. S. W. See Gregg, S. J., 388.
Singleterry, C. R. See Kaufman, S., 604.
Singleton, W. S. See Ward, T. L., 696.
Sirois, E. H. See Brown, A. S., 701.
Skau, E. L. See Mod, R. R., 1016.
Slabaugh, W. H. Synthesis of org.-bentonite anhydrides 748
Smith, R. P. See Eyring, H., 972.
Smoluchowski, R., Mayer, J. E., and Weyl, W. A. Phase Transformations in Solids (book review) 288
Spencer, W. F., and Gieseking, J. E. Org. derivs. of montmorillonite 751
Spiegler, K. S., and Coryell, C. D. Electromigration in a cation exchange resin (II) detailed analysis of 2-component systems 106
Stamm, A. J. See Tarkow, H. 262, 266.
Steacie, E. W. R. See Ivin, K. J., 967.
Steidlitz, M. E., Rosen, F. D., Shiflett, C. H., and Davis, W., Jr. Ionization of fluorocarbon gases by U-234 α-particles 1010
Steigman, J. See Adler, I., 493.
Stein, B. R. See Schweitzer, G. K., 692.
Stoughton, R. W. See Waggener, W. C., 1.
Stowe, V. M. Activated alumina: heat of wetting by water, 484; activated alumina: heat of wetting by hydrocarbons 487
Stranks, D. R., and Harris, G. M. Isotope effect in some reacns. of C^{14}-labeled carbonatotetrammine cobaltic complex ion 906
Sutherland, G. B. B. M. See Costain, C. C., 321.
Sutton, L. E. See Gilchrist, A., 319.
Svirbely, W. J., and Lewis, B. W. Alkaline hydrolysis of monoethyl malonate ion in isodielec. media . . . 1006
Swoboda, T. J. See Wall, F. T., 50.
Szwarc, M. Energy problems of mol. formation processes 368

TALBOT, E. L. See Cook, M. A., 412.
Tarkow, H., and Stamm, A. J. Reacn. of formic acid with carbohydrates (I) reacn. of formic acid with sugars, 262; (II) polysaccharides: new method for detg. accessibility 266
Tarn, W. H. See Hall, W. K., 688.
Taube, H. See Plane, R. A., 33.
Taylor, H. A. See Anderson, R. D., 161, 498.
Templeton, C. C., and Daly, L. K. System Ni(II) nitrate–water–*n*-hexyl alc. at 25° 215
Thacher, H. C., Jr. Dielec. properties of dispersed liquids (I) theory of dielec. const. 795
Thamer, B. J., and Voigt, A. F. Spectrophotometric detn. of overlapping dissocn. consts. of dibasic acids —acid consts. of isophthalic, terephthalic and chloranilic acids 225
Thibault, H. G. See Brown, A. S., 701.
Thompson, J. B., Washburn, E. R., and Guildner, L. A. Adsorption of CO_2 by glass 979
Thompson, L. R., and Wilmarth, W. K. Binuclear peroxo compds. of tri- and tetrapositive Co 5
Thompson, R. N. Explanation of "tackypyknosis" . . 766
Thompson, S. O., Turkevich, J., and Irsa, A. P. Study of Fischer–Tropsch reacn. using D gas 243
Thornton, J. L., Jr. See Walling, C., 989.
Tofias, A. See Brown, A. S., 701.
Toole, R. C. See Anderson, R., 473; Schnizlein, J. G., 233.
Topol, L. E. See MacDougall, F. H., 1090.
Torkington, P. Possible motions of vibrating mols. and their interpretation in terms of mol. structure . . . 336
Trautman, R., and Gofman, J. W. Hydrodynamic factors in moving boundary electrophoresis—introduction to electrophoretic study of lipoproteins 464
Tripp, V. W., Conrad, C. M., and Mares, T. Some relations between intrinsic and sp. viscosity in cellulose solns. at a controlled velocity gradient 693
Turkevich, J. See Thompson, S. O., 243.

UDIN, H. See Buttner, F. H., 657.
Urquhart, J. M. See Klotz, I. M., 77.

VERNON, A. A. See Hughes, V. L., 927.
Vernon, L. W. See Milligan, W. O., 145.
Voigt, A. F. See Thamer, B. J., 225.
Vold, R. D., Grandine, J. D., 2nd, and Schott, H. Characteristic X-ray spectrometer patterns of satd. Na soaps 128
Volman, D. H., and Doyle, G. J. Retentivity of charcoals by approx. isotherm method—effect of moisture on retentivity of Me Et ether, neopentane and MeOH 182

WAGGENER, W. C., and Stoughton, R. W. Chemistry of Th in aq. solns. (II) chloride complexing as a function of ionic strength 1
Wagner, G. H., and Dobay, D. G. O deficient silica phosphors 538
Waldock, K. T., and Frizzell, L. D. Study of functional groups of cation exchangers by infrared absorption 654
Wall, F. T. See Kimpton, D. D., 715.
Wall, F. T., and Swoboda, T. J. Electrolytic interacn. of nylon with aq. solns. of NaOH 50
Wall, L. A. See Simha, R., 707.
Walling, C., Ruff, E. E., and Thornton, J. L., Jr. Improved apparatus for study of foams 989
Wang, H. L., and Hackerman, N. Sorption of gases on metal powders and subsequent change in metal reactivity at room temp. 771
Ward, T. L., and Singleton, W. S. Phys. properties of fatty acids (II) some dilatometric and thermal properties of palmitic acid 696
Washburn, E. R. See Dunning, H. N., 235; Thompson, J. B., 979.
Wehner, P., and Hindman, J. C. Chloro complexes of Ru(IV) 10
Welsh, J. Y., and Garrett, A. B. Dissoln. of metals over temp. range of 25 to -60° (III) dissoln. of Zn in HCl–MeOH–H_2O solns. 727
West, W., Carroll, B. H., and Whitcomb, D. H. Adsorption of sensitizing dyes in photographic emulsions 1054
Weyl, W. A. See Smoluchowski, R., 288.
Whitcomb, D. H. See West, W., 1054.
White, W. C. See Henri, V. P., 153.
Whitehurst, H. B. See Milligan, W. O., 1073.
Wicke, E. Dissocn. energy of F 358
Wijnen, M. H. J. See Ivin, K. J., 967.
Wilcox, O. W. See Mason, D. M., 1008.
Wilkinson, G. Review of "College Chemistry" (Pauling) 672
Williams, R. R., Jr. See Gevantman, L. H., 569.
Wilmarth, W. K. See Thompson, L. R., 5.
Winsor, P. A. Interpretation of published X-ray measurements on detergent solns. on basis of an intermicellar equil. 391
Wirtz, K. See Gierer, A., 914.
Wolfgang, R. L., and Dodson, R. W. Isotopic exchange between valence states of Hg 872
Wood, B. B., Jr. See Hough, E. W., 996.
Wood, G. B. See Kurbatov, M. H., 698.

YOSIM, S., and Davies, T. H. Recoil atoms from slow neutron capture by Au and In surfaces 599
Young, F. E., Jones, F. T., and Lewis, H. J. D-Fructose dihydrate, 738; D-fructose–H_2O phase diagram 1093

ZISMAN, W. A. See Baker, H. R., 405; Merker, R. L., 399.
Zucker, D. See Foster, J. F., 170, 174.
Zucker, D., Foster, J. F., and Miller, G. H. Design and performance of a photoelec. circuit for measurement of streaming birefringence and dichroism 166

Subject Index to Volume LVI, 1952

ABSORPTION, variables in self-, of low-energy β-particles ... 541
Acetamide, binary f.-p. diagrams for, with oleic and elaidic acids ... 1016
Acetic acid, adsorption on Al_2O_3, 373; cryoscopy of, in formamide, 281; magnetic susceptibility of adsorbed ... 1073
Acetylene, low vapor pressure measurement of, 660; adsorption on C blacks, 756; charge transfer in radiation chemistry of ... 842
Activity coefficients, in ion exchange equil. ... 92
Adsorption, isotherms in soap–H_2O systems, 123; of N, O and A on rutile at low temps., 140; mathematics of, 148; retentivity of charcoals by approx. isotherm method, 182; rate-detg. steps in radial, analysis, 373; approximate, isotherms for a mixt. of 2 isotopes, 384; competitive, from soln. between hydrophilic and hydrophobic mols. and ions, 399; of hydrophobic monolayers of carboxylic acids, 405; of UX_1 and Ra E by Aquadag coated dipping Geiger–Mueller tube, 493; of aq. xanthate on galena surfaces, 616; role of, in redn. of org. Hg compds. at dropping Hg electrode, 648; of O on Ag, 657; preferential capillary, of water from solns. of alcs. by silica gel, 665; mathematics of, in beds, 683, 984; rate of, of CO^{++} on hyd. Fe_2O_3, 698; of CO_2 by glass, 979; of Co and Ba ions by hyd. Fe_2O_3, 982; at H_2O–He, –CH_4 and –N interfaces, 996; of sensitizing dyes in photographic emulsions, 1054; isotherms, of H_2O, *n*-PrOH, AcOH, salicylaldehyde and *n*-heptane on silica gel ... 1073
Air, collision diameters of ... 797
Albumin, thermal denaturation of X-rayed egg, 789, (corrn.) ... 1110
Alcohols, potentials of adsorption–desorption capacity peaks for, 935; peak and minimum capacities of adsorption–desorption for, 941; film formation at aq. saline–Hg interface ... 945
Alkali halide, luminescence of, crystals subjected to ionizing radiation ... 548
n-Alkanecarboxylic acids, crit. concns. of K salts of . 953, 959
Alkanes, energy of vaporization of ... 420
Alumina, surface structure of colloidal, 136; adsorption of N, O and A on, 140; satn. of, with $CuSO_4$ and HAc soln., 373; γ-, from gibbsite, 388; heat of wetting of activated, by water, 484, and by hydrocarbons, 487; factors governing hardness and transparency of, gels ... 762
Aluminum bromide, phase rule studies in anhyd. ... 730
Aluminum chloride, Brownian movement and elec. effects ... 272
Amines, adsorption of hydrophobic monolayers on, 405; reacn. between *t*-, and org. acids in non-polar solvents, 604; sorption of, by silica gels ... 733
Ammonia, H exchange reacns. over Fe synthetic. catalysts, 258; potential barriers restricting inversion in, 321; adsorption on C blacks ... 756
Amylose, length of I–, complex as detd. by streaming dichroism, 170; streaming birefringence behavior of subfractionated ... 174
Apatite, radiophosphorus for measuring surface phosphate on hydroxyl- ... 630
Argon, adsorption on rutile, 140; collision diameters of ... 797
Arsine, potential barriers restricting inversion in ... 321
Attapulgite, titration curves of ... 633

BARIUM. adsorption of Ba ions by hyd. Fe_2O_3 ... 982
Bentonite, synthesis of org.-, anhydrides ... 748
Benzene, affinity of water–, mixt. for C, 193; interfacial contact angles in mercury–water–, system, 453; interfacial tension between Hg and, 532; heat capacity of, sorbed on SiO_2 gel ... 921
Bimolecular reactions, probability factor in ... 1101
Binary mixtures, liquid, viscosity of liquid, mixts ... 1052
Birefringence, photoelec. circuit for measurement of streaming, 166; streaming, behavior of subfractionated amyloses ... 174
Boehmite, from gibbsite ... 388
Bond energy, problem of, 289; structure of, and isovalent hybridization, 295; problems of mol. formation processes ... 368
Bond length, factors affecting, in conjugated and aromatic mols. ... 311
Bonds, relations between length and reactivity in some C–halogen, 319; H, in org. crystals ... 502
Bond strength, method of detg. potential barriers restricting inversion in NH_3, PH_3, and AsH_5 from vibrational force consts., 321; some problems of internal rotation, 324; of C halides, 326; of C–C bonds in paraffins, 328; of vibrating mols., 336; of volatile fluorides, 343; of subsd. methanes and acyclic aliphatic hydrocarbons, 351; in O acids and related substances, 361; in conjugated mols. ... 365
Boundary tension, at water–org. liquid interfaces ... 480
Bromine, kinetics of oxidn. of Fe(II) by ... 877
Bromine fluoride, spectra and dissocn. energies of ... 316
Brom phenol blue, reacn. with $AgNO_3$ ... 189
Brownian movement, and elec. effects ... 272
Butane, adsorption on C blacks ... 756
Butane compounds, saponification rate of 3-butene-3-ol and 3-butyn-2-ol ... 461
Butyl alcohol, boundary tension at water–, interfaces. 480
Butyl alcohols, diffusion coeffs. and related properties of ... 235
Butyric acid, solv. of Ag salt of, in aq. $NaNO_3$ ... 491

CADMIUM, dissoln. in HCl–MeOH–H_2O solns. ... 449
Cadmium dimethyl, prepn. and phys. consts. of, 161; photolysis of ... 498
Calcium, Ca^{45}, low-energy β-particles from ... 541
Calcium nitrate, soly. in monoalkyl ethers of ethylene glycol ... 185
Capillary condensation theory, calorimetric evidence for ... 921
Carbon, affinity of liquids for activated, 193; temp. coeff. of, oxidn., 745; reacns. of CO with coke, 778; mechanism of CO_2–C reacn., 785; structure of graphite oxide ... 929
Carbon, $C^{12,13,14}$, isotope subsn., 823; relative rates of hydrolysis of urea containing ... 917
Carbon, C^{13}. enrichment of isotope by difference in rates for irreversible, reacns., 893; effect of, subsn. on collision properties of CO_2 mol. ... 911
Carbon, $C^{13,14}$, in decompn. of oxalic acid ... 897
Carbon. C^{14}. cataphoresis study of tridecanoates, 238; in decarboxylation of malonic acids, 901; isotope effect in, labeled carbonatotetrammine cobaltic ion. 906
Carbon black, sorption of GR-S type of polymer on commercial, 740; surface complexes on ... 753, 756
Carbon bonds, factors affecting bond lengths in conjugated and aromatic mols., 311; relations between length and reactivity in some halogen– ... 319
Carbon dioxide on C black surface, 753; mechanism of C–, reacn., 785; collision properties of, mol., 911; adsorption of, by glass ... 979
Carbon monoxide, reacns. with coke ... 778
Carbon tetrachloride, heat capacity of, sorbed on SiO_2 gel ... 921
Carboxylase, kinetics of an artificial, catalysis ... 722
Carboxylic acids, adsorption of hydrophobic monolayers of ... 405
Catalysis. activity of some reduced vanadate salts, 662; kinetics of an artificial carboxylase, 722; of cerous–ceric electron exchange reacn. by fluoride ... 869
Catalysts. H exchange reacns. over Fe synthetic NH_3, 258; oxidn. and redn. of fused Fe, 688; Ni molybdate and chromate as, for vapor phase redn. of 1-nitropropane ... 1082
Cataphoresis, study in hydrocarbon oil by radioactive and microscopic methods ... 238
Cellulose, viscosity in, solns. at controlled velocity gradient ... 693

Cerium compounds, fluoride catalysis of cerous–ceric electron exchange 869
Chain depolymerization, kinetics of 707
Charcoal, retentivity of, by approx. isotherm method. 182
Chemistry, College (Pauling, book review) 672
Chloranilic acid, acid dissocn. consts. of 225
Chlorine, sorption on metal powders 771
Chlorine fluoride, isotope exchange reacns. of F^{18} with 885
Chromatography, distribution of liq. ascending in a filter paper, 625, (corrn.) 1110; mathematics of . . . 984
Chromium, sorption of gases on, powder 771
Chromium compounds, kinetics of exchange of H_2O between $Cr(H_2O)_6{}^{+++}$ and solvent, 33; racemization studies on K tris-(oxalato)-chromate (III), 428; retarding effect of $CrO_4^{=}$ in polymn. of silicic acid, 678; catalytic activity of reduced Ni chromate 1082
Cobalt compounds, binuclear peroxo compds. of tri- and tetrapositive, 5; complex, 16; aquation and hydrolysis of acetatopentammine-cobalt (III) ions, 22; effects of Co γ-radiation on water and aq. solns., 587; rate of adsorption of Co^{++} on hydrous Fe_2O_3, 698; isotopic effect in C^{14}-labeled carbonatotetrammine cobaltic ion, 906; adsorption of Co ions by hyd. Fe_2O_3, 982; photonuclear prepn. of Co-58, Co-58m 1097
Collision diameters, of some gases as functions of temp. 797
Conductance, measurement of high field, of electrolytes 999
Contact angles, interfacial, in mercury–benzene–water system 453
Copper, Cu(II)–cyanide reacn., 19; electron microscopic study of cystine–, complex 768
Copper sulfate, saturation of Al_2O_3 with, soln. 373
Corundum, from gibbsite 388
Cryoscopic studies, of chlorides and org. acids in formamide, 281; data resulting from addn. of acids to amines in benzene 604
Crystal structure, of heavy metal orthovanadates, 145; H bond in org. crystals 502
Cyanide, Cu(II)–, reacn. 19
Cyclohexane, chem. effects of α-particles on 153
Cyclohexylcarboxylic acid, adsorption on Pt 399
Cyclopropane, polymn. of 156
Cystine, electron microscopic study of Cu–, complex . . 768

DEUTERIUM, study of Fischer–Tropsch reacn. using, gas, 243; significance of isotopic reacns. in rate theory 889
Deuterium oxide, study of Joshi effect of H_2O and, vapor 218
Deuterium peroxide, force consts. in 340
Deuteron, proton and, transfer over H 914
Diacetone alcohol, phys. properties of 1013
Dichroism, photoelec. circuit for measurement of, 166; length of amylose–I complex as detd. by streaming. 170
Dielectric constant, theory of 795
Dielectric properties, of *o*-nitrophenol sorbed on silica gel 198
Diffusion, process for organolite exchangers, 97; effect of intraparticle, in agitated static systems, 148; effect of intraparticle, in flow systems in fixed beds, 683; effect of longitudinal, in ion exchange and chromatographic columns 984
Diffusion coefficient, of Bu alcs., 235; detn. of, from rates of evaporation 715
Diffusion current, relation between, and frequency and amplitude of vibration 439
Dissociation energy, of BrF and IF, 316; of F 358
Dodecylbenzenesulfonic acid, foam production with Na salts of 989
Dyes, interacn. of optically isomeric, with bovine serum albumin, 70; adsorption of sensitizing, in photographic emulsions 1054
Dynamical systems, statistical mechanics of, with integrals other than energy 1039

ELAIDIC acid, binary f.-p. diagrams for acetamide with oleic and 1016
Electric moment, dielec. properties of dispersed liquids 795
Electrochemical properties, of a permionic anion membrane 100
Electrolysis, interacn. of nylon with aq. NaOH solns. . 50
Electrolytes, X-ray measurements of colloidal, and ethylene oxide derivs., 391; measurement of high field conductance of 999
Electromigration, in a cation exchange resin—2-component systems 106
Electron diffraction, of C bonds, 324; of volatile fluorides, 343; study of films formed by $NaNO_2$ on Fe. 451
Electron microscope, in study of Cu–cystine complex. 768
Electron, transfer, interacn. of electron donors and acceptors, 801; measurement in gases at low pressure, 837; in radiation chemistry of gases, 842; processes and oxidn.–redn. reacns. of hexacyanoferrate(III) ion, 858; theory of, reacns. in aq. soln., 863; reacn. of $Ce^{+++} \rightleftarrows Ce^{++++}$ 869
Electrophoresis, hydrodynamic factors in moving boundary, of lipoproteins, 464; analysis of protein interacn. 717
Emulsions, structural colors in 510
Energy, interacn. of electron donors and acceptors 801
Energy of vaporization, of non-ionic, non-associated substances 420
Enthalpy, calcn. of, changes from free-energy data . . . 427
Entropy, calcn. of, changes from free-energy data, 427; of palmitic acid 696
Enzyme models 723
Ethane, free radicals in radiolysis of, 569; vapor pressure of 660
Ethyl alcohol, interfacial tension between Hg and 532
Ethylene, vapor pressure of 660
Ethylenediamine, complex ions from Fe and, tetraacetate, 25; viscosity of 1008
Ethylenediaminetetraacetic acid, complexes of metals with 993
Ethylene glycol, soly. of Ca and Sr nitrate in, ethers . . 185
Ethylene oxide, polymer of, in foaming of non-ionic surface active agent 963
Ethylenetriamine, formation consts. of complex ions of di- and tri-, with divalent ions 16
Ethyl radicals, reacns. of 967
Europium, kinetics of Eu(II)–Eu(III) reacn. 853
Evaporation, kinetics of, 475; detn. of diffusion coeffs. from rates of 715

FISCHER-TROPSCH reaction, study of, using D gas, 243; studies of synthesis 688
Flotation, surface oxidn. of galena in relation to its, 610; collector-depressant equil. in 637, 643
Fluorides, prepn. and purification of OF_2, 233; structures of volatile, 343; catalytic effect of, in polymn. of silicic acid, 680; catalysis of cerous–ceric electron exchange, 869; soly. of metal, in liq. HF 1106
Fluorine, dissocn. energy of, 358; isotope exchange reacns. of, with halogen fluorides 885
Fluorocarbon, ionization of, gases by U-234 α-particles 1010
Foam, mechanical, destruction of young and old, films, 164; of non-ionic surface active agents, 963; improved apparatus for study of 989
Force constants, in H and D peroxides 340
Formaldehyde, in ion exchange study of complex ions. 113
Formamide, cryoscopy of chlorides and org. acids in . . 281
Formic acid, reacn. with sugars, 262; reacn. of polysaccharides with, 266; ionizing radiation in aq. solns. of 594
Free radicals, in radiolysis of alkanes and alkyl iodides 569
D-Fructose, H_2O–, phase diagram 1093
D-Fructose dihydrate 738
Furfuryl alcohol, viscosity of 1008

GALENA, surface oxidn. of, in relation to its flotation, 610; adsorption of aq. xanthate on, surfaces 616
Gases, new relation of transport properties of 1034
Germanium compounds, Raman spectra of 355
Gibbsite, effect of heat on surface properties of 388
Glass, adsorption of CO_2 by glass 979
Glass electrode, theory of membrane potential 1017
γ-Globulin, interacn. of β-lipoprotein and 85
Glyoxylic acid, thermal, catalyzed decarboxylation of Ph-, by 3-amino-α-naphthoxindole 722
Gold, recoil atoms from neutron capture by, surfaces . . 599
Graphite, adsorption of UX_1 and Ra E by Aquadag coated dipping tube 493
Graphite oxide, structure of 929

HALOGEN, length and reactivity of C-, bonds, 319; Ge–H bond in $GeHX_3$ and mobility of, bond 355
Heat capacity, of benzene and CCl_4 sorbed on SiO_2 gel 921
Heat of fusion, of palmitic acid 696
Heat of wetting, of activated alumina by water, 484, and by hydrocarbons 487
Helium, adsorption isotherms for, 384; mobilities of positive ions of, 832; α-ray energy in radiation chemistry, 920; adsorption at He–H_2O interface 996
n-Heptane, structural colors in emulsions of, with benzene and nitromethane, 510; interfacial tension between Hg and, 532; magnetic susceptibility of adsorbed 1073
Heptanes, heat of wetting of activated alumina by 487
Heptanoic acid, salt effect on crit. concns. of K salt of 959
Hexane, chem. effect of α-particles on 153
n-Hexane, production of Ni_3C by decompn. of, on metallic Ni 706
n-Hexyl alcohol, system Ni(II) nitrate–water– 215
Hybridization, magic formula, structure of bond energies and isovalent, 295; factor affecting bond lengths in conjugated and aromatic mols 311
Hydrazine, viscosity of 1008
Hydrocarbons bond strengths in conjugated, 365; radiolysis of, mixts 560
Hydrochloric acid, dissoln. of Zn in MeOH–H_2O–, solns 727
Hydrofluoric acid, solv. of fluorides of metals in liq. 1106
Hydrogen, chemisorption on ZnO–MoO_3 catalyst, 220; exchange reacns. over Fe synthetic NH_3 catalysts, 258; Joshi effect in, 457; mobilities of positive ions of, 832; measurement of electron exchange in, at low pressure, 837; theory of electron exchange reacn., 863; proton and deuteron transfer over 914
Hydrogen bond, in org. crystals 502
Hydrogen peroxide, force consts. in, 34; reacn. with donor particles 279
Hydrolysis, surface, in Na lauryl sulfate solns., 412; relative rates of, of urea containing C^{14}, C^{13} and C^{12} 917

INDIUM, recoil atoms from neutron capture by, surfaces 599
Insulin monomers, interacn. of 85
Interfacial tension, between Hg and other liquids 532
Iodine, length of amylose–, complex as detd. by streaming dichroism, 170; thermal conductivity of, vapor 358
Iodine, I^{131}, in radiolysis of alkyl iodides 569
Iodine fluoride, spectra and dissocn. energies of 316
Ion exchange. See under *Resins*.
Ionization, of fluorocarbon gases by U-234 α-particles 1010
Ions, chloride complexing as a function of ionic strength, 1; binuclear peroxo complex compds. of Co, 5; chloro complexes of Ru(IV), 10; formation consts. of di- and triethylenetetramine with divalent, 16; Cu(II)–cyanide reacn., 19; aquation and hydrolysis of acetatopentamminecobalt(III), 22; complex, from Fe and ethylenediaminetetraacetate, 25; macro-, 43; distribution in solns. of weak electrolytes, 60; charge transfer and mobility of rare gas, 829; mobilities of positive, in their parent gases 832
Iron, electron diffraction study of films formed by $NaNO_2$ solns. on, 451; structural changes of a reduced, catalyst on reoxidn., 688; sorption of gases on stainless steel 771
Iron compounds, ethylenediaminetetraacetate–, ions, 25; H exchange reacns. over, synthetic NH_3 catalysts, 258; exchange reacn. between 2 oxidn. states of, 846; hexacyanoferrate(III) ion in aq. soln., 858; kinetics of oxidn. of Fe(II) by Br_2 877
Iron oxide, pptn. of colloidal Fe_2O_3 by corrosion inhibitor ions, 671; adsorption of Co^{++} on hydrous Fe_2O_3, 698; adsorption of Co and Ba ions by hyd. Fe_2O_3 982
Isoelectric point, Brownian movement and elec. effects 272
Isophthalic acid, acid dissocn. consts. of 225
Isopropylamine, viscosity of 1008
Isotopes, effects of, subsn. on rates of chem. reacns. 823

JACOBIAN method, for calcn. of thermodynamic derivs 799
Joshi effect, in H_2O and D_2O vapor, 218; production of, under direct current excitation 457

KINETIC theory, relation among, cross-section integrals 1034
Krypton, sorption on metal powders 771

LAURIC acid, mechanical destruction of young and old foam films of 164
Lauryl alcohol, surface hydrolysis in Na lauryl sulfate solns 412
Laurylpyridinium chloride, micelle concn. of 701
Lead sulfide, surface oxidn. of galena in relation to its floatation, 610; adsorption of xanthate on, 616; inorg. depressants for 637, 643
Linoleic acid, solv. in common org. solvents 1068
Lipoprotein, interacn. of γ-globulin and β-, 85; electrophoretic study of 464
Lithium fluoride, storage of radiation energy in crystalline, 546; luminescence of 548
Luminescence, of alkali halide crystals subjected to ionizing radiation 548
Macroscopic equations of transport 1048
Magnetic susceptibility, of adsorbed vapors 1073
Malonic acid, C^{14} in decarboxylation of, 901; alkaline hydrolysis of monoethyl malonate ion in isodielec. media 1006
Manganate ion, disproportionation of 882
Mechanics, statistical, of dynamical systems with integrals other than energy 1039
Membrane potential, theory of 1017
Mercury, interfacial contact angles in benzene–water–, system, 453; interfacial tension between, and other liquids, 532; oxide film formation on, surfaces in aq. solns., 621; role of adsorption in redn. of org. compds. at dropping, electrode, 648; isotopic exchange between the valence states of, with Hg_2O_3, 872; potentials of desorption–adsorption capacity peaks in polarography 935, 941, 945
Mercury diethyl, photosensitized decompn. of 967
Mesityl oxide, phys. properties of 1013
Metallurgy, irreversible phenomena in 1025
Metals, solv. of, fluorides in liq. HF 1106
Metamict minerals, storage of radiation energy in 546
Methacrylic acid, poly- 43
Methane, vapor pressure of, 660; adsorption at CH_4–H_2O interface 996
Methanes, bond distance relations in subsd 351
Methanol, retentivity when adsorbed on charcoal 182
Methyl alcohol, dissoln. of Cd in HCl–MeOH–H_2O, 449; dissoln. of Zn in HCl–H_2O–, solns 727
Methylamine, adsorption on C blacks 756
Methyl ethyl ether, retentivity when adsorbed on charcoal 182
Methyl isobutyl ketone, phys. properties of 1013
Methyl orange, boundary anomaly in serum albumin–, system 717
Micelle concentration, crit., by bubble pressure method 701
Molecular weight, average polymer 489
Molybdenum, sorption of gases on, powder 771
Molybdenum compounds, catalytic activity of reduced Ni molybdate 1082
Molybdenum oxide, chemisorption of H on ZnO–, catalyst 220
Montmorillonite, org. derivs. of 751
Moving boundary electrophoresis, hydrodynamic factors in, of lipoproteins 464

NAPHTHALENE, redn. of nitro-, to 1-naphthylamine 662
α-Naphthoxindole, thermal, catalyzed decarboxylation of phenylglyoxylic acid by 3-amino- 722
Neon, charge transfer and mobility of, ions 829
Neopentane, retentivity when adsorbed on charcoal 182
Neutron, decompn. of H_2O, 575; recoil atoms from, capture by Au and In surfaces 599
Nickel, sorption of gases on, powder 771
Nickel, N^{63}, self-absorption phenomena in measurement of radioactivity of 692
Nickel compounds, racemization rate studies on tris-(2,2′-dipyridyl)–Ni(II) chloride, 195; system Ni(II) nitrate–water–n-hexyl alc., 215; production of Ni_2C by decompn. of n-hexane on metallic Ni, 706; $Ni(CO)_4$ in C^{13} enrichment reacn., 893; catalytic activity of reduced Ni molybdate and chromate 1082

Nickel plating, by chem. redn. 187
Nitrates, photolysis of crystalline 764
Nitric acid, viscosity of red and white fuming 1008
Nitrogen, adsorption on rutile, 140; collision diameters of, 797; adsorption at N–H_2O interface 996
Nitrogen, $N^{14,15}$, isotope subsn. 823
Nontronite, titration curves of 633
Nylon, electrolytic interacn. with aq. NaOH solns. 50

OCTADECYLAMINE, dual adsorption of stearic acid and, on steel 524
n-Octylamine, adsorption on Pt 399
Oleic acid, binary f.-p. diagrams for acetamide with elaidic and, 1016; solv. in common org. solvents 1068
Organic compounds, assocn. between polysilicic acid and polar 673
Organolite, diffusion process for, exchangers 97
Oscilloscope, application of cathode-ray to polarographic phenomena 250, 255, 935, 941, 945
Osmosis, phenomenology of electro-, and streaming potential 775
Oxalic acid, isotope effect in decompn. of 897
Oxygen, adsorption on rutile, 140; adsorption on Ag, 657; collision diameters of 797
Oxygen, $O^{16,18}$, isotope subsn. 823
Oxygen acids, interat. distances in, and related substances 361
Oxygen fluoride, prepn. and purification of, 233; viscosity, d. and crit. consts. of 473

PALMITIC acid, dilatometric and thermal properties of 696
Paraffin, prediction of isomeric differences in, properties, 328; bond distance relations in subsd. methanes and acyclic aliphatic 351
Particles, chem. effect of α-, on C_6-hydrocarbons, 153; logarithmico-normal distribution of, size—homogeneity and heterogeneity, 442; variables in self-absorption of low-energy β-, 541; growth, in aq. polymn. of vinyl acetate 1077
Pentane compounds, saponification rate of 3-Me-1-pentyn-3-ol and 3-Me-1-penten-3-ol 461
Percolation, theory of, for 2 solutes 949
Periodic law, in math. form, 178, (corrn.) 1110; of chem. thermodynamic functions 202
Permionic anion membrane, electrochem. properties of a 100
Peroxo compounds, binuclear, of tri- and tetrapositive Co 5
Phase rule, studies in anhyd. $AlBr_3$, 730; D-fructose–H_2O phase diagram 1093
Phase transformations, in Solids (Smoluchowski, Mayer, Weyl, book review) 288
Phenol, freezing phenomenon of *o*-nitro-, sorbed on silica gel 198
Phosphine, potential barriers restricting inversion in 321
Phosphoric acid, condensation reacns. involving KH orthophosphates, 38; radiophosphorus for measuring surface phosphate on hydroxylapatite and phosphate rock, 630; quaternary ammonium salts of high mol. wt. polymeta- 1086
Phosphors, O deficient silica 538
Phosphorus, P^{32}, in measurement of surface phosphate 630
Phosphotungstic acid, extent of photochem. redn. of 1084
Photochemistry, redn. of phosphotungstic acid 1084
Photolysis, of $CdMe_2$, 498; of crystalline nitrates 764
Phthalein, reacn. of tetrabromophenolsulfon-, and $AgNO_3$ 189
Pinacyanole, in detn. of crit. concns. of K *n*-alkanecarboxylates 953, 959
Platinum, adsorption of *n*-octylamine on 300
Polarography, application of cathode-ray oscilloscope to, phenomena, 250, 255, 935, 941, 945; vibrating micro-electrodes in 439
Polydentate groups, inorg. complex compds. containing 16
Polyelectrolytes, theory of, 57; interacn. of proteins with synthetic 64
Polymer, average, mol. wt. 489
Polymerization, and de-, phenomena in phosphate–metaphosphate systems, 38; of cyclopropane, 156; of silicic acid, 678, 680; kinetics of chain de-, 707; particle growth in aq., of vinyl acetate 1077
Polystyrene, phys.-chem. properties of 514
Potassium chloride, cryoscopy of, in formamide, 281; polarography of 935, 941, 945
Potential, Hg–HgO electrode, 621; phenomenology of electro-osmosis and streaming, 775; ionic equil. in solns. of Ag acetate and monochloroacetate 1090
Probability factor, in bimol. reacns. 1101
Propane, reduced Ni molybdate and chromate as catalysts for vapor phase redn. of 1-nitro- 1082
1,2,3-Propanetricarboxylic acid, ion distribution in 60
Propionic acid, solv. of Ag salt of, in aq. $NaNO_3$ 491
n-Propyl alcohol, magnetic susceptibility of adsorbed 1073
2-Propyl-1-ol, saponification rate of 461
Proteins, interacn. with synthetic polyelectrolytes, 64; binding of org. ions by 77; protein–protein interacns., 85; H bond in org. crystals, 502; electrophoretic analysis of, interacn. 717
Proton, and deuteron transfer over H 914
Pyridine cpds, racemization rate studies on tris-(2,2′-dipyridyl)–Ni(II) chloride 195

QUATERNARY ammonium salts, solys. of, in org. solvents, 927; of high mol. wt. polymetaphosphoric acid 1086
Quebracho, depressant action of 643

RACEMIZATION, rate studies on K tris-(oxalato)-chromate(III) 428
γ-Radiation, decompn. of H_2O and aq. solns. under mixed fast neutron and, 575; H_2O decompn. by, 587; ionizing, in aq. solns. of formic acid 594
Radiation chemistry, symposium on, 545; charge transfer mechanisms in, 555; luminescence of alkali halide crystals subject to ionizing, 548; charge transfer in, of gases, 842; distribution of α-ray energy in 920
Radiation energy, storage of, in crystalline LiF 546
Radioactivity, self absorption, phenomena in measurement of, Ni-63 692
Radiolysis, of hydrocarbon mixts., 560; free radicals in, of alkanes and alkyl iodides 569
Radium E, adsorption of UX_1 and Ra E by Aquadag coated dipping tube 493
Rare earths, complexes with ethylenediaminetetraacetic acid 993
Rare gas, charge transfer and mobility of, ions 829
Reactions. See Fischer-Tropsch reaction.
Reaction velocity, of aquation and hydrolysis of acetatopentamminecobalt(III) ions, 22; of exchange of H_2O between $Cr(H_2O)_6^{+++}$ and solvent, 33; racemization, studies on tris-(2,2′-dipyridyl)–Ni(II) chloride, 195; reacn. of H_2O_2 with donor particles, 279; rate-detg. steps in radial adsorption analysis, 373; racemization studies on K tris-(oxalato)-chromate(III), 428; saponification rate of acetates of unsatd. alcs., 461; kinetics of evaporation, 475; decompn. of water and aq. solns. under mixed fast neutron and γ-radiation, 575; of chain depolymn., 707; of an artificial carboxylase catalysis, 722; photolysis of crystalline nitrates, 764; of thermal denaturation of X-rayed egg albumin, 789, (corrn.) 1110; effects of isotopic subsn. on rates of chem. reacns., 823; exchange reacn. between 2 oxidn. states of Fe, 846; of Eu(II)–Eu(III) exchange reacn., 853; of $Fe^{++} \leftrightarrows Fe^{+++}$, 858; isotopic exchange between valence states of Hg, 872; oxidn. of Fe(II) by Br_2, 877; of $MnO_3^{=} \leftrightarrows MnO_2 + MnO_4^{-}$, 882; significance of isotopic reacns. in rate theory, 889; enrichment of isotopes by differences in rates for isotopic reacns., 893; hydrolysis of urea, 917; of Et radical reacns., 967; recent developments in, theory, 972; frequency factors of some bimol. reacns., 976; alkaline hydrolysis of monoethyl malonate ion 1006
Reduction, Ni plating by chem. 187
Resins, ion exchange, radioactive exchange in complex ions from Fe and ethylenediaminetetraacetate, 25; activity coeffs. in, equil., 92; diffusion process for Organolite exchangers, 97; studies of complex ions as function of temp., ionic strength and presence of formaldehyde, 113; sepns. based on ionic size, 118; adsorption of KCl, 373; theory of per-

colation for 2 solutes, 949; effect of longitudinal diffusion in, and chromatographic columns........ 984
Resin, cation exchange, electromigration in, 106; study of functional groups of cation exchangers by infrared absorption........ 654
Rubber, viscosities of 0.25 to 90% GR-S, solns., 432; sorption of GR-S type of polymer on C black...... 740
Ruthenium, chloro complexes of Ru(IV)........ 10
Rutile, adsorption of N, O and A on........ 140

SACCHARIDES, reacn. of formic acid with poly-.... 266
Salicylaldehyde, magnetic susceptibility of adsorbed.. 1073
Serum albumin, complexing of bovine, 64; interacn. of optically isomeric dyes with bovine, 70; comparison of binding of bovine and human, 77; interacn. of human, with its homologous equine antibody, 85; boundary anomaly in Me orange-bovine, system........ 717
Silica, surface structure of colloidal, 136; O deficient, phosphors........ 538
Silica gel, freezing phenomenon of *o*-nitrophenol sorbed on, 198; capillary adsorption of water from alc. by, 665; sorption of amines by........ 733
Silicic acid, assocn. between poly-, and polar org. compds. 673; retarding effect of $CrO_4^=$ in polymn. of, 678; catalytic effect of fluoride in polymn. of.. 680
Silver, adsorption of O on........ 657
Silver compounds, ionic equil. of Ag acetate and monochloroacetate........ 1090
Silver nitrate, reacn. of tetrabromophenolsulfonphthalein and........ 189
Silver oxide, soly. in alkali solns........ 417
Soap, isobaric and isothermal studies in H_2O-, system, 123; X-ray spectrometer patterns of satd. Na..... 128
Sodium, Na,^{22} in ion exchange........ 106
Sodium hydroxide, electrolytic interacn. of nylon with aq., solns........ 50
Sodium nitrite, electron diffraction of films formed by, soln. on Fe........ 451
Solubility, constitution and stability of complex ions from, minima........ 417
Sorption, of amines by silica gels, 733; of GR-S type of polymer on C black, 740; of gases on metal powders........ 771
Spectra, absorption, of Ru(IV) chloro complexes, 10; for isophthalic, terephthalic and chloranilic acids... 225
Spectra, emission, and dissocn. energies of BrF and IF 316
Spectra, infrared absorption, of deuterated hydrocarbons, 243; and Raman, of C bonds, 324; study of functional groups of cation exchangers by........ 654
Spectra, Raman, in study of Ge-H bond in $GeHX_3$ mols........ 355
Spectra, X-ray, of Na soaps........ 128
Spectra, vibrational, of H and D peroxides........ 340
Stearic acid, dual adsorption of, and octadecylamine on steel........ 524
Steel, dual adsorption of polar org. compds. on........ 524
Strontium nitrate, soly. in ethylene glycol ethers........ 185
Styrene, phys.-chem. properties of poly-........ 514
Sugars, reacn. of formic acid with, 262; prepn. of D-fructose dihydrate........ 738
Sulfur, S^{35}, low-energy β-particles from........ 541
Sulfur dioxide, bond strength in........ 361
Surface, displacement pressure method for measuring affinity of liquids for solids, 193; thermodynamics and quasi-thermodynamics of plane and spherical.. 526
Surface complexes, on C blacks........753, 756
Surface structure, of colloidal SiO_2 and Al_2O_3........ 136
Surface tension, ring method of measuring, for liquids of high d. and low, 284; crit. micelle concns. by bubble pressure method........ 701

"TACKYPYKNOSIS," explanation of........ 766
Tannic acid, depressant action of........ 643
Temperature coefficient, of heterogeneous reacns..... 745
Terephthalic acid, acid dissocn. consts. of........ 225
Thermodynamic derivatives, Jacobian method for rapid evaluation of, without use of tables........ 799
Thermodynamic functions, periodicity of chem........ 202
Thermodynamics, and quasi-, of 2-phase transition region, 526; of irreversible processes in metallurgy, 1025; statistical method of Gibbs in irreversible, 1030; macroscopic eqns. of transport........ 1048
Thixotropy, explanation of "tackypyknosis"........ 766
Thorium, chloride complexing of, as function of ionic strength........ 1
Toluene, boundary tension at water-, interfaces........ 480
Tridecanoic acid, cataphoresis study of, salts........ 238
Tungsten compounds, photochem. redn. of phosphotungstic acid........ 1084

URANIUM, U^{234}, ionization of fluorocarbon gases by, α-particles........ 1010
Urea, relative rates of hydrolysis of, containing C^{14}... 917

VALENCE, problem of bond energies........ 289
Vanadium compounds, crystal structure of heavy metal orthovanadates, 145; catalytic activity of reduced vanadate salts........ 662
Vapor pressure, of OF_2, 233; low, measurement and thermal transpiration........ 66
Vibrating molecules, possible motions of, and their interpretation in terms of mol. structure........ 336
Vibrational force constants, method of detg. potential barriers restricting inversion in NH_3, PH_3, AsH_3 from........ 321
Vibrational frequencies, of simple derivs. of sym. mols. 326
Vinyl acetate, particle growth in aq. polymn. of...... 1077
Viscosity, of 0.25 to 90% GR-S rubber solns., 432; in cellulose solns. at controlled velocity gradient, 693; of several liquids, 1008; of binary liq. mixts....... 1052

WATER, study of Joshi effect in, and D_2O vapor, 218; interfacial tension between Hg and, 532; decompn. of, under mixed fast neutron and γ-radiation, 575; effects of Co γ-radiation on, and aq. solns., 587; magnetic susceptibility of adsorbed.... 1073
Wien effect, measurement of high field conductance of electrolytes........ 999

XANTHATE, adsorption of aq., on galena surfaces... 616
X-Rays, spectrometer patterns of satd. Na soaps, 128; interpretation of published, measurements correlated with intermicellar equil., 391; thermal denaturation of egg albumin, 789, (corrn.)........ 1110

ZINC, dissoln. of, in HCl-MeOH-H_2O solns........ 727
Zinc, Zn^{65}, in ion exchange........ 106
Zinc oxide, chemisorption of H on MoO_3-, catalyst... 220

New Schedule

BACK ISSUE PRICES

AMERICAN CHEMICAL SOCIETY JOURNALS

Effective January 1, 1952

Single copies or complete volumes of nearly all the ACS journals listed below may be purchased at these prices.

	Current Year		Back Years			
Journal	Member	Non-Member	Member	Non-Member	Foreign Postage	Canadian Postage
ANALYTICAL CHEMISTRY	$0.40	$0.50	$0.60	$0.75	$0.15	$0.05
Analytical Edition (I&EC)						
Volumes 1–4	....	....	1.60	2.00	.15	.05
Volumes 5–8	....	....	1.00	1.25	.15	.05
Volume 9, et seq	....	....	.60	.75	.15	.05
CHEMICAL ABSTRACTS (Vols. 11–44)						
Numbers 1–22, each	....	....	1.00	1.25	.15	.05
Numbers 23 and 24, each	....	....	2.40	3.00*	.45	.15
CHEMICAL ABSTRACTS (Vol. 45, et seq.)						
Numbers 1–22	1.00**	2.00	1.00**	1.25	.15	.05
Number 23 (Author Index)	6.00**	12.00	9.60**	12.00	Free	Free
Number 24 (Subject, Patent, Formula Indexes, complete)	12.00**	24.00	19.20**	24.00	Free	Free
CHEMICAL AND ENGINEERING NEWS	.15	.15	.15	.15	.05	Free
INDUSTRIAL AND ENGINEERING CHEMISTRY	.60	.75	.80	1.00	.15	.05
INDUSTRIAL AND ENGINEERING CHEMISTRY (Industrial Edition)	....	....	.80	1.00	.15	.05
JOURNAL OF THE AMERICAN CHEMICAL SOCIETY (From Vol. 32)	.50	.75	1.00	1.25	.15	.05
JOURNAL OF PHYSICAL CHEMISTRY	1.00	1.25	Not available		.15	.05

RATES FOR VOLUMES OF BACK NUMBERS

Journal	Member	Non-Member	Foreign Postage	Canadian Postage
ANALYTICAL CHEMISTRY (formerly Analytical Edition)	$ 6.00	$ 7.50	$0.75	$0.25
CHEMICAL ABSTRACTS (Vols. 11–44)	20.00	25.00	2.40	.80
CHEMICAL ABSTRACTS (Vol. 45, et seq.)	50.80**	63.50	2.40	.80
CHEMICAL AND ENGINEERING NEWS (1–24)	2.80	3.50	2.25	.75
CHEMICAL AND ENGINEERING NEWS (25, et seq.)	5.60	7.00	2.25	.75
INDUSTRIAL AND ENGINEERING CHEMISTRY	8.80	11.00	2.25	.75
JOURNAL OF THE AMERICAN CHEMICAL SOCIETY (From Vol. 32)	12.00	1.50	1.50	.50
JOURNAL OF PHYSICAL CHEMISTRY—Order from Walter Johnson 125 East 23rd Street, New York 10, New York				

* Each part, when divided.
** The member discount for Volumes 45, et seq. applies only if purchase is for personal use and not for resale.

•

AMERICAN CHEMICAL SOCIETY

Back Issue Department

1155 Sixteenth St., N.W.
Washington 6, D. C.